Universitat Autònoma de Barcelona

The embryo-endometrium crosstalk during human implantation: a focus on molecular determinants and microbial environment

Paula Vergaro Varela

The embryo-endometrium crosstalk during human implantation: a focus on molecular determinants and microbial environment

Paula Vergaro Varela

Thesis for Doctoral Degree in Cell Biology by Universitat Autònoma de Barcelona, Department of Cell Biology, Physiology and Immunology

Barcelona, 2019

Supervisors: Dr. Rita Vassena and Prof. Josep Santaló Pedro

A meus pais e a miña irmá,

SUMMARY

Implantation failure is a major cause of human infertility and currently the most limiting step in Assisted Reproductive Technologies (ART). It can be caused by both maternal and embryonic factors, as well as by defective crosstalk between them. Due to technical and ethical limitations, it is not possible to study human implantation *in vivo*. The knowledge about implantation has been mainly obtained from animal models which fail to represent the physiology of the human process. Additionally, a number of *in vitro* studies have investigated the molecular mechanisms underlying implantation, mostly focussing on either the embryo or the endometrium in a unilateral manner. Many authors have also tried to use indirect, non-invasive approaches to predict implantation success. Despite these efforts, the molecular and environmental determinants precluding pregnancy success remain largely unknown.

In this thesis, we used an *in vitro* model to study the embryo-endometrium interactions during the early stages of implantation. In a first approach, we focused on the different transcriptional responses of the system upon attachment according to the epithelial receptivity (co-culture of trophoblast spheroids with receptive *vs*. non-receptive endometrial epithelium). The results showed that the receptive epithelium is able to trigger a transcriptional response to the trophoblast challenge otherwise muted when it is non-receptive. We further characterized the transcriptional dynamics at earlier time points during the attachment of the trophoblast to the receptive epithelium, aiming to mimic the successful establishment of pregnancy. It resulted in a series of dynamic changes in gene expression, characterized by an early and transient transcriptional up-regulation in the receptive epithelium, while the trophoblast response was more dynamic. Using an *in silico* integrative strategy, we predicted the trophoblast and endometrial protein pairs that interact during these different time points and could mediate attachment and early invasion during implantation. Finally, we used an indirect approach to investigate the environmental determinants influencing implantation by evaluating the vaginal microbiota composition at the day of embryo transfer and its relationship with the reproductive outcomes. Our data suggested that vaginal microbiota profile at the embryo transfer does not directly affect implantation in women undergoing IVF with donated oocytes.

RESUMEN

El fracaso de la implantación es una causa importante de infertilidad humana y, en la actualidad, el paso más limitante en las Tecnologías de Reproducción Asistida (del inglés, ART). Puede ser causado por factores maternos y embrionarios, así como por una comunicación defectuosa entre ellos. Debido a limitaciones técnicas y éticas, no es posible estudiar la implantación humana *in vivo*. El conocimiento sobre la implantación se ha obtenido principalmente a partir de modelos animales que no representan la fisiología del proceso humano. Además, varios estudios *in vitro* han investigado los mecanismos moleculares subyacentes a la implantación, centrándose principalmente en el embrión o el endometrio de manera unilateral. Muchos autores también han intentado utilizar enfoques indirectos y no invasivos para predecir el éxito de la implantación. A pesar de estos esfuerzos, los determinantes moleculares y ambientales que imposibilitan el éxito del embarazo siguen siendo en gran medida desconocidos.

En esta tesis, utilizamos un modelo *in vitro* para estudiar las interacciones embrión-endometrio durante las primeras etapas de la implantación. En un primer enfoque, nos centramos en las diferentes respuestas transcripcionales del sistema tras la adhesión de acuerdo a la receptividad epitelial (co-cultivo de esferoides trofoblásticos con epitelio endometrial receptivo *vs*. no receptivo). Los resultados mostraron que el epitelio receptivo es capaz de desencadenar una respuesta transcripcional al contacto con el trofoblasto por el contrario silenciada cuando no es receptivo. Además, caracterizamos la dinámica transcripcional en tiempos más tempranos durante la unión del trofoblasto al epitelio receptivo, tratando de mimetizar el establecimiento exitoso del embarazo. Esto resultó en una serie de cambios dinámicos de expresión génica, caracterizados por una regulación transcripcional positiva temprana y transitoria en el epitelio receptivo, mientras que la respuesta del trofoblasto fue más dinámica. Usando una estrategia de integración *in silico*, predijimos los pares de proteínas del trofoblasto y del endometrio que interactúan durante estas fases de tiempo y que podrían mediar en la adhesión e invasión temprana durante la implantación. Finalmente, utilizamos un enfoque indirecto para investigar los determinantes ambientales que afectan la implantación mediante la evaluación de la composición de la microbiota vaginal en el día de la transferencia embrionaria y su relación con los resultados reproductivos. Nuestros datos sugirieron que el perfil de microbiota vaginal en la transferencia de embriones no afecta directamente la implantación en mujeres sometidas a fecundación *in vitro* (del inglés, IVF) con ovocitos donados.

ABBREVIATIONS LIST

3-D:	Three dimensions
ART:	Assisted reproductive technologies
ATCC:	American type culture collection
ATP:	Adenosine triphosphate
BH:	Broad Hallmark
cAMP:	Cyclic adenosine monophosphate
CT:	Cytotrophoblast
DAPI:	Diamidino-2-phenylindole
DNA:	Deoxyribonucleic acid
DPBS:	Dulbecco's phosphate-buffered saline
ECACC:	European collection of authenticated cell cultures
ECM:	Extracellular matrix
EGA:	Embryonic genome activation
EMT:	Epithelial to mesenchymal transition
ER Map®:	Endometrial receptivity map
ERA®:	Endometrial receptivity array
ESHRE:	European Society of Human Reproduction and Embryology
ET:	Embryo transfer
EVT:	Extravillous trophoblast
FACS:	Fluorescence-activated cell sorting
FBS:	Fetal bovine serum
FSH:	Follicle stimulating hormone
GEO:	Gene expression omnibus
GFP:	Green fluorescent protein
GnRH:	Gonadotropin-releasing hormone
GO:	Gene ontology
GOBP:	Gene ontology biological process
GSEA:	Gene set enrichment analysis
GTP:	Guanosine-5'-triphosphate
hCG:	Human chorionic gonadotropin
HIV:	Human immunodeficiency virus
ICM:	Inner cell mass

ICMART: International Committee for Monitoring Assisted Reproductive Technology

ICSI: Intra-cytoplasmic sperm injection

IGFBP-1: Insulin-like growth factor binding protein-1

IL: Interleukin

IVF: *in vitro* fertilization

LH: Luteinizing hormone

MEM: Minimum essential medium

MET: Mesenchymal to epithelial transition

MMP: Matrix metalloproteinase

MOI: Multiplicity of infection

MSC: Mesenchymal stem/stromal cell

NLR: NOD-like receptor

PAMP: Pathogen-associated molecular pattern

PC: Principal component

PCA: Principal component analysis

PRL: Prolactin

PRR: Pattern recognition receptor

qPCR: Quantitative polymerase chain reaction

RIF: Recurrent implantation failure

RNA-seq: RNA sequencing

RNA: Ribonucleic acid

ROS: Reactive oxygen species

RPL: Recurrent pregnancy loss

SCT: Syncytiotrophoblast

TLR: Toll-like receptor

uNK: Uterine natural killer

WHO: World Health Organization

WOI: Window of implantation

TABLE OF CONTENTS

LIST OF FIGURES

RESULTS - Chapter 4:

DISCUSSION:

LIST OF TABLES

INTRODUCTION

1. Infertility, ART and implantation failure

Human world population is currently over 7 billion and growing at over 1% annually. In spite of that, reproduction in our species is far from being extremely efficient. The average monthly fecundity rate, i.e. the probability of achieving pregnancy within one menstrual cycle, is around 30% (Zinaman et al., 1996). This percentage is very low compared to that from to other species as the baboon, which can reach 80% (Stevens, 1997).

According to the International Committee for Monitoring Assisted Reproductive Technology (ICMART) and the World Health Organization (WHO), infertility is defined as "a disease of the reproductive system defined by the failure to achieve a clinical pregnancy after 12 months or more of regular unprotected sexual intercourse" (Zegers-Hochschild et al., 2009). As many as 48.5 million couples are estimated to suffer from infertility worldwide (Mascarenhas et al., 2012). However, there is little consensus on whether studies estimating the prevalence of infertility should include variables such as the elapsed time to pregnancy or the women´s age (Gurunath et al., 2011). As a result, the definition and prevalence of infertility remains ambiguous.

Risk factors affecting fertility are diverse, including genetic, environmental, social and physiological parameters (Petraglia, Serour, and Chapron, 2013). With the development of Assisted Reproductive Technologies (ART), many infertile couples have managed to conceive. The clinical data registries of the European Society of Human Reproduction and Embryology (ESHRE) indicate continuing expansion of both the number and variety of ART treatments; a total of 291235 treatment cycles in a population of ~208 million inhabitants were performed in Europe in 2014 (De Geyter et al., 2018). After the birth of Louise Brown in 1978, over 8 million babies have been born from *in vitro* fertilization (IVF) worldwide (De Geyter et al., 2018). However, pregnancy rates in IVF are still around 30% mainly limited by failure of embryos to implant (Pandian, Gibreel, and Bhattacharya, 2015). Implantation failure is a major problem when treating infertility and a bottleneck in ART success. This clinical condition is difficult to manage for both patients and physicians as it entails stress, frustration and increased costs of the treatments (Coughlan et al., 2014). A prerequisite for successful implantation is the acquisition of a receptive endometrium in synchrony with competent embryo development. Furthermore, a highly regulated interaction between both elements is required. Many researchers have tried to increase our understanding of these mechanisms, but it is not possible to approach them *in vivo*. Most studies have used animal models or *in vitro* systems with limited extrapolation to the human clinical setting. The molecular mechanisms underlying implantation remain poorly characterized and there

is still a lack of reliable markers and therapeutic tools for implantation dysfunction. For these reasons, implantation is a topic of key relevance in IVF and there is a pressing need to understand its mechanisms in order to increase ART success rates.

2. Recurrent implantation failure (RIF)

After embryo transfer, implantation is usually confirmed in 14 days as biochemical pregnancy (beta-human chorionic gonadotropin (βhCG) levels measured in blood) and at 7 weeks as clinical pregnancy with the confirmation of fetal heartbeat by ultrasonography. However, successful embryo implantation is not a likely event. The implantation rate per IVF cycle of a single cell-stage embryo is 30% on average, increasing up to 40% with the transfer of a blastocyst (Coughlan et al., 2014). This high probability of failure is an important contributor to the low pregnancy and delivery rates after fresh IVF/ICSI cycles (approximately 28% and 21%, respectively; De Geyter et al., 2018). Importantly, this does not mean that ART techniques are inefficient, as in the fertile population, an estimated 70% of conceptions are spontaneously lost prior to live birth, most of them before becoming clinically detectable (**Figure 1**).

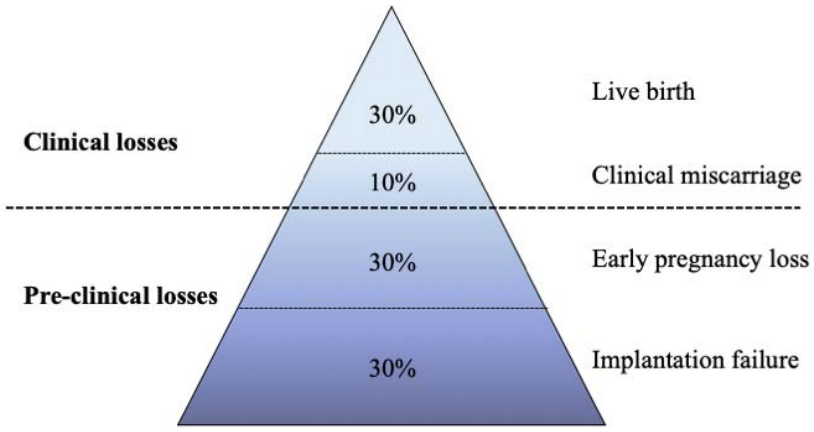

Figure 1. Estimated percentages of pregnancy losses in human spontaneous conceptions. 70% of conceptions are lost prior to live birth, most of them before clinical confirmation of the pregnancy (represented by dotted line) (Adapted from Macklon, Geraedts, and Fauser, 2002).

The term ‘implantation failure’ can be applied to both patients trying to conceive naturally and those undergoing IVF. Recurrent or repeated implantation failure (RIF) refers to a situation of implantation failure after successive IVF attempts. However, a universal definition of this clinical condition has not been agreed upon yet. The variety of definitions includes different parameters such as the number of IVF attempts, the number, quality and stage of the transferred embryos and the age of the woman. In general, the lack of consensus among the research community has led to

controversy surrounding the definition of RIF. A commonly used definition of RIF proposed some years ago was "the absence of a gestational sac visible by ultrasound after 5 weeks post-embryo transfer in more than 3 embryo transfers with high quality embryos or the transfer of 10 or more embryos in multiple transfers; exact numbers to be determined by each centre" (Thornhill et al., 2005). A mathematical model has recently predicted that this definition leads to increased false positives and to possible over-treatments (Somigliana et al., 2018). More recently, other definitions have been proposed; Polanski et al. have defined RIF as "the absence of implantation after two consecutive cycles of IVF, ICSI or frozen embryo replacement cycles where the cumulative number of transferred embryos was no less than four for cleavage-stage embryos and no less than two for blastocysts, with all embryos being of good quality and of appropriate developmental stage" (Polanski et al., 2014). Coughlan et al. have proposed this alternative definition: "failure to achieve a clinical pregnancy after the transfer of at least four good-quality embryos in a minimum of three fresh or frozen cycles in a woman under the age of 40 years" (Coughlan et al., 2014). Of note, it is important to distinguish between RIF and recurrent pregnancy loss (RPL), which is defined by the European Society of Human Reproduction and Embryology (ESHRE) as two or more pregnancy losses (including biochemical pregnancies) before 24 weeks gestation (Bender-Atik et al., 2018).

Due to this variety of definitions, the prevalence of RIF is very difficult to determine. Some reports have estimated that RIF occur in 4-10% of the IVF/ICSI cycles (Margalioth et al., 2006; Shohayeb and El-Khayat, 2012; Koot et al., 2012). The available therapeutic interventions for RIF in the IVF clinics include the freeze-all strategy, administration of antithrombotic agents (i.e. heparin), immunotherapy (e.g. immunosuppressive drugs, intravenous immunoglobulin, peripheral blood mononuclear cells and granulocyte colony stimulating factor), treatment with antibiotics, endometrial injury (i.e. scratching) and molecular evaluation of endometrial receptivity (e.g. Endometrial Receptivity Array (ERA®) and Endometrial Receptivity Map (ER Map®)) (Magdi et al., 2017; Berker et al., 2011; Nakagawa et al., 2015; Li et al., 2013; Yu et al., 2016; Li, Mo, and Chen, 2017; Cicinelli et al., 2015; Vitagliano et al., 2019; Diaz-Gimeno et al., 2011; Enciso et al., 2018). Of note, none of these therapies has been universally proven and their therapeutic effectiveness is controversial.

The urgent need to find effective treatments for RIF led us to develop an *in vitro* model to gain insights into the mechanisms underlying early implantation. In particular, we focused on the interaction between the trophoblast and the endometrial epithelium upon co-culture. Additionally, we aimed to explore the environmental determinants of implantation in order to find indirect, non-

invasive approaches to predict pregnancy success. To achieve this, we studied the relationship between the vaginal microbial environment and reproductive outcomes in women undergoing IVF. Of note, implantation occurs in a complex physical and physiological environment involving the embryo, the endometrium and their interactions. In the following sections of this introduction, we give an overview of these aspects in order to understand the context of implantation and our study approaches.

3. The endometrium

The endometrium is the innermost of the three layers composing the uterus, together with the myometrium (the middle layer) and the perimetrium (the outer layer). Histologically, it is divided into the *stratum functionalis* and the *stratum basalis*. The *stratum functionalis* is a compact superficial layer that accounts for the two thirds of the endometrial mass. It is dynamically regulated by ovarian hormones (estrogen and progesterone) and it is shed in each menstrual cycle in absence of conception. This layer is formed by a compact zone which includes the luminal epithelium and the stromal cells immediately beneath as well as a spongy zone with glands that give twisty appearance. After the menstrual bleeding, the *stratum functionalis* is regenerated by the subjacent *stratum basalis*, which is found beneath the spongy zone and close to the myometrium; the *stratum basalis* contains deep glands and the vasculature (Lessey and Young, 2019) (**Figure 2**).

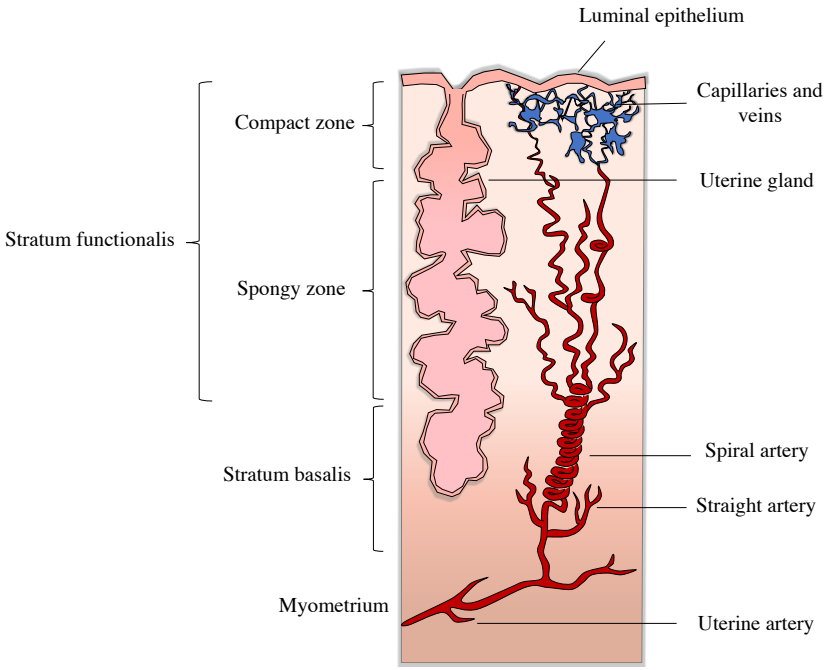

Figure 2. Histologic distribution of the secretory-phase endometrium (Modified from Lessey and Young, 2019).

The endometrium is a dynamic and specialized tissue. If no fertilization occurs, the tissue undergoes cyclic proliferation, differentiation, breakdown and repair during each menstrual cycle along the reproductive life of a woman. If fertilization does occur, this mucosal lining is able to remodel in order to host the embryo, leading to invasive placentation and pregnancy support (Evans et al., 2016). Due to its functions, the endometrium is usually defined as a polarized tissue composed by epithelial (luminal and glandular) and stromal cells, as well as a minority of stem cells, endothelial cells and immune cells (Lessey and Young, 2019). These compartments and components of the endometrium are described in the following sections:

3.1 The epithelium

The endometrial epithelium can be divided into two distinct compartments: the luminal epithelium and the glandular epithelium. The luminal epithelium is a single layer of columnar epithelial cells that covers the uterine surface; it provides the site for embryo implantation and acts as a barrier protecting the uterus against infections (McRae and Kennedy, 1983; Meseguer et al., 2001; Wira, Grant-Tschudy and Crane-Godreau, 2005). The glandular epithelium is composed by columnar epithelial cells and glands that secrete autocrine and paracrine factors regulating endometrial differentiation and embryo implantation (Hempstock et al., 2004; Kelleher et al., 2018). The morphology of this compartment is profoundly influenced by the dynamic hormonal levels during the menstrual cycle. Under the dominance of estrogen during the proliferative phase, epithelial glands are straight and adopt a more intricate structure due to the influence of progesterone in the following secretory phase. Both luminal and glandular epithelium include varying proportions of ciliated cells; heterogeneity is greater in the glandular compartment, where cell surface glycosylation differs among neighbouring cells suggesting that their secretory function could differ as well (Campbell et al., 2000).

3.2 The stroma

The uterine stromal compartment is a layer of connective tissue mainly composed by spindle-shaped fibroblasts and extracellular matrix (ECM) during the proliferative phase of the menstrual cycle. Stromal cells are loosely distributed within the *stratum functionalis* while densely packed in the *stratum basalis* (Lessey and Young, 2019). In the secretory phase, stromal cells undergo a transformation directed by the ovarian steroids to prepare the tissue for potential embryo implantation; this process named decidualization completes the differentiation of the stromal cells. Decidualization is a key event for implantation and it will be discussed in more detail in the context of the endometrial cycle.

3.3 Stem cells

Self-repair of the cycling endometrium led researchers to focus on finding cell populations of stem cells, namely self-renewal, clonogenicity and differentiation (Teixeira, Rueda and Pru, 2008). Experimental identification of endometrial stem cells is usually performed by retention of DNA label and Hoechst 33342 dye exclusion through the ATP-binding cassette transporter and demonstration of clonogenicity (Teixeira, Rueda and Pru, 2008). Some specific stem/progenitor cell populations that could be involved in tissue repair have been identified, including epithelial stem/progenitor cells, mesenchymal stem/stromal cells (eMSCs), and side population cells. Although identified as clonogenic, endometrial epithelial stem/progenitor cells have not been sufficiently characterized to conclude that they are specific to the endometrium, and there are no available markers to identify and isolate them (Gargett, Schwab and Deane, 2016). Clonogenic eMSCs have been localized in perivascular areas of both the *stratum functionalis* and *stratum basalis*; specific markers of eMSCs include co-expression of endothelial cell adhesion molecule cluster of differentiation 146 (CD146) and platelet- derived growth factor receptorβ (PDGFRβ) and single expression of sushi domain-containing protein 2 (SUSD2) (Schwab and Gargett, 2007; Masuda et al., 2012). The side population cells express high levels of ATP binding cassette subfamily G member 2 (ABCG2) and have also been identified in perivascular areas of both the *functionalis* and *basalis* layers (Cervello et al., 2010).

3.4 Endothelial cells

Endothelial cells are located in the endometrial vasculature (in the walls of arteries and veins) and are essential in angiogenesis, i.e. the formation of new blood vessels from pre-existing ones (Carmeliet and Jain, 2011). Angiogenesis plays a key role in endometrial maturation and regeneration, as well as in embryo implantation. During the proliferative and early secretory phases, angiogenesis occurs in the subepithelial region of the *stratum functionalis*; by contrast, during menstruation and endometrial regeneration it only occurs in the *stratum basalis* (Gargett and Rogers, 2001). Endothelial cell proliferation is regulated by the levels of ovarian steroids and the vascular endothelial growth factor (VEGF), but their mechanisms of action are not completely known (Gargett et al., 1999; Kayisli et al., 2004; Chen et al., 2015).

3.5 Immune cells

The human endometrium contains lymphoid cells, macrophages, neutrophils and uterine natural killer (uNK) cells. Lymphoid cells form aggregates comprising a B cell core surrounded by $CD8^+$

T-cells and an outer layer of macrophages (Yeaman et al., 1997). The function of this aggregates is unknown, although it is thought that they could participate in controlling pathogen infections during the menstrual cycle and regulating immunotolerance to the blastocyst during implantation (Zhou, Way and Chen, 2018). Macrophages, neutrophils and uNK cell populations are dynamically regulated during the menstrual cycle, suggesting that in addition to their role in immunity, they could be implicated in tissue breakdown and repair before and after menses. Furthermore, imbalanced composition of leukocyte populations has been associated with infertility (Stewart-Akers et al., 1998; Quenby et al., 1999). Numbers of both macrophages and neutrophils are increased in endometrial tissue areas undergoing remodelling and repair after breakdown (Kaitu'u-Lino, Morison and Salamonsen, 2007; Cousins et al., 2016); macrophages contribute to tissue repair after menstruation by up-regulating cell adhesion molecules such as ICAM-1 and CD71. During early pregnancy, the population of decidual macrophages also increases and contributes to creating a non-cytotoxic pro-inflammatory environment that favours trophoblast invasion by secreting cytokines and chemokines (Fest et al., 2007). uNK cells are the most abundant leukocyte cells in the endometrium and show a different phenotype than that of blood NK cell populations; unlike peripheral blood NK cells that are mainly $CD16^{+}$ $CD56^{-/lo}$, uterine NK cells are predominantly $CD16^{-}$ $CD56^{high}$ (Koopman et al., 2003). uNK cells are predominant in the stroma around the spiral arteries, the endometrial glands and the extravillous trophoblast during early pregnancy; they are scarce in the stroma underlying the epithelial surface. Indeed, increased amount of uNKs in this compartment during the peri-implantation period has been associated with pregnancy loss (Quenby et al., 2009). uNK cells produce angiogenic and chemotactic factors (e.g. VEGF), placental growth factor (PLGF), interleukin (IL)-8 and interferon-inducible protein (IP)-10) that are critical for tissue remodelling, trophoblast invasion and placentation (Koopman et al., 2003; Hannan et al., 2006). Although the mechanisms regulating these processes are not yet elucidated, it has been postulated that uNK cells participate in tissue homeostasis maintenance and endometrial remodelling during implantation through the clearance of senescent decidual cells subpopulations (Brighton et al., 2017). Recent findings revealed the existence of three subsets of uNK cells in the maternal-fetal interface with likely functions as mediators in trophoblast invasion and coordinators of immunomodulatory pathways involving myeloid cells, T cells and stromal cells (Vento-Tormo et al., 2018).

As mentioned, the endometrium is a highly complex and dynamic tissue that undergoes cyclic changes involving its different compartments and components. These series of changes are part of

the menstrual cycle which includes the ovarian and the endometrial cycles, as detailed in the following section.

4. The menstrual cycle

The menstrual cycle refers to the cyclic events involving the action of the hypothalamus, pituitary, ovary and endometrium with the aim of releasing a competent oocyte and preparing the uterus for pregnancy. In a normal, regular cycle, it lasts around 28 days and extends during the reproductive lifespan of a woman. The menstrual cycle is driven by hormonal feedback mechanisms that cause cyclic effects in ovaries, uterus, vagina and mammary glands (Barbieri, 2014). The main effector of this hormonal control is the hypothalamus-pituitary-gonadal axis; the hypothalamus secretes pulses of Gonadotropin-releasing hormone (GnRH), which regulates the production of gonadotropins, i.e. follicle stimulating hormone (FSH) and luteinizing hormone (LH), by the anterior pituitary gland also in a pulsatile manner. Gonadotropins exert their action in the ovaries, where they bind to their receptors and promote sex steroid production. In turn, sex steroid hormones regulate gonadotropin secretion by dual positive and negative feedback control according to their circulating levels (Plant, 2015). The menstrual cycle is usually divided into the ovarian cycle and the endometrial cycle.

4.1 Ovarian cycle

The ovarian cycle includes oogenesis (oocyte generation) and folliculogenesis (growth and development of ovarian follicles harbouring oocytes). The ovarian cycle depends on functional interactions among the oocyte, granulosa and theca cells as well as the vascular and immune systems (Richards, 2018). It is further classified into the follicular phase (lasting from menses to ovulation) and the luteal phase (lasting from ovulation to the following menses) (**Figure 3**):

4.1.1 Follicular phase

The first phase of the ovarian cycle describes the development of the follicle from the primordial stage until the pre-ovulatory stage in response to the FSH secreted by the anterior pituitary gland. FSH levels start to increase during the last days of the previous menstrual cycle; after menses, FSH levels continue to rise and peak during the first week of the follicular phase. This rise in FSH levels stimulates several Graafian follicles to re-enter meiosis. These follicles compete for dominance and, eventually, a single follicle will be ovulated. FSH also promotes granulosa cell proliferation in developing follicles as well as their expression of LH receptors. Under the influence of FSH,

the granulosa cells secrete estradiol, the main steroid hormone during this period. The selected dominant follicle will grow and develop until ovulation, while the rest will undergo atresia. The dominant follicle further increases estrogens levels, which results in a rise in FSH levels and a pronounced peak in LH production; these hormonal peaks trigger ovulation, i.e. the rupture of a mature ovarian follicle and release of an oocyte, which normally occurs approximately 30 hours after the LH surge (Plant, 2015; Richards, 2018).

4.1.2 Luteal phase

After ovulation, the remaining cells of the dominant follicle transform into the corpus luteum, which produces high levels of progesterone and, to a lesser extent, estrogens. Progesterone is responsible for rising the basal body temperature and directing the endometrial remodelling needed to acquire receptivity to implantation. The corpus luteum lasts for around 14 days in absence of conception, when it atrophies due to the fall in levels of FSH and LH. The atrophy of the corpus luteum decreases the levels of progesterone and estrogen, which in turn results in rising levels of FSH; this leads to the recruitment of new follicles and the beginning of a new cycle with menstruation. If implantation occurs, the hCG produced by the embryo maintains the corpus luteum, which produces progesterone until the placenta is able to sustain its own endocrinological function (Plant, 2015; Richards, 2018).

4.2 Endometrial cycle

The endometrial cycle comprises the series of morphological and physiological changes that the endometrium undergoes to acquire the optimal receptive phenotype for hosting the blastocyst upon fertilization and arrival to the uterus. The endometrial cycle includes a proliferative and a secretory phase, separated by ovulation (**Figure 3**).

4.2.1 Proliferative phase

Coinciding with the follicular phase of the ovarian cycle, the endometrial proliferative phase begins with menstruation (days 1 to 4 of the cycle). After the menstrual bleeding, the thin endometrium proliferates under the influence of estrogens, growing from approximately 4.5 mm on day 4 of the cycle to approximately 10 mm on day 9 (Bromer, Aldad and Taylor, 2009). This tissue regeneration and proliferation is directed by the permanent basal layer, which retains the responsiveness to sex steroid hormones and is able to regenerate a thick functional endometrium. Apart from epithelial and stromal cells, the proliferative phase involves glands and blood vessels,

which contribute to the characteristic morphological appearance of the tissue in each cycle phase, as illustrated in **Figure 3**.

During the early proliferative phase (days 4-7 of the cycle), the endometrial tissue is composed by straight short glands and compact stroma, which show large nuclei and rare mitotic activity. The mid proliferative phase (days 8-10) is characterized by columnar epithelial cells, longer curving glands and stromal edema with numerous mitotic events. In the late proliferative endometrium (days 11-14), the epithelium shows undulant surface and pseudo-stratification; glands are tortuous, with active mitotic activity and the moderately dense stroma also evidences active growth (Noyes, Hertig and Rock, 1975).

4.2.2 Secretory phase

The rise in progesterone levels produced by the corpus luteum induces high secretory activity in the endometrium, while estrogen promotes slight additional proliferation. The secretory phase begins with ovulation, which occurs around the 14^{th} day of the cycle and it is in some cases characterized by the presence of subnuclear vacuoles in half of glands. However, no significant changes compared to the late proliferative phase are considered until the day 16^{th}, when subnuclear vacuolation becomes evident. From day 18, the vacuoles become smaller in size, intraluminal secretions appear and both pseudo-stratification and mitoses are absent. Intraluminal secretions and edema are maximal in the following days (20-22). By day 25, most of the endometrial surface is occupied by stromal cells with abundant cytoplasm and large nuclei, feature that is generalized on day 27 (Noyes, Hertig and Rock, 1975). These changes are accompanied by sequential increase in gland tortuosity, size and secretory products; the cytoplasm of stromal cells accumulates glycogen and lipids and undergoes structural transformation, which is known as decidualization. Altogether, the transformation of the endometrium into a secretory tissue aims to provide the optimal conditions for embryo implantation and pregnancy support. The endometrium becomes receptive to implantation for approximately 5 days (days 19-20 to 23-24 of the cycle) (Macklon, Geraedts and Fauser, 2002; Evans et al., 2016).

After having reviewed the histology and physiology of the endometrium, we will summarize the most relevant features for the correct development of decidualization and endometrial receptivity as critical events required for embryo implantation.

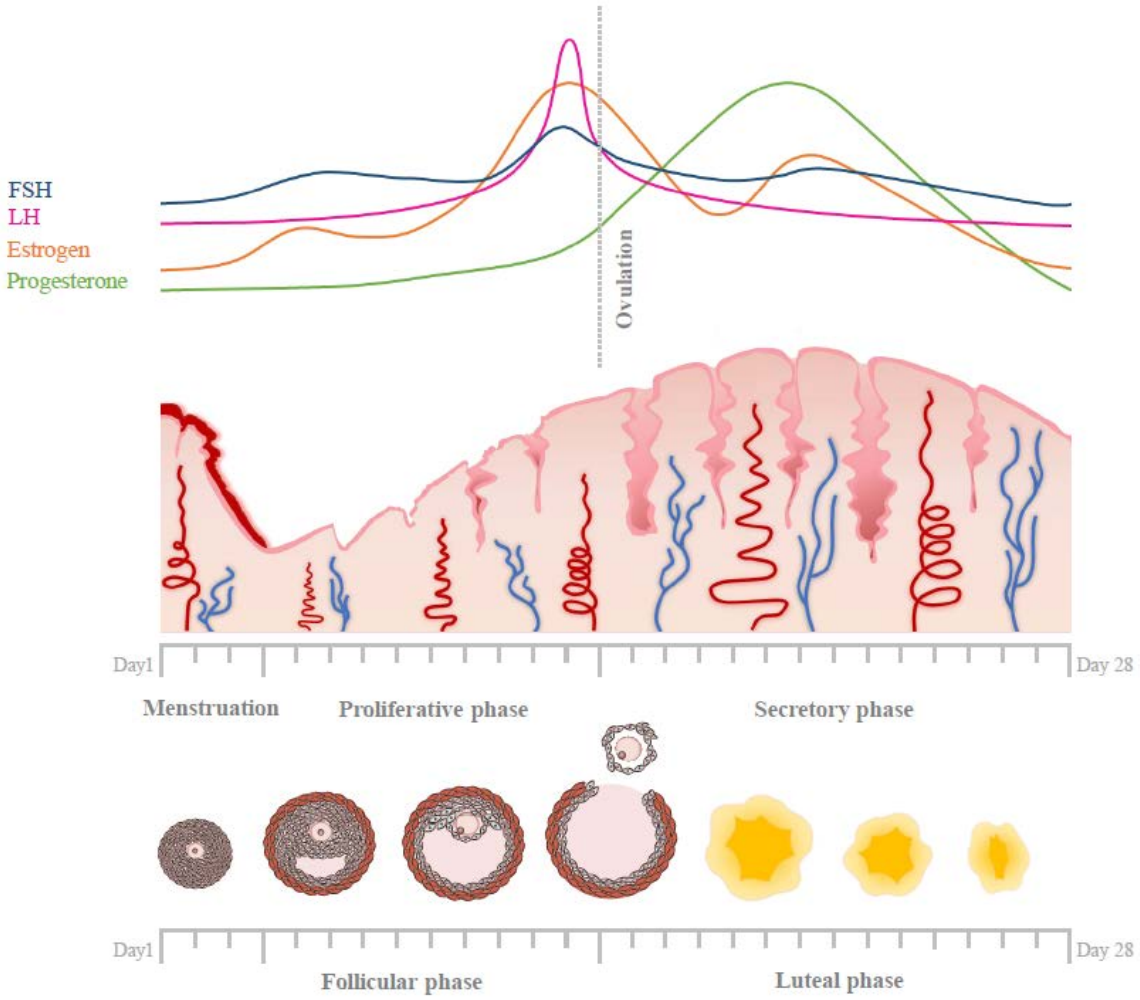

Figure 3. Representation of normal 28-day endometrial (middle panel) **and ovarian** (lower panel) **cycles in relation with gonadotropins and steroid hormone levels** (upper panel). The endometrial cycle is divided into three phases: menstruation, proliferative and secretory. Cycling changes in endometrial tissue are regulated by the levels of ovarian hormones estrogen and progesterone as well as gonadotropins LH and FSH (upper panel). After menstrual bleeding, most of the functional endometrium is shed. Mainly driven by estrogen action, the endometrial epithelium is repaired and increases its thickness during the proliferative phase (middle panel). This coincides with the follicular phase of the ovarian cycle, when follicles develop from the primordial stage until the pre-ovulatory stage in response to FSH. The dominant follicle is selected and grow until ovulation, while the rest will undergo atresia (lower panel). Following ovulation at mid-cycle, which results from a rise in FSH levels and a pronounced peak in LH, the oocyte is released and remaining cells of the dominant follicle transform into the corpus luteum (luteal phase, lower panel). Endometrial cells increase their secretory activity and start to differentiate, driven by progesterone in the presence of estrogen (secretory phase, middle panel). The endometrium is receptive to embryo implantation during a short period in the mid-secretory phase (days 20-24). In a conception cycle, the blastocyst secretes hCG, that maintains the corpus luteum and enables the establishment of pregnancy. If implantation does not occur, the atrophy of the corpus luteum decreases the levels of progesterone and estrogen, leading to rising levels of FSH and the beginning of a new cycle with menstruation.

5. Decidualization

The term decidualization refers to the complex differentiation of the endometrial stromal fibroblasts into specialized secretory epithelioid-like decidual cells; this process involves different cell types, including the secretory transformation of the uterine glands, influx of uNK cells and monocytes as well as vascular remodelling. This series of morphological and biochemical changes make the stroma an immuno-privileged and nutritive environment favourable to embryo implantation and placental development; the stroma is then termed "decidua", which occurs spontaneously in the mid to late secretory phase of each menstrual cycle regardless of the presence of an embryo, as opposed to other species. Instead, human decidualization is mainly driven by the post-ovulatory rise in circulating progesterone but also by estrogen along with increasing local cAMP levels. Once initiated, decidual cells secrete paracrine factors (e.g. hormones, cytokines, chemokines, lipids and non-coding RNAs) that spread the decidualization signal as a wave trough the endometrium. In non-conceptional cycles, the decidual tissue is shed and repaired in response to falling progesterone levels, leading to the beginning of a new cycle (Gellersen and Brosens, 2014; Evans et al., 2016).

Upon decidualization, endometrial stromal cells undergo dramatic phenotypic transformation (**Figure 4**). In the proliferative phase, stromal cells show a fibroblast-like morphology with little cytoplasm, prominent Golgi apparatus and rough endoplasmic reticulum as well as elongated nuclei. They then transform into decidual cells with expanded cytoplasm due to the accumulation of glycogen and lipids, dilated Golgi apparatus and rough endoplasmic reticulum, more abundant nucleoli and rounded nuclei. In the late secretory phase, the number of phagosomes and lysosomes increases and decidual cells present pseudopodia-like structures that may contribute to the ECM remodelling (Cornillie, Lauweryns and Brosens, 1985; Kajihara et al., 2014). The ECM also undergoes characteristic changes during decidualization, marked by increased collagen IV and laminin surrounding decidual cells (Iwahashi et al., 1996). Decidual cells are characterized by the expression of prolactin (*PRL*) and insulin-like growth factor binding protein-1 (*IGFBP-1*), which are well established decidual markers (Golander et al., 1978; Rutanen et al., 1985). Other decidual markers include NODAL-signalling pathway inhibitor left-right determination factor 2 (*LEFTY2*), forkhead box protein O1 (*FOXO1*), CCAAT/enhancer-binding protein- (*C/EBP*), wingless-type mouse mammary tumour virus integration site family member 5A (*WNT-5A*), prokineticin-1 (*PROK1*) and dickkopf-1 (*DKK1*) (Tabibzadeh, Lessey and Satyaswaroop, 1998; Christian et al., 2002; Evans et al., 2008; Matsuoka et al., 2010, Macdonald et al., 2011).

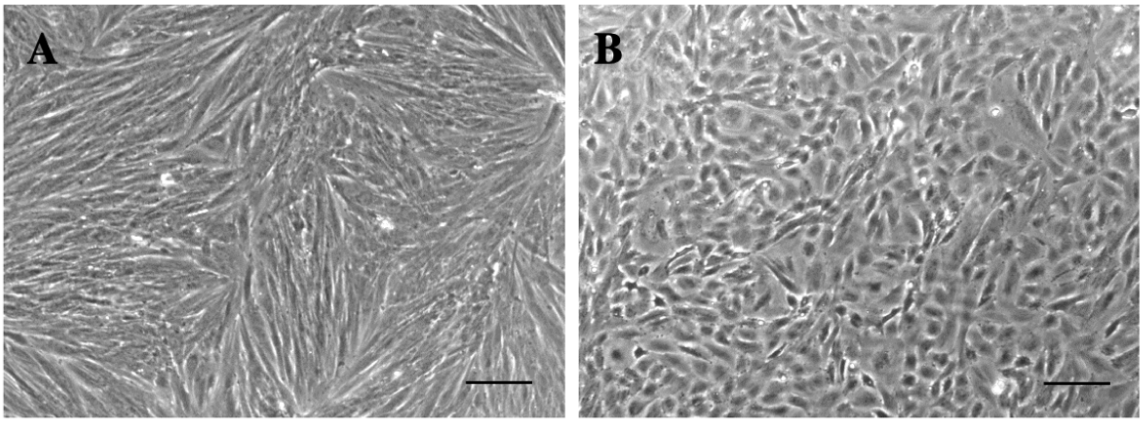

Figure 4. Primary human endometrial stromal cells: (**A**) Untreated controls. (**B**) After inducing *in vitro* decidualization with 0,5 mM 8-Bromoadenosine-3-5-cyclic monophosphate and 1 μM Medroxyprogesterone 17-acetate for 5 days. Scale bars represent 100 μm length.

Although involved in the process, the specific role in decidualization of other cell types different from stromal cells is not clear (Evans et al., 2016). A recent study has found that uterine glands affect decidualization and regulate on-time embryo implantation in mice (Kelleher et al., 2018). It seems that uNK cells could be responsible for creating a balanced inflammatory and immune tolerant environment in the maternal-fetal interface through chemokine-mediated control of decidualized stromal cells (Nancy et al., 2012; Vento-Tormo et al., 2018).

Cyclic tissue decidualization, shedding and repair have been proposed as evolutionary mechanisms of adaptation for the aggressive human haemochorial placentation; this repeated preconditioning could protect the endometrial tissue from the hyperinflammation and oxidative stress caused by placentation and pregnancy (Brosens et al., 2009). Additionally, decidualization could be a mechanism of maternal control to avoid the implantation of genetically impaired embryos. The decidualized cells have the unique property of acting as biosensors of embryo quality, responding differently to implanting embryos depending on their viability (Teklenburg et al., 2010; Brosens et al., 2014). Defective decidualization is linked to non-selective acceptance of low quality embryos, which may be responsible for the increased receptivity and subsequent miscarriage in women suffering RPL. Conversely, a too restrictive decidua leads to the rejection of high quality embryos and implantation failure (Salker et al., 2012; Weimar et al., 2012).

6. Endometrial receptivity and the WOI

Endometrial receptivity is defined as the transient state in the mid to late secretory phase during which the endometrium is favourable to accommodate the blastocyst. Although it is not completely defined, it is often framed around days 19-20 to 23-24 of a regular menstrual cycle (Macklon, Geraedts and Fauser, 2002; Evans et al., 2016). During the rest of the cycle, the endometrium remains refractory to embryo implantation. This period of endometrial receptivity is also termed "window of implantation" (WOI); it comprises a series of molecular and cellular changes directed by the increase of circulating hormonal levels that include, but are not limited to, the decidualization of the stromal compartment. The luminal epithelium also undergoes differentiation during the receptive period to facilitate blastocyst attachment and penetration. The epithelial surface transformation comprises epithelial to mesenchymal transition (EMT), loss of epithelial polarity, loss of cell-cell adhesions and glycocalyx remodelling to weaken the luminal barrier. During the first days of the WOI (19-21), bleb-like protrusions become apparent on the apical surface (Usadi et al., 2003). These structures are called pinopodes or uterodomes and have been related with cytokines secretion and mediation of embryo attachment (Kabir-Salmani et al., 2005; Nejatbakhsh et al., 2012). However, the role of pinopodes in endometrial receptivity and embryo implantation is still a matter of debate (Quinn and Casper, 2009; Qiong et al., 2017). Simultaneously to surface remodelling, the stroma undergoes decidualization accompanied by eosinophilic proliferation around arterioles, stimulation of glycogen accumulation in decidual cells, increase of glandular epithelial secretion and boost of stromal vascularity. Populations of uNK cells and macrophages also increase during this period, contributing to create an optimal environment to embryo implantation (Lessey, 2000; Evans et al., 2016; Salamonsen et al., 2016). The interaction between the blastocyst and the endometrial luminal epithelium further enhances receptivity, while the factors secreted by the decidual cells (such as hormones, cytokines, chemokines and lipids) promote decidualization throughout the stroma (Evans et al., 2016) (**Figure 5**).

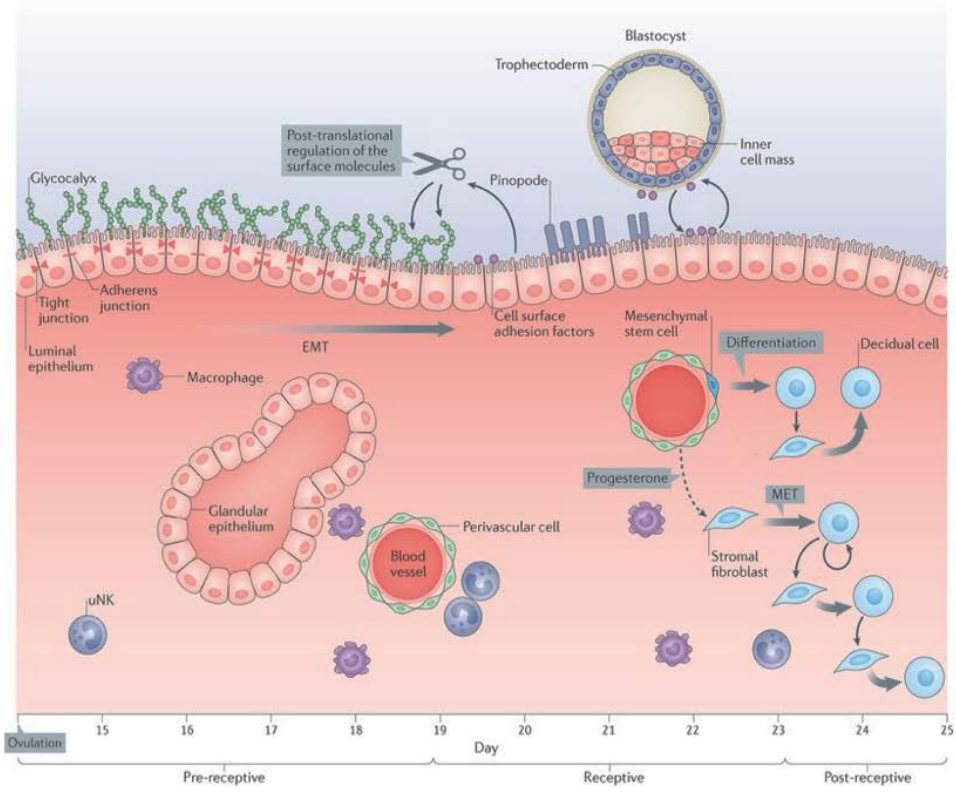

Figure 5. **Representative figure of the main histological changes during the pre-receptive, receptive and post-receptive endometrium.** During the pre-receptive period (coinciding with the secretory phase, from ovulation until around day 20), the luminal epithelium is highly polarized with lateral junctions that keep cells tightly together. The glandular epithelium becomes highly secretory, uNK cells proliferate and peripheral macrophages come to the endometrium. The luminal epithelium is remodelled in order to become receptive: the glycocalyx is modified, surface cells undergo epithelial to mesenchymal transition (EMT), leading to a less polarized epithelium with fewer lateral junctions. The variety of cell adhesion molecules of the luminal surface changes and pinopodes appear, although its role in implantation is unclear. In parallel, the stromal compartment undergoes decidualization which is initiated by progesterone in those areas around blood vessels. These cells undergo mesenchymal to epithelial transition (MET), becoming rounded and acquiring a secretory phenotype. Decidual cells express PRL and IGFBP-1 and secrete factors that promote decidualization throughout the endometrium (Adapted from Evans et al., 2016).

6.1 Evaluation of endometrial receptivity

Suboptimal endometrial receptivity is an important cause of implantation failure and must be carefully evaluated when treating RIF. The clinical application of proven diagnostic tests and treatments for suboptimal endometrial receptivity is, hitherto, very limited. Since first described in 1975, the main method for the assessment of pathologic conditions and receptivity is histologic evaluation of endometrial sections using the Noyes criteria (Noyes, Hertig and Rock, 1975). It is an invasive method, as it requires an endometrial biopsy, and it is somewhat subjective. A

commonly used non-invasive method is ultrasonography, which allows for the evaluation of endometrial thickness, appearance and vascularization. Morphometric methods are easy to implement in the clinical routine and provide valuable information about the overall state of the tissue but cannot generally predict endometrial receptivity.

Currently, the most precise characterization of endometrial status relies on transcriptomic profiling. Transcriptomics has emerged as a powerful tool to characterize physiological and pathological conditions in multiple biological processes, including endometrial receptivity and embryo implantation. This approach has enabled the development of molecular tools to predict the receptive endometrial phase and personalize embryo transfers such as the ERA® and the ER Map® (Diaz-Gimeno et al., 2011; Simon et al., 2016; Enciso et al., 2018). The ERA® is the most widely used molecular test in the clinical practice, which is based on the expression of 238 genes previously selected as representative of the receptive endometrial signature. The bioinformatics algorithm of ERA® showed sensitivity of 0.99 and specificity of 0.88 for endometrial dating, while for pathological classification the specificity was of 0.15 and the sensitivity of 0.99. These numbers have added a greater value for the clinical application of this method compared with histology (Diaz-Gimeno et al., 2011; Diaz-Gimeno et al., 2013; Simon et al., 2016). However, the universal application of ERA® in fertility treatments is still a matter of debate. ERA® has shown improved reproductive outcomes in RIF patients (Ruiz-Alonso et al., 2013; Hashimoto et al., 2017), while it has not been useful in patients with good prognosis (Bassil et al., 2018). Inconsistency in ERA® results has also been reported (Dahan and Tan, 2018). This customized array is based on a set of genes that were selected from a population of fertile women and might not be correctly extrapolated to the infertile population. RIF is a pathology with multiple etiologies including not only out of phase receptivity but also impaired transcriptional profiles, which can be a cause of misdiagnosis in some patients (Koot et al., 2016; Sebastian-Leon et al., 2018). Indeed, there are intermediate transcriptional profiles that cannot be predicted as either healthy nor RIF, leading to a non-binary classification that correlates with the severity of the implantation failure and therefore suggesting that there are different degrees of RIF (Koot et al., 2016). It is needed to further refine the definition of endometrial transcriptional signatures for RIF *vs*. healthy women in order to maximize prediction accuracy. Additionally, large prospective studies are required to validate any clinical benefit of using ERA® in ART.

The ER Map® is a more recent transcriptional and bioinformatics tool restricted to the expression of 40 genes during the WOI analyzed by qPCR. These genes, which are differentially expressed in infertile and fertile women, are involved in endometrial proliferation and immune response

associated with embryo implantation (Enciso et al., 2018). Compared to ERA®, ER Map® has the advantages of reducing the interpatient variability (i.e. samples were obtained at days LH+2 and LH+7 from the same women within the same cycle) and the easier accessibility to the qPCR for the clinical setting. Likewise, these results need to be confirmed in randomized controlled trials before its reliable application in the clinical practice.

An important issue leading to variability in transcriptomic analysis is the heterogeneity in endometrial tissue composition. The proportion of epithelial and stromal cells in endometrial biopsies is dependent on the phase of the menstrual cycle and affects the whole-tissue gene expression profiles. In order not to mask mechanisms affecting endometrial receptivity, it is required to adjust the expression profiles for tissue cellular composition (Suhorutshenko et al., 2018). Another controversial point is the inter-cycle variability of endometrial gene expression profiles. Fertile women have shown a stable expression pattern of genes related with implantation, which was not affected even with repeated sampling on the same cycle (Evans et al., 2018); whether this pattern is reproduced by infertile women has not been addressed. Overall, the use of transcriptomics is still challenging due to the lack of guidelines and experience in managing the big amount of data generated by these approaches. Furthermore, comparing studies is very difficult due to the variability of the studied populations and sampling methods as well as the different methodologies used for the analysis (Altmae et al., 2014).

Other "omics" used for reproductive biology studies include proteomics, lipidomics, secretomics, and metabolomics, which generate long lists of candidates presumably involved in the acquisition of the endometrial receptive phenotype but still need further research. The development of non-invasive methods with clinical applicability is required. Some sources include blood, urine and endometrial fluid, but their clinical usefulness is still to be proven. Endometrial fluid might be an interesting source as it seems to be more direct than blood or urine; state of the art techniques are being used in the research of receptivity biomarkers in endometrial fluid with promising results, e.g. lipidomics and secretomics (Chan et al., 2013; Vilella, Ramirez and Simon, 2013; Azkargorta et al., 2018). It is minimally invasive compared to endometrial curettage and it has been proven that it does not affect pregnancy outcome (van der Gaast et al., 2003). Novel players affecting endometrial receptivity and ultimately the reproductive outcome include reproductive tract bacteria (i.e. vaginal and endometrial microbiota), as further discussed in **Chapter 4**.

A receptive endometrium is a requisite but not the unique to ensure successful implantation and establishment of pregnancy. The embryo plays the same essential role in these processes and the correct pre-implantation embryo development to a competent blastocyst is critical. The following section highlights the most relevant steps during embryo development in order to better understand its role in implantation.

7. Preimplantation embryo development

After fertilization, i.e. the multistep process that ends up with the fusion of a sperm and an oocyte in the ampulla of the fallopian tubes, the preimplantation embryo is transported to the uterine luminal epithelium pulled by cilia movements and muscle contractions (Croxatto, 2002). Along this journey of around five days, preimplantation development involves the transition from almost transcriptionally silent gametes to the formation of a competent blastocyst with ability to implant in the uterus. One of the most important mechanisms during this period is the gene expression control, which switches from maternal to embryonic in a tightly regulated manner. Oocyte development is characterized by active transcription and mRNA storage in the cytoplasm. Transcriptional activity is silenced during oocyte maturation (germinal vesicle to metaphase II oocyte transition) and restored upon fertilization, sustaining early embryonic development (Niakan et al., 2012). This maternal control of gene expression is taken by the embryo upon the major wave of embryonic genome activation (EGA) which occurs on day 3 of human embryo development, at the 8-cell stage. However, this process is dynamic and waves of active transcription have been seen as early as at the 2-cell and 4-cell stages, which could anticipate the subsequent major EGA (Vassena et al., 2011). The translation and degradation of the cytoplasmic maternal mRNAs is also dynamic and highly regulated; it begins even before fertilization and continues until the EGA, selecting those transcripts required for each developmental stage (Zhang and Smith, 2015).

In IVF treatments, embryos are usually cultured from 3 to 5 days before being transferred to the maternal uterus. During these days, the embryos undergo a series of molecular and morphological changes that have been primarily characterized by phase-contrast and time-lapse microscopy. The characterization of these changes also provides a tool for embryo grading, aiming to select and transfer top quality embryos. The main events during embryo development are represented in **Figure 6** and described as following:

- **Day 0**: Fertilization is considered the reference starting point of preimplantation embryo development and it is referred as day 0. The initial stage after fertilization includes key events as the oocyte meiotic resumption and second polar body extrusion, sperm head de-condensation, maternal and paternal pronuclei formation and juxtaposition as well as pronuclear membrane breakdown (Payne et al., 1997). Additionally, there is a reorganization of the nucleolar precursor bodies and cytoplasmic movements. All of these processes are determinant for the future embryo development and therefore the assessment of this stage is essential. A detailed morphokinetic description of the events regulating fertilization has been recently published, providing a source of novel embryo quality parameters (Coticchio et al., 2018).
- **Day 1**: The first cell cleavage occurs around 27-29 hours after fertilization, generating a 2-cell stage embryo (Motato et al., 2016). High quality characteristics at this stage include similar, mononucleated daughter cells (blastomeres) with low percentage of fragmentation (less than 20%) (Gardner and Balaban, 2016).
- **Day 2**: Around 44-46 hours post-fertilization, a high quality embryo is expected to have four or five symmetric, mononucleated blastomeres and little fragmentation (Gardner and Balaban, 2016).
- **Day 3**: From 66 to 68 hours post-fertilization, a high quality embryo should have more than six (7-9) symmetric, mononucleated blastomeres and little fragmentation (Gardner and Balaban, 2016). The number and size of the blastomeres in this stage have been strongly associated with the clinical outcome after embryo transfer (Paternot et al., 2013), which coincides with the major wave of EGA (Vassena et al., 2011).
- **Day 4**: EGA is followed by compaction, which leads to the tight adhesion between the blastomeres into a clustered structure termed morula. It is the first morphological indication of symmetry breaking, which is also dependent on embryonic transcriptional waves (Shi et al., 2015).
- **Day 5**: Sequential embryo cleavage and cavitation lead to the formation of the blastocyst, which comprises a fluid-filled cavity (blastocoel) containing the inner cell mass (ICM) and a surrounding thin layer of trophectoderm cells. The extra-embryonic trophectoderm will provide the placental structures, while the ICM will give rise to the fetal structures later in pregnancy. Just before embryo implantation, the ICM differentiates into the epiblast or ectoderm (pluripotent stem cells that will give rise to all the tissues of the fetus and the extra-embryonic mesoderm) and the hypoblast or primitive endoderm (multipotent cells

which will give rise to the extra-embryonic membranes, mainly the yolk sac) (Niakan et al., 2012).

From day 5 on, the blastocyst expands and the zona pellucida (extracellular glycoprotein layer from oocyte origin surrounding the early embryo that keep the blastomeres together) breaks down, concomitant with dynamic contraction movements (Huang, Chinn, et al., 2016). Evidences from *in vitro* studies suggest that the zona pellucida is not critical for embryo development but it is likely that facilitates embryo transport through the oviduct due to its non-adhesive nature (Carson et al., 2000) and to protect the developing embryo from the maternal immunological system (Clark and Schust, 2013). Then, the blastocyst hatches from the zona pellucida and the trophoblast cells will lead the implantation in the uterus. Implantation occurs around the day 7 and it is essential for further embryo development.

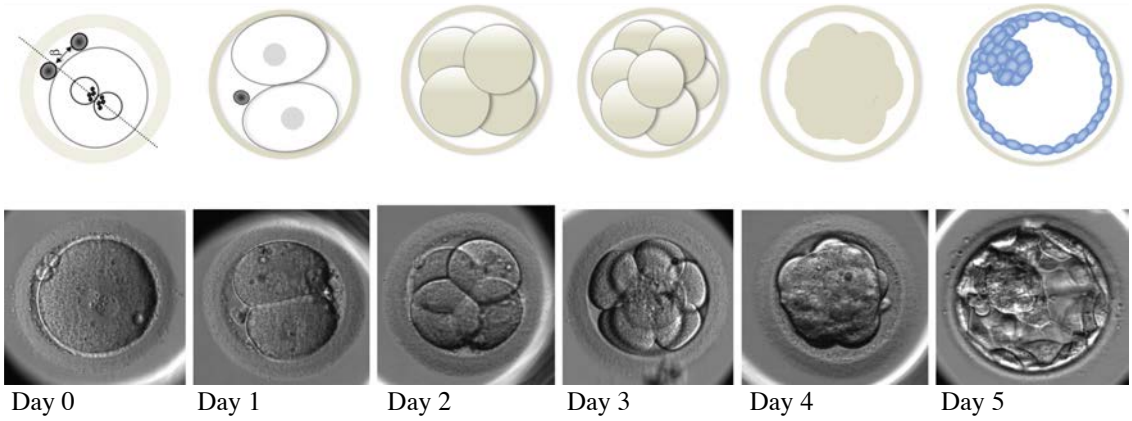

Figure 6. **Graphic representations and images of the key morphological features during human embryo development** from fertilization (day 0) until blastocyst stage (day 5) (adapted from Gardner and Balaban, 2016, with permission).

8. Embryo implantation

Implantation is the first interaction between a viable embryo and the receptive endometrium for the establishment of successful pregnancy. This crosstalk needs to be highly coordinated not to result in out of phase or defective implantation. It is estimated that 30% of failed pregnancies are caused by implantation failure, 30% are lost after implantation but before clinical confirmation and 10% are later stage miscarriages (Macklon, Geraedts and Fauser, 2002). The highest implantation rates are achieved with embryo-endometrial developmental synchrony of

approximately ±1.5 days; therefore, it can be inferred that successful implantation can occur with maximum asynchrony of 3 days (Wilcox, Baird and Weinberg, 1999).

Implantation is a sequential process usually divided into three main steps (illustrated in **Figure 7)**:

8.1 Apposition

When the blastocyst arrives to the endometrial lining, the trophoblast establishes a weak and reversible interaction with the endometrial luminal epithelial cells. As opposed to implantation in mice, the human trophoblast apposition is led by the polar trophectoderm, i.e., the area of trophectoderm closest to the ICM (Lindenberg, 1991; Grewal et al., 2008; Aberkane et al., 2018). Although the importance of blastocyst orientation in human has not been sufficiently explored to make conclusions, it could be related with proper trophoblast invasion and placentation. Blastocyst apposition is mainly driven by paracrine signalling, involving secreted factors and their correspondent receptors as well as exosomes and microvesicle trafficking. These extracellular vesicles are mainly released to the uterine fluid by the epithelial cells and internalized by the trophoblast cells (Ng et al., 2013; Greening, Nguyen, Evans, et al., 2016).

8.2 Attachment

After loose apposition, the embryo becomes firmly attached to the luminal epithelium; this interaction is termed attachment (or adhesion) and is characterized by irreversible trophoblast-epithelium union and active molecular communication (Aplin and Kimber, 2004). The main players are the ECM and cell adhesion molecules such as integrins, cadherins, selectins and immunoglobulins, whose ligands or receptors are expressed in the uterine luminal epithelium and blastocyst surfaces; cell–cell interactions have been demonstrated *in vivo*, *in vitro* and *in silico* (Haouzi et al., 2011; Altmae et al., 2012; Singh and Aplin, 2015; Aberkane et al., 2018). Once firm attachment is established, trophoblast cells differentiate into an outside layer of syncytiotrophoblasts (SCT) and an inner layer of cytotrophoblast (CT), which can also follow two subsequent pathways. Through the villous pathway, CT cells fuse to form multinucleated syncytiotrophoblasts (syncytium), which are important for the initial invasion and for maternal-fetal gas and nutrient exchange. By contrast, CT cells acquire an invasive phenotype through the extravillous pathway and differentiate into interstitial extravillous trophoblasts or endovascular extravillous trophoblasts (EVTs). The interstitial extravillous trophoblasts deeply invade the decidua to anchor the growing fetus, whereas the EVTs remodel the maternal vascular system (Sharma, Godbole and Modi, 2016).

8.3 Invasion

The epithelial breaching and invasion of the underlying stroma aim to allow the penetration of the blastocyst into the decidualized maternal tissue. Cell adhesion molecules also play an important role by promoting chemotaxis and cell migration in the stromal compartment (Gellersen et al., 2013). Invasion is mainly driven by the lytic activity of the SCT, which leads to the remodelling of the maternal spiral arteries and maternal blood supply needed for hemochorial placentation. Various proteinases including serine proteases, matrix metalloproteinases (MMPs) and collagenases are responsible for the ECM degradation and tissue remodelling (Cohen, Meisser and Bischof, 2006). SCTs synthesize specific proteins including hCG, which promotes the establishment and maintenance of the ovarian corpus luteum and the spread of the decidual signalling wave throughout the endometrium in order to support the ongoing pregnancy (Melford, Taylor and Konje, 2014).

Trophoblast-decidual interactions determine placental formation and pregnancy development; deficiencies as shallow trophoblast invasion and insufficient vascular remodelling cause adverse pregnancy outcomes such as preeclampsia and intrauterine growth restriction, while excessive invasion is related with placenta accreta and choriocarcinoma (Lunghi et al., 2007). A balanced control of trophoblast invasion is achieved by trophoblast and decidual secretory products with the dual action of activating and inhibiting the process; these products include a wide range of cytokines (e.g. IL-1β, IL-5, IL-6, IL-7, IL-8, IL-9, IL-10, IL-12, IL-13 and IL-15) growth factors (e.g. VEGF, EGF, placental growth factor (PlGF), CSF-1, IGF-I or IGF-II) and enzymes such as the tissue inhibitors of MMPs (TIMPs) that limit the proteolytic activity of the MMPs (Cohen, Meisser and Bischof, 2006; Knofler, 2010; Sharma, Godbole and Modi, 2016). Secretory products of endometrial glands (e.g. EGF, VEGF and LIF) also contribute to control trophoblast invasion, especially during earlier stages (Burton and Reid, 2002).

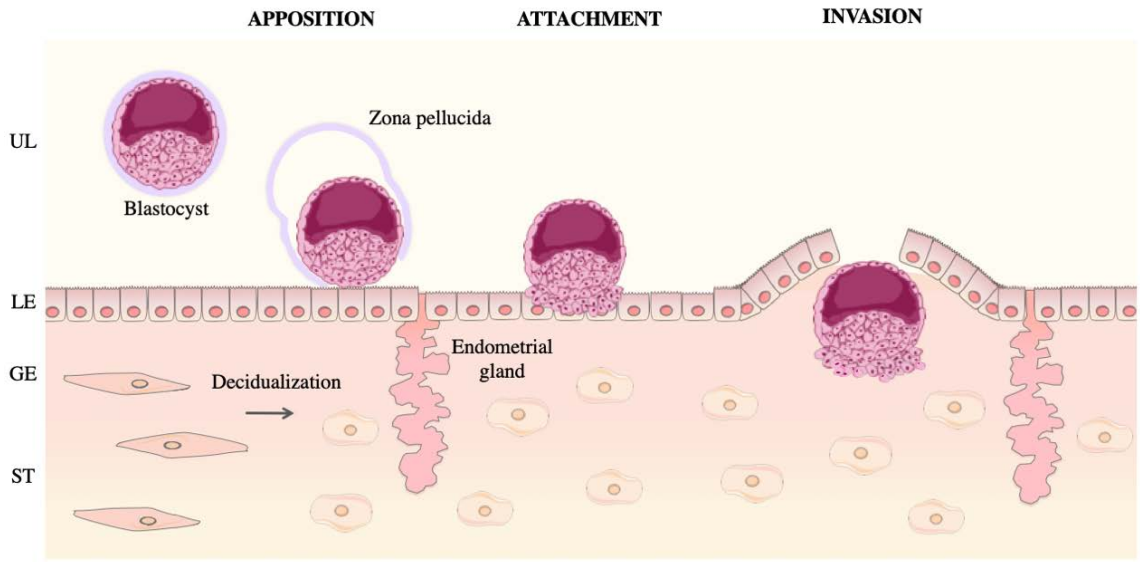

Figure 7. **Simplified figure representing the main events involved in human implantation.** Upon fertilization, the human embryo is transported through the Fallopian tube and arrives to the uterine cavity around day 5 after fertilization. It orients the inner cell mass towards the luminal epithelium and hatches from the zona pellucida. Around day 7, the embryo establishes a weak contact with the endometrium (apposition), followed by a stronger interaction (attachment) via the polar trophectoderm and will eventually invade the underlying glandular epithelium and the decidualized stromal compartment. UL: uterine lumen; LE: luminal epithelium; GE: glandular epithelium; ST: stroma.

9. Approaches to study human implantation

Although the process of implantation has been widely studied and the cellular events have been, overall, well defined, the specific molecules and regulatory networks directing implantation still need further research. For ethical and practical reasons, it is not possible to study human implantation *in vivo*. Most of the information about the implantation process has been obtained from animal (both *in vivo* and *in vitro*) and human *in vitro* studies, as discussed below. However, all these systems represent the *in vivo* situation to a certain extent and the results must be extrapolated with caution.

9.1 Animal models

Implantation is a species-specific process; however, some steps are similar and animal studies allow getting clues about how human implantation is regulated.

9.1.1 Mice

Among the wide range of species in which implantation has been evaluated, mice provided most of the current knowledge about this process at the molecular level. The main advantage of using murine models is the easy animal handling and the great knowledge about their genetics. Both human and mice are characterized by hemochorial placentation. Nevertheless, the mechanisms of implantation between mice and human are different in several aspects. Implantation in mice occurs inside crypts, which are structures surrounding the blastocyst after attachment. These crypts are formed through an eccentric mechanism of epithelial invagination that is subsequently shed by apoptosis, while implantation in humans follows an interstitial mechanism of epithelial breaching and stromal invasion (Lee and DeMayo, 2004; Wang and Dey, 2006). The timing and mechanisms of attachment are also different; in mice, apposition occurs on day 4, with the blastocyst orienting the mural trophectoderm (area of trophectoderm located on the opposite and furthest site from the ICM) towards the epithelium. In human, apposition occurs at day 6-7 and it is the polar trophectoderm which orients towards the epithelium (Cha, Sun and Dey, 2012). Additionally, the decidual response in mice is not spontaneous but elicited by the blastocyst during apposition to the luminal epithelium; however, decidualization is intrinsic to uterine stromal cells and can be mechanically stimulated (Wang and Dey, 2006). The rapid events during the first stages do not make the murine a good model for early implantation. By contrast, it is a good model to study the mechanisms of decidualization and the signalling between the endometrium and the embryo (Carson et al., 2000; Lee and DeMayo, 2004).

9.1.2 Guinea pigs

These rodents share some similarities with human regarding implantation, as it is interstitial rather than eccentric. The blastocyst forms a cone at the opposite side of the ICM, which is mainly composed by syncytial trophoblast. The blastocyst breaches the epithelium and the basal layer, penetrating into the stromal compartment while hatching from the zona pellucida. Once blastocyst is embedded within the stroma, decidualization occurs. Their implantation mechanism makes them a more suitable model for studying apposition and attachment, although they are more difficult to manage than mice due to their longer estrous cycle and not so evident implantation sites (Carson et al., 2000).

9.1.3 Rabbits

Rabbit blastocyst first adheres to the apical ends of the epithelial cells to subsequently fuse with them. This well documented attachment mechanism is useful as a model to study cell-cell communication and fusion during early implantation (Carson et al., 2000).

9.1.4 Domestic animals

The relevance of studying implantation in domestic animals such as pigs, cows, sheep and horses goes beyond the extrapolation of conclusions to the human process. Important events such as conceptus elongation and epitheliochorial placentation differ from those in human, but some characteristics make it worth to develop domestic animal models. For instance, pigs and sheep are good candidates to study early stages of implantation, as they share extended apposition and attachment phases (Lee and DeMayo, 2004). Implantation is superficial in pigs, with absence of epithelial penetration by the trophoblast. In sheep and cows, some binucleate trophoblast cells fuse with uterine luminal epithelial cells and form placentomes, which participate in gas and micronutrient exchange through the placenta (Carson et al., 2000; Lee and DeMayo, 2004). In the case of horses, implantation is mostly non-invasive, with development of apical–apical union between trophoblast and uterine epithelial cells. A unique process of placentation involves a specialized belt of trophectoderm cells (chorionic girdle) surrounding the conceptus. The binucleate girdle cells are intimately associated with the endometrium; they migrate through the uterine luminal epithelium, the basal lamina and the stroma and produce equine chorionic gonadotropin (Bowen and Burghardt, 2000). Dogs and cats present central implantation with isolated plaques of syncytial trophoblast that invade the luminal epithelium, which is subsequently eliminated in the area where the placental band is formed. The syncytium penetrates the epithelial basal lamina and surround the maternal vessels to remodel them (Carson et al., 2000). They can be a good model to study syncytial invasion.

9.1.5 Non-human primates

As opposed to other animals, the most studied non-human primate species (macaque, marmoset, baboon and rhesus monkey) have similar mechanisms for trophoblast invasion to the human. The syncytial trophoblast that breaches the luminal epithelium is first formed in the polar pole, near the ICM. Therefore, they are a suitable model for the later phases of implantation. The use of non-human primate models is limited by the low fecundity and difficult determination of early pregnancy in most species, with exception of marmosets and rhesus monkeys. In these two species,

epithelial breaching takes several days and early pregnancy can be assessed by circulating levels of progesterone. These features make marmosets and rhesus monkeys good models to study early implantation.

A large, spreading implantation site is formed while the blastocyst remains superficial; it is composed of CTs and SCTs and this period is known as the trophoblastic plate stage. After it, the connected lacunae are formed and eventually filled with maternal blood. Studies in macaque have shown that this connection between the maternal circulation and the trophoblast-lined lacunae is regulated by the SCT, which penetrates the superficial endothelium and reaches the maternal vasculature. The macaque is, therefore, a good animal model for studying late implantation and placentation (Lee and DeMayo, 2004).

9.2 *In vitro* models

Many studies have tried to fill the gap of knowledge regarding the molecular regulation of human implantation using *in vitro* systems. Combined with current molecular techniques including "omics" (e.g. transcriptomics and proteomics), these customized systems allow for multiple possibilities and overcome the limitation of extrapolating results from other species. In the context of implantation, molecular techniques have been used to characterize the embryo and the endometrium in a unilateral manner. Many studies reporting the transcriptional and proteomic profiles of the receptive endometrium and pre-implantation embryo have appeared in the last decade, as well as some characterizing their secretory products (Haouzi et al., 2011; Altmae et al., 2012; Hood et al., 2015; Durruthy-Durruthy et al., 2016; Koot et al., 2016; Diaz-Gimeno et al., 2017; Giacomini et al., 2017; Enciso et al., 2018; Sebastian-Leon et al., 2018; Stirparo et al., 2018). *In vitro* models have extended this picture focusing on specific embryo- or endometrium-derived signals and their response during the embryo-endometrium interaction. Additionally, the possibility of studying both elements and several steps during implantation compared to the static snapshots obtained from molecular unilateral studies adds important value. *In vitro* models also allow for studying the activity of drugs of interest, focusing on their specific metabolic and genetic effects otherwise very difficult to assess. Nevertheless, the extrapolation of the results needs caution due to the intrinsic differences between *in vitro* and *in vivo* biological processes.

Overall, *in vitro* models are composed by an element representing the blastocyst (human or mice blastocysts, primary trophoblast spheroids or explants and trophoblast cell lines) and an element representing the endometrium (endometrial explants, primary endometrial epithelial cells, endometrial epithelial cell lines, primary endometrial stromal cells and endometrial stromal cell

lines). Such models focus on the different phases of the implantation process, i.e. apposition, attachment and invasion, introducing more or less elements to simulate the *in vivo* environment. A wide variety of *in vitro* models can be designed, ranging from co-cultured single cell layers to sophisticated 3-D multi-layered systems:

9.2.1 Monolayer co-culture systems

The simplest *in vitro* models comprise an embryo-like structure, usually spheroid shaped, co-cultured on a monolayer of endometrial cells. This approach is useful to study the first stages of apposition and attachment, where the embryo establishes the first cell-cell contacts with the uterine epithelial barrier. One of the first studies using an *in vitro* model described the embryo-endometrium interactions by electron microscopy. This system included IVF embryos co-cultured with monolayers of endometrial epithelial cells, which were isolated from endometrial biopsies at the time of ovulation (Lindenberg, Nielsen and Lenz, 1985). Later studies have employed this approach aiming to reveal the molecular regulation that the embryo induces on the epithelial compartment. Long lists of embryo-regulated candidates at the gene expression and protein levels appeared, including chemokine receptors (e.g. *CXCR1*, *CXCR4*, *CCR5* and *CCR2B*) (Dominguez et al., 2003), integrins (e.g. integrins beta 3, alpha 4, and alpha 1) (Simon et al., 1997), chemokines (e.g. IL-8, IL-1) (Caballero-Campo et al., 2002; Gonzalez et al., 2003), hormones (e.g. leptin) (Gonzalez et al., 2000; Gonzalez et al., 2003) and cell adhesion molecules (e.g. MUC-1) (Meseguer et al., 2001).

Embryo-epithelium co-cultures were also investigated in the context of ART treatments. With the aim of improving *in vitro* embryo development, day 2 embryos were co-cultured with autologous epithelial cell monolayers until the blastocyst stage, when they were transferred to the uterus (Simon et al., 1999). A follow-up study from the same group concluded that co-culture is only effective in patients with implantation failure undergoing oocyte donation but not IVF patients with autologous cycles (Rubio et al., 2000). However, increased blastocyst and implantation rates have also been reported in the IVF population (Mercader et al., 2003). Although this practice seems to be safe, the outcomes are still controversial and its use is limited.

Culturing epithelial cells is technically challenging and the isolation of both glandular and luminal epithelial cells is even more difficult. The vast majority of the studies employing primary epithelial cells mix both compartments and fail to represent the correct structure of the tissue. An alternative to overcome these limitations is the use of endometrial epithelial cell lines, which will be detailed below. However, there are a large number of publications in the literature employing *in vitro* co-

culture systems of embryos or embryo-like surrogates with primary stromal cells. This is mainly due to the easier technical handling of stromal *vs*. epithelial cells an also after finding such a relevant role of decidualization in the implantation process. Such models have provided much information, e.g. about the morphological changes and ligand-receptor interactions during invasion (Carver et al., 2003), the role of GTPases, histone modifications and androgen signalling in stromal migration and remodelling (Grewal et al., 2008; Grewal et al., 2010; Estella et al., 2012; Wongwananuruk et al., 2016) and the stromal derived paracrine signalling regulating trophoblast invasion (Gonzalez et al., 2011). Popovici et al. studied the stromal gene expression profile after the interaction with the trophoblast by the co-culture of trophoblast explants on non-decidualized primary stromal cells. Using bioinformatic functional analysis, the study also showed the main pathways that were influenced by the co-culture, from which they highlighted inflammation, immune response and haematological and developmental processes (Popovici et al., 2006). Co-culture *in vitro* studies have revealed unique properties of decidual cells, changing the traditional concept that the endometrium was a passive player in the implantation process. These properties include the ability of the decidual cells to migrate in response to the trophoblast and to give specific transcriptional and secretory responses dependent on embryo viability (Gellersen et al., 2010; Teklenburg et al., 2010; Salker et al., 2012; Weimar et al., 2012; Gellersen et al., 2013; Brosens et al., 2014).

In vitro models involving the interaction between the embryo and the stromal compartment mimic the stage of invasion, but most of them lack the previous contact between the embryo and the luminal epithelium. A recent study has demonstrated that apposition to epithelial cells is needed to activate mouse blastocysts, allowing them to breach the epithelial barrier and go on to invade the underlying stroma (Ruane et al., 2017). Overall, simple monolayer co-culture systems cannot represent the interactions between the different layers of the endometrium. Although the tissue is a continuum, the luminal and glandular epithelia and the stroma have different transcriptional and protein profiles which are, indeed, interdependent (Evron, Goldman and Shalev, 2011; Evans et al., 2014). Cell-cell and cell-ECM interactions as well as paracrine signalling are missing and the tissue polarization is lost while growing on flat plastic surfaces. These systems also lack other components of the implantation environment, i.e. endothelial, immune and stem cells.

9.2.2 3-D co-culture systems

More complex and sophisticated *in vitro* models are the multi-layered systems, usually comprising embryos or embryo-like elements on top of an ECM or epithelial surface growing on a monolayer of stromal cells. The more elements they include the more attractive these systems are, but they also become very difficult to handle and to control. One of the firsts 3-D models used epithelial cells embedded onto a Matrigel matrix with an underlying monolayer of stromal cells; the model succeeded to represent the architecture of the endometrial implantation site and allowed its characterization by scanning electro-microscopy (Bentin-Ley et al., 1999; Bentin-Ley et al., 2000). Other studies have focused on the embryonic regulation of specific mechanisms such as apoptosis (Galan et al., 2000) or on providing a more comprehensive understanding of the three phases, i.e. apposition, attachment and invasion, during implantation (Wang et al., 2012). 3-D *in vitro* models of implantation have also been employed to test contraceptive drugs (Petersen et al., 2005; Lalitkumar et al., 2007; Meng et al., 2009; Berger et al., 2015; Boggavarapu et al., 2016) and to study the interactions between the different cell types (Arnold et al., 2001; Pierro et al., 2001; Blauer et al., 2005).

Apparently, tissue explants could provide good models, as all the layers are included and the integrity and structure of the endometrium is maintained. However, the high levels of necrosis, lack of polarization and their limited lifespan make them technically inconvenient (Landgren et al., 1996). Recently, novel organoid systems have been developed that mimic the three-dimensional structure and physiology of both the trophoblast and the endometrium (Boretto et al., 2017; Turco et al., 2017). Both endometrial and trophoblast organoid systems are long-term, hormone responsive and recapitulate morphological and functional features of the tissue of origin (Boretto et al., 2017; Turco et al., 2017; Haider et al., 2018; Turco et al., 2018). Undoubtedly, these systems will be used in the context of embryo implantation and early pregnancy, providing promising tools to understand these processes in healthy and pathological conditions.

9.3 Cell lines

As human embryos for research purposes are very scarce and endometrial biopsies can be difficult to obtain, a large number of studies have co-cultured mouse embryos or embryo-like spheroids with endometrial epithelial cell lines (Hohn, Linke and Denker, 2000; Heneweer et al., 2003; Heneweer et al., 2005; Mo et al., 2006; Uchida et al., 2007; Aboussahoud et al., 2010; Ho et al., 2012; Holmberg et al., 2012; Xiong et al., 2012). Cell lines usually come from carcinoma origin and are already committed matured cells, which in the case of the trophoblast represent a later

developmental stage than embryo cells during *in vivo* implantation. Although the extrapolation of results warrants caution, some positive aspects encourage the use of established cell lines for implantation *in vitro* models. For instance, gene and protein expressions in primary endometrial cells are conditioned by the endometrial dating at the moment of the biopsy. Experimental easiness, reproducibility and genetic homogeneity are also advantages.

9.3.1 Trophoblast cell lines

The selection of the cell lines to devise an *in vitro* model is important and depends on the phase of the process that is simulated and the technical approach that is used. For instance, to study attachment and early invasion most trophoblast cell lines are suitable, but the options for invasion assays involving syncytialization are almost limited to the BeWo cell line (Hannan et al., 2010). If targeted molecular approaches are used, it is advisable to check the mRNA expression of essential mediators and receptors for the correspondent processes in each cell line, if it is available from previous studies.

Trophoblast cell lines share the epithelial marker Keratin 7 (KRT7), which is expressed by trophectoderm, SCTs, CTs and EVts as well as by glandular epithelial cells but not by other cell types in the first trimester maternal-fetal interface (Maldonado-Estrada et al., 2004). They can be obtained from normal placenta or embryonic carcinomas differentiated to trophoblast, but most of them are from choriocarcinoma origin (King, Thomas and Bischof, 2000). Currently available trophoblast cell lines include HTR-8/SVneo (from first trimester villous explants), JEG-3 (from choriocarcinoma explants), JAR (from gestational choriocarcinoma), BeWo (from choriocarcinoma), SGHPL-4 (from primary extravillous trophoblast) and AC1M-88 (fusion of JEG-3 and term trophoblast). Apart from HTR-8/SVneo and BeWo, which present both EVT and CT phenotype, the other cell lines present an EVT phenotype (Hannan et al., 2010).

The cell line JEG-3 is a common choice to study implantation in the literature (Kliman, Feinberg and Haimowitz, 1990; Zygmunt et al., 1998; Hohn, Linke and Denker, 2000; Karmakar, Dhar and Das, 2004; Godbole et al., 2011; Estella et al., 2012; Liu et al., 2013; Bohlmann et al., 2014; Buck et al., 2015; Hakam et al., 2017). Since first established in 1971 (Kohler and Bridson, 1971), JEG-3 cell line has been extensively characterized at the cytogenetic, physiological and transcriptional levels (Frank et al., 2000; Burleigh et al., 2007; Bilban et al., 2010; Rothbauer et al., 2017). JEG-3 cells constitutively express *HLAG* mRNA, as well as hCG and hCGR (Handschuh et al., 2007). McConkey et al. have provided evidences of syncytialization of JEG-3 cells while grown in 3-D systems, which was concomitant with transcriptional profiles and secretory activities similar to

those from primary syncytiotrophoblasts (McConkey et al., 2016). Additionally, JEG-3 cells present specific characteristics that closely resemble normal primary trophoblast cells, such as hCG production, glucose transport and cell barrier integrity (Huang, Luthi et al., 2016). Altogether, JEG-3 cell line can be trustingly chosen for *in vitro* studies of implantation and early pregnancy.

9.3.2 Endometrial cell lines

As mentioned before, the luminal and glandular epithelium as well as the stromal compartment undergo critical phenotypical changes along the menstrual cycle. To correctly represent each compartment in a certain moment of the cycle, it is needed to choose the correct cell line from those available. Since epithelial primary culture is technically challenging, there are several immortalized epithelial cell lines commercially available. Among them, some represent the luminal epithelium, other the glandular epithelium and some present mixed characteristics of both. The most popular epithelial cell lines currently available are: ECC-1 (from adenocarcinoma, luminal phenotype), Ishikawa (from adenocarcinoma, luminal and glandular phenotype), HEC-1-A (from adenocarcinoma, luminal and glandular phenotype), HEC-1-B (from adenocarcinoma, luminal and glandular phenotype) and RL95-2 (from moderately differentiated adenosquamous carcinoma, glandular phenotype) (Hannan et al., 2010; Buck et al., 2015). Commercially available stromal cell lines include T hESCs (from non-malignant myoma), SHT290 (from non-pathological uterine biopsies), KC02-44D (from leiomyoma) and St-T1b (from non-pathological uterine biopsies) (Krikun et al., 2004; Barbier et al., 2005; Samalecos et al., 2009; Yuhki et al., 2011).

Due to their functional characteristics, epithelial cells are usually referred as model for receptive or non-receptive epithelium. This classification is based on their surface adhesive properties, resembling the receptive and refractory phases of the endometrial cycle. The most widely used cell lines for modelling the receptive epithelium are Ishikawa and RL95-2; by contrast, HEC-1-A is the most common choice for non-receptive epithelium due its low adhesiveness. Ishikawa has the advantage of presenting both luminal and glandular phenotypes, making it very versatile. It was established on 1985 (Nishida et al., 1985) and it has been broadly used in adhesion assays as well as to simulate normal endometrial function (Singh et al., 2010; Schaefer et al., 2010; Berger et al., 2015; Ruane et al., 2017; Aberkane et al., 2018). Ishikawa cells are hormonally responsive and express a wide repertoire of molecules involved in endometrial receptivity and embryo attachment (e.g. cell adhesion molecules, cytokines and ECM molecules as well as estrogen, progesterone, androgen and luteinizing hormone receptors) (Lessey et al., 1996; Heneweer et al., 2005; Hannan et al., 2010). After treatment with estrogen, Ishikawa cells increase proliferation, while

progesterone causes the opposite effect (Croxtall, Elder and White, 1990). As mentioned before, HEC-1-A is a usual model for the refractory epithelium (Dominguez et al., 2003; Harduf, Goldman and Shalev, 2007, 2009; Dominguez et al., 2010; Wang et al., 2012; Wang et al., 2013). The poorly adhesive HEC-1-A cell line shares with Ishikawa the expression of estrogen and progesterone receptors and a variety of molecules also present in receptive cell lines (e.g. TGF, VEGF and IGFBP protein families) (Kuramoto, Tamura and Notake, 1972; Kurarmoto, Hamano and Imai, 2002). Some studies have compared receptive and non-receptive cell lines focusing on molecules that could be responsible for their phenotypes such as metalloproteinases, genes involved in estrogen biosynthesis and metabolism as well as genes targeted by steroid hormone receptors (Dominguez et al., 2003; Tamm et al., 2009; Dominguez et al., 2010; Schropfer et al., 2010; Hevir-Kene and Rizner, 2015). However, the molecular programmes that determine receptive or non-receptive status in these cell lines are not fully unravelled.

AIMS

The main aim of this thesis was to gain insights into the molecular mechanisms regulating endometrial receptivity and human implantation and the effect of microbial environment on these events. Specifically, we aimed to accomplish the following:

1) To devise an *in vitro* co-culture system that allowed for dissecting the transcriptional responses of the trophoblast and the endometrial epithelium (receptive *vs*. non-receptive) upon their interaction.

2) To explore the sequence of early transcriptional events preceding successful implantation in a compartment- and time-dependent manner.

3) To identify candidates which potentially regulate the successful trophoblast-epithelium interaction during implantation.

4) To determine the relationship between the vaginal microbiota profile at the time of embryo transfer and reproductive outcomes in women undergoing IVF.

RESULTS

Chapter 1. Transcriptomic analysis of trophoblast interactions with receptive *vs*. non-receptive endometrial epithelium: an *in vitro* model of human implantation

Reproductive biology has not escaped the "omics" revolution; a large number of studies have researched the transcriptional profiles of the embryo and the endometrium during last decades, many of them focusing on deciphering the transcriptional signature of endometrial receptivity. Indeed, impaired endometrial receptivity is a major limiting factor of IVF success when high quality embryos fail to implant (Miller et al., 2012). The contribution of this factor to defective early embryo-epithelium crosstalk and the specific molecular mechanisms underlying it are intriguing but still unanswered questions. Previous studies have tried to identify the genes involved in the embryo-epithelium interaction by computational analysis of the individual transcriptional profiles of blastocysts and the receptive endometrium during the WOI (Haouzi et al., 2011; Altmae et al., 2012). Surprisingly, very few publications have used "omics" techniques to study the trophoblast-epithelium interaction in a compartment specific manner, and most have focused on the stroma or on animal models (Popovici et al., 2006; Moreno-Moya et al., 2015; Huang et al., 2018).

To overcome this limitation, we present here an *in vitro* model for trophoblast attachment to receptive and non-receptive epithelia. We used the trophoblast cell line JEG-3 as a model of trophoblast, which was modified to express GFP. The receptive and non-receptive epithelial substrates models were the Ishikawa and HEC-1-A cell lines, respectively. GFP fluorescence of the trophoblast allowed for an efficient separation of both compartments by FACS. Through a transcriptomic analysis by RNA-seq, we studied the bulk transcriptional changes occurring in the trophoblast and the epithelium after 48 hours of interaction in a 2-D *in vitro* system.

The results included in **Chapter 1** are part of the manuscript "**Transcriptomic analysis of the interaction of choriocarcinoma spheroids with receptive *vs*. non-receptive endometrial epithelium cell lines: an *in vitro* model for human implantation**" (Paula Vergaro, M.Sc., Gustavo Tiscornia, Ph.D., Amelia Rodríguez, Ph.D , Josep Santaló, Ph.D , Rita Vassena, D.V.M. Ph.D), which has been published in the *Journal of Assisted Reproduction and Genetics* (DOI: 10.1007/s10815-019-01442-9).

1. Abstract

Purpose: Several *in vitro* systems have been reported to model human implantation; however, the molecular dynamics of the trophoblast *vs*. the epithelial substrate during attachment have not been described. We have established an *in vitro* model which allowed us to dissect the transcriptional responses of the trophoblast and the receptive *vs*. non-receptive epithelium after co-culture.

Methods: We established an *in vitro* system based on co-culture of a) immortalized cells representing receptive (Ishikawa) or non-receptive (HEC-1-A) endometrial epithelium with b) spheroids of a trophoblastic cell line (JEG-3) modified to express GFP. After 48 hours of co-culture, GFP+ (trophoblast cells) and GFP- cell fractions (receptive or non-receptive epithelial cells) were isolated by fluorescence-activated flow cytometry (FACS) and subjected to RNA-seq profiling and gene set enrichment analysis (GSEA).

Results: Compared to HEC-1-A, the trophoblast challenge to Ishikawa cells differentially regulated the expression of 495 genes, which mainly involved cell adhesion and extracellular matrix (ECM) molecules. GSEA revealed enrichment of pathways related to cell division, cell cycle regulation and metabolism in the Ishikawa substrate. Comparing the gene expression profile of trophoblast spheroids revealed that 1877 and 323 genes were up-regulated or down-regulated when co-cultured on Ishikawa substrates (compared to HEC-1-A), respectively. Pathways favorable to development, including tissue remodelling, organogenesis and angiogenesis were enhanced in the trophoblast compartment after co-culture of spheroids with receptive epithelium. By contrast, the co-culture with less receptive epithelium enriched pathways mainly related to trophoblast cell proliferation and cell cycle regulation.

Conclusions: Endometrial receptivity requires a transcriptional signature that determines the trophoblast response and drives attachment.

Funding: This work was supported by intramural funding of Clínica EUGIN and by the Secretary for Universities and Research of the Ministry of Economy and Knowledge of the Government of Catalonia (GENCAT 2015 DI 050).

Keywords: Implantation; attachment; endometrial receptivity; transcriptomics

2. Introduction

Despite the efforts to develop *in vivo* and *in vitro* approaches to study human implantation, the molecular mechanisms directing this process are still poorly understood. Successful implantation requires a highly orchestrated process dependent on correct coordination of the molecular crosstalk between the different cellular compartments involved, namely, the trophoblast, and both the epithelium and the stroma of the endometrium (Sharkey and Macklon, 2013). The initial interaction between the embryo and the epithelium is supported by molecules secreted from both compartments into the uterine fluid (Hannan et al., 2006; Hannan et al., 2011; Greening et al., 2016). Initially, the blastocyst establishes a reversible first contact with the luminal epithelial surface (apposition). This is followed by the establishment of a stronger, irreversible interaction (attachment). After the initial interaction with, and breaching of, the luminal epithelium, the trophoblast must invade the underlying stromal compartment to establish a pregnancy (Wang and Dey, 2006). Studies focused on the stroma have highlighted its relevance to the implantation success; this is mainly due to the unique activity of decidualized cells, which act as a biosensor of embryo quality and trigger a transient pro-inflammatory response linked to endometrial receptivity (Teklenburg et al., 2010; Salker et al., 2012; Weimar et al., 2012). How these processes are controlled in the cycling endometrium is still unknown, although it has been proposed that uterine NK cells and the decidualization-associated senescence in endometrial tissue are responsible for endometrial receptivity and remodelling (Brighton et al., 2017). Knowledge of the molecular mechanisms governing the initial attachment of the embryo to the epithelial surface is more limited. Using an *in vitro* model for attachment between mouse blastocysts and carcinoma-derived epithelial cells, Ruane et al. have demonstrated that endometrial molecular signals critically regulate the trophoblast differentiation needed for breaching and invasion (Ruane et al., 2017).

The study of implantation is essential to understand and characterize implantation failure, a frequent cause of human infertility (Polanski et al., 2014). Impaired endometrial receptivity is an important limiting factor of IVF success when high quality embryos are transferred (Miller et al., 2012). Since it is not possible to study implantation *in vivo*, the biological mechanisms underpinning this process are difficult to access; further, *in vitro* assays are hampered by low availability of human embryos and fresh endometrial tissue to establish primary cultures. A number of publications have approached the study of implantation using knock-out mice models (as reviewed in Namiki, Ito and Kashiwazaki, 2018). However, the mechanistic details of implantation are species-specific and limit the usefulness of mice studies to describe human

implantation (Wang and Dey, 2006; Melford, Taylor and Konje, 2014). In particular, the rapid sequence of implantation events and the differences with the human mechanisms of attachment, invasion and placentation do not make the mouse a good model for studying early implantation (Cha, Sun and Dey, 2012; Melford, Taylor and Konje, 2014; Aplin and Ruane, 2017). A common approach to overcome these limitations is the use of cell lines. The epithelial cell lines Ishikawa (receptive) and HEC-1-A (minimally receptive) have been widely used to model different aspects of human implantation due to their differential response to embryo attachment (Dominguez et al., 2003; Heneweer et al., 2005; Uchida et al., 2007; Singh et al., 2010; Tamm-Rosenstein et al., 2013). *In vitro* systems have allowed the study of different stages of implantation by co-culturing both compartments to detect specific molecules at the mRNA transcript or protein levels (Singh et al., 2010; Kang et al., 2014), to test the effect of candidate drugs (Uchida et al., 2007; Berger et al., 2015; Boggavarapu et al., 2016) or to describe morphological changes during implantation (Carver et al., 2003). Importantly, most *in vitro* approaches employed to date analyze the response of the whole co-culture system, without dissecting the response of each compartment. To overcome this limitation, we have devised a system to dissect the transcriptional dynamics of the trophoblast and the epithelium during the attachment and initial invasion. Using the cell line JEG-3 as a proxy for the trophoblast, and the cell lines Ishikawa and HEC-1-A as receptive and non-receptive endometrial epithelia, respectively, our *in vitro* model allows for an efficient separation of both compartments by fluorescence-activated cell sorting (FACS). Through RNA-seq transcriptomic analysis, we quantified the transcriptional changes occurring in the trophoblast and the epithelium (receptive *vs*. minimally receptive) after 48 hours of co-culture in a 2-D *in vitro* system.

3. Materials and methods

Cell culture

The human endometrial adenocarcinoma cell lines Ishikawa (ECACC 99040201) and HEC-1-A (ATCC HTB-112) and the human trophoblast choriocarcinoma cell line JEG-3 (ATCC HTB-36) were cultured as indicated by the provider. Ishikawa cells were maintained in MEM (MEM α, nucleosides, no phenol red) supplemented with 5% fetal bovine serum, 10 mM of non-essential amino acids (MEM Non-Essential Amino Acids Solution) and 100 mg/ml streptomycin and 100 IU/ml penicillin (PenStrep). HEC-1-A were maintained in McCoy´s 5A (McCoy's 5A (Modified)

Medium, GlutaMAX™ Supplement) supplemented with 10% fetal bovine serum and 100 mg/ml streptomycin and 100 IU/ml penicillin (PenStrep). JEG-3 cells were cultured in DMEM (DMEM, high glucose, GlutaMAX™ supplement) containing 10% fetal bovine serum, 1 mM sodium pyruvate and 100 mg/ml streptomycin and 100 IU/ml penicillin (PenStrep). All cell lines were kept at 37ºC and media was changed every other day. Unless otherwise indicated, all reagents were purchased from Gibco, Thermo Fisher Scientific, USA.

Generation of fluorescent JEG-3 spheroids

Recombinant lentiviral particles (third generation self-inactivating vector system) expressing GFP from a PGK promoter were produced as described (Tiscornia, Singer and Verma, 2006) and used to transduce the JEG-3 trophoblast cells. Briefly, trophoblast cells were plated on 12-well plates and cultured to 70% confluence. Aliquots of lentiviral particles were diluted to achieve an estimated multiplicity of infection (MOI) of 10 in a final volume of 500 µl. After 24 hours, cells were rinsed with Dulbecco's Phosphate-Buffered Saline (DPBS without calcium or magnesium) and fresh medium was added. Cells were cultured and passaged three times to avoid lentivirus carryover. Trophoblast cells with the highest GFP levels were sorted and collected for further culture by fluorescence-activated cell sorting (FACS). Cell suspensions of GFP positive JEG-3 cells were diluted to a final concentration of $3x10^4$ cells/ml. 100 µl of the cell suspension (3000 cells) were seeded in U-bottom ultra-low attachment 96-well plates (Corning, NY, USA). Plates were centrifuged at room temperature during 10 min at 250 x g and cultured for 48 hours at 37ºC and 5% CO_2 generating fluorescent spheroids of 250-300 µM (10000 cells).

***In vitro* attachment assay**

An *in vitro* model of implantation was established to mimic the molecular changes during attachment and initial invasion. The cell line Ishikawa was used as a model of receptive epithelium, while the cell line HEC-1-A represented the non-receptive epithelium. Both Ishikawa and HEC-1-A were cultured in 96-well plates (Nunc, Thermo Fisher Scientific, USA) until the cells reached confluence. GFP positive JEG-3 spheroids formed by around 10000 cells were added to each 96-well (one spheroid per well). Our experimental design (see **Figure 1**) used pools of small wells containing a single spheroid to increase trophoblast to epithelium ratio, and optimize the detection of transcriptional changes induced by the interaction in those areas of the substrate far from the spheroid. Co-cultures were maintained for 48 hours in 1:1 mix of MEM/DMEM in case of the Ishikawa-JEG-3 co-culture and 1:1 mix of McCoy´s 5A/DMEM in case of the HEC-1-A-JEG-3

co-culture. In parallel, 96-well plates of confluent Ishikawa, HEC-1-A and JEG-3 spheroids cultured without addition of any other cell type for 48 hours were used as experimental controls for the effect of time of co-culture. After 48 hours, all the monocultures and co-cultures were washed with DPBS and cells were harvested from the 96-well plates using TrypLE™ Express Enzyme and pooled before cell sorting. All reagents were purchased from Gibco, Thermo Fisher Scientific, USA. Co-culture experiments were performed three times as independent biological triplicates.

Cell sorting and RNA extraction

Fluorescence-activated flow cytometry (FACS; BD FACS Aria Fusion II cell sorter (BD Biosciences, USA) was used to separate GFP positive trophoblast cells from unlabelled epithelial substrates after co-culture. The following cell fractions were collected: Ishikawa control (I-c), HEC-1-A control (H-c), JEG-3 spheroids control (S-c), Ishikawa substrates co-cultured with JEG-3 spheroids (I-co-S), HEC-1-A substrates co-cultured with JEG-3 spheroids (H-co-S), JEG-3 spheroids co-cultured with Ishikawa substrates (S-co-I) and JEG-3 spheroids co-cultured with HEC-1-A substrates (S-co-H) (**Figure 1**). To minimize RNA degradation, all handling procedures were performed on ice; the cytometer chamber was cooled to 4ºC before cell sorting. Cell suspensions were filtered through a 70 µm mesh to eliminate cellular aggregates before sorting. 100 µm sorter nozzles were used to minimize clog formation during cell sorting. Dead cells were identified by diamidino-2-phenylindole (DAPI) staining and excluded from the sorted populations. GFP positive and GFP negative fractions were collected in 50 µl of DPBS without calcium or magnesium on ice, centrifuged and cell pellets were stored at -20ºC until processed. RNA from each fraction of the three independent experiments was isolated using the RNeasy Mini Kit (Qiagen N. V., Netherlands) following manufacturer´s recommendations and eluted in 30 µl nuclease free water. RNA was purified using RNase-Free DNase Set (Qiagen N. V., Netherlands) and concentration was measured by fluorometric quantitation (QuBit, Thermo Fisher Scientific, USA). RNA integrity number (RIN) was 8.5 to 10 in all samples as determined by Bioanalyzer 2100 System (Agilent Technologies, USA).

cDNA Library Preparation and RNA-seq

A total of 21 RNA samples (3 replicates of each of the 7 experimental cell populations) were used for cDNA library preparation and RNA-seq analysis. After performing the quality control of the 21 samples, polyA mRNA was isolated using NEBNext Poly(A) mRNA Magnetic Isolation

Module (New England Biolabs, USA) following the manufacturer's instructions. Once mRNA was purified, cDNA generation, End repair and Ligate Adaptor for Illumina were done using the kit NEBNext Ultra II RNA Library Prep for Illumina following the manufacturer's instructions. Samples were amplified with SYBR green to establish the minimum number of cycles required. During the amplification, each sample was labeled with a specific barcode using the NEBNext Multiplex Oligos kit for Illumina (Index Primers Set 1). Finally, three equimolar 7 sample pools were generated, and each pool was sequenced in a single 50 nt Single Read lane of an Illumina Hiseq 2500 system, getting more than 30 million reads per sample.

RNA-Seq data analysis

Reads were aligned to the hg19 version of the human genome with the STAR software v2.3.0e (Dobin et al., 2013) and default parameters. The aligned reads were binarized and sorted with sambamba v0.5.9 (http://lomereiter.github.io/sambamba/). Reads were imported to R (https://www.R-project.org/) with the inbuilt annotation in the Rsubread package (Liao, Smyth and Shi, 2013). Further annotations were downloaded from Biomart (Smedley et al., 2015) using the corresponding R package.

Differential expression was performed with DESeq2 (Love, Huber and Anders, 2014) with processing batch as covariate.

Enrichment analysis

Pathway enrichment was assessed through the pre-ranked version of Gene Set Enrichment Analysis (GSEA) (Subramanian et al., 2005). GSEA was applied to the ranking defined by the log2 Fold Change (log2FC) of the differential expression analysis using DESeq2. Gene sets for analyses belonged to the Gene Ontology (GO) (Ashburner et al., 2000) terms as collected in the GSEABase R package (Morgan, 2017), or to the Hallmark collection (Liberzon et al., 2015) after retrieval from the MsigDB (Liberzon et al., 2011). The significance cut-off for false discovery rate (FDR) was set at 0.1.

In order to assess the enrichment of genes showing significant interaction between HEC-1-A and Ishikawa when comparing co-cultured and non-co-cultured control fractions, we categorized genes with adjusted p-value for the interaction lower than 0.05 in the following four groups: larger effect (either positive or negative) in HEC-1-A than in Ishikawa (absolute value of the size estimate in Ishikawa lower than 0.25 and size estimate higher (lower) than 0.75 (-0.75) in HEC-1-A. Larger

effect (either positive or negative) in Ishikawa than in HEC-1-A (absolute value of the size estimate in HEC-1-A lower than 0.25 and size estimate higher (lower) than 0.75 (-0.75) in Ishikawa. We tested enrichment of these gene signatures in the Gene Ontology collections (Ashburner et al., 2000) and the Hallmarks gene sets from the Broad Institute (Liberzon et al., 2011). Gene sets were filtered for sizes larger than 10 and smaller than 2000. We used a hypergeometric test for statistical significance with Benjamin-Hochberg adjustment for multiple testing.

Statistical analysis

Linear regression and pairwise comparison were used to analyze differential gene expression between cell populations sorted by FACS. Statistical significance was set at an absolute log2 fold change (log2FC) ≥ 1 and a q-value of <0.05 (adjusted p-value <0.05 with Benjamin-Hochberg correction for multiple comparisons).

RNA-seq validation by qPCR

A molecular quantitative analysis was performed to confirm the expression patterns of selected genes among the same samples used in the RNA-seq. The validation was performed using 5 ng (in triplicate) of the cDNA libraries previously constructed in a final volume of 20µl. Gene expressions were quantified using 2x SsoAdvanced Universal SYBR Green Supermix (BioRad, Hercules, CA, USA) on a CFX Real-Time PCR platform (Bio-Rad, Hercules, CA, USA). The selected genes and their forward and reverse primer sequences (5′-3′) were the following: *TMEM255A* (ACCTGCTTCTGCTGTGACCT and TCTTGGCAACTGCTGACATC), *EREG* (CACAGTCGTCGGTTCCAC and CTCTGGATCCCCTGAGGT), *SPDYC* (TCAGCCTTCTGGAGGACAGT and CACCATGGCCAGGAGATACT), *CYP19A1* (GTGGACGTGTTGACCCTTCT and CACGATAGCACTTTCGTCCA), *CASC1* (GGTGGGATGCTGAAGGTAAA and AAAGGTGTCCAGGCTGAATG), *PROM1* (GCCACCGCTCTAGATACTGC and GCTTTTCCTATGCCAAACCA), *TGFA* (TTCCCACACTCAGTTCTGCTT and ACGTACCCAGAATGGCAGAC), *CDC20B* (GTAGTTGGGGCTCTGAGCTG and GGCTACCCGAACATCGTG) and *HPRT1* (TGACACTGGCAAAACAATGCA and GGTCCTTTTCACCAGCAAGCT). The final products were analyzed using the CFX Manager Software (Bio-Rad, Hercules, CA, USA). To select the most stable normalizers, the Integrated Cotton EST Database was used (Xie et al., 2011); *MAP4K4* and *TBP* were used as housekeeping genes, using the following forward and reverse primer sequences (5′-3′): CTTGGATGGTGTGTTCATGC and AGACCGAACAGAGGCAAAGA for

MAP4K4 and TATAATCCCAAGCGGTTTGC and GCTGGAAAACCCAACTTCTG for *TBP*. Gene expression data were calculated as the ratios between the gene expression values of the selected genes and the geometric average of *MAP4K4* and *TBP* expressions (Vandesompele et al., 2002). Amplification specificity was confirmed by analyzing the qPCR melting curves of the final products.

4. Results

Transcriptional changes induced by trophoblast-epithelium interaction

After 48 hours of co-culture, the spheroids attached firmly to the Ishikawa cells, flattened out and expanded radially on the substrate (**Figure 2a**). In contrast, after the interaction with the minimally receptive HEC-1-A cells, the trophoblast spheroids adhered to the monolayer but did not expand onto the substrate cells (**Figure 2b**). After co-culture, trophoblast and epithelial compartments (receptive Ishikawa or minimally receptive HEC-1-A) were isolated by FACS. The transcriptional changes of the sorted cell populations were individually analyzed by comprehensive RNA-seq profiling. GFP positive fractions corresponded to the co-cultured JEG-3 trophoblast spheroids or controls, while GFP negative cell populations corresponded to co-cultured Ishikawa or HEC-1-A, or their respective controls. RNA-seq data are available in the public database Gene Expression Omnibus (GEO) repository (accession GSE121790).

Sample clustering and quality control

Principal component analysis (PCA) was used to identify sample clustering and possible technical bias between experimental triplicates (**Supplementary Figure 1**). PCA clearly revealed distinctive expression patterns among sorted cell populations and clustering of experimental triplicates by sample group; First and second components (PC1 and PC2) accounted for 52.5% and 36.0% of sample variability, respectively.

Transcriptional dynamics of the epithelial substrates

Pairwise comparisons of transcriptome dynamics in both trophoblast spheroids and epithelial compartments were performed. In each of the 3 experimental replicates, a total of 7 gene expression datasets were generated from the cell fractions collected by FACS, including trophoblast or epithelial fractions after co-culture and their correspondent non-co-cultured

controls, as described in the materials and methods section and **Figure 1**. We found striking differences in gene expression profiles when comparing the control receptive *vs*. control non-receptive substrates: as many as 6628 genes were differentially expressed between I-c and H-c (3957 genes up-regulated and 2671 down-regulated in I-c as compared to H-c, respectively; **Figure 3a**, **Supplementary File S1**). After co-culture with spheroids (I-co-S), the receptive substrate (Ishikawa), showed 608 differentially expressed genes (as compared to I-c), of which 310 genes were up-regulated and 298 genes down-regulated (**Figure 3b**, **Supplementary File S2**). The top 10 differentially expressed genes of this set (ranked by absolute log2FC) are listed in **Figure 4**. Interestingly, the comparison between H-co-S and H-c yielded only 9 differentially expressed genes (5 genes up-regulated and 4 genes down-regulated in H-co-S, respectively; **Figure 3c**, **Supplementary File S3**). Three of these genes were also present in I-co-S *vs*. I-c dataset (*SYNGR3, CYP1A1* and *ANK1*) (**Figure 4**). Co-cultured epithelial Ishikawa and HEC-1-A substrates could not be compared directly, as their respective controls were different cell lines; however, when we performed an analysis of differential expression patterns between I-co-S and I-c as compared to the differential expression patterns between H-co-S and H-c, we found 495 genes which changed their expression patterns among both interaction pairs (**Supplementary File S4**).

Transcriptional dynamics of the trophoblast spheroids

Comparison of transcriptome dynamics in the trophoblast compartment after co-culture on Ishikawa (S-co-I) showed important differential gene expression when compared to non-co-cultured control (S-c): a total of 3976 genes were differentially expressed between S-co-I and S-c (3220 genes up-regulated and 756 genes down-regulated in S-co-I compared to S-c, respectively; **Figure 3d**, **Supplementary File S5**). Interestingly, fewer genes significantly changed their expression levels when the transcriptomic profile of S-co-H was compared with that of S-c (only 1038 genes showed differential expression, with 949 genes up-regulated and 89 genes down-regulated, respectively; **Figure 3e**, **Supplementary File S6**).

A direct comparison of JEG-3 spheroids after co-culture on Ishikawa or HEC-1-A (S-co-I *vs*. S-co-H), possible due to the fact that both compartments have the same control (S-c), showed 2200 differentially expressed genes (1877 genes up-regulated and 323 genes down-regulated in S-co-I *vs*. S-co-H, respectively; **Figure 3f**, **Supplementary File S7**). Some of these genes were also differentially expressed in I-co-S *vs.* I-c comparison (209, listed in **Supplementary File S8**, of which the top 10 differentially expressed genes are shown in **Figure 4**), and only two genes (*CYP1A1* and *TACSTD2*) were differentially expressed in H-co-S *vs*. H-c (**Figure 4**).

Enrichment analysis of the epithelial substrates

GSEA was applied to all gene set comparisons to reveal the biological pathways enriched in each group. GOBP and Broad Hallmarks annotations were used to classify functionally related genes over-represented in co-cultured GFP+ and GFP- cell fractions. Biological pathways over-represented in each gene set comparison are showed in **Tables I-V**. Compared to I-c, the pathways enriched in I-co-S were mostly related to spindle organization and cell cycle regulation (e.g. mitotic spindle organization, E2F targets and G2M checkpoint) (**Table I**). In contrast, only one pathway was significantly enriched in the comparison H-co-S *vs*. H-c (regulation of amino acid transport) (**Table II**). A hypergeometric test was used to perform gene enrichment analysis of epithelial substrates in both interactions (I-co-S and I-c *vs*. H-co-S and H-c). Of the four gene expression patterns included in this test, only one achieved statistical significance; it included those genes which were up-regulated in I-co-S *vs*. I-c and down-regulated or unchanged in H-co-S *vs*. H-c (**Table III**). The results suggested that the transcriptional changes in the receptive and non-receptive epithelium after the trophoblast challenge mainly involved pathways related to cell division and cell cycle regulation (e.g. nuclear division, chromosome segregation and metaphase/anaphase transition of mitotic cell cycle) as well as metabolism (i.e. cholesterol biosynthetic process, sterol biosynthetic process and cholesterol homeostasis).

Enrichment analysis of the trophoblast spheroids

The GSEA of the trophoblast spheroids showed involvement of a greater number of pathways than those detected in the epithelial compartments. In the S-co-I *vs*. S-co-H comparison, pathways over-represented in S-co-I suggested increased tissue morphogenesis and organogenesis (e.g. cardiac muscle cell apoptotic process, middle ear morphogenesis and regulation of organ formation), cell differentiation and development (e.g. peripheral nervous system neuron development, regulation of stem cell differentiation and anterior/posterior axis specification, embryo), angiogenesis (e.g. positive regulation of blood vessel endothelial cell migration, hypoxia and angiogenesis), cell signalling (e.g. calcium-mediated signalling using intracellular calcium source, regulation of insulin-like growth factor receptor signalling pathway and Kras signalling) as well as tissue remodelling (e.g. blastoderm segmentation and epithelial to mesenchymal transition) (**Table IV**). By contrast, the pathways over-represented in S-co-H included cell proliferation and cell cycle regulation (e.g. DNA replication initiation, signal transduction involved in cell cycle checkpoint and Myc targets), protein metabolism (e.g. tRNA processing and tRNA metabolic process) and

immune response regulation (e.g. response to interferon-alpha and Interleukin-6 biosynthetic process) (**Table V**).

RNA-seq validation

We used qPCR for validating the RNA-seq results of nine genes: *TMEM255A*, *EREG*, *SPDYC*, *CYP19A1*, *CASC1*, *PROM1*, *TGFA*, *CDC20B* and *HPRT1*. In accordance with the RNA-seq, qPCR results confirmed up-regulation of *EREG* (H-c *vs*. I-c), *SPDYC* (I-co-S *vs*. I-c), *PROM1* (S-co-I *vs*. S-c) and *TGFA* (S-co-I *vs*. S-c), down-regulation of *TMEM255A* (H-c *vs*. I-c), *CYP19A1* (S-co-H *vs*. S-c), *CASC1* (S-co-I *vs*. S-co-H) and *CDC20B* (I-co-S *vs*. I-c) and similar levels of *HPRT1* (H-c *vs*. I-c) (**Figure 5)**.

5. Discussion

To our knowledge, this is the first study to analyze transcriptional dynamics of human implantation in a compartment specific manner. In our *in vitro* model, transcriptional changes in both the embryo and endometrial epithelium proxies were dependent on endometrial receptivity, confirming that endometrium-driven molecular signals during attachment mediate embryo implantation.

Substrate response to embryo attachment

Our system successfully modelled known features of substrate response to contact with the trophoblast. As expected due to their different origins, the differences in the transcriptomic profiles of Ishikawa *vs*. HEC-1-A were numerous, as was their transcriptional response to co-culture with spheroids. Our datasets included genes previously related with implantation, such as *SPP1* (Secreted phosphoprotein 1, which encodes the ECM component osteopontin), *OLFM2* (which encodes the ECM protein olfactomedin-2) and members of the Wnt signalling pathway (e.g. *WNT11*, *FZD8* and *KREMEN2*) (Borthwick et al., 2003; White et al., 2006; Quenby et al., 2007; Kodithuwakku et al., 2011; Kang et al., 2014; Tepekoy, Akkoyunlu and Demir, 2015; Zhang and Yan, 2016; Farah et al., 2017). In accordance with the role of cell adhesion and ECM proteins in the trophectoderm-epithelium interaction established in the literature (Haouzi et al., 2011; Singh and Aplin, 2015; Altmae et al., 2012; Aberkane et al., 2018), our results highlighted important transcriptional differences of genes involved in these processes, including cadherins (e.g. *PCDHA11, PCDHA12, CDH2* and *CDHR1*), claudins (e.g. *CLDN16*), collagens (e.g. *COL9A3*

and *COL5A1*), glycoproteins (e.g. *TNXB*) and metallopeptidases (e.g. *ADAM32*). In addition, the receptive epithelium responded to the trophoblast challenge by promoting pathways including mitotic spindle organization (suggesting increased cell division) and apoptosis, which is involved in the epithelial breaching by the embryo (Arase et al., 2009). Of note, *C10orf10* and *G0S2*, which resulted differentially expressed among the substrates in our analysis, were previously suggested as transcriptomic biomarkers of endometrial receptivity (Altmae et al., 2017).

Additionally, our model revealed emerging candidates in embryo attachment. *CDHR1* (Cadherin-related family member 1) was strongly up-regulated in Ishikawa cells after co-culture with spheroids and remained unchanged in HEC-1-A cells, compared to their respective non-co-cultured controls. The CDHR1 protein in endometrial fluid of healthy women has been suggested to be regulated by 17β-estradiol (Chan et al., 2013) (Humphreys, Ziegler and Nardulli, 2014). Another gene family highlighted by our study is aquaporins. The expression levels *AQP3* and *AQP4* were up-regulated in Ishikawa cells after the co-culture but not in HEC-1-A. Increased expression of *AQP3* has been associated with both epithelial cell migration and endometrial receptivity (Cui et al., 2018), while deficiency of *AQP4* leads to female subfertility in mice (Sun et al., 2009). Other genes upregulated in Ishikawa cells upon trophoblast challenge were desmin (*DES*), adrenomedullin (*ADM*) and intermidin (*ADM2*). DES has been related to decidualization and implantation in rodents (Korgun et al., 2007). *ADM,* which encodes for an endocrine peptide, has been linked to fertility in female mice; reduced expression levels of *ADM* impaired endometrial receptivity and the administration of ADM prior to embryo transfer improved fertility by promoting pinopode formation (Li et al., 2006; Li, Wu and Caron 2008; Matson et al., 2017). In humans, a role for ADM in zygote transport in tubal ectopic pregnancies has been suggested (Liao et al., 2012). The related protein adrenomedullin 2 (also known as intermedin) has been associated with embryo implantation and placental growth (Havemann et al., 2013). The role of these genes in the trophoblast-epithelium interaction remains to be investigated.

Trophoblast response to attachment on epithelial substrates

Our model allowed us to examine the transcriptional response of the trophoblast to receptive or non-receptive substrates. Several trophoblast genes related with cell adhesion and ECM (*CD44*, *CTNND2, THBS1)* underwent upregulation upon co-culture of spheroids with Ishikawa cells (compared to HEC-1A cells), confirming previous reports that these 3 genes are differentially expressed in embryos that do attach to Ishikawa substrates compared to those which do not firmly attach (Aberkane et al., 2018). Other genes followed a similar expression pattern: *TRO* (trophinin,

an adhesion molecule uniquely expressed by human trophoblastic cells) and ErbB4 (a member in the EGFR subfamily of receptor tyrosine kinases) have been proposed as markers of initial embryo attachment (Chobotova et al., 2002; Sugihara et al., 2007). Further, co-culture on Ishikawa cells also resulted in upregulation of *DPY19L2,* a transmembrane protein coding gene was previously related to male infertility; *DPY19L2* deletions are causative of around 70% of globozoospermia cases (Harbuz et al., 2011; Modarres et al., 2016).

Attachment in our model is driven by the endometrial compartment

The lack of receptivity of HEC-1-A is well established in the literature (Dominguez et al., 2003; Tamm et al., 2009). Our study results showed that this lack of receptivity is due to a general inability of this substrate to mount a transcriptional response to the presence of the trophoblast spheroid. Indeed, when co-cultured with spheroids, the number of genes differentially expressed in Ishikawa cells *vs*. HEC-1-A cells was 608 *vs*. 9 genes, respectively. In turn, the different transcriptional responses of the two substrates conditioned the transcriptional response of the trophoblast spheroids. The trophoblast spheroids differentially expressed 3986 *vs.* 1038 genes when co-cultured with receptive *vs.* minimally receptive substrate, respectively, with over-representation of important pathways for future embryo development and pregnancy (e.g. organogenesis, morphogenesis and angiogenesis) after interaction with Ishikawa cells. It has been demonstrated that embryos are able to self-organize while attached to cell-free surfaces, in absence of maternal stimuli (Harrison et al., 2017; Shahbazi et al., 2017; Sozen et al., 2018). These studies highlight the importance of embryo regulation during later stages of development. However, implantation in maternal tissue is, ultimately, essential for developmental progression. We focus on early stages of implantation, where the crosstalk between the embryo and the maternal endometrium is essential (Greening et al., 2016; Ruane et al., 2017; Kang et al., 2014). Maternal induction of trophoblast differentiation has recently been found to be an important regulatory mechanism of implantation; although the mechanistic details have not been elucidated, the invasion needed for successful implantation has been shown to be dependent on maternal juxtacrine signals during apposition and attachment (Ruane et al., 2017). Different endometrial transcriptomic signatures during the window of implantation have been associated with reproductive success or failure (Koot et al., 2016; Diaz-Gimeno et al., 2017; Huang et al., 2017); a defective transcriptional substrate response to the presence of the embryo could underlie those transcriptomic signatures and lead to implantation failures.

Thus, by using a relatively simple 2-D co-culture system, we confirm that the behavior of trophoblast spheroids on receptive *vs*. minimally receptive epithelial substrates was consistent with the expected changes during implantation, as previously described in another model (Wang and Dey, 2006; Wang et al., 2012), and identified several candidate genes for future study.

A strength of our study is a novel experimental design which uses FACS to isolate individual compartments, allowing us to analyze the transcriptional response of each compartment to the other after co-culture. Further, RNA samples were harvested from pools of 96 well plates where each well contained a single spheroid on a fixed area of substrate (keeping the substrate/spheroid ratio constant) and therefore lending reproducibility and robustness to our results. A number of studies have determined the transcriptional signature of the endometrium and its correlation with implantation and reproductive outcome (Altmae et al., 2010; Koot et al., 2016; Diaz-Gimeno et al., 2017; Enciso et al., 2018). Our study highlights the significance of focusing not only on the endometrium per se, but on its ability to mount the correct transcriptional response upon interaction with the embryo.

The convenience of using an *in vitro* experimental approach entails limitations in our study. It has been confirmed that *in vitro* cell culture induces changes in the cell transcriptome, which limits the extrapolation of our study results (Krjutskov et al., 2016). Although broadly used in the literature to study implantation, JEG-3, Ishikawa and HEC-1-A cell lines come from carcinogenic origin and might not represent the physiological conditions of the implantation process (Hannan et al., 2010). Trophoblast spheroids lack communication between the inner cell mass and the trophectoderm and they are committed cells from a later developmental stage; therefore, their response does not fully represent a viable real embryo. Nevertheless, JEG-3 cell line present specific characteristics that resemble normal primary trophoblast cells, such as hCG production, glucose transport and cell barrier integrity (Huang et al., 2016; Rothbauer et al., 2017). The 3-D structure provides transcriptional profiles and secretory activities more similar to those from primary trophoblasts compared to 2-D cultures (McConkey et al., 2016). Of note, no hormones were used during cell culture (e.g. progesterone or estrogen), which could change expression levels of some transcripts (Dassen et al., 2007; Tamm-Rosenstein et al., 2013). We chose a 48 hours co-culture based on the morphological changes observed in our system and previous reports; different end points could give different results. These features in our experimental setup could explain that some genes we were expecting to find involved in attachment based on previous literature such as epithelial *MUC-1*, *LIF*, *HB-EGF* and *HOXA10* as well as trophoblast *IL-1* and *MMP-9* (Lessey and Castelbaum, 2002; Hirota et al., 2009; Paiva et al., 2009; Singh et al., 2010; Plaks et al., 2013;

Franasiak et al., 2014) were not detected in our analysis. Both Ishikawa and HEC-1-A cells express estrogen and progesterone receptors and are responsive to hormones in terms of gene expression (Kurarmoto et al., 2002; Thie et al., 2002; Singh et al., 2010; Tamm-Rosenstein et al., 2013). However, they do not reproduce the non-receptive to receptive phenotype change that epithelial cells undergo during the menstrual cycle under the influence of ovarian steroids. Therefore, hormonal supplementation is not likely to cause a great effect on gene expression in co-culture experiments (Rahimipour et al., 2018).

The application of our methodological approach to primary epithelial and stromal cells obtained from patients will provide extended information about the mechanisms involved in implantation failure. In summary, our transcriptional results suggest that endometrial receptivity determines the degree of trophoblast response and drives attachment during human implantation.

Acknowledgements

The authors wish to thank all members of the Basic Laboratory from Clínica EUGIN, especially Montserrat Barragán and Anna Ferrer, for critical discussion; José Buratini from Sao Paulo State University (Brasil) for critical revision of the manuscript; Camille Stephan Otto from the Biostatistics/Bioinformatics facility of the Institute for Research in Biomedicine (Barcelona) for bioinformatics analysis; Charles Pineau, Natalie Melaine and Emmanuelle Com from Proteomics Core Facility Biogenouest (Rennes) for assistance with data analysis and Prof. Daniel Grinberg from Universitat de Barcelona for technical support.

Conflict of interest

The authors declare that they have no conflict of interest.

Authors roles

Paula Vergaro: experimental execution, study design, data analysis, manuscript preparation. Gustavo Tiscornia: study design and supervision, data analysis, manuscript edition, expert knowledge. Amelia Rodríguez: study supervision. Josep Santaló: study supervision, expert knowledge, manuscript edition. Rita Vassena: study design and supervision, expert knowledge, manuscript edition.

6. Figures

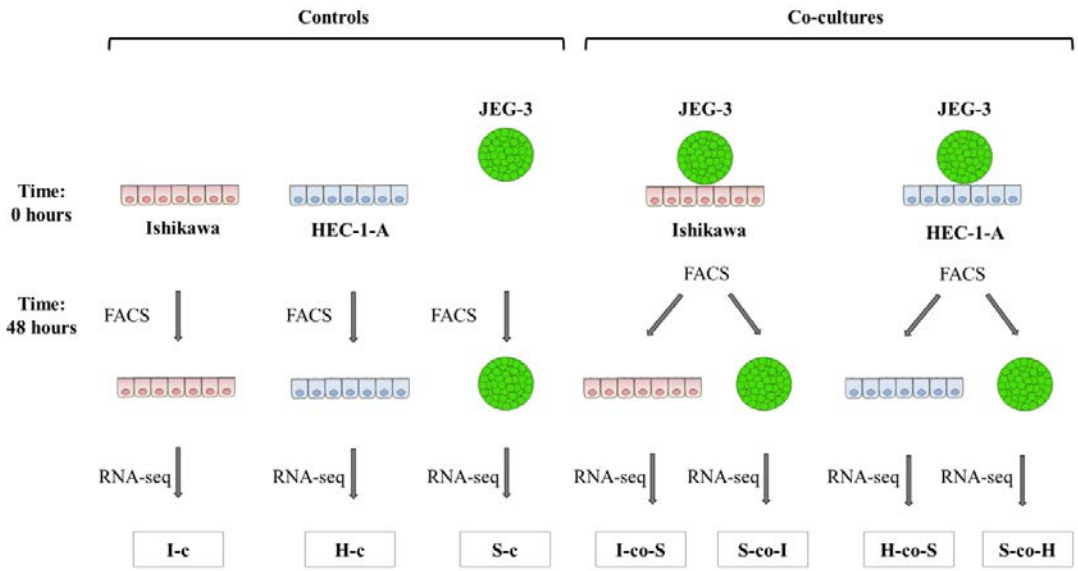

Figure 1. Scheme of the experimental design. Monolayers of receptive (Ishikawa) and non-receptive (HEC-1-A) epithelia were co-cultured with trophoblast spheroids (JEG-3) for 48 hours or maintained in mono-cultures for the same time as controls. Likewise, single spheroids were co-cultured or cultured for 48 hours in absence of any substrate as controls. All the JEG-3 spheroids depicted express GFP. After 48 hours, GFP+ (trophoblast) and GFP- (receptive or non-receptive epithelia) were separated by FACS and analyzed by RNA-seq. The transcriptomic profiles of the following cell fractions were obtained: Ishikawa control (I-c), HEC-1-A control (H-c), JEG-3 spheroids control (S-c), Ishikawa substrates co-cultured with JEG-3 spheroids (I-co-S), HEC-1-A substrates co-cultured with JEG-3 spheroids (H-co-S), JEG-3 spheroids co-cultured with Ishikawa substrates (S-co-I) and JEG-3 spheroids co-cultured with HEC-1-A substrates (S-co-H).

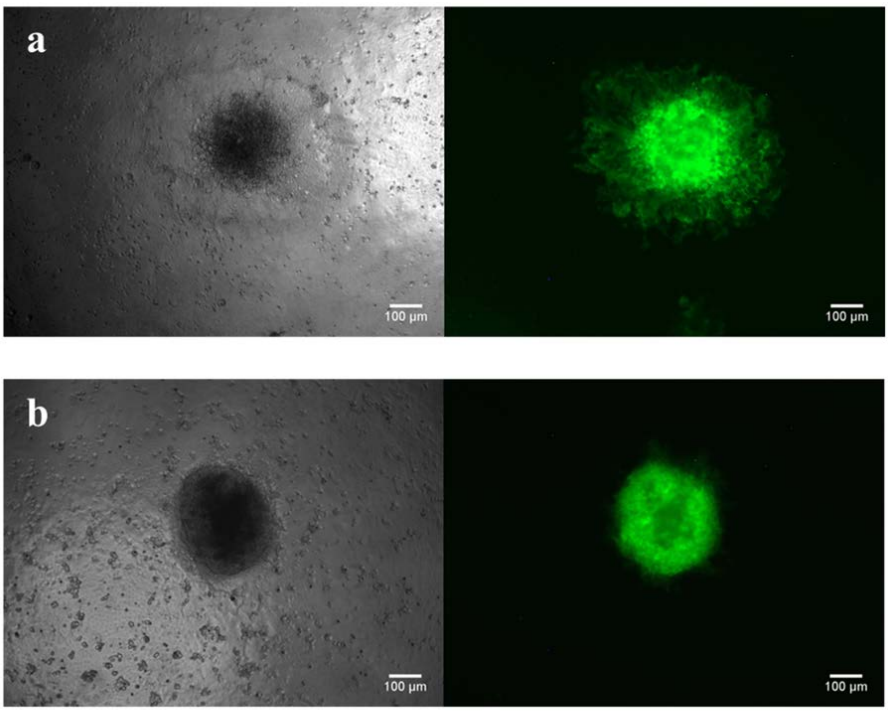

Figure 2. **Representative figures of GFP+ trophoblast spheroids attached to Ishikawa (a) and adhered to HEC-1-A (b) monolayers after 48 hours co-culture**, visualized under 10X magnification.

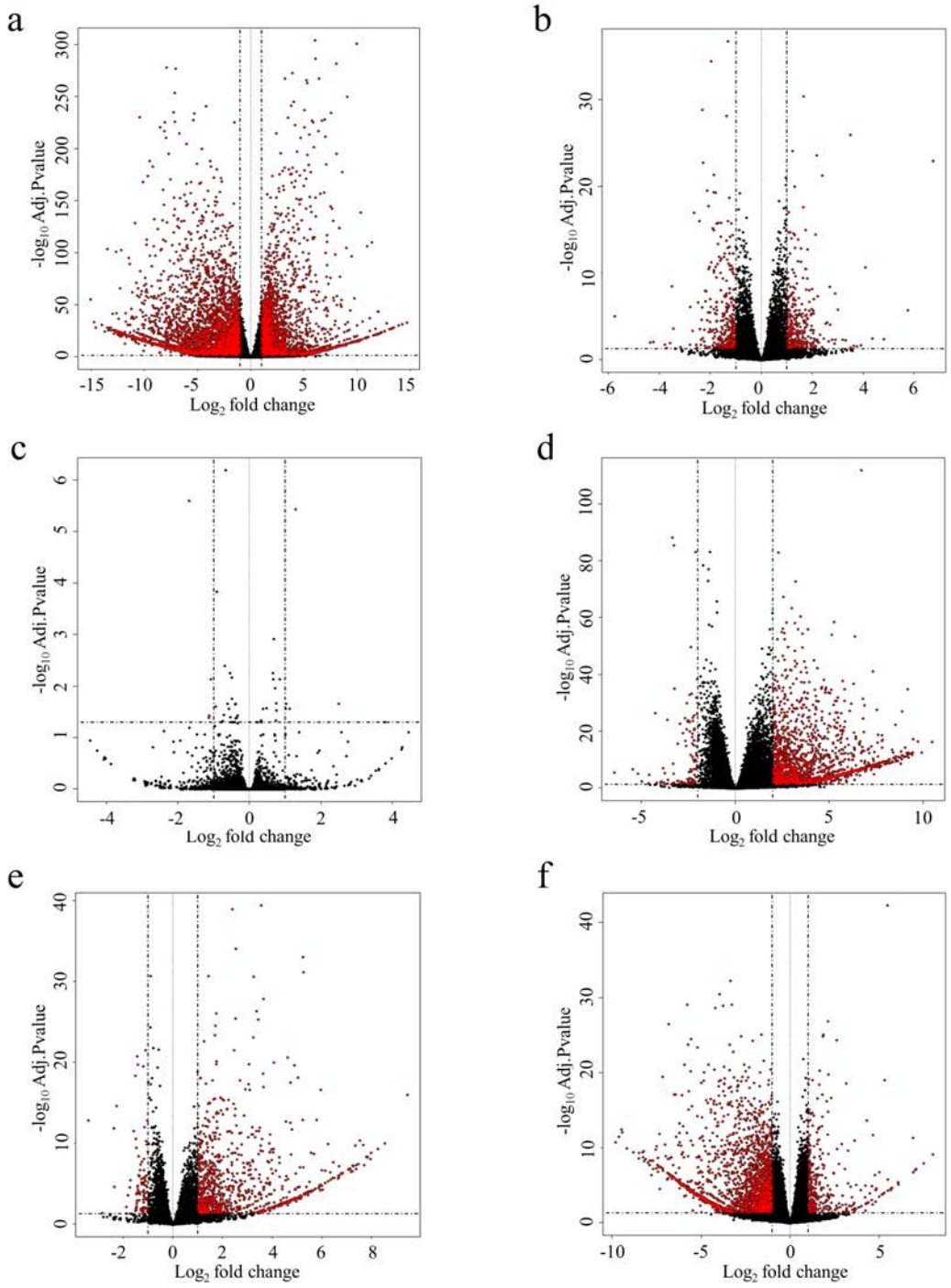

Figure 3: Volcano plots of differentially expressed genes between co-cultured and sorted GFP+ and GFP- cells fractions as well as non-co-cultured controls in pairwise comparisons: **(3a)** Ishikawa control (I-c) *vs*. HEC-1-A control (H-c), **(3b)** Ishikawa substrates co-cultured with JEG-3 spheroids (I-co-S) *vs*. Ishikawa control (I-c), **(3c)** HEC-1-A substrates co-cultured with JEG-3 spheroids (H-co-S) *vs*. HEC-1-A control (H-c), **(3d)** JEG-3 spheroids co-cultured with Ishikawa substrates (S-co-I) *vs*. JEG-3 spheroids control (S-c), **(3e)** JEG-3 spheroids co-cultured with HEC-1-A substrates (S-co-H) *vs*. JEG-3 spheroids control (S-c), **(3f)** JEG-3 spheroids co-cultured with Ishikawa substrates (S-co-I) *vs*. JEG-3 spheroids co-cultured with HEC-1-A substrates (S-co-H).

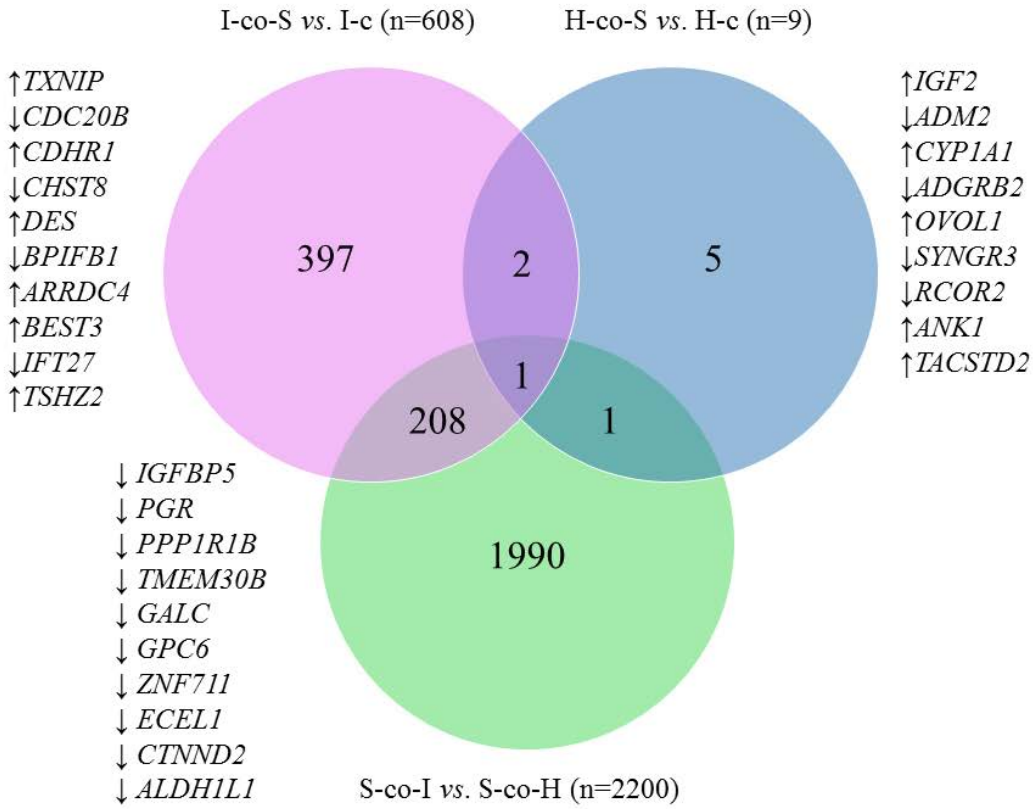

Figure 4. **Venn diagram representing differentially expressed genes among the following pairwise comparisons**: (pink) Ishikawa substrates co-cultured with JEG-3 spheroids (I-co-S) *vs*. Ishikawa control (I-c), top 10 differentially expressed genes of this comparison ranked by absolute log2FC listed on the left; (blue) HEC-1-A substrates co-cultured with JEG-3 spheroids (H-co-S) *vs*. HEC-1-A control (H-c), all nine genes included in this comparison ranked by absolute log2FC listed on the right; (green) JEG-3 spheroids co-cultured with Ishikawa substrates (S-co-I) *vs*. JEG-3 spheroids co-cultured with HEC-1-A substrates (S-co-H), top 10 differentially expressed genes of this comparison ranked by absolute log2FC listed on the left. The arrows show the direction of gene expression changes (↑= up-regulated, ↓= down-regulated).

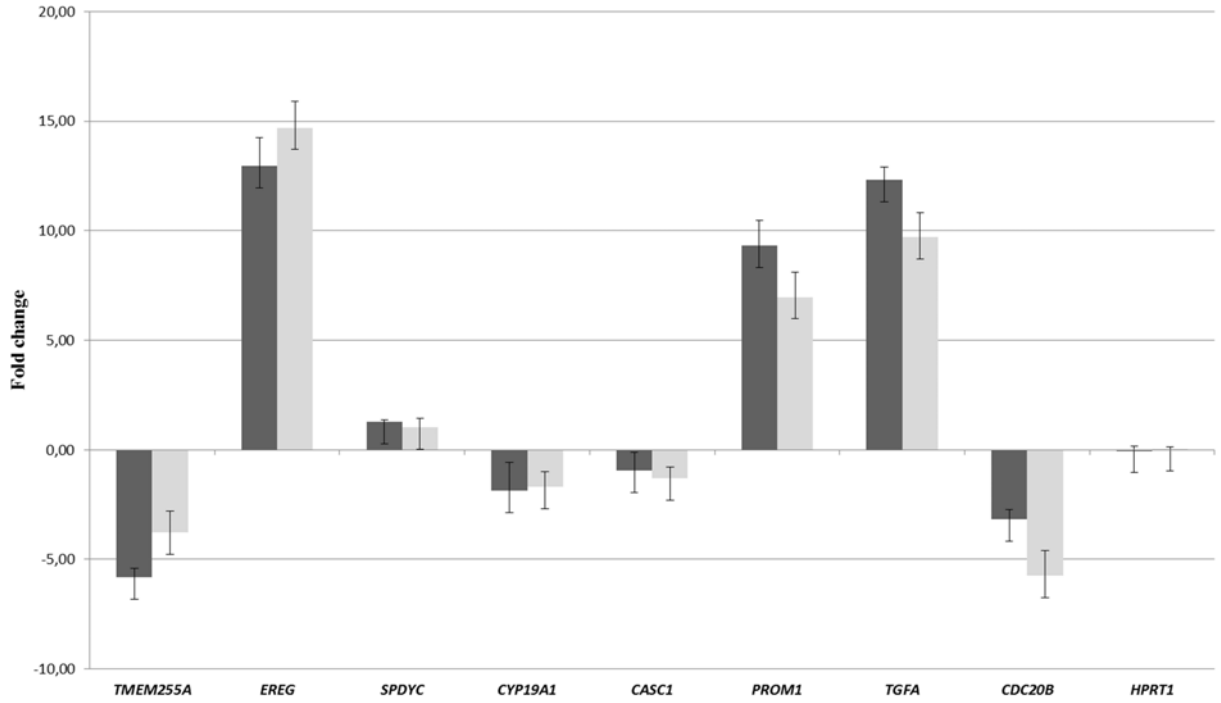

Figure 5. **RNA-seq validation by qPCR**. Dark grey bars represent the differences in gene expression levels among samples (pairwise comparisons) by qPCR and light grey bars represent the differences in gene expression levels among samples (pairwise comparisons) by RNA-seq. The genes and samples tested were: *TMEM255A* (H-c *vs*. I-c), *EREG* (H-c *vs*. I-c), *SPDYC* (I-co-S *vs*. I-c), *CYP19A1*(S-co-H *vs*. S-c), *CASC1* (S-co-I *vs*. S-co-H), *PROM1* (S-co-I *vs*. S-c), *TGFA* (S-co-I *vs*. S-c), *CDC20B* (I-co-S *vs*. I-c) and *HPRT1* (H-c *vs*. I-c). Error bars represent variability between sample triplicates from the original experimental sets.

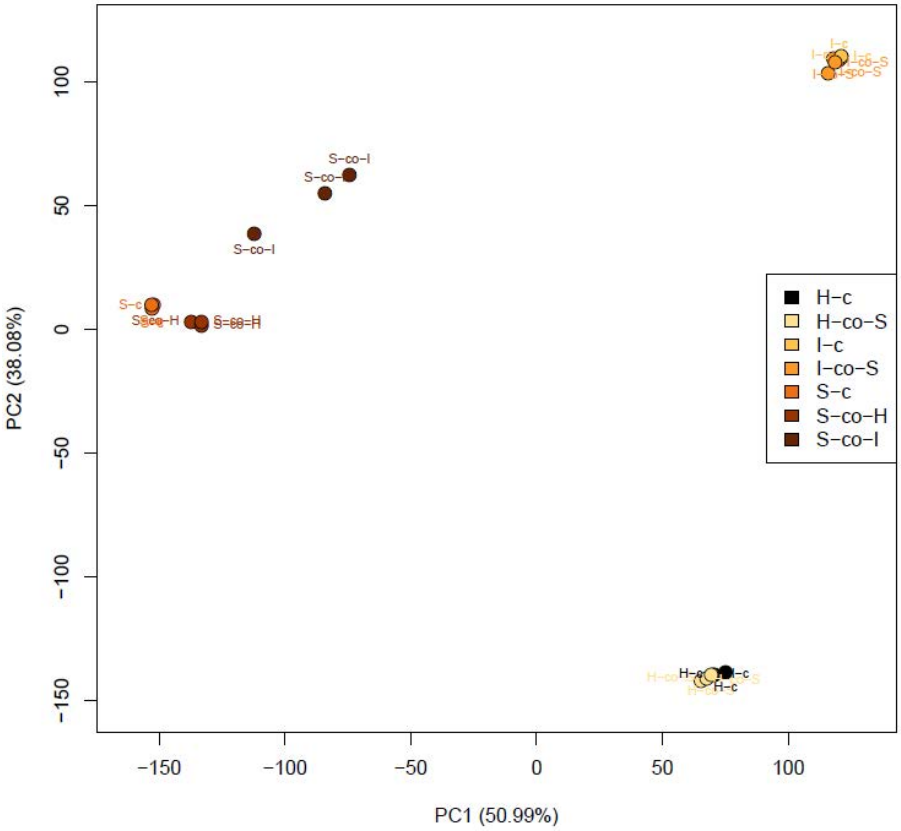

Supplementary Figure 1. Principal component analysis representing all samples from experimental triplicates according to principal component 1 (PC1) and principal component 2 (PC2): HEC-1-A control (H-c), HEC-1-A substrates co-cultured with JEG-3 spheroids (H-co-S), Ishikawa control (I-c), Ishikawa substrates co-cultured with JEG-3 spheroids (I-co-S), JEG-3 spheroids control (S-c), JEG-3 spheroids co-cultured with HEC-1-A substrates (S-co-H) and JEG-3 spheroids co-cultured with Ishikawa substrates (S-co-I).

7. Tables

Table I. Biological pathways over-represented in Ishikawa epithelial substrate after co-culture with JEG-3 spheroids *vs.* Ishikawa control using GOBP and Broad Hallmarks annotations (NES= Normalized enrichment score; FDR= False discovery rate).

Annotation terms	Genes (n)	NES	FDR
Biological processes (GOBP)			
Mitotic spindle organization	38	1.91	0.098
Sister chromatid segregation	55	1.90	0.083
Mitotic sister chromatid segregation	52	1.88	0.079
Spindle organization	86	1.87	0.084
Rhodopsin mediated signalling pathway	34	1.85	0.090
Broad Hallmarks			
E2F targets	196	1.87	0.003
G2M checkpoint	194	1.62	0.032
Allograft rejection	188	1.58	0.033
Apoptosis	158	1.52	0.044

Table II. Biological pathways over-represented in HEC-1-A epithelial substrate after co-culture with JEG-3 spheroids *vs.* HEC-1-A control using GOBP and Broad Hallmarks annotations (NES= Normalized enrichment score; FDR= False discovery rate).

Annotation terms	Genes (n)	NES	FDR
Biological processes (GOBP)			
Regulation of amino acid transport	18	1.94	0.028

Table III. Biological pathways over-represented in the statistically significant gene expression pattern "up-regulated in I-co-S *vs.* I-c and down-regulated or unchanged in H-co-S *vs.* H-c" according to the hypergeometric test using GOBP and Broad Hallmarks annotations.

Annotation terms	Genes (n)	Genes in the intersection (n)	Adj p-value
Biological processes (GOBP)			
Nuclear division	346	32	0,00
Mitosis	346	32	0,00
Organelle fission	373	33	0,00
Chromosome segregation	152	19	0,00
Mitotic cell cycle	816	45	0,00
Mitotic spindle organization	39	9	0,00
Mitotic sister chromatid segregation	53	10	0,00
Sister chromatid segregation	56	10	0,00
Cell division	494	31	0,00
Spindle organization	88	11	0,00
Cell cycle process	1117	49	0,01
Microtubule cytoskeleton organization	297	20	0,01
Microtubule-based process	456	26	0,01
Metaphase/anaphase transition of mitotic cell cycle	43	7	0,02
Metaphase/anaphase transition of cell cycle	43	7	0,02
Cholesterol biosynthetic process	44	7	0,02
Cell cycle	1464	57	0,03
Sterol biosynthetic process	50	7	0,04
Broad Hallmarks			
E2F targets	200	23	0,00
G2M checkpoint	200	22	0,00
Mitotic spindle	200	14	0,00
Cholesterol homeostasis	75	8	0,00

Table IV. Biological pathways over-represented in trophoblast JEG-3 spheroids after co-culture with Ishikawa *vs.* HEC-1-A using GOBP and Broad Hallmarks annotations (NES= Normalized enrichment score; FDR= False discovery rate).

Annotation terms	Genes (n)	NES	FDR
Biological processes (GOBP)			
Cardiac muscle cell apoptotic process	15	-1.86	0.000
Striated muscle cell apoptotic process	18	-1.84	0.002
Peripheral nervous system neuron development	13	-1.82	0.003
Middle ear morphogenesis	24	-1.80	0.006
Regulation of organ formation	36	-1.78	0.012
Peripheral nervous system neuron differentiation	13	-1.78	0.012
Anterior/posterior axis specification, embryo	15	-1.77	0.012
Blastoderm segmentation	15	-1.77	0.013
Tripartite regional subdivision	15	-1.76	0.017
Regulation of cardiac muscle cell apoptotic process	12	-1.76	0.017
Dicarboxylic acid catabolic process	15	-1.75	0.018
Regulation of insulin-like growth factor receptor signalling pathway	19	-1.75	0.018
Regulation of heart morphogenesis	24	-1.75	0.019
Positive regulation of transforming growth factor beta receptor signalling pathway	22	-1.74	0.021
Neuropeptide signalling pathway	56	-1.74	0.022
Heart formation	14	-1.74	0.023
Calcium-mediated signalling using intracellular calcium source	11	-1.73	0.025
Regulation of fibroblast growth factor receptor signalling pathway	25	-1.73	0.025
Regulation of striated muscle cell apoptotic process	15	-1.73	0.026
Cell surface receptor signalling pathway involved in heart development	23	-1.71	0.035
Outflow tract morphogenesis	52	-1.69	0.056
Anterior/posterior axis specification	41	-1.69	0.062
Cartilage development involved in endochondral bone morphogenesis	21	-1.68	0.065
Eating behaviour	22	-1.68	0.064
Glutamate secretion	30	-1.68	0.063
Regulation of cell proliferation involved in heart morphogenesis	15	-1.68	0.062
Regulation of epithelial to mesenchymal transition	42	-1.68	0.061
Face development	39	-1.68	0.060
Embryonic cranial skeleton morphogenesis	38	-1.67	0.066
Cell proliferation involved in heart morphogenesis	15	-1.67	0.065
Insulin-like growth factor receptor signalling pathway	32	-1.67	0.065
Positive regulation of blood vessel endothelial cell migration	21	-1.67	0.064
Clathrin coat assembly	12	-1.66	0.080

Embryonic skeletal system development	111	-1.66	0.079
Regulation of stem cell differentiation	74	-1.66	0.085
Embryonic skeletal system morphogenesis	84	-1.65	0.088
Proximal/distal pattern formation	30	-1.65	0.087
Negative regulation of striated muscle cell apoptotic process	12	-1.65	0.099
Broad Hallmarks			
Hypoxia	194	-1.51	0.090
Epithelial mesenchymal transition	195	-1.46	0.082
Kras signalling dn	181	-1.43	0.095
Angiogenesis	35	-1.42	0.075

Table V. Biological pathways over-represented in trophoblast JEG-3 spheroids after co-culture with HEC-1-A *vs.* Ishikawa using GOBP and Broad Hallmarks annotations (NES= Normalized enrichment score; FDR= False discovery rate).

Annotation terms	Genes (n)	NES	FDR
Biological processes (GOBP)			
Detection of chemical stimulus involved in sensory perception of smell	21	2.32	0.002
Chromosome localization	22	2.26	0.003
Establishment of chromosome localization	21	2.20	0.007
tRNA processing	78	2.16	0.012
tRNA metabolic process	124	2.14	0.013
Metaphase plate congression	17	2.07	0.033
DNA strand elongation involved in DNA replication	33	2.07	0.031
Sensory perception of smell	43	2.06	0.029
Positive regulation of ubiquitin-protein ligase activity involved in mitotic cell cycle	72	2.04	0.035
Mitotic metaphase plate congression	13	2.04	0.033
Sister chromatid segregation	55	2.01	0.046
Negative regulation of ubiquitin-protein ligase activity involved in mitotic cell cycle	67	1.99	0.051
Anaphase-promoting complex-dependent proteasomal ubiquitin-dependent protein catabolic process	83	1.99	0.051
Mitotic sister chromatid segregation	52	1.97	0.058
Regulation of ubiquitin-protein ligase activity involved in mitotic cell cycle	78	1.96	0.061
Mitotic nuclear envelope disassembly	36	1.95	0.063
Response to interferon-alpha	16	1.95	0.059
Cell cycle DNA replication	33	1.94	0.063
Histone exchange	24	1.94	0.060
Actin nucleation	13	1.94	0.058
ATP-dependent chromatin remodelling	30	1.92	0.067
DNA strand elongation	36	1.92	0.065
Detection of chemical stimulus involved in sensory perception	44	1.92	0.064
Positive regulation of ligase activity	86	1.90	0.078
ncRNA processing	206	1.89	0.085
DNA replication initiation	29	1.88	0.082
Interleukin-6 biosynthetic process	18	1.88	0.081
Negative regulation of ubiquitin-protein ligase activity	72	1.87	0.089
Negative regulation of ligase activity	72	1.87	0.087
Signal transduction involved in cell cycle checkpoint	66	1.85	0.098
Positive regulation of ubiquitin-protein ligase activity	82	1.85	0.098
Regulation of interleukin-6 biosynthetic process	16	1.84	0.097
ncRNA metabolic process	292	1.84	0.097
Nuclear envelope disassembly	38	1.83	0.098

Broad Hallmarks			
E2F targets	196	2.79	0.000
G2M checkpoint	194	2.72	0.000
Myc targets v1	196	2.39	0.000
Myc targets v2	58	1.89	0.000
Interferon alpha response	93	1.63	0.013

8. Supplementary files (Available online: https://doi.org/10.1007/s10815-019-01442-9 or upon request to the authors)

Supplementary file S1: List of differentially expressed genes between HEC-1-A control (H-c) *vs*. Ishikawa control (I-c). Statistical significance was set at absolute log2FC cut-off of 1 and adjusted p-value <0.05. Negative fold changes mean that expression in H-c is lower than that in I-c; positive fold changes mean expression in H-c is higher than that in I-c.

Supplementary file S2: List of differentially expressed genes between Ishikawa substrates co-cultured with JEG-3 spheroids (I-co-S) *vs*. Ishikawa control (I-c). Statistical significance was set at absolute log2FC cut-off of 1 and adjusted p-value <0.05. Negative fold changes mean that expression in I-co-S is lower than that in I-c; positive fold changes mean expression in I-co-S is higher than that in I-c.

Supplementary file S3: List of differentially expressed genes between HEC-1-A substrates co-cultured with JEG-3 spheroids (H-co-S) *vs*. HEC-1-A control (H-c). Statistical significance was set at absolute log2FC cut-off of 1 and adjusted p-value <0.05. Negative fold changes mean that expression in H-co-S is lower than that in H-c; positive fold changes mean expression in H-co-S is higher than that in H-c.

Supplementary file S4: List of differential expression patterns between HEC-1-A substrates co-cultured with JEG-3 spheroids (H-co-S) *vs*. HEC-1-A control (H-c) compared to Ishikawa substrates co-cultured with JEG-3 spheroids (I-co-S) *vs*. Ishikawa control (I-c). Statistical significance was set at absolute log2FC cut-off of 1 and adjusted p-value <0.05. Negative fold changes mean that difference in gene expression is enriched in H-co-S *vs*. H-c; positive fold changes mean that difference in gene expression is enriched in I-co-S *vs*. I-c.

Supplementary file S5: List of differentially expressed genes between JEG-3 spheroids co-cultured with Ishikawa substrates (S-co-I) *vs*. JEG-3 spheroids control (S-c), Statistical significance was set at absolute log2FC cut-off of 1 and adjusted p-value <0.05. Negative fold changes mean that expression in S-co-I is lower than that in S-c; positive fold changes mean expression in S-co-I is higher than that in S-c.

Supplementary file S6: List of differentially expressed genes between JEG-3 spheroids co-cultured with HEC-1-A substrates (S-co-H) *vs*. JEG-3 spheroids control (S-c), Statistical significance was set at absolute log2FC cut-off of 1 and adjusted p-value <0.05. Negative fold changes mean that expression in S-co-H is lower than that in S-c; positive fold changes mean expression in S-co-H is higher than that in S-c.

Supplementary file S7: List of differentially expressed genes between JEG-3 spheroids co-cultured with HEC-1-A substrates (S-co-H) *vs*. JEG-3 spheroids co-cultured with Ishikawa substrates (S-co-I). Statistical significance was set at absolute log2FC cut-off of 1 and adjusted p-value <0.05. Negative fold changes mean that expression in S-co-H is lower than that in S-co-I; positive fold changes mean expression in S-co-H is higher than that in S-co-I.

Supplementary file S8: List of the 208 common genes between JEG-3 spheroids co-cultured with Ishikawa substrates and Ishikawa substrates co-cultured with JEG-3 spheroids ("S-co-H *vs*. S-co-I" and "I-co-S *vs.* I-c" comparisons).

9. References

Aberkane, A., W. Essahib, C. Spits, C. De Paepe, K. Sermon, T. Adriaenssens, S. Mackens, H. Tournaye, J. J. Brosens, and H. Van de Velde. 2018. 'Expression of adhesion and extracellular matrix genes in human blastocysts upon attachment in a 2D co-culture system', *Mol Hum Reprod*, 24: 375-87.

Altmae, S., M. Koel, U. Vosa, P. Adler, M. Suhorutsenko, T. Laisk-Podar, V. Kukushkina, M. Saare, A. Velthut-Meikas, K. Krjutskov, L. Aghajanova, P. G. Lalitkumar, K. Gemzell-Danielsson, L. Giudice, C. Simon, and A. Salumets. 2017. 'Meta-signature of human endometrial receptivity: a meta-analysis and validation study of transcriptomic biomarkers', *Sci Rep*, 7: 10077.

Altmae, S., J. A. Martinez-Conejero, A. Salumets, C. Simon, J. A. Horcajadas, and A. Stavreus-Evers. 2010. 'Endometrial gene expression analysis at the time of embryo implantation in women with unexplained infertility', *Mol Hum Reprod*, 16: 178-87.

Altmae, S., J. Reimand, O. Hovatta, P. Zhang, J. Kere, T. Laisk, M. Saare, M. Peters, J. Vilo, A. Stavreus-Evers, and A. Salumets. 2012. 'Research resource: interactome of human embryo implantation: identification of gene expression pathways, regulation, and integrated regulatory networks', *Mol Endocrinol*, 26: 203-17.

Aplin, J. D., and P. T. Ruane. 2017. 'Embryo-epithelium interactions during implantation at a glance', *J Cell Sci*, 130: 15-22.

Arase, T., H. Uchida, T. Kajitani, M. Ono, K. Tamaki, H. Oda, S. Nishikawa, M. Kagami, T. Nagashima, H. Masuda, H. Asada, Y. Yoshimura, and T. Maruyama. 2009. 'The UDP-glucose receptor P2RY14 triggers innate mucosal immunity in the female reproductive tract by inducing IL-8', *J Immunol*, 182: 7074-84.

Ashburner, M., C. A. Ball, J. A. Blake, D. Botstein, H. Butler, J. M. Cherry, A. P. Davis, K. Dolinski, S. S. Dwight, J. T. Eppig, M. A. Harris, D. P. Hill, L. Issel-Tarver, A. Kasarskis, S. Lewis, J. C. Matese, J. E. Richardson, M. Ringwald, G. M. Rubin, and G. Sherlock. 2000. 'Gene ontology: tool for the unification of biology. The Gene Ontology Consortium', *Nat Genet*, 25: 25-9.

Berger, C., N. R. Boggavarapu, J. Menezes, P. G. Lalitkumar, and K. Gemzell-Danielsson. 2015. 'Effects of ulipristal acetate on human embryo attachment and endometrial cell gene expression in an in vitro co-culture system', *Hum Reprod*, 30: 800-11.

Boggavarapu, N. R., C. Berger, C. von Grothusen, J. Menezes, K. Gemzell-Danielsson, and P. G. Lalitkumar. 2016. 'Effects of low doses of mifepristone on human embryo implantation process in a three-dimensional human endometrial in vitro co-culture system', *Contraception*, 94: 143-51.

Borthwick, J. M., D. S. Charnock-Jones, B. D. Tom, M. L. Hull, R. Teirney, S. C. Phillips, and S. K. Smith. 2003. 'Determination of the transcript profile of human endometrium', *Mol Hum Reprod*, 9: 19-33.

Brighton, P. J., Y. Maruyama, K. Fishwick, P. Vrljicak, S. Tewary, R. Fujihara, J. Muter, E. S. Lucas, T. Yamada, L. Woods, R. Lucciola, Y. Hou Lee, S. Takeda, S. Ott, M. Hemberger, S. Quenby, and J. J. Brosens. 2017. 'Clearance of senescent decidual cells by uterine natural killer cells in cycling human endometrium', *Elife*, 6.

Carver, J., K. Martin, I. Spyropoulou, D. Barlow, I. Sargent, and H. Mardon. 2003. 'An in-vitro model for stromal invasion during implantation of the human blastocyst', *Hum Reprod*, 18: 283-90.

Cha, J., X. Sun, and S. K. Dey. 2012. 'Mechanisms of implantation: strategies for successful pregnancy', *Nat Med*, 18: 1754-67.

Chan, C., C. Virtanen, N. A. Winegarden, T. J. Colgan, T. J. Brown, and E. M. Greenblatt. 2013. 'Discovery of biomarkers of endometrial receptivity through a minimally invasive

approach: a validation study with implications for assisted reproduction', *Fertil Steril*, 100: 810-7.

Chobotova, K., I. Spyropoulou, J. Carver, S. Manek, J. K. Heath, W. J. Gullick, D. H. Barlow, I. L. Sargent, and H. J. Mardon. 2002. 'Heparin-binding epidermal growth factor and its receptor ErbB4 mediate implantation of the human blastocyst', *Mech Dev*, 119: 137-44.

Cui, D., L. Sui, X. Han, M. Zhang, Z. Guo, W. Chen, X. Yu, Q. Sun, M. Dong, T. Ma, and Y. Kong. 2018. 'Aquaporin-3 mediates ovarian steroid hormone-induced motility of endometrial epithelial cells', *Hum Reprod*, 33: 2060-73.

Dassen, H., C. Punyadeera, R. Kamps, J. Klomp, G. Dunselman, F. Dijcks, A. de Goeij, A. Ederveen, and P. Groothuis. 2007. 'Progesterone regulation of implantation-related genes: new insights into the role of oestrogen', *Cell Mol Life Sci*, 64: 1009-32.

Diaz-Gimeno, P., M. Ruiz-Alonso, P. Sebastian-Leon, A. Pellicer, D. Valbuena, and C. Simon. 2017. 'Window of implantation transcriptomic stratification reveals different endometrial subsignatures associated with live birth and biochemical pregnancy', *Fertil Steril*, 108: 703-10 e3.

Dobin, A., C. A. Davis, F. Schlesinger, J. Drenkow, C. Zaleski, S. Jha, P. Batut, M. Chaisson, and T. R. Gingeras. 2013. 'STAR: ultrafast universal RNA-seq aligner', *Bioinformatics*, 29: 15-21.

Dominguez, F., S. Avila, A. Cervero, J. Martin, A. Pellicer, J. L. Castrillo, and C. Simon. 2003. 'A combined approach for gene discovery identifies insulin-like growth factor-binding protein-related protein 1 as a new gene implicated in human endometrial receptivity', *J Clin Endocrinol Metab*, 88: 1849-57.

Enciso, M., J. P. Carrascosa, J. Sarasa, P. A. Martinez-Ortiz, S. Munne, J. A. Horcajadas, and J. Aizpurua. 2018. 'Development of a new comprehensive and reliable endometrial receptivity map (ER Map/ER Grade) based on RT-qPCR gene expression analysis', *Hum Reprod*, 33: 220-28.

Farah, O., S. Biechele, J. Rossant, and D. Dufort. 2017. 'Porcupine-dependent Wnt activity within the uterine epithelium is essential for fertility', *Biol Reprod*, 97: 688-97.

Franasiak, J. M., K. J. Holoch, L. Yuan, D. P. Schammel, S. L. Young, and B. A. Lessey. 2014. 'Prospective assessment of midsecretory endometrial leukemia inhibitor factor expression versus alphanubeta3 testing in women with unexplained infertility', *Fertil Steril*, 101: 1724-31.

Greening, D. W., H. P. Nguyen, K. Elgass, R. J. Simpson, and L. A. Salamonsen. 2016. 'Human Endometrial Exosomes Contain Hormone-Specific Cargo Modulating Trophoblast Adhesive Capacity: Insights into Endometrial-Embryo Interactions', *Biol Reprod*, 94: 38.

Hannan, N. J., R. L. Jones, C. A. White, and L. A. Salamonsen. 2006. 'The chemokines, CX3CL1, CCL14, and CCL4, promote human trophoblast migration at the feto-maternal interface', *Biol Reprod*, 74: 896-904.

Hannan, N. J., P. Paiva, E. Dimitriadis, and L. A. Salamonsen. 2010. 'Models for study of human embryo implantation: choice of cell lines?', *Biol Reprod*, 82: 235-45.

Hannan, N. J., P. Paiva, K. L. Meehan, L. J. Rombauts, D. K. Gardner, and L. A. Salamonsen. 2011. 'Analysis of fertility-related soluble mediators in human uterine fluid identifies VEGF as a key regulator of embryo implantation', *Endocrinology*, 152: 4948-56.

Haouzi, D., H. Dechaud, S. Assou, C. Monzo, J. de Vos, and S. Hamamah. 2011. 'Transcriptome analysis reveals dialogues between human trophectoderm and endometrial cells during the implantation period', *Hum Reprod*, 26: 1440-9.

Harbuz, R., R. Zouari, V. Pierre, M. Ben Khelifa, M. Kharouf, C. Coutton, G. Merdassi, F. Abada, J. Escoffier, Y. Nikas, F. Vialard, I. Koscinski, C. Triki, N. Sermondade, T. Schweitzer, A. Zhioua, F. Zhioua, H. Latrous, L. Halouani, M. Ouafi, M. Makni, P. S. Jouk, B. Sele, S. Hennebicq, V. Satre, S. Viville, C. Arnoult, J. Lunardi, and P. F. Ray. 2011. 'A recurrent

deletion of DPY19L2 causes infertility in man by blocking sperm head elongation and acrosome formation', *Am J Hum Genet*, 88: 351-61.

Harrison, S. E., B. Sozen, N. Christodoulou, C. Kyprianou, and M. Zernicka-Goetz. 2017. 'Assembly of embryonic and extraembryonic stem cells to mimic embryogenesis in vitro', *Science*, 356.

Havemann D, Balkrishnan M, Borahay M, Theiler R, Jennings K, Endsley J, Phelps J, Hankins GD, Yallampalli C, and Chauhan M. 2013. 'Intermedin/adrenomedullin 2 is associated with implantation and placentation via trophoblast invasion in human pregnancy', *J Clin Endocrinol Metab*, 98: 695–703.

Heneweer, C., M. Schmidt, H. W. Denker, and M. Thie. 2005. 'Molecular mechanisms in uterine epithelium during trophoblast binding: the role of small GTPase RhoA in human uterine Ishikawa cells', *J Exp Clin Assist Reprod*, 2: 4.

Hirota, Y., Y. Osuga, A. Hasegawa, A. Kodama, T. Tajima, K. Hamasaki, K. Koga, O. Yoshino, T. Hirata, M. Harada, Y. Takemura, T. Yano, O. Tsutsumi, and Y. Taketani. 2009. 'Interleukin (IL)-1beta stimulates migration and survival of first-trimester villous cytotrophoblast cells through endometrial epithelial cell-derived IL-8', *Endocrinology*, 150: 350-6.

Huang, J., H. Qin, Y. Yang, X. Chen, J. Zhang, S. Laird, C. C. Wang, T. F. Chan, and T. C. Li. 2017. 'A comparison of transcriptomic profiles in endometrium during window of implantation between women with unexplained recurrent implantation failure and recurrent miscarriage', *Reproduction*, 153: 749-58.

Huang, X., M. Luthi, E. C. Ontsouka, S. Kallol, M. U. Baumann, D. V. Surbek, and C. Albrecht. 2016. 'Establishment of a confluent monolayer model with human primary trophoblast cells: novel insights into placental glucose transport', *Mol Hum Reprod*, 22: 442-56.

Humphreys, G. I., Y. S. Ziegler, and A. M. Nardulli. 2014. '17beta-estradiol modulates gene expression in the female mouse cerebral cortex', *PLoS One*, 9: e111975.

Kang, Y. J., K. Forbes, J. Carver, and J. D. Aplin. 2014. 'The role of the osteopontin-integrin alphavbeta3 interaction at implantation: functional analysis using three different in vitro models', *Hum Reprod*, 29: 739-49.

Kodithuwakku, S. P., P. Y. Ng, Y. Liu, E. H. Ng, W. S. Yeung, P. C. Ho, and K. F. Lee. 2011. 'Hormonal regulation of endometrial olfactomedin expression and its suppressive effect on spheroid attachment onto endometrial epithelial cells', *Hum Reprod*, 26: 167-75.

Koot, Y. E., S. R. van Hooff, C. M. Boomsma, D. van Leenen, M. J. Groot Koerkamp, M. Goddijn, M. J. Eijkemans, B. C. Fauser, F. C. Holstege, and N. S. Macklon. 2016. 'An endometrial gene expression signature accurately predicts recurrent implantation failure after IVF', *Sci Rep*, 6: 19411.

Korgun, E. T., S. Cayli, M. Asar, and R. Demir. 2007. 'Distribution of laminin, vimentin and desmin in the rat uterus during initial stages of implantation', *J Mol Histol*, 38: 253-60.

Krjutskov, K., S. Katayama, M. Saare, M. Vera-Rodriguez, D. Lubenets, K. Samuel, T. Laisk-Podar, H. Teder, E. Einarsdottir, A. Salumets, and J. Kere. 2016. 'Single-cell transcriptome analysis of endometrial tissue', *Hum Reprod*, 31: 844-53.

Kurarmoto, H., M. Hamano, and M. Imai. HEC-1 cells. 2002. *Human Cell*. 2002; 15:81-95.

Lessey, B. A., and A. J. Castelbaum. 2002. 'Integrins and implantation in the human', *Rev Endocr Metab Disord*, 3: 107-17.

Li, M., Y. Wu, and K. M. Caron. 2008. 'Haploinsufficiency for adrenomedullin reduces pinopodes and diminishes uterine receptivity in mice', *Biol Reprod*, 79: 1169-75.

Li, M., D. Yee, T. R. Magnuson, O. Smithies, and K. M. Caron. 2006. 'Reduced maternal expression of adrenomedullin disrupts fertility, placentation, and fetal growth in mice', *J Clin Invest*, 116: 2653-62.

Liao, S. B., H. W. Li, J. C. Ho, W. S. Yeung, E. H. Ng, A. N. Cheung, F. Tang, and W. S. O. 2012. 'Possible role of adrenomedullin in the pathogenesis of tubal ectopic pregnancy', *J Clin Endocrinol Metab*, 97: 2105-12.

Liao, Y., G. K. Smyth, and W. Shi. 2013. 'The Subread aligner: fast, accurate and scalable read mapping by seed-and-vote', *Nucleic Acids Res*, 41: e108.

Liberzon, A., C. Birger, H. Thorvaldsdottir, M. Ghandi, J. P. Mesirov, and P. Tamayo. 2015. 'The Molecular Signatures Database (MSigDB) hallmark gene set collection', *Cell Syst*, 1: 417-25.

Liberzon, A., A. Subramanian, R. Pinchback, H. Thorvaldsdottir, P. Tamayo, and J. P. Mesirov. 2011. 'Molecular signatures database (MSigDB) 3.0', *Bioinformatics*, 27: 1739-40.

Love, M. I., W. Huber, and S. Anders. 2014. 'Moderated estimation of fold change and dispersion for RNA-seq data with DESeq2', *Genome Biol*, 15: 550.

Matson, B. C., S. L. Pierce, S. T. Espenschied, E. Holle, I. H. Sweatt, E. S. Davis, R. Tarran, S. L. Young, T. A. Kohout, M. van Duin, and K. M. Caron. 2017. 'Adrenomedullin improves fertility and promotes pinopodes and cell junctions in the peri-implantation endometrium', *Biol Reprod*, 97: 466-77.

McConkey, C. A., E. Delorme-Axford, C. A. Nickerson, K. S. Kim, Y. Sadovsky, J. P. Boyle, and C. B. Coyne. 2016. 'A three-dimensional culture system recapitulates placental syncytiotrophoblast development and microbial resistance', *Sci Adv*, 2: e1501462.

Melford, S. E., A. H. Taylor, and J. C. Konje. 2014. 'Of mice and (wo)men: factors influencing successful implantation including endocannabinoids', *Hum Reprod Update*, 20: 415-28.

Miller, P. B., B. A. Parnell, G. Bushnell, N. Tallman, D. A. Forstein, H. L. Higdon, 3rd, J. Kitawaki, and B. A. Lessey. 2012. 'Endometrial receptivity defects during IVF cycles with and without letrozole', *Hum Reprod*, 27: 881-8.

Modarres, P., S. Tanhaei, M. Tavalaee, K. Ghaedi, M. R. Deemeh, and M. H. Nasr-Esfahani. 2016. 'Assessment of DPY19L2 deletion in familial and non-familial individuals with globozoospermia and DPY19L2 genotyping', *Int J Fertil Steril*, 10: 196-207.

Morgan M, Falcon S and Gentleman R. 2017. GSEABase: Gene set enrichment data structures and methods. R package version 1.40.1.'

Namiki, T., J. Ito, and N. Kashiwazaki. 2018. 'Molecular mechanisms of embryonic implantation in mammals: Lessons from the gene manipulation of mice', *Reprod Med Biol*, 17: 331-42.

Paiva, P., E. Menkhorst, L. Salamonsen, and E. Dimitriadis. 2009. 'Leukemia inhibitory factor and interleukin-11: critical regulators in the establishment of pregnancy', *Cytokine Growth Factor Rev*, 20: 319-28.

Plaks, V., J. Rinkenberger, J. Dai, M. Flannery, M. Sund, K. Kanasaki, W. Ni, R. Kalluri, and Z. Werb. 2013. 'Matrix metalloproteinase-9 deficiency phenocopies features of preeclampsia and intrauterine growth restriction', *Proc Natl Acad Sci U S A*, 110: 11109-14.

Polanski, L. T., M. N. Baumgarten, S. Quenby, J. Brosens, B. K. Campbell, and N. J. Raine-Fenning. 2014. 'What exactly do we mean by 'recurrent implantation failure'? A systematic review and opinion', *Reprod Biomed Online*, 28: 409-23.

Quenby, S., M. Anim-Somuah, C. Kalumbi, R. Farquharson, and J. D. Aplin. 2007. 'Different types of recurrent miscarriage are associated with varying patterns of adhesion molecule expression in endometrium', *Reprod Biomed Online*, 14: 224-34.

Rahimipour M, M. Salehnia and M. Jafarabadi. Morphological, ultrastructural, and molecular aspects of in vitro mouse embryo implantation on human endometrial mesenchymal stromal cells in the presence of steroid hormones as an implantation model. 2018. *Cell Journal*, 20:369-376.

Rothbauer, M., N. Patel, H. Gondola, M. Siwetz, B. Huppertz, and P. Ertl. 2017. 'A comparative study of five physiological key parameters between four different human trophoblast-derived cell lines', *Sci Rep*, 7: 5892.

Ruane, P. T., S. C. Berneau, R. Koeck, J. Watts, S. J. Kimber, D. R. Brison, M. Westwood, and J. D. Aplin. 2017. 'Apposition to endometrial epithelial cells activates mouse blastocysts for implantation', *Mol Hum Reprod*, 23: 617-27.

Salker, M. S., J. Nautiyal, J. H. Steel, Z. Webster, S. Sucurovic, M. Nicou, Y. Singh, E. S. Lucas, K. Murakami, Y. W. Chan, S. James, Y. Abdallah, M. Christian, B. A. Croy, B. Mulac-Jericevic, S. Quenby, and J. J. Brosens. 2012. 'Disordered IL-33/ST2 activation in decidualizing stromal cells prolongs uterine receptivity in women with recurrent pregnancy loss', *PLoS One*, 7: e52252.

Shahbazi, M. N., A. Scialdone, N. Skorupska, A. Weberling, G. Recher, M. Zhu, A. Jedrusik, L. G. Devito, L. Noli, I. C. Macaulay, C. Buecker, Y. Khalaf, D. Ilic, T. Voet, J. C. Marioni, and M. Zernicka-Goetz. 2017. 'Pluripotent state transitions coordinate morphogenesis in mouse and human embryos', *Nature*, 552: 239-43.

Sharkey, A. M., and N. S. Macklon. 2013. 'The science of implantation emerges blinking into the light', *Reprod Biomed Online*, 27: 453-60.

Singh, H., and J. D. Aplin. 2015. 'Endometrial apical glycoproteomic analysis reveals roles for cadherin 6, desmoglein-2 and plexin b2 in epithelial integrity', *Mol Hum Reprod*, 21: 81-94.

Singh, H., L. Nardo, S. J. Kimber, and J. D. Aplin. 2010. 'Early stages of implantation as revealed by an in vitro model', *Reproduction*, 139: 905-14.

Smedley, D., S. Haider, S. Durinck, L. Pandini, P. Provero, J. Allen, O. Arnaiz, M. H. Awedh, R. Baldock, G. Barbiera, P. Bardou, T. Beck, A. Blake, M. Bonierbale, A. J. Brookes, G. Bucci, I. Buetti, S. Burge, C. Cabau, J. W. Carlson, C. Chelala, C. Chrysostomou, D. Cittaro, O. Collin, R. Cordova, R. J. Cutts, E. Dassi, A. Di Genova, A. Djari, A. Esposito, H. Estrella, E. Eyras, J. Fernandez-Banet, S. Forbes, R. C. Free, T. Fujisawa, E. Gadaleta, J. M. Garcia-Manteiga, D. Goodstein, K. Gray, J. A. Guerra-Assuncao, B. Haggarty, D. J. Han, B. W. Han, T. Harris, J. Harshbarger, R. K. Hastings, R. D. Hayes, C. Hoede, S. Hu, Z. L. Hu, L. Hutchins, Z. Kan, H. Kawaji, A. Keliet, A. Kerhornou, S. Kim, R. Kinsella, C. Klopp, L. Kong, D. Lawson, D. Lazarevic, J. H. Lee, T. Letellier, C. Y. Li, P. Lio, C. J. Liu, J. Luo, A. Maass, J. Mariette, T. Maurel, S. Merella, A. M. Mohamed, F. Moreews, I. Nabihoudine, N. Ndegwa, C. Noirot, C. Perez-Llamas, M. Primig, A. Quattrone, H. Quesneville, D. Rambaldi, J. Reecy, M. Riba, S. Rosanoff, A. A. Saddiq, E. Salas, O. Sallou, R. Shepherd, R. Simon, L. Sperling, W. Spooner, D. M. Staines, D. Steinbach, K. Stone, E. Stupka, J. W. Teague, A. Z. Dayem Ullah, J. Wang, D. Ware, M. Wong-Erasmus, K. Youens-Clark, A. Zadissa, S. J. Zhang, and A. Kasprzyk. 2015. 'The BioMart community portal: an innovative alternative to large, centralized data repositories', *Nucleic Acids Res*, 43: W589-98.

Sozen, B., G. Amadei, A. Cox, R. Wang, E. Na, S. Czukiewska, L. Chappell, T. Voet, G. Michel, N. Jing, D. M. Glover, and M. Zernicka-Goetz. 2018. 'Self-assembly of embryonic and two extra-embryonic stem cell types into gastrulating embryo-like structures', *Nat Cell Biol*, 20: 979-89.

Subramanian, A., P. Tamayo, V. K. Mootha, S. Mukherjee, B. L. Ebert, M. A. Gillette, A. Paulovich, S. L. Pomeroy, T. R. Golub, E. S. Lander, and J. P. Mesirov. 2005. 'Gene set enrichment analysis: a knowledge-based approach for interpreting genome-wide expression profiles', *Proc Natl Acad Sci U S A*, 102: 15545-50.

Sugihara, K., D. Sugiyama, J. Byrne, D. P. Wolf, K. P. Lowitz, Y. Kobayashi, M. Kabir-Salmani, D. Nadano, D. Aoki, S. Nozawa, J. Nakayama, T. Mustelin, E. Ruoslahti, N. Yamaguchi, and M. N. Fukuda. 2007. 'Trophoblast cell activation by trophinin ligation is implicated in human embryo implantation', *Proc Natl Acad Sci U S A*, 104: 3799-804.

Sun, X. L., J. Zhang, Y. Fan, J. H. Ding, J. H. Sha, and G. Hu. 2009. 'Aquaporin-4 deficiency induces subfertility in female mice', *Fertil Steril*, 92: 1736-43.

Tamm, K., M. Room, A. Salumets, and M. Metsis. 2009. 'Genes targeted by the estrogen and progesterone receptors in the human endometrial cell lines HEC1A and RL95-2', *Reprod Biol Endocrinol*, 7: 150.

Tamm-Rosenstein, K., J. Simm, M. Suhorutshenko, A. Salumets, and M. Metsis. 2013. 'Changes in the transcriptome of the human endometrial Ishikawa cancer cell line induced by estrogen, progesterone, tamoxifen, and mifepristone (RU486) as detected by RNA-sequencing', *PLoS One*, 8: e68907.

Tan, Y., X. Yin, S. Zhang, H. Jiang, K. Tan, J. Li, B. Xiong, F. Gong, C. Zhang, X. Pan, F. Chen, S. Chen, C. Gong, C. Lu, K. Luo, Y. Gu, X. Zhang, W. Wang, X. Xu, G. Vajta, L. Bolund, H. Yang, G. Lu, Y. Du, and G. Lin. 2014. 'Clinical outcome of preimplantation genetic diagnosis and screening using next generation sequencing', *Gigascience*, 3: 30.

Teklenburg, G., M. Salker, M. Molokhia, S. Lavery, G. Trew, T. Aojanepong, H. J. Mardon, A. U. Lokugamage, R. Rai, C. Landles, B. A. Roelen, S. Quenby, E. W. Kuijk, A. Kavelaars, C. J. Heijnen, L. Regan, J. J. Brosens, and N. S. Macklon. 2010. 'Natural selection of human embryos: decidualizing endometrial stromal cells serve as sensors of embryo quality upon implantation', *PLoS One*, 5: e10258.

Tepekoy, F., G. Akkoyunlu, and R. Demir. 2015. 'The role of Wnt signaling members in the uterus and embryo during pre-implantation and implantation', *J Assist Reprod Genet*, 32: 337-46.

Thie M, and HW Denker. In vitro studies on endometrial adhesiveness for trophoblast: cellular dynamics in uterine epithelial cells. 2002. *Cells Tissues Organs*, 172:237-52.

Tiscornia, G., O. Singer, and I. M. Verma. 2006. 'Production and purification of lentiviral vectors', *Nat Protoc*, 1: 241-5.

Uchida, H., T. Maruyama, K. Ohta, M. Ono, T. Arase, M. Kagami, H. Oda, T. Kajitani, H. Asada, and Y. Yoshimura. 2007. 'Histone deacetylase inhibitor-induced glycodelin enhances the initial step of implantation', *Hum Reprod*, 22: 2615-22.

Vandesompele, J., K. De Preter, F. Pattyn, B. Poppe, N. Van Roy, A. De Paepe, and F. Speleman. 2002. 'Accurate normalization of real-time quantitative RT-PCR data by geometric averaging of multiple internal control genes', *Genome Biol*, 3: RESEARCH0034.

Wang, H., and S. K. Dey. 2006. 'Roadmap to embryo implantation: clues from mouse models', *Nat Rev Genet*, 7: 185-99.

Wang, H., F. Pilla, S. Anderson, S. Martinez-Escribano, I. Herrer, J. M. Moreno-Moya, S. Musti, S. Bocca, S. Oehninger, and J. A. Horcajadas. 2012. 'A novel model of human implantation: 3D endometrium-like culture system to study attachment of human trophoblast (Jar) cell spheroids', *Mol Hum Reprod*, 18: 33-43.

Weimar, C. H., A. Kavelaars, J. J. Brosens, B. Gellersen, J. M. de Vreeden-Elbertse, C. J. Heijnen, and N. S. Macklon. 2012. 'Endometrial stromal cells of women with recurrent miscarriage fail to discriminate between high- and low-quality human embryos', *PLoS One*, 7: e41424.

White, F. J., R. C. Burghardt, J. Hu, M. M. Joyce, T. E. Spencer, and G. A. Johnson. 2006. 'Secreted phosphoprotein 1 (osteopontin) is expressed by stromal macrophages in cyclic and pregnant endometrium of mice, but is induced by estrogen in luminal epithelium during conceptus attachment for implantation', *Reproduction*, 132: 919-29.

Xie, F., G. Sun, J. W. Stiller, and B. Zhang. 2011. 'Genome-wide functional analysis of the cotton transcriptome by creating an integrated EST database', *PLoS One*, 6: e26980.

Zhang, Q., and J. Yan. 2016. 'Update of Wnt signaling in implantation and decidualization', *Reprod Med Biol*, 15: 95-105.

Chapter 2. Early implantation is characterized by compartment-specific transcriptional waves and specific biological pathways during co-culture *in vitro*

To date, characterization of embryo apposition and attachment to the epithelial surface remains incomplete. The relevance of these early steps to initiate a successful pregnancy has been highlighted in the literature, as it is understood to be critical for trophoblast differentiation, endometrial breaching and successful implantation (Ruane et al., 2017; Kelleher et al., 2018). In light of this, an important proportion of implantation failures could be caused by defective embryo-endometrium interaction during the first stages of apposition and attachment, before the decidua is invaded by the trophoblast.

In the previous Chapter, we concluded that the receptive epithelium is able to trigger a transcriptional response to the trophoblast challenge that the non-receptive epithelium cannot. The striking transcriptional changes found upon interaction between the trophoblast (modelled by JEG-3 cell line) and the receptive epithelium (modelled by Ishikawa cell line) at 48 hours, prompted us to investigate the transcriptional dynamics of both compartments at shorter timepoints using the same experimental approach.

The results included in **Chapter 2** are included in the manuscript "**The trophoblast-epithelium interaction is characterized by compartment-specific transcriptional waves and biological pathways during co-culture *in vitro***" (Paula Vergaro, M.Sc., Gustavo Tiscornia, Ph.D., Filippo Zambelli, Ph.D; Amelia Rodríguez, Ph.D , Josep Santaló, Ph.D , Rita Vassena, D.V.M. Ph.D), which is in preparation for submission.

1. Abstract

Study question: Which are the early compartment-specific transcriptional responses of the trophoblast and the endometrial epithelium throughout early attachment during implantation?

Summary answer: Successful attachment produced a series of dynamic changes in gene expression, characterized by an early and transient transcriptional up-regulation in the receptive epithelium, in contrast to a more dynamic transcriptional response in the trophoblast.

What is known already: Embryo implantation is the most limiting step in success of infertility treatments. However, the molecular mechanisms regulating human implantation remain poorly known. In order to understand the process of successful implantation and the establishment of pregnancy, a comprehensive description of the compartment-specific gene expression responses that both the embryo and the endometrium undergo during implantation is urgently required.

Study design, size, duration: We developed an *in vitro* model consisting of an endometrial epithelium proxy (confluent monolayers of the receptive cell line Ishikawa) co-cultured with spheroids of a Green Fluorescent Protein (GFP) expressing trophoblast cell line (JEG-3). After 0, 8, and 24 hours of interaction, the co-cultures were sorted by FACS; GFP+ (trophoblast spheroids) and GFP- (epithelial substrates) as well as non-co-cultured control fractions were collected for RNA extraction (in triplicate) and analyzed by RNA-seq.

Participants/materials, setting, methods: The transcriptional changes of both compartments (GFP+ trophoblast and GFP- epithelium) at different time points were analyzed using Illumina Hiseq 2500 system. Differential expression was performed with DESeq2; statistical significance was set at Log2 fold change ≥ 1 and p-value <0.05. Gene set enrichment analysis (GSEA) was performed using GOBP and Broad Hallmarks databases, with false discovery rate cut-off <0.1.

Main results and the role of chance: After 8 hours of co-culture, 200 genes were up-regulated and 95 genes were down-regulated in the epithelial compartment; from 8 to 24 hours, 127 genes were up-regulated and 131 were down-regulated. Trophoblast challenge induced a wave of epithelial transcriptional changes that resulted in over-representation of epithelial to mesenchymal transition (EMT), cell movement, apoptosis, hypoxia, inflammation, allograft rejection, myogenesis and cell signalling (e.g., TNFa/NFkb, KRAS, JAK-STAT cascades) at 8 hours. Interestingly, most pathways subsided at 24 hours (i.e., EMT, cell movement, allograft rejection, myogenesis and cell signalling), while others did not change (hypoxia, inflammation and

apoptosis). In the trophoblast compartment, the transcriptional changes upon co-culture were more dynamic. A total of 1201 and 46 genes were up- and down-regulated after 8 hours, respectively; from 8 to 24 hours, 458 genes were up-regulated and 23 were down-regulated. The GSEA revealed that angiogenesis and hypoxia were over-represented at both 8 and 24 hours, while EMT and cell signalling were only over-represented at 8 hours; from 8 to 24 hours, inflammation and estrogen response were enriched, while proliferation was under-represented.

Limitations, reasons for caution: Our *in vitro* model is based on cell lines of carcinoma origin; therefore, caution is warranted when extrapolating our results to other systems. Our 2-D model does not take into account the involvement of other cell types in the transcriptional changes during implantation.

Wider implications of the findings: We present a comprehensive description of the molecular events regulating early implantation in a time and compartment specific manner, providing a source of candidate molecules involved in successful embryo attachment.

Study funding/competing interest(s): This work was supported by intramural funding of Clínica EUGIN and by the Secretary for Universities and Research of the Ministry of Economy and Knowledge of the Government of Catalonia (GENCAT 2015 DI 050).

Keywords: Implantation; attachment; endometrial receptivity; transcriptomics

2. Introduction

Implantation is still a major bottleneck in human infertility treatments (Polanski et al., 2014). Recurrent implantation failure (RIF) is estimated to occur in approximately 4% of the IVF cycles (Koot et al., 2012), although estimates vary due to the existence of several somewhat different definitions of RIF in the literature. Implantation of the blastocyst stage embryo to the receptive endometrium, a sequential process involving apposition, attachment and invasion precedes the establishment of pregnancy (Wang and Dey, 2006). Successful implantation requires both embryo competence and endometrial receptivity, which are dynamic and highly regulated processes (Wang and Dey, 2006). Apart from genetic disorders, which are a major cause of implantation failure and miscarriage, embryo competence, quality and ultimately developmental potential depend on the embryo achieving the correct regulatory, signalling and metabolic states (Simon and Laufer, 2012; Hourvitz et al., 2006; Lundin, Bergh and Hardarson, 2001; Fu et al., 2009; Sjoblom et al., 2006).

A key determinant of these states are their underlying transcriptional dynamics; for instance, waves of embryonic transcriptional activation direct early development and the symmetry breaking needed for cell fate specification (Vassena et al., 2011; Shi et al., 2015). Endometrial receptivity, driven by ovarian steroids, results in a "window of implantation" which is also dependent on the establishment of correct transcriptional signatures (Diaz-Gimeno et al., 2011; Enciso et al., 2018). During every menstrual cycle, the endometrium undergoes cyclic proliferation and differentiation. If a viable embryo is present, invasive placentation and pregnancy occur; in its absence, the endometrium undergoes breakdown and repair (Evans et al., 2016). The stromal compartment of the endometrium plays an essential role in the establishment and maintenance of pregnancy; upon decidualization, this compartment becomes an embryo quality biosensor (Teklenburg et al., 2010; Brosens et al., 2014). Disordered decidualization is linked to defective embryo selection, which may be responsible for the extended receptivity and non-selective acceptance of low quality embryos in women suffering recurrent pregnancy loss (RPL). Conversely, too restrictive decidua leads to the rejection of high quality embryos and implantation failure (Salker et al., 2012; Weimar et al., 2012).

A particular aspect of a competent blastocyst and a receptive endometrium required to support successful implantation is their ability to coordinate their responses. Asynchrony or faulty molecular cascades occurring during embryo-endometrium interactions may lead to implantation failure, therefore limiting IVF success rates (Koot et al., 2016; Valdes, Schutt and Simon, 2017). The importance of the transcriptional regulation of trophoblast-decidual communication during early pregnancy and placentation has recently been reported (Vento-Tormo et al., 2018). However, the knowledge about the mechanisms regulating the first physical interaction at the maternal-fetal interface, i.e, apposition and attachment of the blastocyst to the epithelial surface, is still limited. Recent studies have demonstrated that molecular signals from the luminal epithelium regulate the trophoblast differentiation needed for barrier breaching during attachment and that uterine glands coordinate on-time implantation (Ruane et al., 2017; Kelleher et al., 2018). Previous studies have compared the individual transcriptional profiles of the preimplantation embryo and the receptive endometrium (Haouzi et al., 2011; Altmae et al., 2017). Nevertheless, the specific transcriptional dynamics of the trophoblast-epithelium cross-talk has not been examined in a compartment specific manner.

Our group has recently determined that the receptive epithelium reacts through a transcriptional response to trophoblast challenge that is severely muted when the epithelium is non-receptive

(Vergaro et al., 2019). Combining cell sorting and RNA-seq analysis, we have characterized the transcriptional responses that the trophoblast (modelled by spheroids of the JEG-3 trophoblast cell line) and the receptive epithelium (modelled by the Ishikawa endometrial epithelial cell line) undergo during the first 8 and 24 hours of attachment *in vitro*, as representative time points for the early and late events that take place during the implantation process. The GSEA revealed a transient transcriptional wave in the epithelium after 8 hours of co-culture, mainly characterized by over-representation of epithelial to mesenchymal transition (EMT), cell movement, apoptosis, hypoxia, inflammation, allograft rejection, myogenesis and cell signalling. Of note, most pathways were over-represented at 24 hours (i.e., EMT, cell movement, allograft rejection, myogenesis and cell signalling). By contrast, the trophoblast counterpart of the co-culture followed a more dynamic gene expression: a total of 1201 and 46 genes were up- and down-regulated after 8 hours, respectively; from 8 to 24 hours, 458 genes were up-regulated and 23 were down-regulated. The GSEA revealed that angiogenesis and hypoxia were over-represented at both 8 and 24 hours, while EMT and cell signalling were only over-represented at 8 hours; from 8 to 24 hours, inflammation and estrogen response were enriched, while proliferation was under-represented.

3. Materials and methods

Cell culture

The human endometrial adenocarcinoma cell line Ishikawa (European Collection of Authenticated Cell Cultures, UK; Cat. N. 99040201) was cultured in Minimum Essential Medium-alpha modification (MEM α, nucleosides, no phenol red) containing 5% fetal bovine serum, 10 mM of non-essential amino acids (MEM Non-Essential Amino Acids Solution) and 100 mg/ml streptomycin and 100 IU/ml penicillin (PenStrep). The human trophoblast choriocarcinoma cell line JEG-3 (American Type Culture Collection, USA; Cat. N. HTB-36) was cultured in Dulbecco's modified Eagle Medium (DMEM, high glucose, GlutaMAX™ supplement) supplemented with 10% fetal bovine serum, 1 mM sodium pyruvate and 100 mg/ml streptomycin and 100 IU/ml penicillin (PenStrep). Cells were maintained at 37ºC and media changed every other day. Unless specified, all reagents were obtained from Gibco, Thermo Fisher Scientific, USA.

Fluorescent trophoblast spheroids

Fluorescent spheroids of the trophoblast cell line JEG-3 were generated by transduction with recombinant lentiviral particles expressing GFP from a PGK promoter (Tiscornia et al., 2006). Briefly, trophoblast cells were grown on 12-well plates until cultures reached 70% confluence. Lentiviral particles were added to the culture at a multiplicity of infection (MOI) of 10. Trophoblast cells with the highest GFP levels were collected by fluorescence-activated cell sorting (FACS) and cultured further. To generate spheroids, suspensions of GFP positive JEG-3 cells were adjusted to a $3x10^4$ cells/ml concentration; 100 µl were seeded in U-bottom ultra-low attachment 96-well plates (Corning, NY, USA) and centrifuged at room temperature during 10 min at 250 x g. The plates were kept for 48 hours at 37ºC and 5% CO_2, resulting in spheroids of around 250 µM diameter.

***In vitro* co-culture assay**

In order to analyze the transcriptional dynamics during the first 24 hours of trophoblast-epithelium interaction, an *in vitro* system modelling embryo attachment was established as previously described (Vergaro et al., 2019) (**Figure 1**). Briefly, Ishikawa cells were used as substrates representing the receptive endometrial epithelium, while GFP positive JEG-3 spheroids represented the embryo trophoblast. The epithelial substrates were grown in 96-well plates (Nunc, Thermo Fisher Scientific, USA) until cells reached confluence; trophoblast spheroids were individually seeded on each well on top of a confluent epithelial substrate. In parallel to co-cultures, 96 well plates with confluent Ishikawa cells only or U-bottom ultra-low attachment 96-well plates with trophoblast spheroids only were kept in culture as experimental controls. At time points 0 hours, 8 hours and 24 hours, all the co-cultures and controls were harvested from the 96-well plates using TrypLE™ Express Enzyme and pooled in single cell suspensions for cell sorting. All reagents were purchased from Gibco, Thermo Fisher Scientific, USA. *In vitro* co-culture assays and controls were repeated in triplicate as independent experiments.

Cell sorting and RNA extraction

After co-culture, fluorescence-activated flow cytometry (FACS; BD FACS Aria Fusion II cell sorter (BD Biosciences, USA) was used to separate GFP positive trophoblast cells from non-fluorescent epithelial substrates from each co-culture at the different time points (0, 8 and 24 hours). In each experimental replicate, 10 cell fractions were obtained (a total of 30 cell fractions). Cell suspensions were maintained on ice and the cytometer chamber was cooled to 4ºC before cell

sorting. To eliminate possible cellular aggregates, cell suspensions were filtered through a 70 µm mesh before sorting and 100 µm sorter nozzles were used to minimize clog formation. Diamidino-2-phenylindole (DAPI) staining allowed excluding dead cells from the isolated cell populations. GFP positive and GFP negative fractions were collected in 50 µl of DPBS without calcium or magnesium and kept on ice. After centrifugation, cell pellets were stored at -80ºC until processed. RNA from each of the 30 fractions (10 fractions from three independent experiments) was isolated using RNeasy Mini Kit (Qiagen N. V., Netherlands) following the manufacturer´s instructions. RNA was eluted in 30 µl nuclease free water and purified using RNase-Free DNase Set (Qiagen N. V., Netherlands). RNA concentration was measured by fluorometric quantitation (QuBit, Thermo Fisher Scientific, USA) and high RNA integrity number (RIN) was determined by Bioanalyzer 2100 System (Agilent Technologies, USA), ranging from 8.6 to 10 in all samples.

cDNA Library Preparation and RNA-seq

A total of 30 RNA samples (3 experimental replicates of each of the 10 cell populations sorted by FACS) were used for cDNA library preparation and subjected to RNA-seq analysis. All 30 samples were subjected to quality control before polyA mRNA purification using NEBNext Poly(A) mRNA Magnetic Isolation Module (New England Biolabs, USA) according to the manufacturer's instructions. cDNA generation, End repair and Ligate Adaptor for Illumina were performed using the kit NEBNext Ultra II RNA Library Prep for Illumina, following the manufacturer's instructions. The minimum number of required cycles was established by amplifying samples with SYBR Green. Each sample was labelled with a specific barcode during the amplification by the NEBNext Multiplex Oligos kit for Illumina (Index Primers Set 1). Three equimolar pools of 10 samples were generated; each pool was sequenced in a single 50 nt Single Read lane of an Illumina Hiseq 2500 system, getting over 30 million reads per sample.

RNA-Seq data analysis

The STAR software v2.3.0e (Dobin et al., 2013) with default parameters was used to align reads to the hg19 version of the human genome. Once aligned, reads were binarized, sorted with sambamba v0.5.9 (http://lomereiter.github.io/sambamba/) and imported to R (https://www.R-project.org/) with the inbuilt annotation in the Rsubread package (Liao, Smyth and Shi, 2013). Biomart (Smedley et al., 2015) was used as a source for further annotations using the corresponding R package. Taking into account processing batch as covariate, differential expression was analyzed with DESeq2 (Love, Huber and Anders, 2014).

Functional analysis

The pre-ranked version of Gene Set Enrichment Analysis (GSEA) was used to assess pathway enrichment (Subramanian et al., 2005) and applied to the ranking defined by the log2 Fold Change (log2FC) of the differential expression analysis using DESeq2. Gene sets for analyses were part of the Gene Ontology (GO) (Ashburner et al., 2000) as included in the GSEABase R package (Morgan, 2017), or of the Hallmark collection (Liberzon et al., 2015) after retrieval from the MsigDB (Liberzon et al., 2011). The false discovery rate (FDR) cut-off for significance was set at 0.1. For visualization of Broad Hallmark gene sets, plots were generated with Circos version 0.67 (Krzywinski et al., 2009).

Statistical analysis

Differential gene expression between the cell fractions collected after FACS was analyzed by linear regression and pairwise comparison. Cut-off for statistical significance was set at absolute log2 fold change (log2FC) ≥1 and adjusted p value <0.05 (with Benjamin-Hochberg correction for multiple comparisons).

RNA-seq validation by quantitative PCR (qPCR)

RNA-seq results were validated by qPCR using 5 ng (in triplicates) of the same cDNA libraries previously obtained. The expressions of selected genes (*CYP19A1*, *CGA*, *SPDYC*, *CASC1*, *TGFA*, *PROM1*, *PRUNE2* and *SLC30A2*) were quantified in a final volume of 20µl using 2x SsoAdvanced Universal SYBR Green Supermix (BioRad, Hercules, CA, USA) on a CFX Real-Time PCR platform (Bio-Rad, Hercules, CA, USA). Forward and reverse primer sequences (5´- 3´) were the following: GTGGACGTGTTGACCCTTCT and CACGATAGCACTTTCGTCCA) for *CYP19A1*, TCTGGTCACATTGTCGGTGT and TTCCTGTAGCGTGCATTCTG for *CGA,* TCAGCCTTCTGGAGGACAGT and CACCATGGCCAGGAGATACT for *SPDYC*, GGTGGGATGCTGAAGGTAAA and AAAGGTGTCCAGGCTGAATG for *CASC1*, TTCCCACACTCAGTTCTGCTT and ACGTACCCAGAATGGCAGAC for *TGFA* GCCACCGCTCTAGATACTGC and GCTTTTCCTATGCCAAACCA for *PROM1*, and TTATGCAGAGCATGGGTGTC and GAAGGTGCAGATGGGGTCTA for *SLC30A2*. *PPIB*, *MAP4K4* and *GUSB* were selected as the most stable housekeeping genes using the Integrated Cotton EST Database (Xie et al., 2011); forward and reverse primer sequences (5´-3´) were the following: CATGTGGTGTTTGGCAAAGT and TTTATCCCGGCTGTCTGTCT for *PPIB*, CTTGGATGGTGTGTTCATGC and AGACCGAACAGAGGCAAAGA for *MAP4K4* and

AAACGATTGCAGGGTTTCAC and CTCTCGTCGGTGACTGTTCA for *GUSB*. Specificity of the qPCR products was confirmed by analyzing the melting curves. Gene expression data were calculated as the ratio between the gene expression values of the selected genes and the geometric average of *PPIB*, *MAP4K4* and *GUSB* expressions (Vandesompele et al., 2002).

4. Results

Along the 24 hours of co-culture, the trophoblast spheroids showed increasing attachment and outgrowth throughout the epithelial monolayer (**Figure 2A**, **B**). The cell fractions were isolated by FACS at different time points (0, 8 and 24 hours) and analyzed by RNA-seq profiling. Each co-culture gave rise to a GFP positive (JEG-3 trophoblast spheroids) and a GFP negative (Ishikawa epithelial substrates) cell populations; non-co-cultured controls of both cell types were also independently sorted. A total of 10 gene expression datasets were obtained (**Table I**). Pairwise comparisons of co-cultured cells and their respective non-co-cultured controls were used to analyze the effect of the trophoblast-epithelium interaction on the compartment specific transcriptional profile over time, divided in two stages of co-culture: stage I (from 0 to 8 hours) and stage II (from 8 to 24 hours). The gene expression profile of co-cultured fractions for 8 hours and 24 hours were compared to those of 0 hours and 8 hours, respectively. RNA-seq results have been submitted to the Gene Expression Omnibus (GEO) repository (accession number to be determined).

Principal component analysis

Principal component analysis (PCA) was used as quality control to identify technical bias between the three independent experiments (**Supplementary Figure 1**). PCA revealed concordant clustering among sample groups and experimental triplicates; the first component (PC1) explained 87.2% of the sample variability.

Gene expression dynamics of the epithelial substrates induced by co-culture with trophoblast spheroids for 8 and 24 hours

Analysis of differential gene expression between non-co-cultured epithelial substrates during stage I and stage II reflected the effect of the time of culture on the epithelium transcriptome; no genes were differentially expressed in non-co-cultured epithelial controls during stage I (I-c T8 *vs*. I-c

T0) and stage II of culture (I-c T24 *vs.* I-c T8) (**Figure 3.A** and **B**), indicating cultures were transcriptionally stable over these timeframes. Co-culture during stage I (I-co-S T8 *vs*. I-c T0) resulted in 295 genes differentially expressed in the epithelial substrates (200 genes up-regulated and 95 down-regulated (**Figure 3.C**; **Supplementary File S1**).

Co-culture during stage II (I-co-S T24 *vs*. I-co-S T8) resulted in differential expression of 258 genes, of which 127 genes were up-regulated and 131 genes were down-regulated; **Figure 3.D**; **Supplementary File S2**). A total of 124 genes were differentially regulated in both stages. Interestingly, 62 out of 124 genes were up-regulated during stage I (I-co-S T8 *vs*. I-c T0), and subsequently down-regulated during stage II (I-co-S T24 *vs*. I-co-S T8), indicating an early wave of upregulation during stage I that subsequently subsided during stage II (**Supplementary File S3**).

Gene expression dynamics of the trophoblast spheroids induced by co-culture with epithelial substrates for 8 and 24 hours

Regarding the transcriptomic changes due to time of culture on the trophoblast compartment, no genes were differentially expressed in the non-co-cultured trophoblast spheroids control during stage I (S-c T8 *vs*. S-c T0; **Figure 3E**). Only 6 genes changed their expression levels during stage II (S-c T24 *vs*. S-c T8); of these, 4 were up-regulated (*PLAC8*, *NRN1*, *IL2RB* and *RHPN1)*, while 2 were down-regulated (*CES1* and *STX11*) (**Figure 3F**).

The variations in gene expression levels on the trophoblast cells associated to the co-culture were numerous. During stage I, spheroids co-cultured with the epithelial substrate (S-co-I T8 *vs*. S-co-I T0) showed differential expression of 1247 genes, of which 1201 and 46 genes were up- and down-regulated, respectively (**Figure 3G**; **Supplementary File S4**). During stage II, 481 genes were differentially expressed, of which 458 genes were up-regulated and 23 genes were down-regulated (S-co-I T24 *vs*. S-co-I T8; **Figure 3H**; **Supplementary File S5**).

Comparing the differentially expressed genes in both stages of co-culture, 260 genes were found to be common between these timeframes (S-co-I T8 *vs.* S-c T0 and S-co-I T24 *vs.* S-co-I T8); most of these genes were persistently up-regulated at both 8 *vs*. 0 hours and at 24 *vs*. 8 hours (252/260) (**Supplementary File S6**).

GSEA of the epithelial substrates

We performed GSEA using GOBP and Broad Hallmarks annotations to identify the biological pathways over-represented in the epithelial substrates during both stages of co-culture. GOBP which were over- or under-represented in epithelial substrates during stage I and stage II are listed in **Tables II** and **III**, respectively. Broad Hallmarks for both stages are illustrated in **Figure 4**. Briefly, during the early interaction with the trophoblast (stage I), the enriched pathways were related to cell movement (e.g. actin-mediated cell contraction, actin-myosin filament sliding and actomyosin structure organization), epithelial to mesenchymal transition (EMT), endocrine response (e.g. endocrine hormone secretion and response to gonadotropin stimulus), cell cycle (e.g. positive regulation of cell cycle and apoptosis), morphogenesis (e.g. cell differentiation involved in embryonic placenta development, myogenesis and tissue morphogenesis), cell signalling (e.g. negative regulation of cAMP metabolic process, regulation of signal transduction by P53 class mediator and regulation of JAK-STAT cascade) and immune response (e.g. inflammatory response and allograft rejection). Many of the pathways over-represented in stage I were found to be under-represented in the second stage of culture (from 8 to 24 hours), including heterophilic cell-cell adhesion actin-mediated cell contraction, rRNA related processes (e.g. ribosome biogenesis, rRNA processing and ncRNA processing) and signalling (e.g. IL6 JAK STAT3 signalling and TNFa signalling via NFKb).

GSEA of the trophoblast spheroids

The trophoblast spheroids were also subjected to a GSEA analysis like that performed on the epithelial compartment. The GOBP annotation terms over-represented in stage I (S-co-I T8 *vs*. S-c T0) are included in **Table VI**; no GOBP annotation term was over-represented in stage II (S-co-I T24 *vs*. S-co-I T8). Significant Broad Hallmarks during both stages are illustrated in **Figure 5**. During stage I, EMT, angiogenesis, signalling (e.g. KRAS signalling up and Wnt beta Catenin signalling) as well as hypoxia were enriched; by contrast, pathways related to protein processing (e.g. tRNA aminoacylation, tRNA modification and unfolded protein response) were under-represented. At 24 hours of co-culture, enriched pathways included hypoxia and angiogenesis as well as inflammatory and estrogen responses. Conversely, cell proliferation pathways (e.g. E2F targets, G2M checkpoint and MYC targets v1 and v2) were under-represented.

RNA-seq validation

The RNA-seq results were validated by confirming gene expression patterns of up- and down-regulation of selected candidates. As in the RNA-seq data, *CYP19A1*, *CGA*, *TGFA* and *PROM1* were up-regulated, while *SPDYC*, *CASC1* and *SLC30A2* were down-regulated (**Figure 6**).

5. Discussion

We used an *in vitro* model to perform a comprehensive transcriptional analysis of trophoblast-epithelium interactions during human implantation. Most transcriptomic studies in human have focused either on endometrial function and receptivity, aiming to understand the maternal mechanisms during implantation treatments (Koler et al., 2009; Altmae et al., 2010; Ledee et al., 2011; Diaz-Gimeno et al., 2011; Ulbrich, Groebner and Bauersachs, 2013; Sebastian-Leon et al., 2018; Enciso et al., 2018) or, alternatively, gene expression regulating human pre-implantation embryo development (Vassena et al., 2011; Blakeley et al., 2015; Petropoulos et al., 2016; Stirparo et al., 2018). However, analysis of the molecular cross-talk during implantation has required development of *in vitro* models (Genbacev et al., 2003; Tapia et al., 2008; Green, Fraser and Day, 2015; Aberkane et al., 2018; Cheng et al., 2017; Heneweer et al., 2003; Laheri et al., 2018; Kakar-Bhanot et al., 2019). Surprisingly, only a few studies have used transcriptomics (Moreno-Moya et al., 2015; Huang et al., 2018; Popovici et al., 2006).

By co-culturing GFP+ trophoblast spheroids with GFP- receptive epithelial cells and separating them by FACS, we have analyzed the transcriptomic response of each element of the model to the other during early and late phases of apposition and attachment.

Trophoblast attachment is characterized by an early transient transcriptional wave in the luminal epithelium

Our data showed that, overall, the co-culture induced a transient wave of transcriptional up-regulation in the endometrial epithelium during the first 8 hours, with many of the up-regulated pathways being down-regulated from 8 to 24 hours. Several genes showed interesting patterns of expression. The most highly differentially expressed gene in stage I was *CYP19A1*, which has been shown to be involved in decidualization as well as increased susceptibility to unexplained female infertility and endometriosis (Altmae et al., 2009; Gibson et al., 2013).

Other differentially expressed genes are considered endometrium-specific (Uhlen et al., 2015), including *CPXM1*, *TMEM158, SOX17* and *ZCCHC12. CPXM1* has been associated with early-onset preeclampsia (Song, Li and An, 2015); *TMEM158* gene expression has been found down-regulated in the post-implantation luminal epithelium of mice compared to that on the preimplantation period (Xiao et al., 2014). SOX17 has been involved in embryo attachment, since it is predominantly located at the luminal epithelium in mice and shows increased levels at the embryo attachment sites (Wallingford, Angelo and Mager, 2013; Hirate et al., 2016); of note, *sox17* haploinsufficiency results in female subfertility and implantation failure in mice (Hirate et al., 2016). *ZCCHC12* (zinc finger CCHC-type containing 12) encodes a transcriptional coactivator in the bone morphogenetic protein (BMP)-signalling pathway (Cho et al., 2008). Although a role in implantation has not been reported, it has been identified as a marker of endometrial receptivity (Hu et al., 2014).

CEMIP (hyaluronic acid binding protein) which positively regulates cell migration by increasing EMT (Liang et al., 2018) was down-regulated during stage II (8 to 24 hours of co-culture), in accordance with the downregulation of biological pathways related with cell motility and EMT. Another interesting candidate is PGR (Progesterone receptor). The depletion of epithelial *PGR* expression levels is a marker of murine endometrial receptivity (Wetendorf et al., 2017); a recent study found that FOXO1-PGR signalling is related to epithelial depolarization and tissue integrity (Vasquez et al., 2018). Our data showed that *PGR* expression did not change in stage I but was up-regulated during stage II, suggesting that after the initial trophoblast-epithelium interaction and barrier breaching, up-regulation of *PGR* is needed to initiate the reconstruction of the epithelial lining.

Regulation of EMT, inflammation and immune response precedes epithelial breeching

The luminal epithelium is the first physical barrier that the embryo needs to breach during implantation. EMT has been suggested as a mechanism to reorganize the structure of the luminal epithelium in order to accommodate the implanting trophoblast and also to regenerate the epithelial tissue once breaching is complete (Uchida et al., 2012; Stone et al., 2016). The roles of inflammatory and immune responses in implantation have also been extensively reported, as reviewed elsewhere (Singh, Chaudhry and Asselin, 2011; Mor et al., 2011; Granot, Gnainsky and Dekel, 2012; Dekel et al., 2014). Increased levels of tumor necrosis factor-α (TNF-α) and Interleukin-6 (IL-6) have been found in women suffering from miscarriage and pathological pregnancies (Quenby et al., 1999; Lockwood et al., 2008; Banerjee et al., 2013). These molecules

interact with Interleukin-11 (IL-11), leukemia inhibitory factor (LIF) and the JAK/STAT pathway, all of them known players in endometrial receptivity and implantation (Dimitriadis et al., 2007; Dimitriadis et al., 2010; Singh, Chaudhry and Asselin, 2011). We found that EMT related pathways as well inflammatory and immune responses (i.e. TNFa signalling via NFKb, IL6-JAK/STAT3 signalling and allograft rejection) were enriched in the substrate during stage I but under-represented as the co-culture progressed through stage II. This could reflect the *in vivo* event of EMT mediate epithelial breaching followed by downregulation of EMT to rebuild the epithelial lining. Activation of other biological pathways could assist the epithelial breaching, namely apical junction, actin filament-based movement and contraction and apoptosis. TGF beta signalling, which we also found enriched in stage I but not stage II, could also be involved in the process, as it has been shown to upregulate the expression of matrix metalloproteinases that promote trophoblast invasion (Jones et al., 2006).

The transcriptional regulation of the trophoblast compartment during attachment is more dynamic than that of the endometrial epithelium

After interacting with the epithelium, the transcriptional response of the trophoblast spheroids followed a more dynamic pattern; overall, it was characterized by early up-regulation during stage I that continued through stage II (from the common 260 genes differentially expressed at stages I and II, 252 were up-regulated at both stages). Several of these genes were included in the Human Protein Atlas database as specific from placenta, showing up-regulation at both stages (*PABPC4L, HOXA13, BIRC7* and *HES7*). Other placental-associated genes were only up-regulated in stage I (*ADAMTS15, IGFBP3* and *SPP1*) or in stage II (*JAM2* and *FLT1*) in our data. These molecules have been related with trophoblast proliferation and invasion (e.g. *IGFBP3*, *SPP1*, *BIRC* and *TIMP3*) (Gleeson et al., 2001; Wu, Liu and Xie, 2015; Li et al., 2006; Whiteside et al., 2001; Chen and Khalil, 2017), placental vascularization (e.g. *HOXA13*) (Shaut et al., 2008), attachment to the endometrial epithelium (e.g. *JAM2*) (Su et al., 2012) and angiogenesis (e.g. *FLT1*) (Douglas et al., 2014). Trophinin has been related to trophoblast invasion due to its dual action on promoting trophoblast proliferation and inducing endometrial epithelium apoptosis (Sugihara et al., 2007). In agreement with the literature, trophinin was up-regulated in the trophoblast spheroids during both stages I and II of our study, suggesting that trophinin could be a marker of successful implantation.

Trophoblast attachment requires time-specific regulation of a wide range of molecular pathways

Our data suggested a number of biological pathways previously related to trophoblast invasion and placental development, such as EMT, the Wingless/β-catenin pathway (canonical Wnt cascade), hypoxia and reduced proliferation (Davies et al., 2016; Knofler and Pollheimer, 2013; Caniggia et al., 2000; Velicky et al., 2018). Trophoblast inflammatory response was up-regulated after 24 hours but not before; once the epithelium is breached, inflammation could act as a regulatory mechanism to prevent excessive invasion. Interestingly, angiogenesis was continuously increased along the 24 hours of co-culture; if extrapolated to the *in vivo* situation, the transcriptional up-regulation during this early time could prime the signalling needed for the future remodelling of maternal vasculature during placental development (Zhou, Genbacev and Fisher, 2003; Kuo et al., 2019). Regulation of unfolded protein response, which is linked to endoplasmic reticulum stress, has been related with placental development (Burton and Yung, 2011; Yung et al., 2014). Our data suggested a modulation of this system in the trophoblast compartment, with under-representation of unfolded protein response during stage I. Hypoxia (continuously enriched throughout both stages) and reactive oxygen species pathway (under-represented in stage I) might take part in this regulation.

In summary, we provide a 2-D *in vitro* system that mimics the early trophoblast attachment and allowed us to characterize the transcriptional dynamics and the molecular mechanisms regulating successful implantation. The comparison of the transcriptional profiles from non-co-cultured experimental controls at different time points confirmed that the transcriptional changes were due to the co-culture and not to cell culture conditions. Additionally, the compartmentalization allowed us to discriminate the processes that are important for trophoblast invasion and epithelial breaching upon trophoblast-epithelium interaction. Compared to previous studies, this methodological advantage provided lists of compartment specific candidate genes and suggested the need to focus not only on embryo quality and endometrial receptivity but also on their reciprocal crosstalk and molecular responses. Future confirmation in primary cells would be useful to find markers of implantation failure with clinical application in both assisted conception and contraception.

Our model could be improved in different ways; the addition of other components of the implantation environment, i.e. stromal, endothelial as well as immune and stem cells, would add great value due to their known interactions (Arnold et al., 2001; Evron, Goldman and Shalev, 2011; Brighton et al., 2017; Vento-Tormo et al., 2018). Although the system comprises embryo and epithelium proxies from carcinoma nature, therefore limiting the extrapolation of our results, these two cell lines have been broadly used for similar purposes. The trophoblast JEG-3 cell line present

transcriptional profile and secretory activity similar to those from primary trophoblasts (McConkey et al., 2016). Likewise, Ishikawa cell line has been selected in many studies as a model for receptive epithelium and normal endometrial function (Singh et al., 2010; Berger et al., 2015; Schaefer et al., 2010; Ruane et al., 2017; Aberkane et al., 2018). However, despite their hormonal responsiveness *in vitro*, Ishikawa cells do not reflect the switch from non-receptive to receptive status driven by the steroid hormone levels *in vivo* (Tamm-Rosenstein et al., 2013) so they are constitutively receptive to the trophoblast and, therefore, hormonal supplementation during co-culture is not required (Ruane et al., 2017).

In conclusion, the successful interaction between the trophoblast and the receptive epithelium preceding the establishment of pregnancy relies on transcriptional programs that are regulated in space and time specific manner. This process is characterized by an early and transient transcriptional up-regulation in the receptive epithelium; in contrast, the transcriptional response of the trophoblast is less structured, with overall up-regulation throughout both stages and involving a different pathways at each stage.

Authors roles

P.V.: designed and performed the experiments, interpreted the data and drafted the manuscript. G.T.: designed and supervised the study, interpreted the data and edited the manuscript. F.Z.: designed data visualization and provided critical discussion. A.R.: supervised the study. J.S.: supervised the study, provided critical discussion and edited the manuscript. R.V.: designed and supervised the study, provided critical discussion and edited the manuscript.

Acknowledgements

The authors wish to thank all members from the Basic Laboratory of Clínica EUGIN for helpful discussion, especially Montserrat Barragán and Anna Ferrer; members from the Biostatistics/Bioinformatics facility of the Institute for Research in Biomedicine (Barcelona) for bioinformatics analysis and Prof. Daniel Grinberg from Universitat de Barcelona for technical support.

Funding

This work was supported by intramural funding of Clínica EUGIN and by the Secretary for Universities and Research of the Ministry of Economy and Knowledge of the Government of Catalonia (GENCAT 2015 DI 050).

Conflict of interest

None of the authors has competing interest to declare.

6. Figures

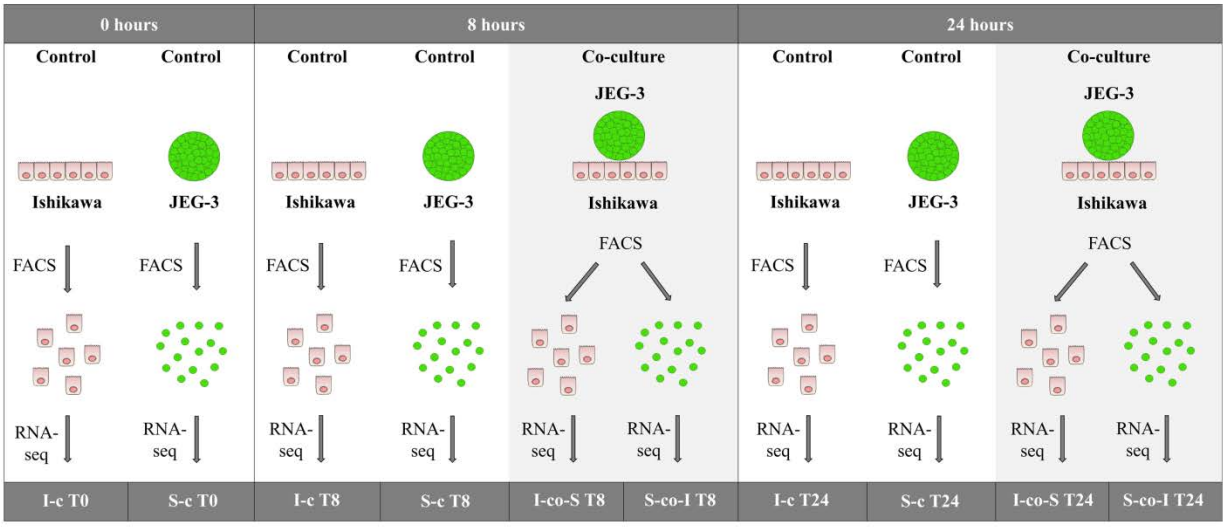

Figure 1. Scheme representing the experimental design: monolayers of receptive epithelium (Ishikawa) were co-cultured with GFP positive trophoblast spheroids (JEG-3) for 0, 8 and 24 hours, or maintained in mono-cultures for the same time intervals as controls. The following cell fractions were obtained and profiled by RNA-seq: Ishikawa control at 0 hours (I-c T0), GFP+ JEG-3 spheroids control at 0 hours (S-c T0), Ishikawa control at 8 hours (I-c T8), GFP+ JEG-3 spheroids control at 8 hours (S-c T8), Ishikawa substrates co-cultured with JEG-3 spheroids for 8 hours (I-co-S T8), GFP+ JEG-3 spheroids co-cultured with Ishikawa substrates for 8 hours (S-co-I T8), Ishikawa control at 24 hours (I-c T24), GFP+ JEG-3 spheroids control at 24 hours (S-c T24), Ishikawa substrates co-cultured with JEG-3 spheroids for 24 hours (I-co-S T24) and GFP+ JEG-3 spheroids co-cultured with Ishikawa substrates for 8 hours (S-co-I T24).

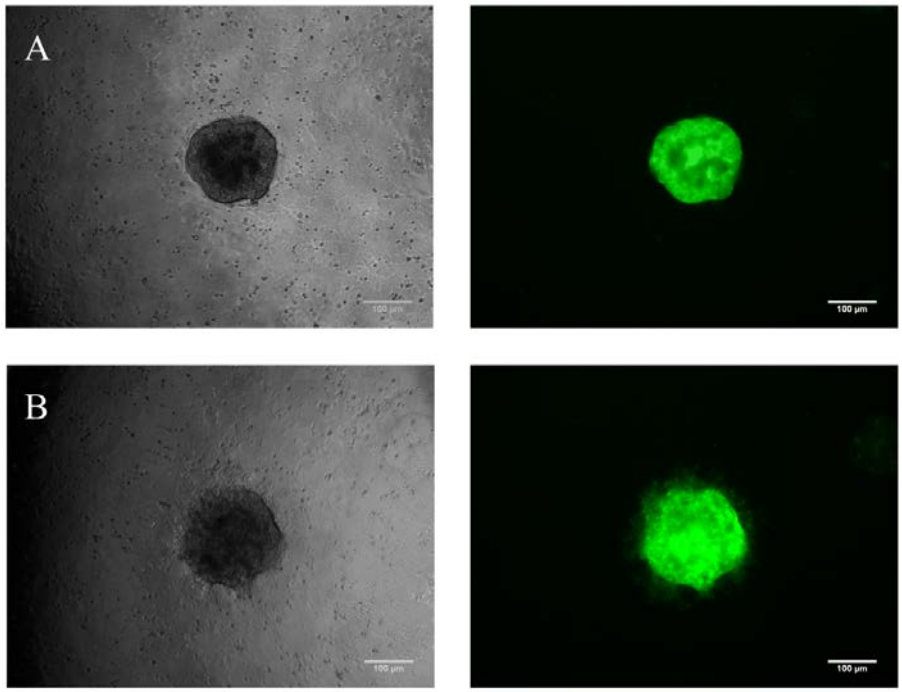

Figure 2. Representative images of GFP+ trophoblast spheroids co-cultured with Ishikawa cell monolayers for 8 hours (A) and 24 hours (B) visualized under 10X magnification with Nikon TE-200 inverted fluorescence microscope (Nikon Corporation, Tokyo, Japan).

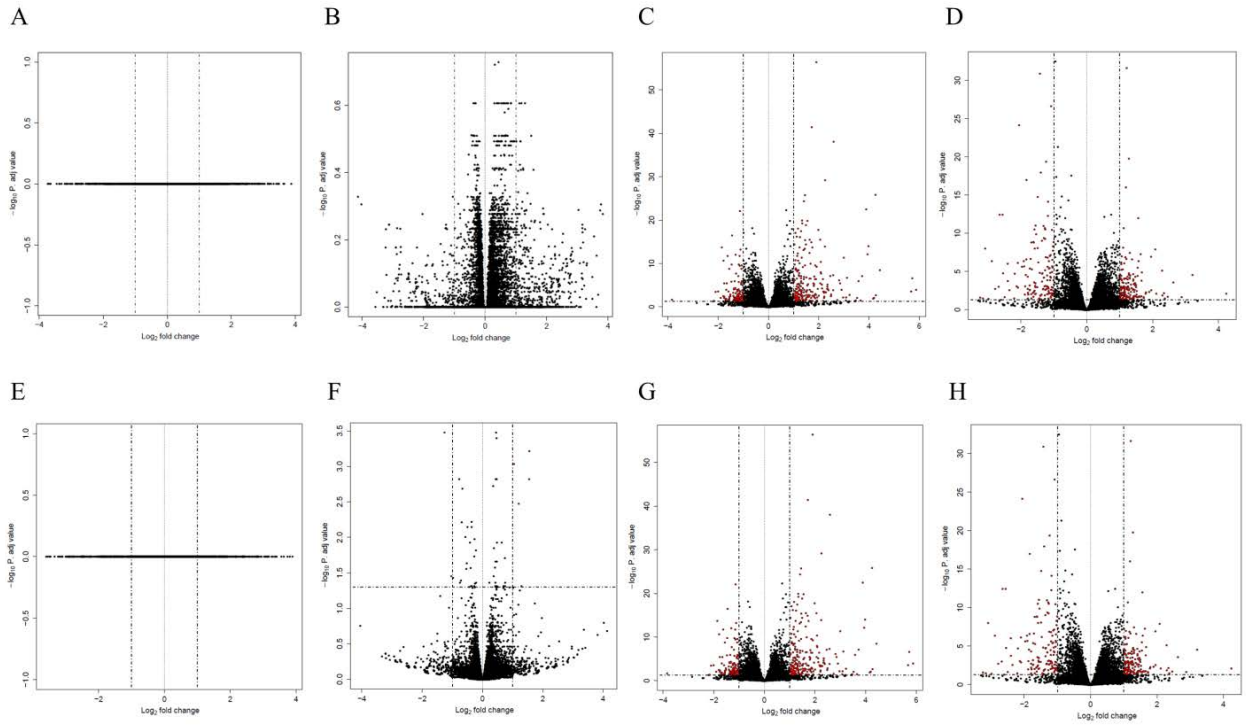

Figure 3. Volcano plots of differentially expressed genes, represented as red dots (Log2FC ≥1, adjusted p-value <0.05) between sorted non-co-cultured controls as well as co-cultured GFP+ and GFP- cells fractions in pairwise comparisons: **(3.A)** Ishikawa control at 8 hours *vs*. Ishikawa control at 0 hours (I-c T8 *vs*. I-c T0), **(3.B)** Ishikawa control at 24 hours *vs*. Ishikawa control at 8 hours (I-c T24 *vs*. I-c T8), **(3.C)** Ishikawa substrates co-cultured with JEG-3 spheroids for 8 hours *vs*. Ishikawa control at 0 hours **(**I-co-S T8 *vs*. I-c T0), **(3.D)** Ishikawa substrates co-cultured with JEG-3 spheroids for 24 hours *vs*. Ishikawa substrates co-cultured with JEG-3 spheroids for 8 hours (I-co-S T24 *vs*. I-co-S T8), **(3.E)** JEG-3 spheroids control at 8 hours *vs*. JEG-3 spheroids control at 0 hours **(**S-c T8 *vs*. S-c T0), **(3.F)** JEG-3 spheroids control at 24 hours *vs*. JEG-3 spheroids control at 8 hours (S-c T24 *vs*. S-c T8), **(3.G)** JEG-3 spheroids co-cultured with Ishikawa substrates for 8 hours *vs*. JEG-3 spheroids control at 0 hours (S-co-I T8 *vs*. S-c T0), **(3.H)** JEG-3 spheroids co-cultured with Ishikawa substrates for 24 hours *vs*. JEG-3 spheroids co-cultured with Ishikawa substrates for 8 hours (S-co-I T24 *vs*. S-co-I T8).

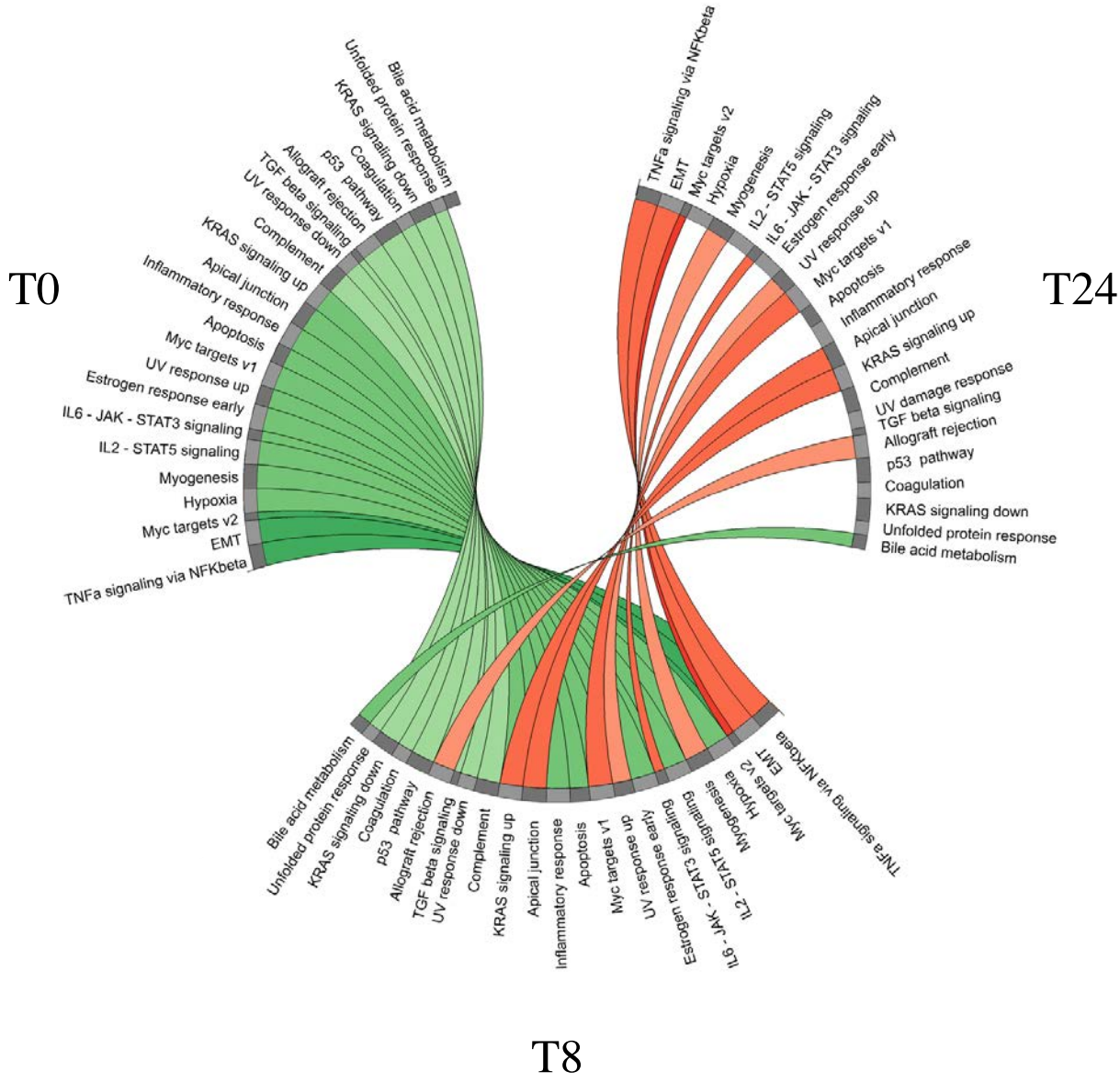

Figure 4. Graphical representation of the Broad Hallmark (BH) gene sets modulation in Ishikawa epithelial substrates co-cultured for 8 and 24 hours with JEG-3 spheroids. Ishikawa non-co-cultured cells were used as T0. Ribbons are colour coded based on the normalized enrichment score (NES) of the pairwise comparison (very dark colours with |NES|>2, dark colours with 1.5<|NES|<2, and light colours with |NES|<1.5). Green and red colours represent enrichment or depletion of the BH gene set, respectively.

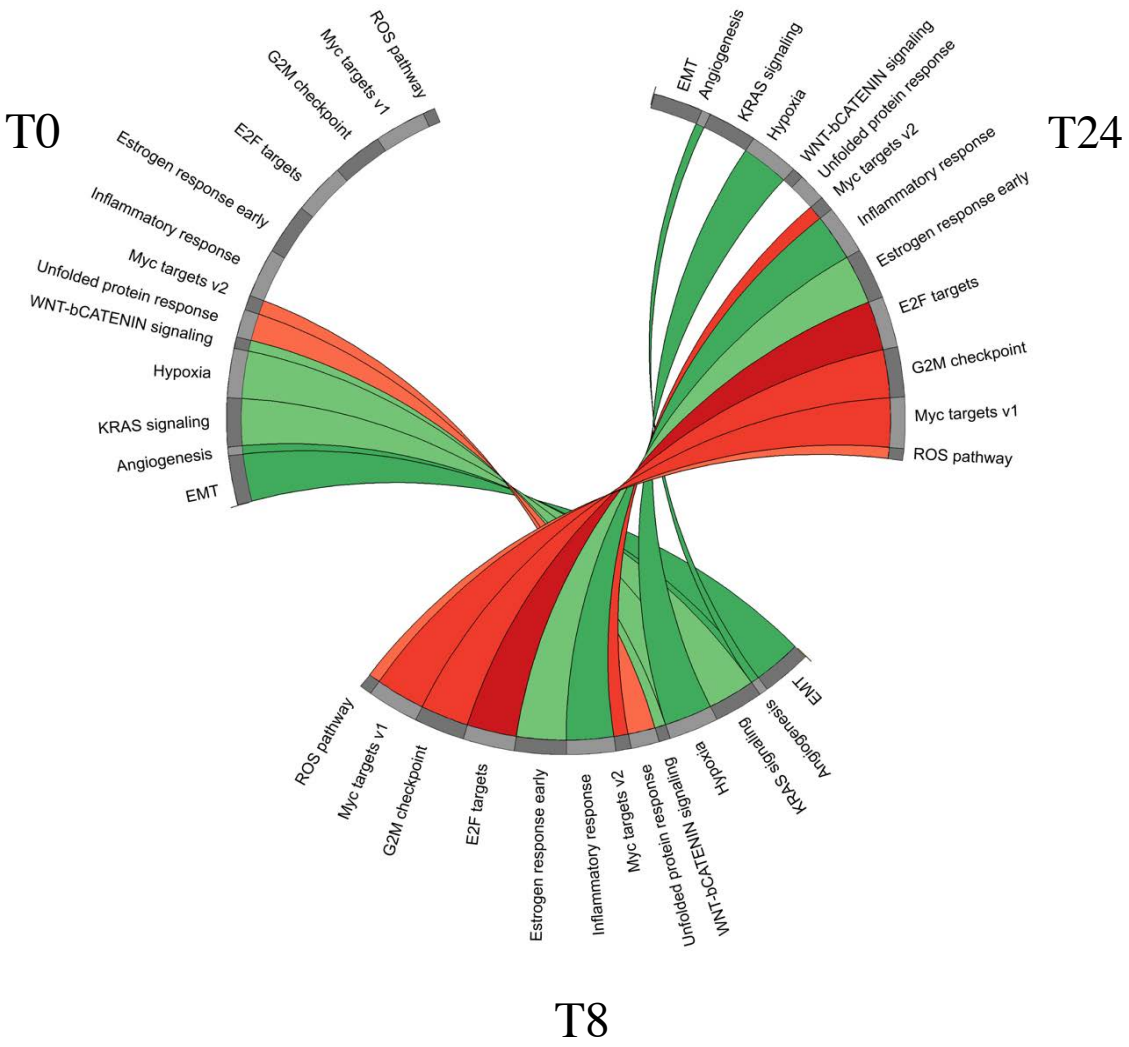

Figure 5. Graphical representation of the Broad Hallmark (BH) gene sets modulation in JEG-3 trophoblast spheroids co-cultured for 8 and 24 hours on Ishikawa substrates. Non-co-cultured JEG3 spheroids were used as T0. Ribbons are colour coded based on the normalized enrichment score (NES) score of the pairwise comparison (very dark colours with |NES|>2, dark colours with 1.5<|NES|<2, and light colours with |NES|<1.5). Green and red colours represent enrichment or depletion of the BH gene set, respectively.

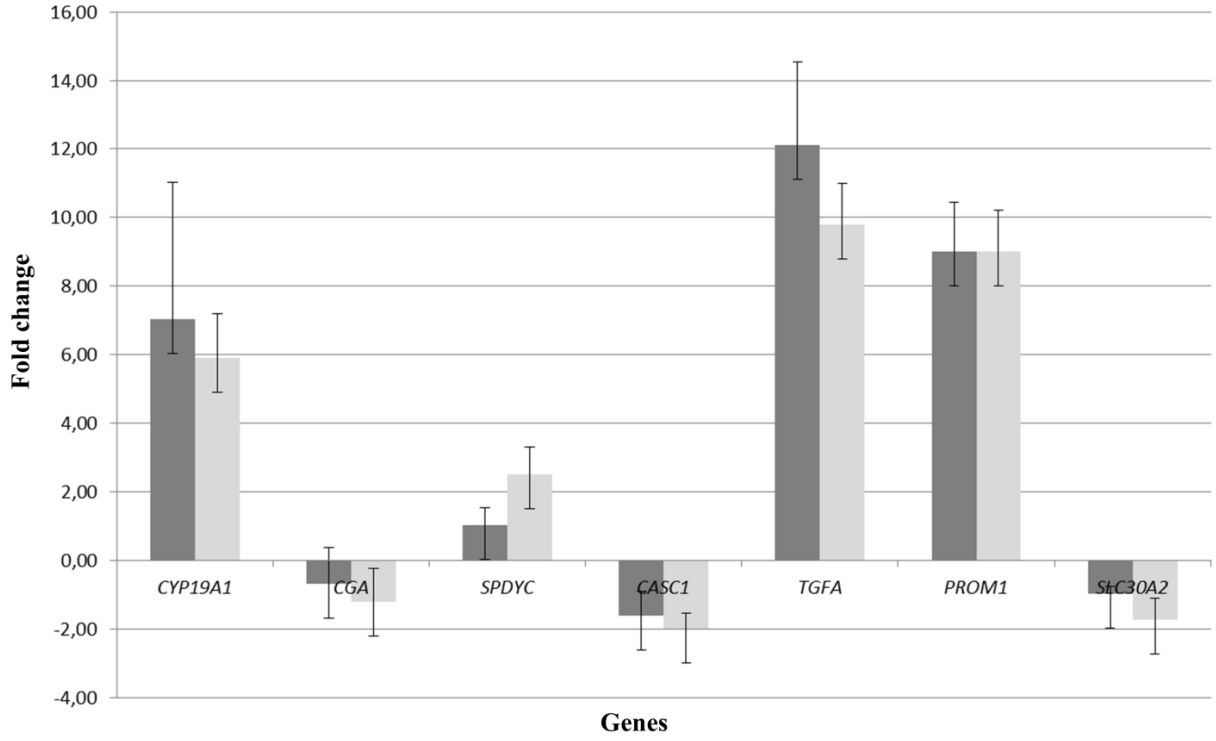

Figure 6. RNA-seq validation by qPCR. Dark grey bars represent the differences in gene expression levels among samples by qPCR and light grey bars represent the differences in gene expression levels among samples by RNA-seq. The genes were compared in the following samples: I-co-S T8 *vs*. I-c T0 for *CYP19A1* and *SPDYC*, I-co-S T24 *vs*. I-co-S T8 for *CGA* and *CASC1* and S-co-I T8 *vs*. S-c T0 for *TGFA*, *PROM1*and *SLC30A2*.

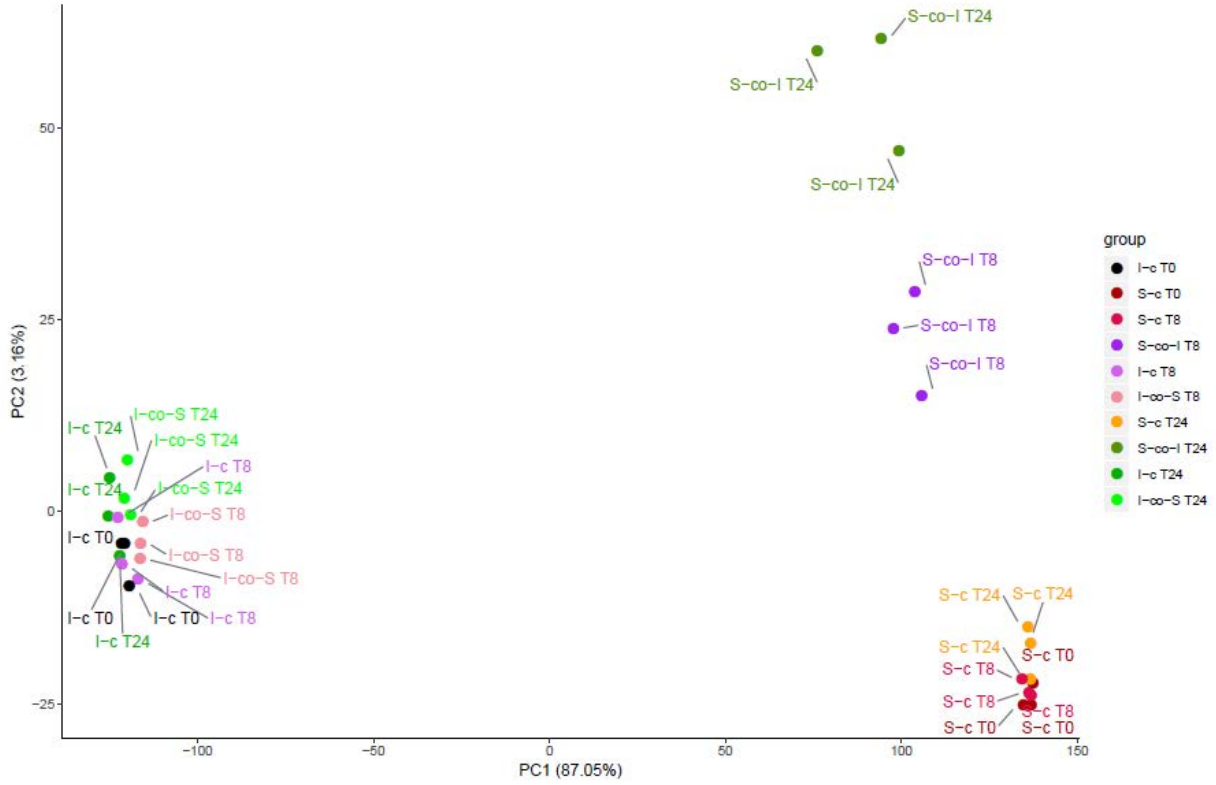

Supplementary Figure 1. Principal component analysis representing all samples from the three experimental replicates according to principal component 1 (PC1) and principal component 2 (PC2): Ishikawa control at 0 hours (I-c T0), JEG-3 spheroids control at 0 hours (S-c T0), Ishikawa control at 8 hours (I-c T8), JEG-3 spheroids control at 8 hours (S-c T8), Ishikawa substrates co-cultured with JEG-3 spheroids for 8 hours (I-co-S T8), JEG-3 spheroids co-cultured with Ishikawa substrates for 8 hours (S-co-I T8), Ishikawa control at 24 hours (I-c T24), JEG-3 spheroids control at 24 hours (S-c T24), Ishikawa substrates co-cultured with JEG-3 spheroids for 24 hours (I-co-S T24) and JEG-3 spheroids co-cultured with Ishikawa substrates for 24 hours (S-co-I T24).

7. Tables

Table I. Cell fractions recovered after FACS from non-co-cultured and co-cultured trophoblast and epithelial substrates at the different time points (0, 8 and 24 hours).

Sorted cell fractions	Nomenclature
Ishikawa control at 0 hours	I-c T0
GFP+ JEG-3 spheroids control at 0 hours	S-c T0
Ishikawa control at 8 hours	I-c T8
GFP+ JEG-3 spheroids control at 8 hours	S-c T8
Ishikawa substrates co-cultured with JEG-3 spheroids for 8hrs	I-co-S T8
JEG-3 spheroids co-cultured with Ishikawa substrates for 8hrs	S-co-I T8
Ishikawa control at 24 hours	I-c T24
GFP+ JEG-3 spheroids control at 24 hours	S-c T24
Ishikawa substrates co-cultured with JEG-3 spheroids for 24hrs	I-co-S T24
JEG-3 spheroids co-cultured with Ishikawa substrates for 24hrs	S-co-I T24

Table II. **Biological pathways over-represented** (positive NES value) **or underrepresented** (negative NES value) **in Ishikawa epithelial substrates co-cultured for 8-hours with JEG-3 spheroids *vs*. non co-cultured Ishikawa epithelial substrates control using GOBP annotation.** (NES= Normalized enrichment score; FDR= False discovery rate)

Annotation terms	Genes (n)	NES	FDR
Biological processes (GOBP)			
Detection of chemical stimulus involved in sensory perception of smell	25	2.32	0.000
Actin-mediated cell contraction	53	2.01	0.003
Actin filament-based movement	70	2.00	0.004
Muscle filament sliding	37	1.97	0.008
Actin-myosin filament sliding	37	1.96	0.006
Endocrine process	64	1.96	0.006
Ribosome biogenesis	148	1.93	0.012
Endocrine hormone secretion	30	1.91	0.019
rRNA processing	106	1.90	0.019
Cell differentiation involved in embryonic placenta development	17	1.89	0.024
Myofibril assembly	40	1.89	0.023
Positive regulation of smooth muscle cell proliferation	39	1.89	0.022
Regulation of ATPase activity	27	1.88	0.022
Actomyosin structure organization	54	1.88	0.022
Regulation of astrocyte differentiation	22	1.87	0.025
Striated muscle cell development	153	1.86	0.030

Regulation of synaptic plasticity	94	1.86	0.031
Response to gonadotropin stimulus	22	1.84	0.039
Tissue morphogenesis	477	1.84	0.037
Regulation of synaptic transmission	175	1.83	0.041
Positive regulation of ATPase activity	17	1.82	0.052
Ovulation	20	1.82	0.052
Cardiac chamber morphogenesis	97	1.81	0.050
Positive regulation of cell cycle	108	1.81	0.049
Regulation of endothelial cell proliferation	66	1.81	0.047
Regulation of transmission of nerve impulse	197	1.81	0.049
Regulation of gene silencing	21	1.81	0.052
Regulation of calcium ion import	19	1.80	0.051
Regulation of establishment or maintenance of cell polarity	12	1.80	0.053
Cellular response to gonadotropin stimulus	15	1.80	0.053
Muscle cell development	163	1.79	0.056
Cardiac muscle cell development	43	1.79	0.058
Regulation of neurological system process	209	1.79	0.061
Negative regulation of monooxygenase activity	11	1.78	0.065
Cardiac muscle tissue morphogenesis	51	1.78	0.063
Sarcomere organization	26	1.78	0.063
Genetic imprinting	25	1.78	0.063
Regulation of muscle hypertrophy	18	1.78	0.063
Positive regulation of tyrosine phosphorylation of stat protein	42	1.77	0.064
Cardiac epithelial to mesenchymal transition	19	1.77	0.062
Cardiac cell development	45	1.77	0.065
Muscle tissue morphogenesis	54	1.77	0.064
Ovulation cycle process	79	1.77	0.064
Regulation of calcium ion transmembrane transporter activity	36	1.77	0.065
Regulation of the force of heart contraction	21	1.77	0.064
Regulation of DNA damage response, signal transduction by p53 class mediator	25	1.76	0.066
Negative regulation of epithelial cell differentiation	21	1.76	0.065
Renal tubule development	39	1.76	0.064
Negative regulation of cAMP metabolic process	31	1.76	0.063
Smooth muscle cell proliferation	69	1.76	0.064
Muscle adaptation	46	1.76	0.063
Heart morphogenesis	181	1.76	0.063
Regulation of signal transduction by P53 class mediator	31	1.76	0.066
Regulation of JAK-STAT cascade	68	1.75	0.067
Renal tubule morphogenesis	22	1.75	0.066
ncRNA processing	205	1.75	0.066
Skeletal muscle adaptation	13	1.75	0.066
Regulation of tyrosine phosphorylation of STAT protein	48	1.75	0.066
Muscle system process	294	1.75	0.067
Connective tissue development	195	1.75	0.066
Response to mechanical stimulus	141	1.75	0.067
Gonad development	177	1.74	0.069
Reproductive structure development	253	1.74	0.068

Negative regulation of ion transmembrane transport	13	1.74	0.068
Heart trabecula formation	14	1.74	0.070
Negative regulation of muscle organ development	19	1.74	0.069
Positive regulation of endothelial cell proliferation	49	1.74	0.069
Gonadotropin secretion	12	1.74	0.070
Regulation of cAMP biosynthetic process	85	1.73	0.070
Regulation of calcium ion transport	132	1.73	0.069
Regulation of ryanodine-sensitive calcium-release channel activity	22	1.73	0.070
Regulation of cAMP metabolic process	92	1.73	0.070
Regulation of system process	453	1.73	0.071
Reproductive system development	255	1.73	0.070
Pharyngeal system development	15	1.73	0.073
Nephron tubule development	38	1.73	0.073
Muscle contraction	257	1.73	0.072
Morphogenesis of an epithelium	381	1.72	0.074
Regulation of smooth muscle cell proliferation	66	1.72	0.073
Nephron tubule morphogenesis	19	1.72	0.074
Inactivation of MAPK activity	26	1.72	0.075
Vascular smooth muscle contraction	15	1.72	0.074
Positive regulation of translation	52	1.72	0.075
Cardiac muscle tissue development	139	1.72	0.074
Heart trabecula morphogenesis	21	1.72	0.076
Endothelial cell proliferation	79	1.72	0.075
Positive regulation of muscle hypertrophy	10	1.72	0.075
Regulation of cardiac muscle hypertrophy	17	1.71	0.076
cAMP biosynthetic process	91	1.71	0.081
Negative regulation of oxidoreductase activity	19	1.71	0.084
Cellular response to ionizing radiation	42	1.71	0.084
Cardiac chamber development	114	1.70	0.085
Positive regulation of cardiac muscle hypertrophy	10	1.70	0.087
Nephron tubule formation	14	1.70	0.087
Regulation of cation channel activity	44	1.70	0.086
Gland development	267	1.70	0.086
Positive regulation of JAK-STAT cascade	49	1.70	0.087
Granulocyte chemotaxis	57	1.70	0.087
Tyrosine phosphorylation of STAT protein	53	1.70	0.087
Positive regulation of extrinsic apoptotic signalling pathway	29	1.70	0.086
Inner ear receptor cell development	19	1.69	0.089
Cellular response to organic cyclic compound	184	1.69	0.089
Positive regulation of cyclic nucleotide biosynthetic process	62	1.69	0.088
Regulation of cyclic nucleotide metabolic process	108	1.69	0.088
Chemokine metabolic process	14	1.69	0.090
Negative regulation of muscle tissue development	18	1.69	0.091
T-Helper 2 cell differentiation	13	1.69	0.091
Regulation of muscle system process	140	1.69	0.092
Cell chemotaxis	141	1.69	0.093
Regulation of tyrosine phosphorylation of STAT3 protein	30	1.68	0.093

Positive regulation of tyrosine phosphorylation of STAT3 protein	25	1.68	0.092
Regulation of nucleotide biosynthetic process	99	1.68	0.092
Positive regulation of transmembrane receptor protein serine/threonine kinase signalling pathway	69	1.68	0.092
Negative regulation of astrocyte differentiation	11	1.68	0.093
Regulation of cyclic nucleotide biosynthetic process	96	1.68	0.093
Estrogen metabolic process	17	1.68	0.096
Ribonucleoprotein complex biogenesis	247	1.68	0.098
Epidermis development	252	1.68	0.097
mRNA transcription	15	1.68	0.097
Positive regulation of purine nucleotide biosynthetic process	64	1.68	0.097
Metanephric nephron tubule development	16	1.67	0.098
Positive regulation of nitric oxide biosynthetic process	27	1.67	0.098
Positive regulation of renal sodium excretion	13	1.67	0.097
Regulation of nitric oxide biosynthetic process	37	1.67	0.098
Striated muscle cell differentiation	258	1.67	0.097
Negative regulation of gliogenesis	27	1.67	0.097
Regulation of purine nucleotide biosynthetic process	99	1.67	0.096
Type 2 immune response	28	1.67	0.096
Positive regulation of camp metabolic process	57	1.67	0.099
Second-messenger-mediated signalling	154	1.67	0.098
Metanephric tubule development	17	1.67	0.098
Positive regulation of urine volume	12	1.67	0.099
Negative regulation of glial cell differentiation	21	1.67	0.098
Positive regulation of calcium ion transport	57	1.67	0.097
Astrocyte differentiation	43	1.67	0.097
Regulation of Interleukin-13 production	11	1.67	0.097
Female gamete generation	82	1.66	0.098
Response to alkaloid	94	1.66	0.098
Cartilage development	160	1.66	0.098
Negative regulation of striated muscle tissue development	17	1.66	0.097
Loop of henle development	10	1.66	0.096
Epidermal cell differentiation	130	1.66	0.096
Inositol phosphate-mediated signalling	19	1.66	0.096
Placenta development	131	1.66	0.099
Ovulation cycle	84	1.66	0.099
Metanephric nephron epithelium development	16	1.66	0.099
Negative regulation of camp biosynthetic process	28	1.66	0.098
Regulation of cholesterol efflux	17	-1.91	0.088

Table III. Biological pathways over-represented (positive NES value) **or underrepresented** (negative NES value) **in Ishikawa epithelial substrates co-cultured for 24-hours with JEG-3 spheroids *vs.* Ishikawa epithelial substrates co-cultured for 8-hours with JEG-3 spheroids using GOBP annotation** (NES= Normalized enrichment score; FDR= False discovery rate).

Annotation terms	Genes (n)	NES	FDR
Biological processes (GOBP)			
Ribosome biogenesis	148	-2.05	0.014
rRNA processing	106	-2.01	0.015
ncRNA processing	205	-1.99	0.014
Ribonucleoprotein complex biogenesis	247	-1.90	0.079
Heterophilic cell-cell adhesion	23	-1.89	0.071
Actin-mediated cell contraction	53	-1.88	0.070
rRNA metabolic process	111	-1.87	0.083

Table IV. Biological pathways over-represented (positive NES value) **or underrepresented** (negative NES value) **in JEG-3 spheroids co-cultured for 8-hours with Ishikawa epithelial substrates *vs.* non co-cultured JEG-3 spheroids control using GOBP and Broad Hallmarks annotations** (NES= Normalized enrichment score; FDR= False discovery rate).

Annotation terms	Genes (n)	NES	FDR
Biological processes (GOBP)			
Amino acid activation	49	-2.10	0.004
tRNA aminoacylation for protein translation	47	-2.08	0.005
tRNA aminoacylation	49	-2.06	0.006
ncRNA processing	205	-2.01	0.014
tRNA modification	21	-1.88	0.072

8. Supplementary material (Available upon request to the authors)

Supplementary figure 1: Principal component analysis representing all samples from the three experimental replicates according to principal component 1 (PC1) and principal component 2 (PC2): Ishikawa control at 0 hours (I-c T0), JEG-3 spheroids control at 0 hours (S-c T0), Ishikawa control at 8 hours (I-c T8), JEG-3 spheroids control at 8 hours (S-c T8), Ishikawa substrates co-cultured with JEG-3 spheroids for 8 hours (I-co-S T8), JEG-3 spheroids co-cultured with Ishikawa substrates for 8 hours (S-co-I T8), Ishikawa control at 24 hours (I-c T24), JEG-3 spheroids control at 24 hours (S-c T24), Ishikawa substrates co-cultured with JEG-3 spheroids for 24 hours (I-co-S T24) and JEG-3 spheroids co-cultured with Ishikawa substrates for 24 hours (S-co-I T24).

Supplementary File S1: List of differentially expressed genes between Ishikawa substrates co-cultured with JEG-3 spheroids for 8 hours *vs*. Ishikawa control at 0 hours **(**I-co-S T8 *vs*. I-c T0). Statistical significance was set at absolute log2FC ≥1 and adjusted p-value <0.05. Negative fold changes mean that expression in I-co-S T8 is lower than that in I-c T0; positive fold changes mean expression in I-co-S T8 is higher than that in I-c T0.

Supplementary File S2: List of differentially expressed genes between Ishikawa substrates co-cultured with JEG-3 spheroids for 24 hours *vs*. Ishikawa substrates co-cultured with JEG-3 spheroids for 8 hours (I-co-S T24 *vs*. I-co-S T8). Statistical significance was set at absolute log2FC ≥1 and adjusted p-value <0.05. Negative fold changes mean that expression in I-co-S T24 is lower than that in I-co-S T8; positive fold changes mean expression in I-co-S T24 is higher than that in I-co-S T8.

Supplementary File S3: List of common genes between I-co-S T8 *vs*. I-c T0 and I-co-S T24 *vs*. I-co-S T8 comparisons.

Supplementary File S4: List of differentially expressed genes between JEG-3 spheroids co-cultured with Ishikawa substrates for 8 hours *vs*. JEG-3 spheroids control at 0 hours (S-co-I T8 *vs*. S-c T0). Statistical significance was set at absolute log2FC ≥1 and adjusted p-value <0.05. Negative fold changes mean that expression in S-co-I T8 is lower than that in S-c T0; positive fold changes mean expression in S-co-I T8 is higher than that in S-c T0.

Supplementary File S5: List of differentially expressed genes between JEG-3 spheroids co-cultured with Ishikawa substrates for 24 hours *vs*. JEG-3 spheroids co-cultured with Ishikawa substrates for 8 hours (S-co-I T24 *vs*. S-co-I T8). Statistical significance was set at absolute log2FC ≥1 and adjusted p-value <0.05. Negative fold changes mean that expression in S-co-I T24 is lower than that in S-co-I T8; positive fold changes mean expression in S-co-I T24 is higher than that in S-co-I T8.

Supplementary File S6: List of common genes between S-co-I T8 *vs*. S-c T0 and S-co-I T24 *vs*. S-co-I T8 comparisons.

9. References

Aberkane, A., W. Essahib, C. Spits, C. De Paepe, K. Sermon, T. Adriaenssens, S. Mackens, H. Tournaye, J. J. Brosens, and H. Van de Velde. 2018. 'Expression of adhesion and extracellular matrix genes in human blastocysts upon attachment in a 2D co-culture system', *Mol Hum Reprod*, 24: 375-87.

Altmae, S., K. Haller, M. Peters, M. Saare, O. Hovatta, A. Stavreus-Evers, A. Velthut, H. Karro, A. Metspalu, and A. Salumets. 2009. 'Aromatase gene (CYP19A1) variants, female infertility and ovarian stimulation outcome: a preliminary report', *Reprod Biomed Online*, 18: 651-7.

Altmae, S., M. Koel, U. Vosa, P. Adler, M. Suhorutsenko, T. Laisk-Podar, V. Kukushkina, M. Saare, A. Velthut-Meikas, K. Krjutskov, L. Aghajanova, P. G. Lalitkumar, K. Gemzell-Danielsson, L. Giudice, C. Simon, and A. Salumets. 2017. 'Meta-signature of human endometrial receptivity: a meta-analysis and validation study of transcriptomic biomarkers', *Sci Rep*, 7: 10077.

Altmae, S., J. A. Martinez-Conejero, A. Salumets, C. Simon, J. A. Horcajadas, and A. Stavreus-Evers. 2010. 'Endometrial gene expression analysis at the time of embryo implantation in women with unexplained infertility', *Mol Hum Reprod*, 16: 178-87.

Arnold, J. T., D. G. Kaufman, M. Seppala, and B. A. Lessey. 2001. 'Endometrial stromal cells regulate epithelial cell growth in vitro: a new co-culture model', *Hum Reprod*, 16: 836-45.

Ashburner, M., C. A. Ball, J. A. Blake, D. Botstein, H. Butler, J. M. Cherry, A. P. Davis, K. Dolinski, S. S. Dwight, J. T. Eppig, M. A. Harris, D. P. Hill, L. Issel-Tarver, A. Kasarskis, S. Lewis, J. C. Matese, J. E. Richardson, M. Ringwald, G. M. Rubin, and G. Sherlock. 2000. 'Gene ontology: tool for the unification of biology. The Gene Ontology Consortium', *Nat Genet*, 25: 25-9.

Banerjee, P., S. K. Jana, P. Pasricha, S. Ghosh, B. Chakravarty, and K. Chaudhury. 2013. 'Proinflammatory cytokines induced altered expression of cyclooxygenase-2 gene results in unreceptive endometrium in women with idiopathic recurrent spontaneous miscarriage', *Fertil Steril*, 99: 179-87.

Berger, C., N. R. Boggavarapu, J. Menezes, P. G. Lalitkumar, and K. Gemzell-Danielsson. 2015. 'Effects of ulipristal acetate on human embryo attachment and endometrial cell gene expression in an in vitro co-culture system', *Hum Reprod*, 30: 800-11.

Blakeley, P., N. M. Fogarty, I. del Valle, S. E. Wamaitha, T. X. Hu, K. Elder, P. Snell, L. Christie, P. Robson, and K. K. Niakan. 2015. 'Defining the three cell lineages of the human blastocyst by single-cell RNA-seq', *Development*, 142: 3151-65.

Brighton, P. J., Y. Maruyama, K. Fishwick, P. Vrljicak, S. Tewary, R. Fujihara, J. Muter, E. S. Lucas, T. Yamada, L. Woods, R. Lucciola, Y. Hou Lee, S. Takeda, S. Ott, M. Hemberger, S. Quenby, and J. J. Brosens. 2017. 'Clearance of senescent decidual cells by uterine natural killer cells in cycling human endometrium', *Elife*, 6.

Brosens, J. J., M. S. Salker, G. Teklenburg, J. Nautiyal, S. Salter, E. S. Lucas, J. H. Steel, M. Christian, Y. W. Chan, C. M. Boomsma, J. D. Moore, G. M. Hartshorne, S. Sucurovic, B. Mulac-Jericevic, C. J. Heijnen, S. Quenby, M. J. Koerkamp, F. C. Holstege, A. Shmygol, and N. S. Macklon. 2014. 'Uterine selection of human embryos at implantation', *Sci Rep*, 4: 3894.

Burton, G. J., and H. W. Yung. 2011. 'Endoplasmic reticulum stress in the pathogenesis of early-onset pre-eclampsia', *Pregnancy Hypertens*, 1: 72-8.

Caniggia, I., H. Mostachfi, J. Winter, M. Gassmann, S. J. Lye, M. Kuliszewski, and M. Post. 2000. 'Hypoxia-inducible factor-1 mediates the biological effects of oxygen on human trophoblast differentiation through TGFbeta(3)', *J Clin Invest*, 105: 577-87.

Chen, J., and R. A. Khalil. 2017. 'Matrix Metalloproteinases in Normal Pregnancy and Preeclampsia', *Prog Mol Biol Transl Sci*, 148: 87-165.

Cheng, X., J. Liu, H. Shan, L. Sun, C. Huang, Q. Yan, R. Jiang, L. Ding, Y. Jiang, J. Zhou, G. Yan, and H. Sun. 2017. 'Activating transcription factor 3 promotes embryo attachment via up-regulation of leukemia inhibitory factor in vitro', *Reprod Biol Endocrinol*, 15: 42.

Cho, G., Y. Lim, D. Zand, and J. A. Golden. 2008. 'Sizn1 is a novel protein that functions as a transcriptional coactivator of bone morphogenic protein signaling', *Mol Cell Biol*, 28: 1565-72.

Davies, J.E., J. Pollheimer, H. E. Yong, M. I. Kokkinos, B. Kalionis, M. Knofler, and P. Murthi. 2016. 'Epithelial-mesenchymal transition during extravillous trophoblast differentiation', *Cell Adh Migr*, 10: 310-21.

Dekel, N., Y. Gnainsky, I. Granot, K. Racicot, and G. Mor. 2014. 'The role of inflammation for a successful implantation', *Am J Reprod Immunol*, 72: 141-7.

Diaz-Gimeno, P., J. A. Horcajadas, J. A. Martinez-Conejero, F. J. Esteban, P. Alama, A. Pellicer, and C. Simon. 2011. 'A genomic diagnostic tool for human endometrial receptivity based on the transcriptomic signature', *Fertil Steril*, 95: 50-60, 60 e1-15.

Dimitriadis, E., E. Menkhorst, L. A. Salamonsen, and P. Paiva. 2010. 'Review: LIF and IL11 in trophoblast-endometrial interactions during the establishment of pregnancy', *Placenta*, 31 Suppl: S99-104.

Dimitriadis, E., A. M. Sharkey, Y. L. Tan, L. A. Salamonsen, and J. R. Sherwin. 2007. 'Immunolocalisation of phosphorylated STAT3, interleukin 11 and leukaemia inhibitory factor in endometrium of women with unexplained infertility during the implantation window', *Reprod Biol Endocrinol*, 5: 44.

Dobin, A., C. A. Davis, F. Schlesinger, J. Drenkow, C. Zaleski, S. Jha, P. Batut, M. Chaisson, and T. R. Gingeras. 2013. 'STAR: ultrafast universal RNA-seq aligner', *Bioinformatics*, 29: 15-21.

Douglas, N. C., R. C. Zimmermann, Q. K. Tan, C. S. Sullivan-Pyke, M. V. Sauer, J. K. Kitajewski, and C. J. Shawber. 2014. 'VEGFR-1 blockade disrupts peri-implantation decidual angiogenesis and macrophage recruitment', *Vasc Cell*, 6: 16.

Enciso, M., J. P. Carrascosa, J. Sarasa, P. A. Martinez-Ortiz, S. Munne, J. A. Horcajadas, and J. Aizpurua. 2018. 'Development of a new comprehensive and reliable endometrial receptivity map (ER Map/ER Grade) based on RT-qPCR gene expression analysis', *Hum Reprod*, 33: 220-28.

Evans, J., L. A. Salamonsen, A. Winship, E. Menkhorst, G. Nie, C. E. Gargett, and E. Dimitriadis. 2016. 'Fertile ground: human endometrial programming and lessons in health and disease', *Nat Rev Endocrinol*, 12: 654-67.

Evron, A., S. Goldman, and E. Shalev. 2011. 'Effect of primary human endometrial stromal cells on epithelial cell receptivity and protein expression is dependent on menstrual cycle stage', *Hum Reprod*, 26: 176-90.

Fu, J., X. J. Wang, Y. W. Wang, J. Sun, K. Gemzell-Danielsson, and X. X. Sun. 2009. 'The influence of early cleavage on embryo developmental potential and IVF/ICSI outcome', *J Assist Reprod Genet*, 26: 437-41.

Genbacev, O. D., A. Prakobphol, R. A. Foulk, A. R. Krtolica, D. Ilic, M. S. Singer, Z. Q. Yang, L. L. Kiessling, S. D. Rosen, and S. J. Fisher. 2003. 'Trophoblast L-selectin-mediated adhesion at the maternal-fetal interface', *Science*, 299: 405-8.

Gibson, D. A., K. J. McInnes, H. O. Critchley, and P. T. Saunders. 2013. 'Endometrial Intracrinology-generation of an estrogen-dominated microenvironment in the secretory phase of women', *J Clin Endocrinol Metab*, 98: E1802-6.

Gleeson, L. M., C. Chakraborty, T. McKinnon, and P. K. Lala. 2001. 'Insulin-like growth factor-binding protein 1 stimulates human trophoblast migration by signaling through alpha 5

beta 1 integrin via mitogen-activated protein Kinase pathway', *J Clin Endocrinol Metab*, 86: 2484-93.

Granot, I., Y. Gnainsky, and N. Dekel. 2012. 'Endometrial inflammation and effect on implantation improvement and pregnancy outcome', *Reproduction*, 144: 661-8.

Green, C. J., S. T. Fraser, and M. L. Day. 2015. 'Insulin-like growth factor 1 increases apical fibronectin in blastocysts to increase blastocyst attachment to endometrial epithelial cells in vitro', *Hum Reprod*, 30: 284-98.

Haouzi, D., H. Dechaud, S. Assou, C. Monzo, J. de Vos, and S. Hamamah. 2011. 'Transcriptome analysis reveals dialogues between human trophectoderm and endometrial cells during the implantation period', *Hum Reprod*, 26: 1440-9.

Heneweer, C., H. G. Adelmann, L. H. Kruse, H. W. Denker, and M. Thie. 2003. 'Human uterine epithelial RL95-2 cells reorganize their cytoplasmic architecture with respect to Rho protein and F-actin in response to trophoblast binding', *Cells Tissues Organs*, 175: 1-8.

Hirate, Y., H. Suzuki, M. Kawasumi, H. M. Takase, H. Igarashi, P. Naquet, Y. Kanai, and M. Kanai-Azuma. 2016. 'Mouse Sox17 haploinsufficiency leads to female subfertility due to impaired implantation', *Sci Rep*, 6: 24171.

Hourvitz, A., L. Lerner-Geva, S. E. Elizur, M. Baum, J. Levron, B. David, D. Meirow, R. Yaron, and J. Dor. 2006. 'Role of embryo quality in predicting early pregnancy loss following assisted reproductive technology', *Reprod Biomed Online*, 13: 504-9.

Hu, S., G. Yao, Y. Wang, H. Xu, X. Ji, Y. He, Q. Zhu, Z. Chen, and Y. Sun. 2014. 'Transcriptomic changes during the pre-receptive to receptive transition in human endometrium detected by RNA-Seq', *J Clin Endocrinol Metab*, 99: E2744-53.

Huang, M. Y., W. Q. Zhang, M. Zhao, C. Zhu, J. P. He, and J. L. Liu. 2018. 'Assessment of Embryo-Induced Transcriptomic Changes in Hamster Uterus Using RNA-Seq', *Cell Physiol Biochem*, 46: 1868-78.

Jones, R. L., J. K. Findlay, P. G. Farnworth, D. M. Robertson, E. Wallace, and L. A. Salamonsen. 2006. 'Activin A and inhibin A differentially regulate human uterine matrix metalloproteinases: potential interactions during decidualization and trophoblast invasion', *Endocrinology*, 147: 724-32.

Kakar-Bhanot, R., K. Brahmbhatt, B. Chauhan, R. R. Katkam, T. Bashir, H. Gawde, N. Mayadeo, U. K. Chaudhari, and G. Sachdeva. 2019. 'Rab11a drives adhesion molecules to the surface of endometrial epithelial cells', *Hum Reprod*, 34: 519-29.

Kelleher, A. M., J. Milano-Foster, S. K. Behura, and T. E. Spencer. 2018. 'Uterine glands coordinate on-time embryo implantation and impact endometrial decidualization for pregnancy success', *Nat Commun*, 9: 2435.

Knofler, M., and J. Pollheimer. 2013. 'Human placental trophoblast invasion and differentiation: a particular focus on Wnt signaling', *Front Genet*, 4: 190.

Koler, M., H. Achache, A. Tsafrir, Y. Smith, A. Revel, and R. Reich. 2009. 'Disrupted gene pattern in patients with repeated in vitro fertilization (IVF) failure', *Hum Reprod*, 24: 2541-8.

Koot, Y. E., G. Teklenburg, M. S. Salker, J. J. Brosens, and N. S. Macklon. 2012. 'Molecular aspects of implantation failure', *Biochim Biophys Acta*, 1822: 1943-50.

Koot, Y. E., S. R. van Hooff, C. M. Boomsma, D. van Leenen, M. J. Groot Koerkamp, M. Goddijn, M. J. Eijkemans, B. C. Fauser, F. C. Holstege, and N. S. Macklon. 2016. 'An endometrial gene expression signature accurately predicts recurrent implantation failure after IVF', *Sci Rep*, 6: 19411.

Krzywinski, M., J. Schein, I. Birol, J. Connors, R. Gascoyne, D. Horsman, S. J. Jones, and M. A. Marra. 2009. 'Circos: an information aesthetic for comparative genomics', *Genome Res*, 19: 1639-45.

Kuo, C. Y., M. Shevchuk, J. Opfermann, T. Guo, M. Santoro, J. P. Fisher, and P. C. Kim. 2019. 'Trophoblast-endothelium signaling involves angiogenesis and apoptosis in a dynamic bioprinted placenta model', *Biotechnol Bioeng*, 116: 181-92.

Laheri, S., N. Ashary, P. Bhatt, and D. Modi. 2018. 'Oviductal glycoprotein 1 (OVGP1) is expressed by endometrial epithelium that regulates receptivity and trophoblast adhesion', *J Assist Reprod Genet*, 35: 1419-29.

Ledee, N., C. Munaut, J. Aubert, V. Serazin, M. Rahmati, G. Chaouat, O. Sandra, and J. M. Foidart. 2011. 'Specific and extensive endometrial deregulation is present before conception in IVF/ICSI repeated implantation failures (IF) or recurrent miscarriages', *J Pathol*, 225: 554-64.

Li, M., D. Yee, T. R. Magnuson, O. Smithies, and K. M. Caron. 2006. 'Reduced maternal expression of adrenomedullin disrupts fertility, placentation, and fetal growth in mice', *J Clin Invest*, 116: 2653-62.

Liang, G., X. Fang, Y. Yang, and Y. Song. 2018. 'Silencing of CEMIP suppresses Wnt/beta-catenin/Snail signaling transduction and inhibits EMT program of colorectal cancer cells', *Acta Histochem*, 120: 56-63.

Liao, Y., G. K. Smyth, and W. Shi. 2013. 'The Subread aligner: fast, accurate and scalable read mapping by seed-and-vote', *Nucleic Acids Res*, 41: e108.

Liberzon, A., C. Birger, H. Thorvaldsdottir, M. Ghandi, J. P. Mesirov, and P. Tamayo. 2015. 'The Molecular Signatures Database (MSigDB) hallmark gene set collection', *Cell Syst*, 1: 417-25.

Liberzon, A., A. Subramanian, R. Pinchback, H. Thorvaldsdottir, P. Tamayo, and J. P. Mesirov. 2011. 'Molecular signatures database (MSigDB) 3.0', *Bioinformatics*, 27: 1739-40.

Lockwood, C. J., C. F. Yen, M. Basar, U. A. Kayisli, M. Martel, I. Buhimschi, C. Buhimschi, S. J. Huang, G. Krikun, and F. Schatz. 2008. 'Preeclampsia-related inflammatory cytokines regulate interleukin-6 expression in human decidual cells', *Am J Pathol*, 172: 1571-9.

Love, M. I., W. Huber, and S. Anders. 2014. 'Moderated estimation of fold change and dispersion for RNA-seq data with DESeq2', *Genome Biol*, 15: 550.

Lundin, K., C. Bergh, and T. Hardarson. 2001. 'Early embryo cleavage is a strong indicator of embryo quality in human IVF', *Hum Reprod*, 16: 2652-7.

McConkey, C. A., E. Delorme-Axford, C. A. Nickerson, K. S. Kim, Y. Sadovsky, J. P. Boyle, and C. B. Coyne. 2016. 'A three-dimensional culture system recapitulates placental syncytiotrophoblast development and microbial resistance', *Sci Adv*, 2: e1501462.

Mor, G., I. Cardenas, V. Abrahams, and S. Guller. 2011. 'Inflammation and pregnancy: the role of the immune system at the implantation site', *Ann N Y Acad Sci*, 1221: 80-7.

Moreno-Moya, J. M., N. A. Franchi, S. Martinez-Escribano, J. A. Martinez-Conejero, S. Bocca, S. Oehninger, and J. A. Horcajadas. 2015. 'Transcriptome of early embryonic invasion at implantation sites in a murine model', *Reprod Fertil Dev*.

Morgan M, Falcon S and Gentleman R. 2017. 'Morgan M, Falcon S and Gentleman R (2017). GSEABase: Gene set enrichment data structures and methods. R package version 1.40.1.'.

Petropoulos, S., D. Edsgard, B. Reinius, Q. Deng, S. P. Panula, S. Codeluppi, A. Plaza Reyes, S. Linnarsson, R. Sandberg, and F. Lanner. 2016. 'Single-Cell RNA-Seq Reveals Lineage and X Chromosome Dynamics in Human Preimplantation Embryos', *Cell*, 165: 1012-26.

Polanski, L. T., M. N. Baumgarten, S. Quenby, J. Brosens, B. K. Campbell, and N. J. Raine-Fenning. 2014. 'What exactly do we mean by 'recurrent implantation failure'? A systematic review and opinion', *Reprod Biomed Online*, 28: 409-23.

Popovici, R. M., N. K. Betzler, M. S. Krause, M. Luo, J. Jauckus, A. Germeyer, S. Bloethner, A. Schlotterer, R. Kumar, T. Strowitzki, and M. von Wolff. 2006. 'Gene expression profiling of human endometrial-trophoblast interaction in a coculture model', *Endocrinology*, 147: 5662-75.

Quenby, S., M. Bates, T. Doig, J. Brewster, D. I. Lewis-Jones, P. M. Johnson, and G. Vince. 1999. 'Pre-implantation endometrial leukocytes in women with recurrent miscarriage', *Hum Reprod*, 14: 2386-91.

Ruane, P. T., S. C. Berneau, R. Koeck, J. Watts, S. J. Kimber, D. R. Brison, M. Westwood, and J. D. Aplin. 2017. 'Apposition to endometrial epithelial cells activates mouse blastocysts for implantation', *Mol Hum Reprod*, 23: 617-27.

Salker, M. S., J. Nautiyal, J. H. Steel, Z. Webster, S. Sucurovic, M. Nicou, Y. Singh, E. S. Lucas, K. Murakami, Y. W. Chan, S. James, Y. Abdallah, M. Christian, B. A. Croy, B. Mulac-Jericevic, S. Quenby, and J. J. Brosens. 2012. 'Disordered IL-33/ST2 activation in decidualizing stromal cells prolongs uterine receptivity in women with recurrent pregnancy loss', *PLoS One*, 7: e52252.

Schaefer, W. R., L. Fischer, W. R. Deppert, A. Hanjalic-Beck, L. Seebacher, M. Weimer, and H. P. Zahradnik. 2010. 'In vitro-Ishikawa cell test for assessing tissue-specific chemical effects on human endometrium', *Reprod Toxicol*, 30: 89-93.

Sebastian-Leon, P., N. Garrido, J. Remohi, A. Pellicer, and P. Diaz-Gimeno. 2018. 'Asynchronous and pathological windows of implantation: two causes of recurrent implantation failure', *Hum Reprod*, 33: 626-35.

Shaut, C. A., D. R. Keene, L. K. Sorensen, D. Y. Li, and H. S. Stadler. 2008. 'HOXA13 Is essential for placental vascular patterning and labyrinth endothelial specification', *PLoS Genet*, 4: e1000073.

Shi, J., Q. Chen, X. Li, X. Zheng, Y. Zhang, J. Qiao, F. Tang, Y. Tao, Q. Zhou, and E. Duan. 2015. 'Dynamic transcriptional symmetry-breaking in pre-implantation mammalian embryo development revealed by single-cell RNA-seq', *Development*, 142: 3468-77.

Simon, A., and N. Laufer. 2012. 'Repeated implantation failure: clinical approach', *Fertil Steril*, 97: 1039-43.

Singh, H., L. Nardo, S. J. Kimber, and J. D. Aplin. 2010. 'Early stages of implantation as revealed by an in vitro model', *Reproduction*, 139: 905-14.

Singh, M., P. Chaudhry, and E. Asselin. 2011. 'Bridging endometrial receptivity and implantation: network of hormones, cytokines, and growth factors', *J Endocrinol*, 210: 5-14.

Sjoblom, P., J. Menezes, L. Cummins, B. Mathiyalagan, and M. F. Costello. 2006. 'Prediction of embryo developmental potential and pregnancy based on early stage morphological characteristics', *Fertil Steril*, 86: 848-61.

Smedley, D., S. Haider, S. Durinck, L. Pandini, P. Provero, J. Allen, O. Arnaiz, M. H. Awedh, R. Baldock, G. Barbiera, P. Bardou, T. Beck, A. Blake, M. Bonierbale, A. J. Brookes, G. Bucci, I. Buetti, S. Burge, C. Cabau, J. W. Carlson, C. Chelala, C. Chrysostomou, D. Cittaro, O. Collin, R. Cordova, R. J. Cutts, E. Dassi, A. Di Genova, A. Djari, A. Esposito, H. Estrella, E. Eyras, J. Fernandez-Banet, S. Forbes, R. C. Free, T. Fujisawa, E. Gadaleta, J. M. Garcia-Manteiga, D. Goodstein, K. Gray, J. A. Guerra-Assuncao, B. Haggarty, D. J. Han, B. W. Han, T. Harris, J. Harshbarger, R. K. Hastings, R. D. Hayes, C. Hoede, S. Hu, Z. L. Hu, L. Hutchins, Z. Kan, H. Kawaji, A. Keliet, A. Kerhornou, S. Kim, R. Kinsella, C. Klopp, L. Kong, D. Lawson, D. Lazarevic, J. H. Lee, T. Letellier, C. Y. Li, P. Lio, C. J. Liu, J. Luo, A. Maass, J. Mariette, T. Maurel, S. Merella, A. M. Mohamed, F. Moreews, I. Nabihoudine, N. Ndegwa, C. Noirot, C. Perez-Llamas, M. Primig, A. Quattrone, H. Quesneville, D. Rambaldi, J. Reecy, M. Riba, S. Rosanoff, A. A. Saddiq, E. Salas, O. Sallou, R. Shepherd, R. Simon, L. Sperling, W. Spooner, D. M. Staines, D. Steinbach, K. Stone, E. Stupka, J. W. Teague, A. Z. Dayem Ullah, J. Wang, D. Ware, M. Wong-Erasmus, K. Youens-Clark, A. Zadissa, S. J. Zhang, and A. Kasprzyk. 2015. 'The BioMart community portal: an innovative alternative to large, centralized data repositories', *Nucleic Acids Res*, 43: W589-98.

Song, J., Y. Li, and R. F. An. 2015. 'Identification of Early-Onset Preeclampsia-Related Genes and MicroRNAs by Bioinformatics Approaches', *Reprod Sci*, 22: 954-63.

Stirparo, G. G., T. Boroviak, G. Guo, J. Nichols, A. Smith, and P. Bertone. 2018. 'Integrated analysis of single-cell embryo data yields a unified transcriptome signature for the human pre-implantation epiblast', *Development*, 145.

Stone, R. C., I. Pastar, N. Ojeh, V. Chen, S. Liu, K. I. Garzon, and M. Tomic-Canic. 2016. 'Epithelial-mesenchymal transition in tissue repair and fibrosis', *Cell Tissue Res*, 365: 495-506.

Su, R. W., B. Jia, H. Ni, W. Lei, S. L. Yue, X. H. Feng, W. B. Deng, J. L. Liu, Z. A. Zhao, T. S. Wang, and Z. M. Yang. 2012. 'Junctional adhesion molecule 2 mediates the interaction between hatched blastocyst and luminal epithelium: induction by progesterone and LIF', *PLoS One*, 7: e34325.

Subramanian, A., P. Tamayo, V. K. Mootha, S. Mukherjee, B. L. Ebert, M. A. Gillette, A. Paulovich, S. L. Pomeroy, T. R. Golub, E. S. Lander, and J. P. Mesirov. 2005. 'Gene set enrichment analysis: a knowledge-based approach for interpreting genome-wide expression profiles', *Proc Natl Acad Sci U S A*, 102: 15545-50.

Sugihara, K., D. Sugiyama, J. Byrne, D. P. Wolf, K. P. Lowitz, Y. Kobayashi, M. Kabir-Salmani, D. Nadano, D. Aoki, S. Nozawa, J. Nakayama, T. Mustelin, E. Ruoslahti, N. Yamaguchi, and M. N. Fukuda. 2007. 'Trophoblast cell activation by trophinin ligation is implicated in human embryo implantation', *Proc Natl Acad Sci U S A*, 104: 3799-804.

Tamm-Rosenstein, K., J. Simm, M. Suhorutshenko, A. Salumets, and M. Metsis. 2013. 'Changes in the transcriptome of the human endometrial Ishikawa cancer cell line induced by estrogen, progesterone, tamoxifen, and mifepristone (RU486) as detected by RNA-sequencing', *PLoS One*, 8: e68907.

Tapia, A., L. A. Salamonsen, U. Manuelpillai, and E. Dimitriadis. 2008. 'Leukemia inhibitory factor promotes human first trimester extravillous trophoblast adhesion to extracellular matrix and secretion of tissue inhibitor of metalloproteinases-1 and -2', *Hum Reprod*, 23: 1724-32.

Teklenburg, G., M. Salker, M. Molokhia, S. Lavery, G. Trew, T. Aojanepong, H. J. Mardon, A. U. Lokugamage, R. Rai, C. Landles, B. A. Roelen, S. Quenby, E. W. Kuijk, A. Kavelaars, C. J. Heijnen, L. Regan, J. J. Brosens, and N. S. Macklon. 2010. 'Natural selection of human embryos: decidualizing endometrial stromal cells serve as sensors of embryo quality upon implantation', *PLoS One*, 5: e10258.

Tiscornia, G., O. Singer, and I. M. Verma. 2006. 'Production and purification of lentiviral vectors', *Nat Protoc*, 1: 241-5.

Uchida, H., T. Maruyama, S. Nishikawa-Uchida, H. Oda, K. Miyazaki, A. Yamasaki, and Y. Yoshimura. 2012. 'Studies using an in vitro model show evidence of involvement of epithelial-mesenchymal transition of human endometrial epithelial cells in human embryo implantation', *J Biol Chem*, 287: 4441-50.

Uhlen, M., L. Fagerberg, B. M. Hallstrom, C. Lindskog, P. Oksvold, A. Mardinoglu, A. Sivertsson, C. Kampf, E. Sjostedt, A. Asplund, I. Olsson, K. Edlund, E. Lundberg, S. Navani, C. A. Szigyarto, J. Odeberg, D. Djureinovic, J. O. Takanen, S. Hober, T. Alm, P. H. Edqvist, H. Berling, H. Tegel, J. Mulder, J. Rockberg, P. Nilsson, J. M. Schwenk, M. Hamsten, K. von Feilitzen, M. Forsberg, L. Persson, F. Johansson, M. Zwahlen, G. von Heijne, J. Nielsen, and F. Ponten. 2015. 'Proteomics. Tissue-based map of the human proteome', *Science*, 347: 1260419.

Ulbrich, S. E., A. E. Groebner, and S. Bauersachs. 2013. 'Transcriptional profiling to address molecular determinants of endometrial receptivity--lessons from studies in livestock species', *Methods*, 59: 108-15.

Valdes, C. T., A. Schutt, and C. Simon. 2017. 'Implantation failure of endometrial origin: it is not pathology, but our failure to synchronize the developing embryo with a receptive endometrium', *Fertil Steril*, 108: 15-18.

Vandesompele, J., K. De Preter, F. Pattyn, B. Poppe, N. Van Roy, A. De Paepe, and F. Speleman. 2002. 'Accurate normalization of real-time quantitative RT-PCR data by geometric averaging of multiple internal control genes', *Genome Biol*, 3: RESEARCH0034.

Vasquez, Y. M., E. C. Mazur, X. Li, R. Kommagani, L. Jiang, R. Chen, R. B. Lanz, E. Kovanci, W. E. Gibbons, and F. J. DeMayo. 2015. 'FOXO1 is required for binding of PR on IRF4, novel transcriptional regulator of endometrial stromal decidualization', *Mol Endocrinol*, 29: 421-33.

Vasquez, Y. M., X. Wang, M. Wetendorf, H. L. Franco, Q. Mo, T. Wang, R. B. Lanz, S. L. Young, B. A. Lessey, T. E. Spencer, J. P. Lydon, and F. J. DeMayo. 2018. 'FOXO1 regulates uterine epithelial integrity and progesterone receptor expression critical for embryo implantation', *PLoS Genet*, 14: e1007787.

Vassena, R., S. Boue, E. Gonzalez-Roca, B. Aran, H. Auer, A. Veiga, and J. C. Izpisua Belmonte. 2011. 'Waves of early transcriptional activation and pluripotency program initiation during human preimplantation development', *Development*, 138: 3699-709.

Velicky, P., G. Meinhardt, K. Plessl, S. Vondra, T. Weiss, P. Haslinger, T. Lendl, K. Aumayr, M. Mairhofer, X. Zhu, B. Schutz, R. L. Hannibal, R. Lindau, B. Weil, J. Ernerudh, J. Neesen, G. Egger, M. Mikula, C. Rohrl, A. E. Urban, J. Baker, M. Knofler, and J. Pollheimer. 2018. 'Genome amplification and cellular senescence are hallmarks of human placenta development', *PLoS Genet*, 14: e1007698.

Vento-Tormo, R., M. Efremova, R. A. Botting, M. Y. Turco, M. Vento-Tormo, K. B. Meyer, J. E. Park, E. Stephenson, K. Polanski, A. Goncalves, L. Gardner, S. Holmqvist, J. Henriksson, A. Zou, A. M. Sharkey, B. Millar, B. Innes, L. Wood, A. Wilbrey-Clark, R. P. Payne, M. A. Ivarsson, S. Lisgo, A. Filby, D. H. Rowitch, J. N. Bulmer, G. J. Wright, M. J. T. Stubbington, M. Haniffa, A. Moffett, and S. A. Teichmann. 2018. 'Single-cell reconstruction of the early maternal-fetal interface in humans', *Nature*, 563: 347-53.

Vergaro, P., G. Tiscornia, A. Rodriguez, J. Santalo, and R. Vassena. 2019. 'Transcriptomic analysis of the interaction of choriocarcinoma spheroids with receptive vs. non-receptive endometrial epithelium cell lines: an in vitro model for human implantation', *J Assist Reprod Genet*, 6: 857-873.

Wallingford, M. C., J. R. Angelo, and J. Mager. 2013. 'Morphogenetic analysis of peri-implantation development', *Dev Dyn*, 242: 1110-20.

Wang, H., and S. K. Dey. 2006. 'Roadmap to embryo implantation: clues from mouse models', *Nat Rev Genet*, 7: 185-99.

Weimar, C. H., A. Kavelaars, J. J. Brosens, B. Gellersen, J. M. de Vreeden-Elbertse, C. J. Heijnen, and N. S. Macklon. 2012. 'Endometrial stromal cells of women with recurrent miscarriage fail to discriminate between high- and low-quality human embryos', *PLoS One*, 7: e41424.

Wetendorf, M., S. P. Wu, X. Wang, C. J. Creighton, T. Wang, R. B. Lanz, L. Blok, S. Y. Tsai, M. J. Tsai, J. P. Lydon, and F. J. DeMayo. 2017. 'Decreased epithelial progesterone receptor A at the window of receptivity is required for preparation of the endometrium for embryo attachment', *Biol Reprod*, 96: 313-26.

Whiteside, E. J., M. M. Jackson, A. C. Herington, D. R. Edwards, and M. B. Harvey. 2001. 'Matrix metalloproteinase-9 and tissue inhibitor of metalloproteinase-3 are key regulators of extracellular matrix degradation by mouse embryos', *Biol Reprod*, 64: 1331-7.

Wu, L. Z., X. L. Liu, and Q. Z. Xie. 2015. 'Osteopontin facilitates invasion in human trophoblastic cells via promoting matrix metalloproteinase-9 in vitro', *Int J Clin Exp Pathol*, 8: 14121-30.

Xiao, S., H. Diao, F. Zhao, R. Li, N. He, and X. Ye. 2014. 'Differential gene expression profiling of mouse uterine luminal epithelium during periimplantation', *Reprod Sci*, 21: 351-62.

Yung, H. W., D. Atkinson, T. Campion-Smith, M. Olovsson, D. S. Charnock-Jones, and G. J. Burton. 2014. 'Differential activation of placental unfolded protein response pathways implies heterogeneity in causation of early- and late-onset pre-eclampsia', *J Pathol*, 234: 262-76.

Zhou, Y., O. Genbacev, and S. J. Fisher. 2003. 'The human placenta remodels the uterus by using a combination of molecules that govern vasculogenesis or leukocyte extravasation', *Ann N Y Acad Sci*, 995: 73-83.

Chapter 3. Implantation is a two-way dialogue: *in silico* predicted protein-protein interactions between the trophoblast and the receptive endometrial epithelium

To gain insight into the reciprocal embryo-maternal interactions, we performed a computational analysis to construct putative protein networks underlying the trophoblast-epithelium interaction during implantation. This analysis is based on the premise that the transcriptional changes during trophoblast-epithelium co-culture lead to the establishment of protein-protein interactions that ultimately induce signal transduction and coordinate both compartments. In our *in silico* approach, we integrated trophoblast and epithelial transcriptomic profiles with databases of reported physical protein-protein interactions (membrane/membrane or secreted ligand/membrane interacting protein pairs). Our analysis revealed sets of proteins that are likely to mediate the interaction within the trophoblast and the endometrial epithelium at different time points along the successful attachment process.

1. Materials and methods

In silico protein interaction network analysis

To predict protein-protein interactions between the trophoblast and the receptive epithelium, an integrative omics approach was used following the *in silico* strategy published by Chalmel et al. (Chalmel et al., 2014). This allowed for the prediction of membrane and secreted proteins from each compartment and their presumed interactions (membrane/membrane, secreted ligand/membrane and membrane/secreted ligand from the trophoblast or the epithelium, respectively). We did not include protein interactions between secreted protein from both compartments. The *in silico* interactomics analysis was first performed using the transcriptomics data of Ishikawa epithelial substrates and trophoblast spheroids after co-culture for 48 hours compared to their respective non-co-cultured controls (**Chapter 1**). The subsets of differentially expressed genes were catalogued according to a more restrictive criteria, using absolute log2FC ≥ 2 and adjusted p-value<0.05, as using more lax parameters would result in an unreasonably long list of protein-protein potential interactions. To further explore the protein-protein interactions involved in the receptive epithelium-trophoblast interactions in earlier stages of adhesion and attachment, the same strategy was used comparing the differentially expressed genes found in the time-course analysis described in **Chapter 2**. This analysis included the transcriptional profiles of co-cultured Ishikawa epithelial substrates for 8 *vs*. 0 hours (non-co-cultured control) and 24 *vs*. 8 hours as well as those of the trophoblast counterpart, i.e. co-cultured JEG-3 spheroids for 8 *vs*. 0 hours (non-co-cultured control) and 24 *vs*. 8 hours. In this case, the thresholds to filter differentially expressed genes were set at absolute log2FC ≥ 1 and adjusted p-value<0.05, as the lists of protein-protein interactions were feasible to handle. The gene expression datasets compared by the *in silico* analysis, the nomenclature according to the fractions obtained after FACS and the size of the datasets are listed in **Table I**.

Table I. Transcriptomic datasets selected for *in silico* protein interaction network analysis and number of genes included in each dataset (n) using absolute log2FC ≥2 and adjusted p-value<0.05 (white, results included in **Chapter 1**) or absolute log2FC ≥1 and adjusted p-value<0.05 (dark grey, results included in **Chapter 2**) cut-offs.

Transcriptomic dataset	Nomenclature	Size (n genes)
Ishikawa substrates co-cultured with JEG-3 spheroids for 48 hours *vs*. Ishikawa control (48 hours)	I-co-S *vs*. I-c	90
Ishikawa substrates co-cultured with JEG-3 spheroids for 8 hours *vs*. Ishikawa control at 0 hours	I-co-S T8 *vs*. I-c T0	295
Ishikawa substrates co-cultured with JEG-3 spheroids for 24 hours *vs*. Ishikawa substrates co-cultured with JEG-3 spheroids for 8 hours	I-co-S T24 *vs*. I-co-S T24	258
JEG-3 spheroids co-cultured with Ishikawa substrates for 48 hours *vs*. GFP+ JEG-3 spheroids control (48 hours)	S-co-I *vs*. S-c	2001
JEG-3 spheroids co-cultured with Ishikawa substrates for 8 hours *vs*. GFP+ JEG-3 spheroids control at 0 hours	S-co-I T8 *vs*. S-c T0	1247
JEG-3 spheroids co-cultured with Ishikawa substrates for 24 hours *vs*. JEG-3 spheroids co-cultured with Ishikawa substrates for 8 hours	S-co-I T24 *vs*. S-co-I T24	481

To identify membrane proteins in our transcriptomic datasets, we used the public collection of the predicted human membrane proteome, which was generated according to the majority decision-based method (MDM). This predicted human membrane proteome comprises 5480 transmembrane proteins selected by seven prediction methods: MEMSAT3, MEMSAT-SVM, Phobius version 1.01, SCAMPI multi-sequence-version, SPOCTOPUS, TMHMM and THUMBUP (Fagerberg et al., 2010). The MDM method selects membrane proteins when they present at least one transmembrane segment and overlapping predictions by four out of the seven methods. To identify secreted proteins, the Human Protein Atlas (HPA) database was used, which included 2933 predicted candidates containing a peptide signal sequence by three prediction methods: SignalP4.0, Phobius and SPOCTOPUS (Uhlen et al., 2015). Similarly to the MDM, this collection used a majority decision-based method for secreted proteins (MDSEC) selecting those candidates expressing the signal peptide sequence that are included by two out of the three different prediction methods. Some secreted and membrane proteins present the signal peptides; if these proteins are also predicted as transmembrane by the MDM, they are considered anchored to the membrane and therefore not secreted. Both collections are freely accessible on the Human Protein Atlas website (https://www.proteinatlas.org). By integrating our transcriptomic data with

predicted membrane and secreted protein collections, we identified predicted membrane and secreted proteins in both the trophoblast and epithelial compartments.

Genome annotation entries (Ensembl gene IDs) of our predicted membrane and secreted proteins datasets were converted into their corresponding Uniprot entries using the Uniprot Retrieve/ID mapping tool (https://www.uniprot.org/); only protein entries retrieved from the Swiss-Prot manually annotated and reviewed database were included.

Finally, the interacting protein partners involved in trophoblast-epithelial crosstalk were predicted using MENTHA tool (http://mentha.uniroma2.it), which includes five source databases: MINT, IntAct, DIP, MatrixDB and BioGRID (Calderone, Castagnoli and Cesareni, 2013). The MENTHA interactomics network was built from predicted direct protein-protein interactions between the two sets of proteins (epithelial membrane proteins or secreted proteins *vs*. trophoblast membrane proteins or secreted proteins).

Validation of predicted protein-protein interactions by immunofluorescence

In order to validate the predicted protein-protein interactions between the trophoblast and the epithelial compartments, a validation by immunofluorescence was performed on selected protein pairs. The transcriptomic data used for validation experiments were those obtained in the study described in **Chapter 1**, i.e. those genes that resulted differentially expressed after 48 hours co-culture in both compartments: I-co-S *vs*. I-c and S-co-I *vs*. S-c. Only membrane-membrane interactions were tested to increase the probability of detecting protein co-localization by confocal imaging. The proteins were selected according to their relevance in previous publications and the availability of specific antibodies. The list of selected protein pairs as well as the antibodies and dilutions used are described in **Table II**.

Table II. Detailed information of the antibodies used for immunofluorescence validation of the *in silico* predicted protein-protein interactions.

Ishikawa membrane proteins		
	Primary antibody	**Working dilution**
CDHR-1	Anti-CDHR1 polyclonal antibody produced in rabbit (Sigma-Aldrich, Merck KGaA, Germany #HPA 036819)	1:250
CDHR-1	Anti-CDHR1 monoclonal antibody produced in mouse (Santa Cruz Biotechnology, USA #SC514764)	1:50
LAMP-3	Anti-LAMP-3 monoclonal antibody produced in mouse (Abcam, UK #ab215891)	1:100
CLDN-6	Anti-CLDN-6 polyclonal antibody produced in rabbit (Abcam, UK #ab107059)	1:50
JEG-3 membrane proteins		
	Primary antibody	**Working dilution**
PROM-1	Anti-PROM-1 monoclonal antibody produced in mouse (Thermo Fisher Scientific, USA #MA1219)	1:100
TMEM-30-B	Anti-TMEM-30-B polyclonal antibody produced in rabbit (Thermo Fisher Scientific, USA #PA5-60263)	1:50
ABCA-3	Anti-ABCA-3 polyclonal antibody produced in rabbit (Thermo Fisher Scientific, USA #PA5-52478)	1:25
MUC-1	Anti-MUC-1 monoclonal antibody produced in mouse (Abcam, UK #ab36690)	1:5

Immunostaining was performed on co-cultures of trophoblast spheroids and Ishikawa monolayers as described above using chambered coverslips suitable for confocal imaging (treated 8 well-chambered coverslips; Ibidi, Germany #80827). After 48 hours, the co-cultures were rinsed three times in 1X DPBS, fixed in 4% formaldehyde (PFA) (from 16% PFA formaldehyde; Thermo Fisher Scientific, USA #28908) in 1X DPBS for 15 min at room temperature and washed three times in 0.1% DPBS-T (DPBS 0.1% Tween-20; Sigma-Aldrich, Merck KGaA, Darmstadt, Germany #P7949). Fixed samples were stored in 1X DPBS-T at 4ºC until processed. For immunostaining, co-cultures were permeabilized in 0.2% Triton-X-100 (Sigma-Aldrich, Merck KGaA, Darmstadt, Germany #T8787) in DPBS for 15 min, rinsed three times in 1X DPBS and blocked for 3 hours at room temperature in a solution of 5% goat serum (Sigma-Aldrich, Merck KGaA, Darmstadt, Germany #G9023) in DPBS-TB (DPBS 0.1% Tween-20 and 2% BSA; Bovine serum albumin fraction V, Gibco #15260037). Double immunostaining was performed by incubating the two primary antibodies of each protein interaction to be tested in the same well

(CDHR-1 and PROM-1, CDHR-1 and TMEM-30-B, LAMP-3 and ABCA-3, CLDN-6 and MUC-1). Primary antibodies were incubated overnight at 4ºC in blocking solution diluted at the concentrations showed in **Table II**. Samples were then rinsed three times in DPBS-T and incubated for one hour at room temperature with secondary antibodies (see **Table II** for concentrations). Additional wells of negative controls (no primary but only secondary incubation) were added for each interaction pair. After secondary incubation, samples were rinsed again three times with DPBS-T and stained for nuclei visualization with 50µg/ml Hoechst 33342 (Thermo Fisher Scientific, USA #H3570) for 30 minutes at room temperature. Samples were rinsed three times in DPBS and stored at 4ºC until visualized under the confocal microscope (Leica TCS-SP5 confocal microscope at 63X with oil; Leica Microsystems, Wetzlar, Germany or Zeiss 780 confocal/multiphoton microscope at 63X with 80% glycerol; Zeiss International, Oberkochen, Germany).

2. Results

The interactome of *in vitro* implantation: a prediction based on 48 hours co-culture

Among the 90 genes differentially expressed in the Ishikawa epithelial substrate upon 48 hours co-culture (I-co-S *vs*. I-c), we found 25 predicted membrane proteins and 21 predicted secreted proteins; from the list of 2001 genes differentially expressed in the trophoblast spheroids (S-co-I *vs*. S-c), 654 were predicted to encode membrane proteins and 116 were predicted to encode secreted proteins. The *in silico* predicted interactome strategy revealed 21 different direct protein-protein interactions, some of them included in more than one group (**Table III**): 12 interactions between epithelial secreted ligands and trophoblast membrane receptors, 16 direct interactions between epithelial and trophoblast membrane proteins and 3 interactions between trophoblast secreted ligands and epithelial membrane receptors.

Table III. Trophoblast-receptive epithelium interaction network after 48 hours of co-culture predicted by MENTHA tool. Protein pairs are shown in columns: epithelial secreted ligands and trophoblast membrane receptors, direct interactions between epithelial and trophoblast membrane proteins, and trophoblast secreted ligands and epithelial membrane receptors.

Epithelial secreted	Trophoblast membrane	Epithelial membrane	Trophoblast membrane	Epithelial membrane	Trophoblast secreted
LAMP3	SEL1L3	LAMP3	SEL1L3	CDHR1	PROM1
LAMP3	ATL3	LAMP3	ATL3	CLDN6	MUC1
LAMP3	ARL10	LAMP3	ARL10	ISLR2	UPK1B
LAMP3	SLC22A18	LAMP3	SLC22A18		
CDHR1	PROM1	CDHR1	PROM1		
GDF6	BMPR1B	CCDC155	UPK1B		
LAMP3	ABCA3	LAMP3	ABCA3		
CHST8	MOXD1	CDHR1	TMEM30B		
CDHR1	TMEM30B	MFSD12	SYPL2		
CALCRL	ADM	PDZK1IP1	NSG1		
CHST8	ARL10	PDZK1IP1	AQP2		
CHST8	FRAS1	CLDN6	MUC1		
		GPR161	UPK1B		
		ISLR2	UPK1B		
		CERS4	UPK1B		
		PLLP	SYPL2		

The dynamics of the interactome during *in vitro* implantation

Based on the results described in **Chapter 2**, we further investigated the interactome between the trophoblast and the receptive endometrial epithelium in a time-dependent manner (stage I: between 0 hours and 8 hours of co-culture and stage II: from 8 hours to 24 hours of co-culture). From the dataset of transcriptional changes occurring in the epithelial compartment in stage I (I-co-S T8 *vs*. I-c T0, 295 differentially expressed genes), a total of 74 and 50 genes were predicted to encode membrane proteins and secreted proteins, respectively. In the trophoblast spheroid compartment, 427 and 253 out of the 1247 differentially expressed genes during stage I (S-co-I T8 *vs*. S-c T0 comparison) were predicted to encode membrane and secreted proteins, respectively. We predicted a total of 62 different protein-protein interactions between compartments, with several of them occurring in more than one group: 17 interactions between epithelial secreted ligands and trophoblast membrane receptors, 43 direct interactions between epithelial and trophoblast membrane proteins and 25 interactions between trophoblast secreted ligands and epithelial membrane receptors (**Table IV**).

Table IV. Trophoblast-receptive epithelium interaction network during stage I (after 8 hours of co-culture) predicted by MENTHA tool. Protein pairs are shown in columns: epithelial secreted ligands and trophoblast membrane receptors, direct interactions between epithelial and trophoblast membrane proteins, and trophoblast secreted ligands and epithelial membrane receptors.

Epithelial secreted	Trophoblast membrane	Epithelial membrane	Trophoblast membrane	Epithelial membrane	Trophoblast secreted
LAMA1	ITGA2	EPHA2	ITGB3	JAG1	APBB1
CD44	EGFR	CLDN1	CLDN3	EPHA2	ITGB3
CTGF	EGFR	ADRB2	CLGN	ADRB2	CLGN
SCAMP5	PLAU	CAV1	ABCB1	CAV1	PTGS1
FAT4	PDGFB	MYADM	CD7	MYADM	CD7
LAMA3	CD44	TPM1	EGFR	TPM1	EGFR
L1CAM	NRP1	CD44	EGFR	CD44	EGFR
CTGF	ITGA5	EPHA2	EGFR	EPHA2	EGFR
NRG1	EGFR	HBEGF	EGFR	HBEGF	EGFR
CX3CL1	ITGB3	MYADM	MRAP2	CD44	SPP1
CX3CL1	ITGA5	CAV1	CD44	CAV1	CD44
SLC7A11	CD44	HBEGF	CD44	LAMA3	CD44
CD44	CD44	CAV1	GJA1	HBEGF	CD44
INSIG2	PRLR	CAV1	GJB2	L1CAM	NRP1
ANGPT1	TEK	MYADM	CD83	NRG1	EGFR
LAMA3	SDC2	PBXIP1	P2RX5	MYADM	IL1R2
TNFRSF12A	SLC30A2	HBEGF	CD82	CX3CL1	ITGB3
		NRG1	EGFR	ATP2B3	CLGN
		MYADM	IL1R2	CD44	CD44
		CX3CL1	ITGB3	CLDN6	IGFBP5
		GPR50	SDC2	CAV1	PDGFRB
		MYADM	NCR3LG1	CD44	VCAN
		BNIP3	BCL2	CAV1	PTGS2
		PBXIP1	PRKAA2	CAV1	ID1
		ATP2B3	CLGN	CAV1	EGFR
		CAV1	CXCR4		
		PBXIP1	PTGER3		
		MYADM	PTGER3		
		SLC7A11	CD44		
		CD44	CD44		
		TACSTD2	CLDN1		
		EPHA2	GOLIM4		
		APOL2	EMP1		
		FAXDC2	TMPRSS2		
		BNIP3	TMPRSS2		
		BNIP3	PLP2		
		SLC19A3	C4ORF3		
		EPHA2	EPHA2		
		CAV1	PDGFRB		
		CAV1	EGFR		

			TNFRSF12A	SLC30A2			
			BNIP3	BNIP3L			
			BNIP3	BNIP3			

Taking the transcriptional changes occurring in stage II (from 8 to 24 hours), a total of 68 membrane proteins and 56 secreted proteins were predicted in the epithelial compartment (I-co-S T24 *vs*. I-co-S T8, 258 differentially expressed genes). Regarding the trophoblast spheroids, a total of 169 and 116 membrane and secreted proteins were predicted, respectively (S-co-I T24 *vs*. S-co-I T24, 481 differentially expressed genes). Our *in silico* strategy allowed us to predict 16 different protein-protein interactions, some of them included in different groups: 6 interactions between epithelial secreted ligands and trophoblast membrane receptors, 13 direct interactions between epithelial and trophoblast membrane proteins and 9 interactions between trophoblast secreted ligands and epithelial membrane receptors (**Table V**).

Table V. Trophoblast-receptive epithelium interaction network in stage II (from 8 to 24 hours of co-culture) predicted by MENTHA tool. Protein pairs are shown in columns: epithelial secreted ligands and trophoblast membrane receptors, direct interactions between epithelial and trophoblast membrane proteins, and trophoblast secreted ligands and epithelial membrane receptors.

Epithelial secreted	**Trophoblast membrane**		**Epithelial membrane**	**Trophoblast membrane**		**Epithelial membrane**	**Trophoblast secreted**
SECTM1	CD7		CAV1	TNFRSF1B		TNFRSF12A	TNFSF12
EPHA7	EPHA4		ITGB8	RHBDL1		CAV1	TNFRSF1B
CA9	CA9		SECTM1	CD7		CAV1	PTGS1
EPHA7	EFNA3		EPHA7	EPHA4		SECTM1	CD7
EPHA7	EPHA3		CA9	CA9		EPHA7	EPHA4
SECTM1	EMP3		PTPRN	MAL		CA9	CA9
			EPHA7	EFNA3		EPHA7	EPHA3
			CAV1	CXCR4		CAV1	PDGFRB
			TACSTD2	CLDN1		CAV1	PTGS2
			EPHA7	EPHA3			
			SECTM1	EMP3			
			PTPRN	PTPRN			
			CAV1	PDGFRB			

Validation of *in silico* predicted protein-protein interactions

In order to confirm the interactions predicted by our *in silico* strategy, we performed immunofluorescent staining of selected protein-protein pairs. Despite repeated attempts, we were unable to show protein co-localization of predicted interactions in both the trophoblast and the epithelium compartments by confocal imaging (**Figures 1-4**). Some antibodies did not work (e.g. PROM-1 and ABCA-3) while others resulted in signal in both the trophoblast and the epithelium (e.g. CDHR-1 and MUC-1). All the selected proteins were expected to present membrane distribution; however, only CDHR-1, CLDN-6 and MUC-1 showed a clear membrane distribution in some cells (**Figures 2 and 3**). The validation of specific protein-protein interactions is ongoing work in our lab.

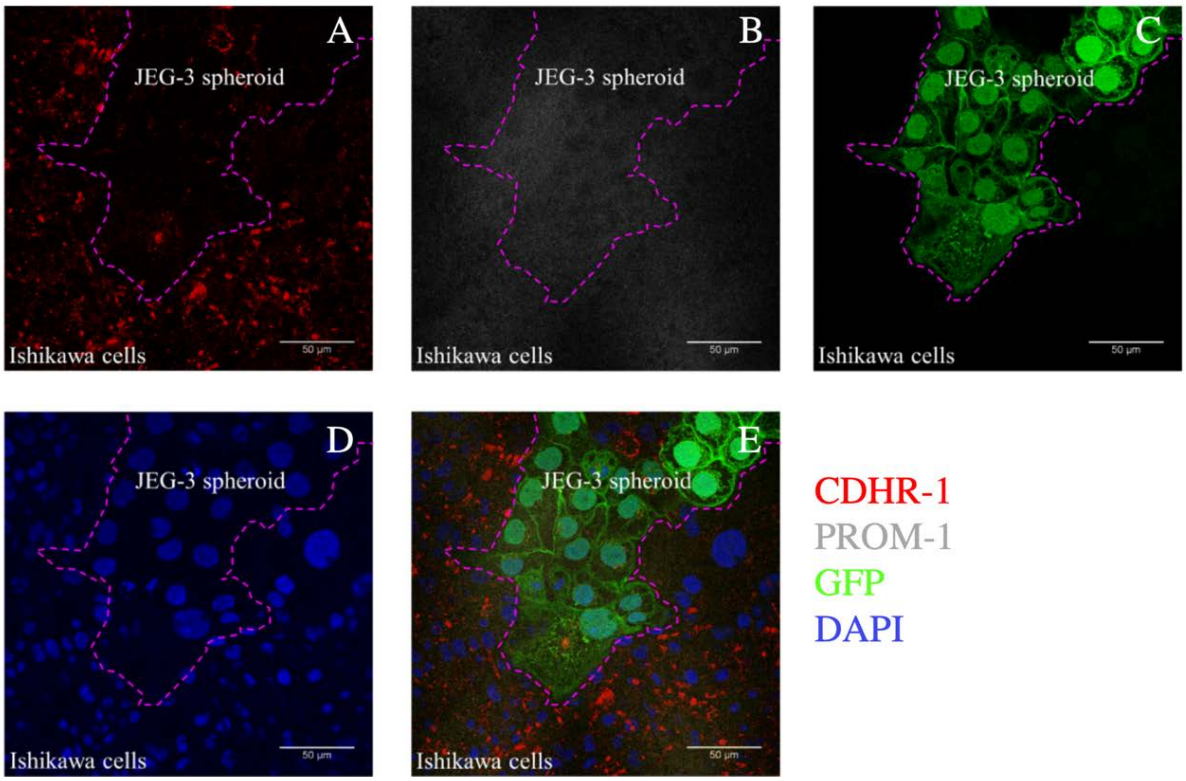

Figure 1. Representative image of immunofluorescence validation of the CDHR-1 (presumed in Ishikawa) **– PROM-1** (presumed in JEG-3 spheroids) **interaction predicted by our integrative *in silico* analysis**. Immunostaining for CDHR-1 is shown in red (**A**), immunostaining for PROM-1 is shown in grey (**B**) and GFP is shown in green (**C**). Nuclei were labelled with DAPI and are shown in blue (**D**). Panel **E** shows a merge of all the channels. Pink dotted lines delimit the extension of GFP+ JEG-3 spheroids co-cultured on monolayers of Ishikawa cells. Images were obtained under 63X magnification with a confocal microscope; panels from **A** to **E** show a single Z-stack of the same sample. Scale bars represent 50 µm length.

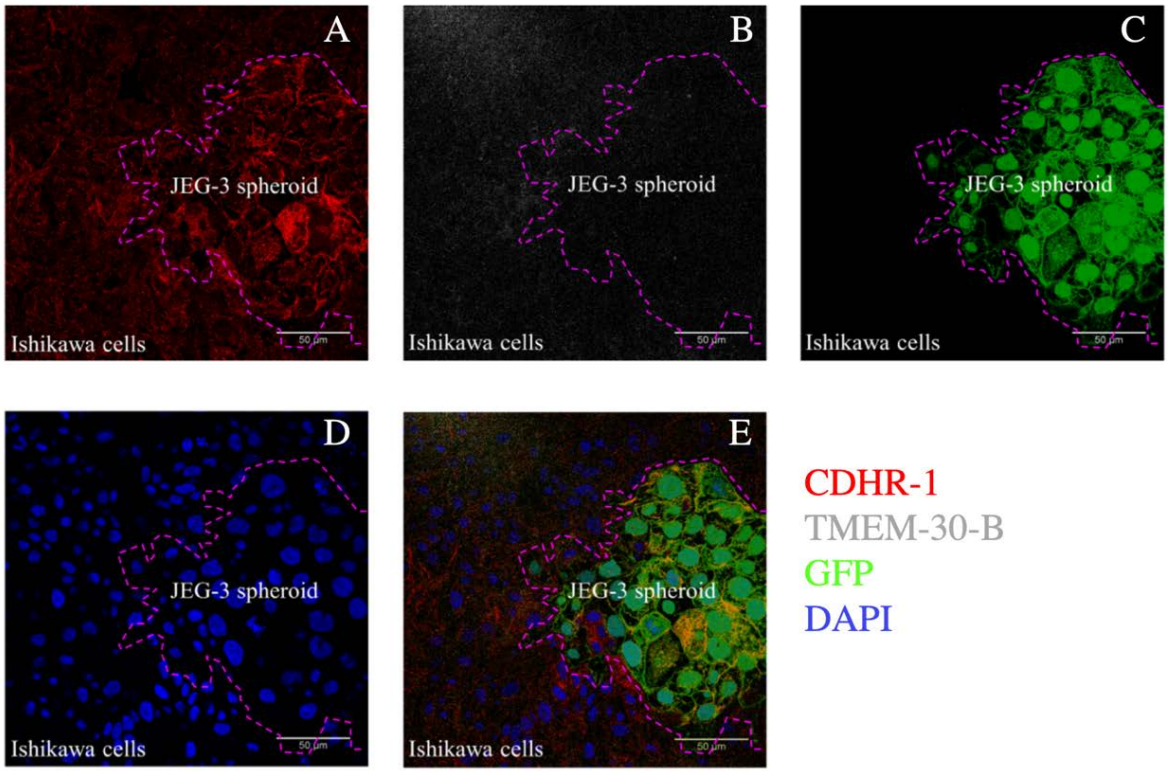

Figure 2. Representative image of immunofluorescence validation of the CDHR-1 (presumed in Ishikawa) **– TMEM-30-B** (presumed in JEG-3 spheroids) **interaction predicted by our integrative *in silico* analysis**. Immunostaining for CDHR-1 is shown in red (**A**), immunostaining for TMEM-30-B is shown in grey (**B**) and GFP is shown in green (**C**). Nuclei were labelled with DAPI and are shown in blue (**D**). Panel **E** shows a merge of all the channels. Pink dotted lines delimit the extension of GFP+ JEG-3 spheroids co-cultured on monolayers of Ishikawa cells. Images were obtained under 63X magnification with a confocal microscope; panels from **A** to **E** show a single Z-stack of the same sample. Scale bars represent 50 µm length.

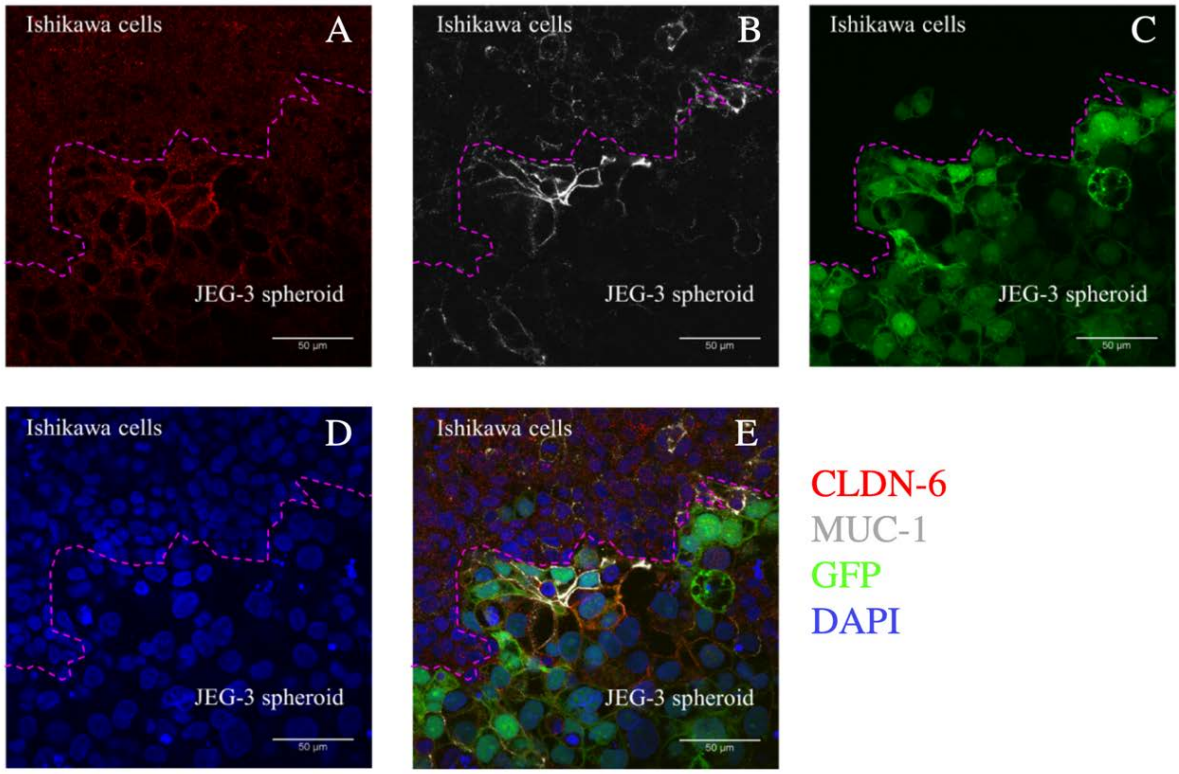

Figure 3. Representative image of immunofluorescence validation of the CLDN-6 (presumed in Ishikawa) **– MUC-1** (presumed in JEG-3 spheroids) **interaction predicted by our integrative *in silico* analysis**. Immunostaining for CLDN-6 is shown in red (**A**), immunostaining for MUC-1 is shown in grey (**B**) and GFP is shown in green (**C**). Nuclei were labelled with DAPI and are shown in blue (**D**). Panel **E** shows a merge of all the channels. Pink dotted lines delimit the extension of GFP+ JEG-3 spheroids co-cultured on monolayers of Ishikawa cells. Images were obtained under 63X magnification with a confocal microscope; panels from **A** to **E** show a single Z-stack of the same sample. Scale bars represent 50 µm length.

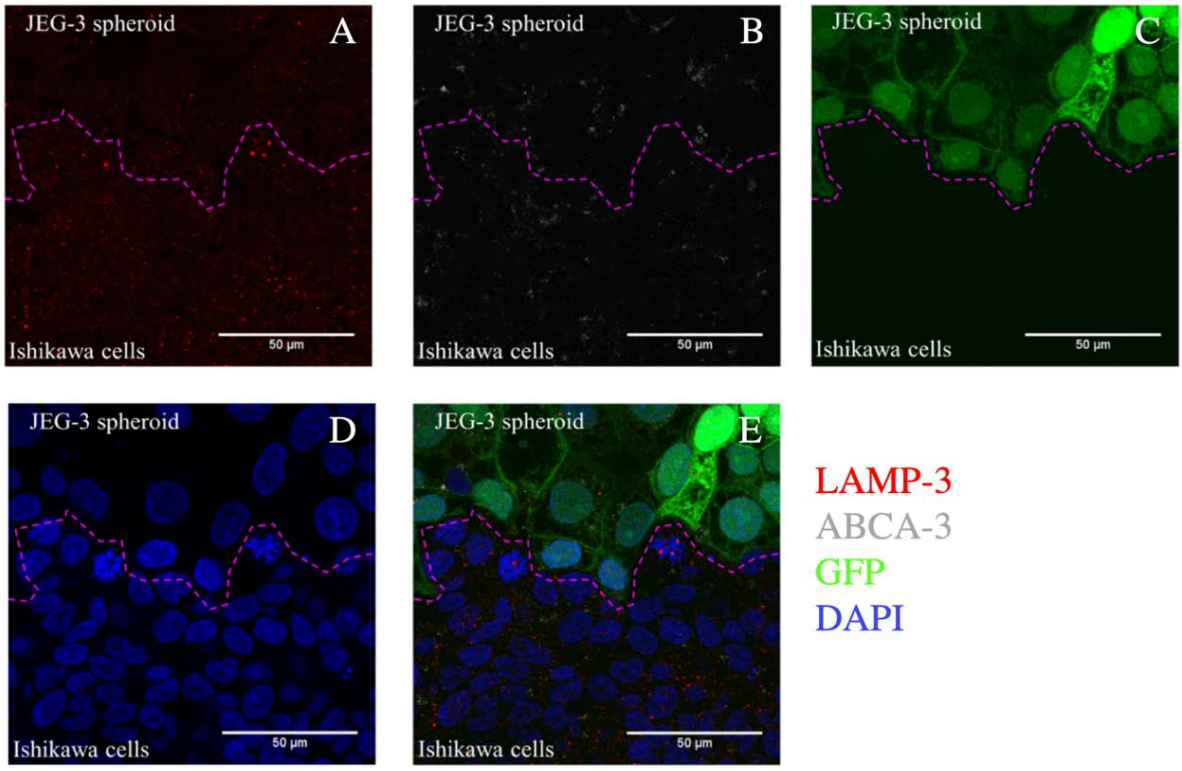

Figure 4. Representative image of immunofluorescence validation of the LAMP-3 (presumed in Ishikawa) **– ABCA-3** (presumed in JEG-3 spheroids) **interaction predicted by our integrative *in silico* analysis**. Immunostaining for LAMP-3 is shown in red (**A**), immunostaining for ABCA-3 is shown in grey (**B**) and GFP is shown in green (**C**). Nuclei were labelled with DAPI and are shown in blue (**D**). Panel **E** shows a merge of all the channels. Pink dotted lines delimit the extension of GFP+ JEG-3 spheroids co-cultured on monolayers of Ishikawa cells. Images were obtained under 63X magnification (zoomed in) with a confocal microscope; panels from **A** to **E** show a single Z-stack of the same sample. Scale bars represent 50 µm length.

3. Discussion

To our knowledge, this is the first integrative analysis using transcriptional data from both the trophoblast and the epithelium compartments after their physical interaction in a co-culture model. Previous studies used similar strategies to build protein-protein interaction networks at the maternal-fetal interface (Haouzi et al., 2011; Altmae et al., 2012). However, their analyses were based on unilateral transcriptional profiles of the embryo and the endometrium and provide a static snapshot of the dynamic process of implantation. In addition, these studies report implantation markers in day 5 blastocysts which might not be fully concordant with those on day 6 or 7, when implantation takes place.

Using the datasets generated from the experiments described in **Chapter 1**, our *in silico* analysis identified adhesion and ECM molecules such as CDHR-1, CLDN-6 and MUC-1, suggesting a

potential functional role of these proteins in attachment. As previously mentioned, the role of cell adhesion and ECM proteins in the trophectoderm-epithelium interaction has been broadly established in the literature. MUC-1 is a widely known marker of endometrial receptivity and implantation (Singh et al., 2010; Horne et al., 2005; Bastu et al., 2015). Both MUC-1 mRNA and protein were found increased in receptive compared to non-receptive endometrium, and MUC-1 down-regulation is needed for implantation to occur (Meseguer et al., 2001; Singh et al., 2010). In our study, MUC-1 was predicted in the trophoblast, which has also been previously reported (Meseguer et al., 2001). The role of embryo-derived MUC-1 seems to be important for later stages of pregnancy, as MUC-1 expression has been found increased during human placental development and linked to trophoblast invasion (Shyu et al., 2008). Since we did not identify the interaction of trophoblast MUC-1 within the earlier 8 and 24-hour timepoints of co-culture analysis, this suggests that the trophoblast-epithelium co-culture at 48 hours is more representative of the early invasion stage of implantation rather than the attachment stage.

Among the results of the analysis using the data reported in **Chapter 2**, many other adhesion and ECM molecules appeared in both the trophoblast and the endometrial epithelium components of our system (e.g. CLDN-1, CLDN-3, ITGA5 and L1CAM). Some of them have previously been reported in the literature for their roles in reproduction. For instance, the cell surface glycoprotein CD44 has shown up in both stages of the time course analysis (8 hours *vs*. 0 hours and 24 hours *vs*. 8 hours), suggesting that it is an important mediator of the trophoblast-receptive epithelium interactions. The distribution of CD44 protein has been previously described in the trophoblast and the endometrial epithelium. CD44 acts as a receptor for collagens, matrix metalloproteinases and other ligands such as OPN. Ligand binding to epithelial CD44 leads to changes in cell motility, gene expression and growth (Senbanjo and Chellaiah, 2017). The interaction between embryonic CD44 with endometrial hyaluronic acid seems to promote EVT invasion during placentation (Takahashi et al., 2014). A recently published study highlighted the role of the CD44-hyaluronic acid protein pair in the embryo-epithelium interaction in a similar co-culture system using mouse embryos and Ishikawa cells. Functional blocking of embryonic CD44 leads to delayed attachment during early stages (Berneau et al., 2019). In our study, embryonic CD44 is predicted to interact with epithelial CAV1, HB-EGF, SLC7A11, CD44, LAMA-3. On the other hand, epithelial CD44 is predicted to interact with EGFR, CD44, SPP1 (OPN) and VCAN. These specific interacting pairs have not been previously described in the context of implantation, but some of them appear in the literature as involved in reproductive events. The expression and localization of CAV1 in the endometrial epithelium is increased during first stages of pregnancy in rats; it has been

suggested that it may play a role in trafficking proteins and maintaining a polarised epithelium (Madawala et al., 2014). *ERBB4* and *HB-EGF* have been proposed as trophoblast and endometrial markers of embryo attachment, respectively (Chobotova et al., 2002; Sugihara et al., 2007; Zhang et al., 2013). Unexpectedly, our *in silico* analysis did not predict *ERBB4* as a trophoblast protein interacting partner of endometrial HB-EGF. *HB-EGF* transcriptional levels were not different after 24 or 48 hours of co-culture but only earlier (after 8 hours) suggesting that it may exert a role as mediator in the initial apposition and attachment of the trophoblast to the receptive epithelium. Although the mechanisms by which this molecule contribute to the success of embryo implantation are unknown, there is evidence that HB-EGF elicits intracellular Ca^{2+} signalling and induces competence to the trophoblast for adhesion and invasion in the mouse (Wang et al., 2000). The highest HB-EGF expression in the human endometrial epithelium coincides with the presence of pinopodes during the WOI (Stavreus-Evers et al., 2002). Furthermore, human endometrial HB-EGF seems to be hormonally regulated by progesterone and estradiol; these hormones not only increase HB-EGF expression levels but also the ability of HB-EGF to induce the expression of other molecules related with implantation in the epithelium (i.e. LIF, HOXA-10 and ITGB3) (Lessey et al., 2002). Supporting the putative role of HB-EGF in implantation and trophoblast invasion, it has been shown that pre-eclampsia underlies defective HB-EGF signalling leading to altered trophoblast invasion and placentation (Armant et al., 2015).

CX3CL1, also known as fractalkine, is a chemokine presumed to be involved in the maternal-fetal crosstalk required for successful pregnancy. After implantation, fractalkine may regulate trophoblast invasion and remodelling of uteroplacental arteries (Kervancioglu Demirci, Salamonsen and Gauster, 2016). In our analysis, Ishikawa CX3CL1 was predicted to interact with the integrins ITGB3 and ITGA5; although these two integrins were known to be expressed by the trophoblast (Hannan et al., 2010), their most relevant roles are related with endometrial receptivity and regulation of trophoblast invasion by the endometrial epithelium (Zhu et al., 2013; Chung et al., 2016). TPM1 is an actin-binding protein involved in cytoskeleton organization and smooth muscle contraction (Lin et al., 2008). The *tpm1* gene was differentially expressed in mice peri-implantation luminal epithelium compared to other stages and suggested as a marker of endometrial receptivity (Xiao et al., 2014). In our data, TPM1 was predicted as an epithelial membrane protein interacting with the epidermal growth factor receptor (EGFR) in the trophoblast during the first 8 hours of attachment. As mentioned in **Chapter 2**, cell movement, muscle contraction and cytoskeleton organization were over-represented in the receptive epithelium upon interaction with the trophoblast at 8 hours. The signal transduction regulating these molecular

cascades could require the interaction of membrane and secreted proteins such as TPM1-EGFR, that might ultimately mediate trophoblast attachment. Of note, the expression of *TPM1* in Ishikawa cells is estradiol-dependent (Tamm-Rosenstein et al., 2013); this feature makes it an interesting candidate for endometrial receptivity and implantation and its expression along the women´s endometrial cycle should be evaluated.

Despite several attempts, we have not been able to demonstrate the co-localization of the protein-protein interactions we selected by immunofluorescence. It is worth mentioning that our *in silico* strategy is based on transcriptomic data; protein expression does not necessarily reflect transcription. Additionally, the absence of immunofluorescence signals for some of our targets does not necessarily mean absence of the proteins due to antibody characteristics or factors related to sample processing. Validation of these predicted interactions using alternative methods is still pending.

In summary, the *in silico* interactomics strategy we describe here allowed us to identify a number of potential protein-protein interactions among the receptive endometrial epithelium and the trophoblast at different time points. Most of these proteins had not been described in the context of reproduction, while others had been related with implantation and endometrial receptivity in mice or human. Using the data obtained from the experiments described in **Chapter 1**, we predicted the protein candidates regulating the process at 48 hours; the results suggested that this time point corresponded to those changes expected during the beginning of invasion. With the ulterior analysis at different time points, we not only studied the dynamics of the process during the initial stages but also refined the analysis: we selected defined time frames (0 to 8 hours and 8 to 24 hours), therefore excluding redundant proteins that could also be involved in other stages. The validation of direct physical interactions between the trophoblast and the endometrial epithelium as well as functional assays to demonstrate their role in implantation would be very valuable. If confirmed, these interactions should be tested in viable human embryos and primary endometrial epithelial cells in order to be considered as clinical markers of implantation.

Chapter 4. The microbial environment in reproductive success

The concept of the uterus as a non-sterile cavity has been intensively discussed in the recent years, as well as its putative impact on reproductive outcomes. The vaginal microbiota composition has also been related with reproductive success, as some reports found negative results in vaginal fluid samples with high loads of anaerobic bacteria. Of note, the assessment of endometrial receptivity and implantation requires the development of non-invasive methods for clinical application. In this Chapter, we present a study that correlated the vaginal microbiota profile at the day of embryo transfer with live birth rates in IVF cycles using donated oocytes.

The results included in **Chapter 4** are part of the manuscript "**Vaginal microbiota profile at the time of embryo transfer does not affect live birth rate in IVF cycles with donated oocytes"** (Paula Vergaro, M.Sc., Gustavo Tiscornia, Ph.D., Montserrat Barragán, Ph.D; Amelia Rodríguez, Ph.D , Josep Santaló, Ph.D , Rita Vassena, D.V.M. Ph.D), which has been published in the *Reproductive Biomedicine Online* journal (https://doi.org/10.1016/j.rbmo.2018.12.019).

1. Abstract

Research question: What is the relationship between the vaginal microbiota profile at the time of embryo transfer (ET) and live birth rates in women undergoing IVF/ICSI with donated oocytes?

Design: 150 Caucasian women receiving donated oocytes were prospectively included in the study from March 2017 to January 2018. Samples of vaginal fluid were taken immediately before fresh single blastocyst transfer, and genomic DNA (gDNA) was extracted. Bacterial load as well as the presence of 4 lactobacilli (*L. crispatus, L. gasseri, L. jensenii* and *L. iners*) and 4 species related with BV (BVB) (*Gardnerella vaginalis, Atopobium vaginae, Mycoplasma hominis* and *Prevotella spp.*) were determined by qPCR. Vaginal microbiota profiles for each patient were characterized and correlated with reproductive results.

Results: Although bacterial load was variable, a majority of samples were dominated by a single species (80.7%, 121/150). Most samples (76.7%, 115/150) were dominated by *Lactobacillus spp*., while 23.3% (35/150) were dominated by BV associated bacteria. The distribution of microbiota profiles among women who achieved live birth and women who did not was similar ($p = 0.43$). Interestingly, we found a significantly higher proportion of *L. crispatus*-dominated samples in women achieving live birth compared to those who did not ($p = 0.021$); this correlation was also statistically significant for biochemical pregnancy ($p = 0.039$) and clinical pregnancy ($p = 0.015$).

Conclusions: Our data suggest that BV-like vaginal microbiota at the ET does not directly affect live birth rate.

Key message: Imbalances in vaginal microbiota leading to communities dominated by bacterial anaerobic species can result in bacterial vaginosis (BV). Published results are controversial regarding the relationship between BV-like microbiota and a detrimental effect on IVF outcome. The results of the present study suggest that a vaginal microbiota profile associated with BV at the day of embryo transfer is not linked with decreased live birth rate in IVF cycles with donated oocytes.

Funding: This work was supported by intramural funding of Clínica EUGIN and by the Secretary for Universities and Research of the Ministry of Economy and Knowledge of the Government of Catalonia (GENCAT 2015 DI 050). The authors declare no competing interests.

Keywords: vaginal microbiota; qPCR; bacterial vaginosis; IVF.

2. Introduction

The human body is colonized by millions of microorganisms which contribute to essential physiological processes such as immunity and metabolism (Guven-Maiorov, Tsai and Nussinov, 2017). Microbial diversity is dependent on environmental conditions and host factors, and varies considerably from site to site, between individuals, and in a time-dependent manner (Costello et al., 2009). Vaginal microbiota, i.e. the community of bacterial species colonizing the vaginal mucosae, plays an important role in the physiology of the female genital tract. Vaginal microbiota composition varies with ethnicity, personal hygiene, sexual activity and phase of the menstrual cycle (Ravel et al., 2011; Gajer et al., 2012), among others. Commonly, healthy vaginal microbiota is dominated by lactic acid-producing bacteria pertaining to *Lactobacillus spp*. This acidic environment might confer protective properties against pathogenic microorganisms such as *Chlamydia* and HIV (Gong et al., 2014; Nunn et al., 2014). Although more than 250 species of the vaginal microbial community have been characterized by sequencing, the microbiota of the vagina is usually dominated by just one or two species. The most frequent dominant species are *L. crispatus, L. gasseri, L. iners* and *L. jensenii* (Datcu et al., 2013; Li et al., 2012; Mendling, 2016). Imbalances in vaginal microbiota leading to communities dominated by facultative or strict anaerobes such as *Gardnerella vaginalis* and *Atopobium vaginae* can result in a clinical (or subclinical) condition known as bacterial vaginosis (BV). Overgrowth of BV-like bacterial species and depletion of Lactobacilli increases the vaginal pH and causes clinical symptoms in approximately half of the cases: itchiness, redness, vaginal discharge, and unusual odor (Mendling, 2016). BV is a relatively common vaginal disorder in women of reproductive age, with an estimated prevalence of 19% among infertile women (van Oostrum et al., 2013).

Clinically, a diagnosis of BV requires meeting the microbiological criteria of either Amsel, or more recently, Nugent (Amsel et al., 1983; Nugent, Krohn and Hillier, 1991). These methods rely on the morphological identification of bacteria using specific histological stains and clinical signs such as odor, discharge, presence of clue cells and vaginal pH > 4.5. In recent years, molecular techniques have emerged as promising tools to characterize vaginal microbiota, showing that the bacterial community involved in BV is more complex than previously realized (Burton and Reid, 2002; Hyman et al., 2005; Hyman et al., 2012; Fredricks et al., 2007; Srinivasan and Fredricks, 2008; Ravel et al., 2011; Balashov et al., 2014; Hilbert et al., 2016).

Published data have linked BV with reproductive outcomes, including higher risk of early pregnancy loss (Ralph, Rutherford and Wilson, 1999; Nelson et al., 2015), late miscarriage

(Nelson et al., 2007) and preterm birth (Foxman et al., 2014). To date, few studies have been conducted in women undergoing IVF, with contradictory results regarding the relationship between certain vaginal microbiota compositions and reproductive outcomes. Haar et al. suggested a significant negative impact of BV-like vaginal microbiota on clinical pregnancy rate (Haahr et al., 2016). Mangot-Bertrand et al. also found a relation between BV and decreased embryo implantation rate, albeit without statistical significance (Mangot-Bertrand et al., 2013). In contrast, Moini et al. found similar implantation, pregnancy, preterm delivery and live birth rates in women with diagnosed BV and healthy controls (Moini et al., 2017). Heterogeneity among women populations studied, technical approaches and sampling times makes direct comparisons between studies difficult and precludes reaching solid conclusions (Ralph, Rutherford and Wilson, 1999; Liversedge et al., 1999; Nelson et al., 2007; Mangot-Bertrand et al., 2013; Moini et al., 2017; Haahr et al., 2016). Therefore, the effect of vaginal microbiota composition on reproductive outcome remains controversial. In many of these studies, vaginal samples were collected during the ovum pick-up (Ralph, Rutherford and Wilson, 1999; Liversedge et al., 1999; Mangot-Bertrand et al., 2013; Moini et al., 2017); in our study, we avoided oocyte and ovarian stimulation related factors by including only recipients of donated oocytes.

We conducted a study to evaluate whether vaginal microbiota composition at the time of ET could influence IVF outcome in women receiving donated oocytes. Microbiota profiles were established according to qPCR-based species determination and related with live birth rate as the main outcome, as well as biochemical pregnancy and clinical pregnancy rates.

3. Materials and methods

Study population

A total of 150 Caucasian women undergoing IVF/ICSI with donated oocytes were prospectively included in the study from March until December 2017. Patients with medical conditions involving immunodeficiency, with clinically diagnosed BV in the six months prior to ET or those who had been treated with antibiotics within two months of the ET were excluded from the study. None of the participants were subjected to BV diagnosis at the moment of the fertility treatment, and none referred symptoms (e. g. vaginal discharge, discomfort or odor). Only fresh single blastocyst transfers were included in the analysis. Characteristics of the study population are outlined in

Table I. Of note, in cycles using frozen samples (most of the partner samples and all the donor samples), motility was evaluated after thawing.

Endometrial preparation

Women with ovarian function and menses received GnRH agonists in the midluteal phase for pituitary desensitization. Women who did not show ovarian function did not receive GnRH agonists. All the patients received 6 mg a day of oral oestradiol valerate for the endometrial preparation. The treatment lasted a variable period in accordance with the availability of a matching donor, ranging from 12 to 45 days. From the day of the donor oocyte retrieval, 800 mg of micronized progesterone was administered vaginally for luteal phase support.

Vaginal samples

One vaginal sample per patient was obtained on the day of ET. A sterile cotton swab (Cat. No. 300263, Deltalab Barcelona, Spain) was used to collect vaginal mucus from the fornix during speculum examination, immediately before introducing the transfer catheter. Samples were stored at -20ºC in empty plastic vials until processed.

Whole gDNA extraction

Whole gDNA was extracted from each vaginal swab following the manufacturer´s recommendation (QIAamp DNA mini kit protocol; Qiagen N. V., Venlo, Netherlands). Samples were eluted in 100 µl of AE buffer (10 mM Tris-Cl, 0.5 mM EDTA; pH 9.0), and gDNA concentration was quantified by measurement of absorbance at λ = 260 nm (Quawell, San Jose, USA). gDNA from the following bacterial species was purchased from the Leibniz Institute DSMZ (German Collection of Microorganisms and Cell Cultures, Brunswick, Germany): *Lactobacillus crispatus* (Cat# DSM 20584), *Lactobacillus gasseri* (Cat# DSM 20243), *Lactobacillus jensenii* (Cat# DSM 20557), *Lactobacillus iners* (Cat# DSM 13336), *Gardnerella vaginalis* (Cat# DSM 4944), *Atopobium vaginae* (Cat# DSM 15829), *Prevotella bivia* (Cat# DSM 20514), *and Mycoplasma hominis* (Cat# DSM 102144). GenBank reference numbers and genomic characteristics of the mentioned microorganisms are listed in **Table II**.

QPCR analysis

A molecular quantitative analysis was performed to both bacterial and human gDNA extracted from vaginal fluid samples. All qPCR reactions were performed in a final volume of 20µl, using

2x SsoAdvanced Universal SYBR Green Supermix (BioRad, Hercules, CA, USA), in a CFX Real-Time PCR system (Bio-Rad, Hercules, CA, USA). Primer sequences and literature sources are shown in **Table III**. Each bacterial gDNA was used to construct a standard curve based on serial 10-fold dilutions. Slopes of qPCR assays ranged between -3.4 and -3.7, with 85 to 96% efficiency and linearity values ≥0.99 in all the cases. Number of copies per ng of gDNA was calculated for each microorganism, taking into account their specific genome sizes (**Table II**). Vaginal fluid samples were analyzed by qPCR targeting the bacterial species previously mentioned, using 10 ng (in triplicate) of the total gDNA extracted from the vaginal swabs. Total bacterial load and the load of the human gene RPLP0 were also determined for each sample. Threshold setting, absolute and relative measurements were determined using the CFX Manager Software (Bio-Rad, Hercules, CA, USA). Melting points of the PCR products from vaginal fluid samples and standards were confirmed to be identical by analyzing the qPCR melting curves.

Vaginal microbiota profiling by qPCR

We established a vaginal microbiota profile for each sample based on two methods of analysis: i) number of copies of each microorganism per vaginal fluid sample (10 ng of the gDNA extracted and used as input in qPCR reactions) and ii) relative abundance of each bacterial species normalized to the total bacterial load detected and adjusted for human gDNA content. Taking into account the genome length of each bacterial species, we calculated the number of genome copies per ng of gDNA input according to the following calculation: 6.022×10^{23}/(number of bacterial genome base pairs*10^9*650). Standard curves from bacterial gDNA (of commercial origin, described in **Table II**) were used as references to calculate the number of copies of each microorganism in the samples. Relative abundance was calculated as the abundance of each bacterial species relative to the total bacteria detected with the qPCR primers as previously described (Brukner et al., 2015); in this approach, human RPLP0 gene content detected per sample was used as a normalizer. In both methods of analysis, vaginal fluid samples were defined as *Lactobacillus*-dominated microbiota profiles (≥90% *Lactobacillus spp.*: *L. crispatus, L. gasseri, L. jensenii,* and *L. iners*) or BVB-dominated microbiota profiles (>10% *G. vaginalis, A. vaginae, Prevotella spp.* and *M. hominis*) (Moreno et al., 2016).

Reproductive outcome analysis

The main outcome of this prospective study was live birth. Biochemical pregnancy (βhCG levels measured in blood 14 days after single blastocyst transfer) and clinical pregnancy (fetal heartbeat proven by ultrasonography at 7 weeks of gestation) were also evaluated.

Statistical analysis

The values of bacterial genome quantification obtained by qPCR were used to create a vaginal bacterial species profile for each patient. Univariate analysis using one-way Chi-square test was applied to study differences in microbiota profile distribution between live birth and no live birth or pregnant and non-pregnant groups according to biochemical and clinical pregnancy. All p-values were two-sided and significance level was established at $p<0.05$.

Ethical approval

The project was conducted under permission of the local CEIC (Ethics Committee for Clinical Research). All procedures performed were in accordance with the ethical standards of the institutional research committees and with the 1964 Helsinki declaration, as revised in 2013. All women signed an informed consent form before inclusion in the study.

4. Results

Although samples showed a wide range of bacterial loads, most of them were dominated by a single species (80.7%, 121/150). Evaluation of microorganism genome copy number of each species showed that 76.7% of our samples had *Lactobacillus*-dominated profiles (115/150), while the remaining 23.3% samples (35/150) had BVB-dominated profiles. Using the relative abundance analysis gave similar results: *Lactobacillus*-dominated samples were 77.3% (116/150), while BVB-dominated samples were 22.7% (34/150). Distribution of vaginal microbiota profiles was not statistically different between both methods of analysis ($p = 1.00$).

L. crispatus and *L. iners* were the most frequently dominant species, together dominating 48.0% of all samples. Among BVB, *G. vaginalis* was the most abundant species, dominating 14.0% of the samples. **Figure 1** shows the overall abundance of samples dominated by each single species with respect to all analyzed species.

Reproductive outcomes

We have live birth results of 149 out of the 150 women included in the study (one patient could not be contacted); the overall live birth rate was 37.6% (56/149). Among women who achieved live birth, the prevalence of *Lactobacillus*-dominated profiles was 80.4% (45/56) when the number of bacterial genome copies was analyzed. The remaining 19.6% (11/56) had BVB-dominated profiles. These proportions were similar to those found among women who did not achieve live birth (p =0.43), where microbiota profiles distributed as following: 74.2% (69/93) *Lactobacillus*-dominated and 25.8% (24/93) BVB-dominated profiles. A similar distribution of profiles was obtained when using the relative abundance analysis: 78.6% (44/56) *Lactobacillus*-dominated and 21.4% (12/56) BVB-dominated profiles in women achieving live birth *vs*. 76.3% (71/93) *Lactobacillus*-dominated and 23.7% (22/93) BVB-dominated profiles in women who did not achieve live birth. Again, there were no statistically significant differences in microbiota profile distribution between both study groups (p =0.84).

Overall, samples among live birth and non-live birth groups did not differ in terms of which species of bacteria was dominant, with a single exception; interestingly, one *Lactobacillus* species (*L. crispatus*) showed a significant predominance in women achieving live birth compared to those who did not achieve it (p = 0.021) (**Figure 2**).

We also analyzed the relationship between vaginal microbiota and earlier stages in pregnancy by assessing biochemical pregnancy and clinical pregnancy rates. The overall biochemical pregnancy rate was 54.0% (81/150), with microbiota profiles distributed as follows: 79.0% (64/81) *Lactobacillus*-dominated and 21.0% (17/81) BVB-dominated profiles among pregnant women *vs*. 73.9% (51/69) *Lactobacillus*-dominated and 26.1% (18/69) BVB-dominated profiles in non-pregnant women. Clinical pregnancy was confirmed in 42.7% (64/150) of all patients. The prevalence of *Lactobacillus* and BVB-dominated profiles among pregnant women confirmed by ultrasonography was 82.8% (53/64) and 17.2% (11/64), respectively. In non-pregnant women, *Lactobacillus*-dominated microbiota accounted for 72.1% (62/86) of all the samples and BVB microbiota for the remaining 27.9% (24/86). According to these reproductive outcomes (pregnant *vs.* non-pregnant) none of the groups showed differences in *Lactobacillus*-dominated and BVB-dominated profiles distribution. Regarding biochemical pregnancy, p-values were 0.56 and 0.85 according to the number of bacterial genomes and the relative abundance methods of analysis, respectively. P-value for clinical pregnancy was 0.17 analyzing the number of bacterial genomes and 0.69 using the relative abundance approach.

Examination of the dominance of each individual bacterial species revealed a significantly higher proportion of profiles dominated by *L. crispatus* in pregnant women compared to those non-pregnant ($p = 0.039$ for biochemical pregnancy, $p = 0.015$ for clinical pregnancy). **Figures 3** and **4** show the overall abundance of samples dominated by each single species with respect to all analyzed species for biochemical and clinical pregnancy.

5. Discussion

In our study, we found a BV-like vaginal microbiota in 23.3% of the patients population, in accordance with previously reported studies. Wilson et al., found a prevalence of BV-like vaginal microbiota in infertile women of 24.3% (Wilson, Ralph and Rutherford, 2002). Haahr et al. found similar values among IVF population, with 21% BV prevalence (as determined by Nugent score) and 28% BV prevalence by qPCR determination (Haahr et al., 2016). Proportions of *Lactobacillus*-dominated microbiota profiles were as high as 76.7% of those defined by number of copies of each microorganism and 77.3% of the profiles defined by our relative abundance analysis. This is similar to other studies which included Caucasian women (Ravel et al., 2011; Hyman et al., 2012).

Adjusting the specific content of each bacterial species for total bacterial load and human cellular content did not change the outcome. This is supported by a recent study where adjustment for total bacterial and human cell loads did not significantly improve sensitivity or specificity of molecular diagnosis of BV (Plummer et al., 2017).

The hypothesis of a relationship between an abnormal vaginal microbiota composition and reproductive outcomes has gained importance after recent reports indicating that the endometrium is not a sterile cavity (Franasiak et al., 2016; Moreno et al., 2016; Verstraelen et al., 2016), as previously thought. Several studies suggested an implication of vaginal microbiota in reproductive outcome including preterm and live birth rates. By sequencing the 16S ribosomal RNA gene, Hyman et al. showed temporal variability along IVF treatment and a correlation between composition at the day of ET and live birth rate (Hyman et al., 2012). Foxman et al. found a significant correlation between the presence of BV associated species (*Mycoplasma spp.*, *Mobiluncus* and *Atopobium*) and higher risk of preterm birth (Foxman et al., 2014). In a study population of 867 women undergoing IVF, Ralph et al. found higher risk of early pregnancy loss in women with BV, even though conception rates were not significantly decreased (Ralph, Rutherford and Wilson, 1999). A study published by Nelson et al. reached an opposite conclusion

after studying later reproductive outcomes; although BV and low levels of Lactobacilli during first trimester increased the risk of miscarriage, they did not find a significant correlation between overall levels of BV-associated bacteria and second trimester pregnancy loss (Nelson et al., 2007). Sample sizes, heterogeneous ethnicities of studied populations and different reproductive procedures make these studies difficult to compare.

The effect of vaginal microbiota in reproductive outcome has been examined mainly by focusing on implantation and clinical pregnancy. Salah et al. referred to BV as a cause of infertility in women suffering polycystic ovarian disease, with significantly increased clinical pregnancy rates in subsequent cycles after BV treatment (Salah et al., 2013). Haahr et al. recently reported a negative correlation between an abnormal vaginal microbiota and clinical pregnancy rate in women undergoing IVF (Haahr et al., 2016). By contrast, a study relating vaginal microbiota at the time of oocyte retrieval during IVF procedure did not support adverse effects of BV in implantation and early pregnancy (Liversedge et al., 1999).

The objective of the present study was to establish a vaginal microbiota profile of the most common species in the literature and relate it with reproductive success or failure; we did not find any correlation between vaginal microbiota profile on the day of the ET and live birth rate. The vaginal microbiota profile distribution in our study was not different either between pregnant and non-pregnant women for both implantation and clinical pregnancy. However, we found a significantly higher proportion of women achieving live birth harboring *L. crispatus*-dominated microbiota compared to women who failed ($p = 0.021$). This correlation also achieved statistical significance when biochemical and clinical pregnancy results were analyzed. Previous studies support our findings. Ravel et al. found predominance of *L.crispatus* in vaginal microbiota of asymptomatic women of reproductive age (Ravel et al., 2011). Hyman et al. also reported a dominance of *L.crispatus* among Lactobacilli, and also suggested a positive effect of vaginal microbiota mainly composed by Lactobacilli compared to that mixed on live birth outcome (Hyman et al., 2012). It is worth mentioning that our overall study population included women receiving donated oocytes who did not undergo ovarian stimulation, which excluded the hormonal regulation of vaginal microbiota composition reported in the literature (Hyman et al., 2012; Freitas et al., 2017) Therefore, it is difficult to compare our results with other studies; future research is needed to confirm a relationship between *L.crispatus*-dominated vaginal microbiota and reproductive outcome.

We only included SET at blastocyst stage with embryos obtained from donated oocytes; this excludes the oocyte factor which would undoubtedly affect the reproductive outcome. The fact that all the recipients underwent the same endometrial preparation and that all the samples were taken on the day of the ET also strengthens our results.

We recognize some limitations in our study. We focused on few bacterial species commonly studied in vaginal microbiota; as novel molecular approaches have revealed new species in the female tract microenvironment, the panel of detected bacteria by qPCR might be accordingly increased. Our results come from a population of Caucasian women and need to be confirmed in women with other ethnicities.

In conclusion, our results suggest that overall vaginal microbiota status at the time of ET does not directly affect implantation after IVF. We speculate that vaginal bacterial composition does not affect endometrial receptivity; previous evidences in the literature could derive from underlying mechanisms involving overall infection or abnormal immune conditions. It would be interesting to investigate whether the vaginal and endometrial microbiotas are correlated between them and with reproductive outcomes before using them as predictive variables in IVF.

Acknowledgements

We would like to thank the medical team and Laetitia Jimenez from Clínica Eugin for their help in samples collection.

Manuscript reprinted by permission from Elsevier, Reproductive Biomedicine Online (https://doi.org/10.1016/j.rbmo.2018.12.019).

Conflict of interest

None of the authors has competing interest to declare.

6. Figures

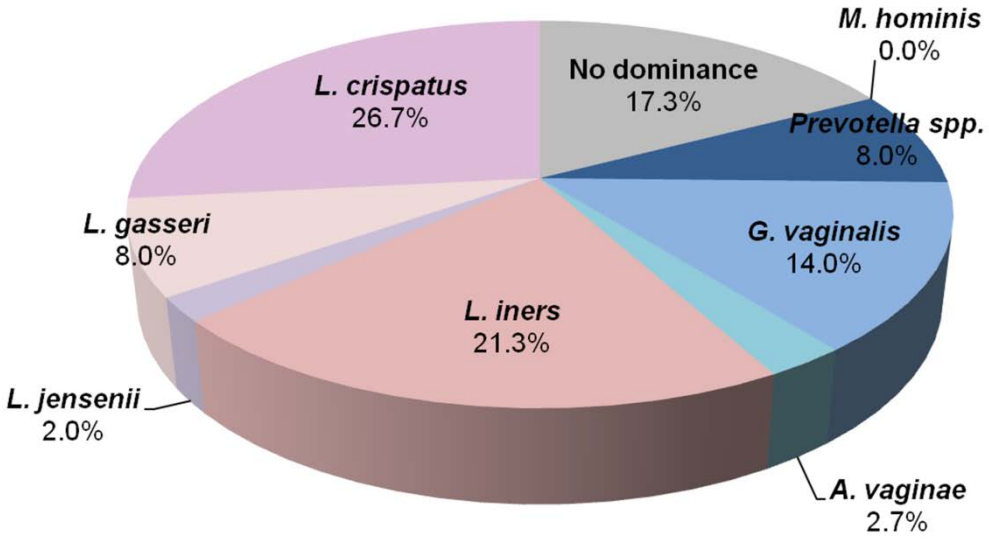

Figure 1. **Relative abundance of samples dominated by a single bacterial species**, calculated as the percentage of women from the overall population presenting a vaginal microbiota dominated by a single species.

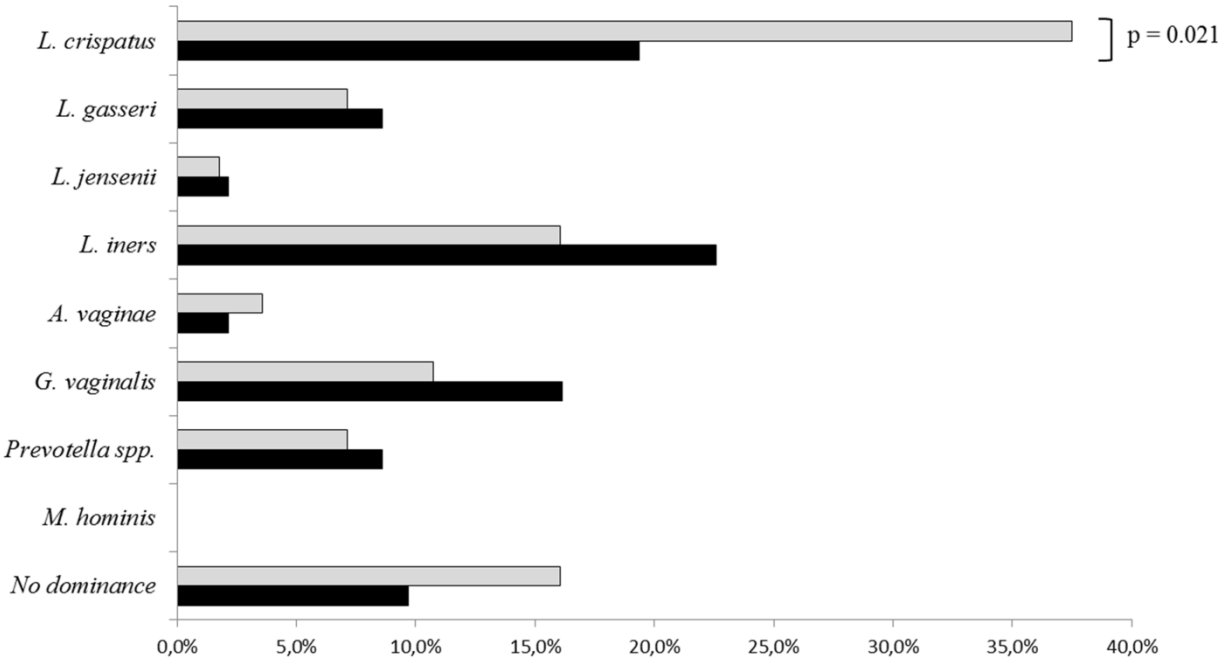

Figure 2. **Relative abundance of samples dominated by a single bacterial species (calculated using the number of copies detected by qPCR), expressed as the percentage of women achieving live birth** (grey bars) ***vs.*** **women who did not** (black bars).

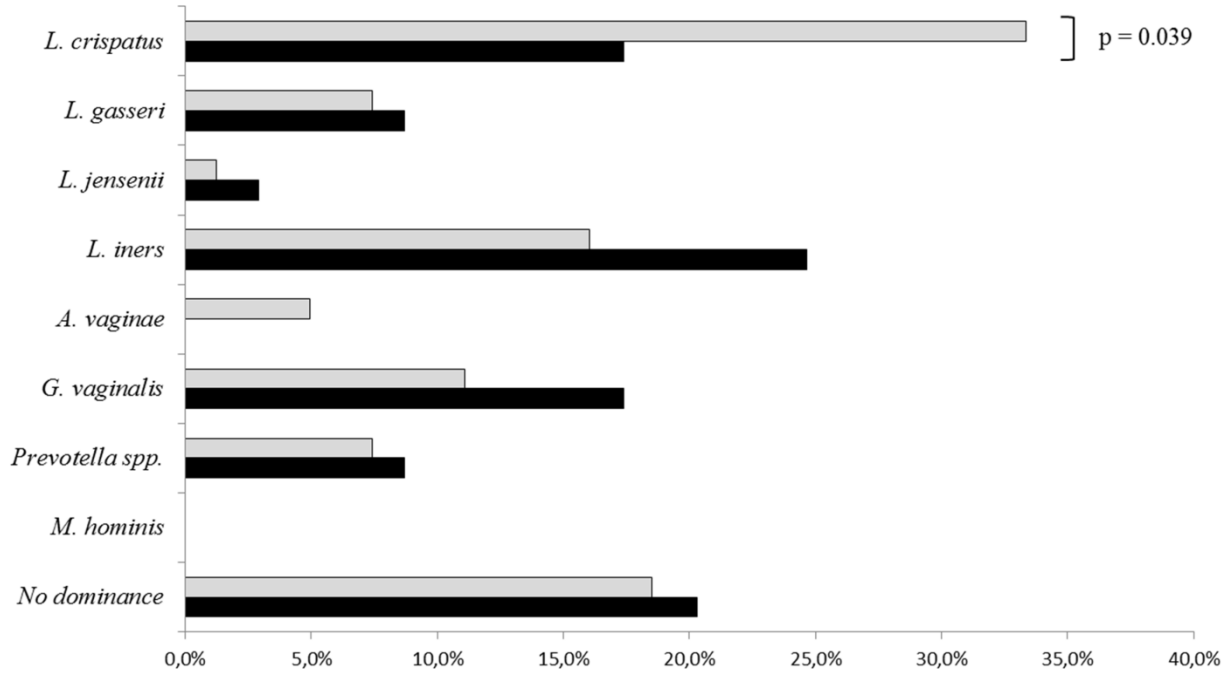

Figure 3. **Relative abundance of samples dominated by a single bacterial species (calculated using the number of copies detected by qPCR) expressed as the percentage of pregnant** (grey bars) ***vs.*** **non-pregnant women** (black bars) **according to biochemical pregnancy**.

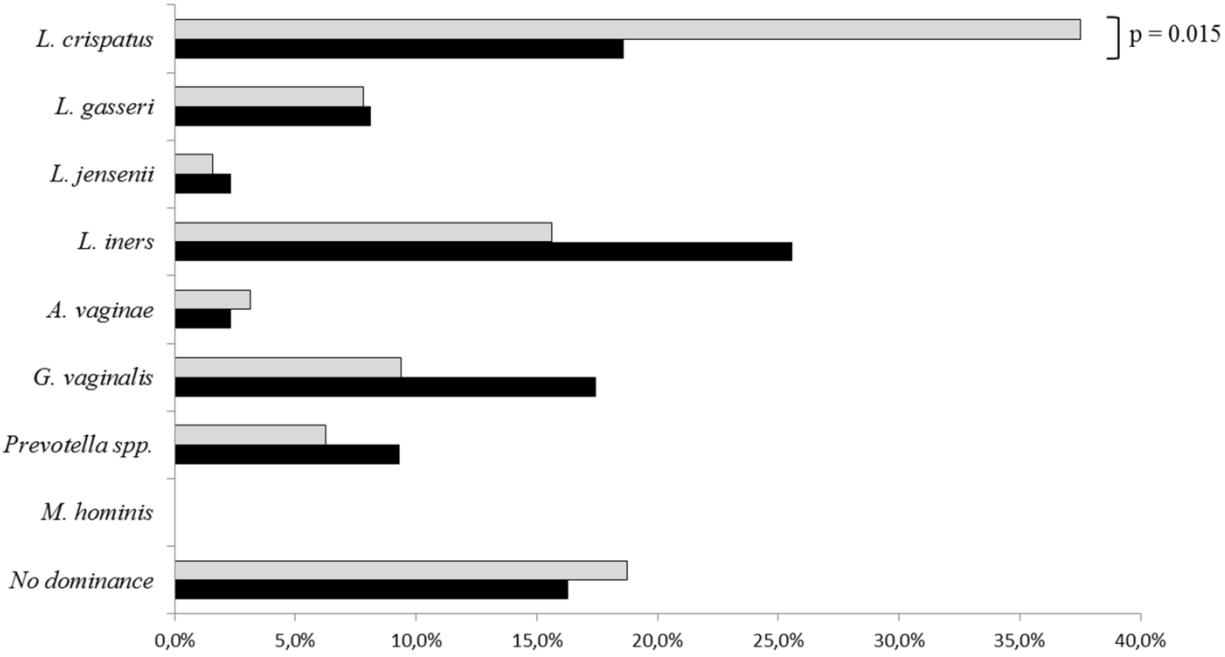

Figure 4. **Relative abundance of samples dominated by a single bacterial species (calculated using the number of copies detected by qPCR) expressed as the percentage of pregnant** (grey bars) ***vs.*** **non-pregnant women** (black bars) **according to clinical pregnancy.**

7. Tables

Table I. Demographic characteristics overall and by study group.

	Overall (n=150)	*Lactobacillus*-dominated (n=115)	BVB-dominated (n=35)
Patient´s Age, Mean (SD)	41.5 (4.7)	41.2 (4.4)	42.3 (5.5)
Patient´s BMI, Mean (SD)	24.4 (4.6)	26.2 (4.3)	26.3 (4.2)
Donor´s Age, Mean (SD)	26.2 (4.3)	24.2 (4.6)	25.6 (4.8)
Donor´s BMI, Mean (SD)	22.5 (3.2)	22.5 (3.1)	22.4 (3.5)
Reason for treatment, n (%)			
Age	50 (33.3)	36 (31.3)	14 (40.0)
IVF failure	39 (26.0)	34 (29.6)	5 (14.3)
Ovarian failure	37 (24.7)	28 (24.3)	9 (25.7)
Menopause	11 (7.3)	8 (7.0)	3 (8.6)
Reciprocal partner oocyte donation	1 (0.7)	0 (0.0)	1 (2.9)
Male factor	5 (3.3)	4 (3.5)	1 (2.9)
Genetic factor	3 (2.0)	1 (0.9)	2 (5.7)
Endometriosis	3 (2.0)	3 (2.6)	0 (0.0)
Recurrent miscarriage	1 (0.7)	1 (0.9)	0 (0.0)
Previous cycles with donated oocytes, n (%)			
None	111 (74.0)	83 (72.2)	28 (80.0)
One	33 (22.0)	29 (25.2)	4 (11.4)
More than one	6 (4.0)	3 (2.6)	3 (8.6)
Origin of sperm, n (%)			
Partner	122 (81.3)	95 (82.6)	27 (77.1)
Donor	28 (18.7)	20 (17.4)	8 (22.9)
Status of sperm, n (%)			
Frozen	122 (81.3)	95 (82.6)	27 (77.1)
Fresh	28 (18.7)	20 (17.4)	8 (22.9)

Table II. **List of bacteria species tested, GenBank accession number, genome size and number of genome copies per ng.**

Microorganism	GenBank no.	Genome size (Mb)	No. Copies per ng
Lactobacillus crispatus	NC_014106.1	2.2	421118.9
Lactobacillus gasseri	NC_008530.1	1.89	489156
Lactobacillus jensenii	NZ_CP018809.1	1.67	554767.4
Lactobacillus iners	NZ_ACLN00000000.1	1.29	718187.2
Gardnerella vaginalis	NC_014644.1	1.60	578167
Atopobium vaginae	NZ_ACGK00000000.2	1.43	647875.2
Mycoplasma hominis	NC_013511.1	0.65	1415633.8
Prevotella bivia	NZ_AJVZ00000000.1	2.52	367643.5

Table III. List of bacterial species, primer sequences and sources in the literature.

Microorganism	Primer sequence (5´to 3´)		Reference
	Forward	Reverse	
L. crispatus	GATTTACTTCGGTAATGACGTTAGGA	AGCTGATCATGCGATCTGCTTTC	(Zozaya-Hinchliffe et al. 2010)
L. gasseri	TGGAAACAGRTGCTAATACCG	CAGTTACTACCTCTATCTTTCTTCACTAC	(Byun et al. 2004)
L. jensenii	CCTTAAGTCTGGGATACCATT	ACGCCGCCTTTTAAACTTCTT	(De Backer et al. 2007)
L. iners	GTCTGCCTTGAAGATCGG	ACAGTTGATAGGCATCATC	(De Backer et al. 2007)
G.vaginalis	TTACTGGTGTATCACTGTAAGG	CCGTCACAGGCTGAACAGT	(Zariffard et al. 2002)
A. vaginae	GCAGGGACGAGGCCGCAA	GTGTTTCCACTGCTTCACCTAA	(Fredricks et al. 2007)
M. hominis	CATGCATGTCGAGCGAGGTT	CCATGCGGTTCCATGCGT	(Datcu et al. 2013)
Prevotella spp.	GGATGCGTCTGATTAGCTTGTT	GCACGCTACTTGGCTGGTTC	(Datcu et al. 2013)
Total bacteria load	AATAAATCATAAACTCCTACGGGAGGCAGCAGT	AATAAATCATAACCTAGCTATTACCGCGGCTGCT	(Brukner et al. 2015)
Human load (*RPLP0*)	CCCATTCTATCATCAACGGGTACAA	CAGCAAGTGGGAAGGTGTAATCC	(Torra-Massana et al. 2018)

8. References

Amsel, R., P. A. Totten, C. A. Spiegel, K. C. Chen, D. Eschenbach, and K. K. Holmes. 1983. 'Nonspecific vaginitis. Diagnostic criteria and microbial and epidemiologic associations', *Am J Med*, 74: 14-22.

Balashov, S. V., E. Mordechai, M. E. Adelson, J. D. Sobel, and S. E. Gygax. 2014. 'Multiplex quantitative polymerase chain reaction assay for the identification and quantitation of major vaginal lactobacilli', *Diagn Microbiol Infect Dis*, 78: 321-7.

Brukner, I., Y. Longtin, M. Oughton, V. Forgetta, and A. Dascal. 2015. 'Assay for estimating total bacterial load: relative qPCR normalisation of bacterial load with associated clinical implications', *Diagn Microbiol Infect Dis*, 83: 1-6.

Burton, J. P., and G. Reid. 2002. 'Evaluation of the bacterial vaginal flora of 20 postmenopausal women by direct (Nugent score) and molecular (polymerase chain reaction and denaturing gradient gel electrophoresis) techniques', *J Infect Dis*, 186: 1770-80.

Byun, R., M. A. Nadkarni, K. L. Chhour, F. E. Martin, N. A. Jacques, and N. Hunter. 2004. 'Quantitative analysis of diverse Lactobacillus species present in advanced dental caries', *J Clin Microbiol*, 42: 3128-36.

Costello, E. K., C. L. Lauber, M. Hamady, N. Fierer, J. I. Gordon, and R. Knight. 2009. 'Bacterial community variation in human body habitats across space and time', *Science*, 326: 1694-7.

Datcu, R., D. Gesink, G. Mulvad, R. Montgomery-Andersen, E. Rink, A. Koch, P. Ahrens, and J. S. Jensen. 2013. 'Vaginal microbiome in women from Greenland assessed by microscopy and quantitative PCR', *BMC Infect Dis*, 13: 480.

De Backer, E., R. Verhelst, H. Verstraelen, M. A. Alqumber, J. P. Burton, J. R. Tagg, M. Temmerman, and M. Vaneechoutte. 2007. 'Quantitative determination by real-time PCR of four vaginal Lactobacillus species, Gardnerella vaginalis and Atopobium vaginae indicates an inverse relationship between L. gasseri and L. iners', *BMC Microbiol*, 7: 115.

Foxman, B., A. Wen, U. Srinivasan, D. Goldberg, C. F. Marrs, J. Owen, D. A. Wing, and D. Misra. 2014. 'Mycoplasma, bacterial vaginosis-associated bacteria BVAB3, race, and risk of preterm birth in a high-risk cohort', *Am J Obstet Gynecol*, 210: 226 e1-7.

Franasiak, J. M., M. D. Werner, C. R. Juneau, X. Tao, J. Landis, Y. Zhan, N. R. Treff, and R. T. Scott. 2016. 'Endometrial microbiome at the time of embryo transfer: next-generation sequencing of the 16S ribosomal subunit', *J Assist Reprod Genet*, 33: 129-36.

Fredricks, D. N., T. L. Fiedler, K. K. Thomas, B. B. Oakley, and J. M. Marrazzo. 2007. 'Targeted PCR for detection of vaginal bacteria associated with bacterial vaginosis', *J Clin Microbiol*, 45: 3270-6.

Freitas, A. C., B. Chaban, A. Bocking, M. Rocco, S. Yang, J. E. Hill, D. M. Money, and Vogue Research Group. 2017. 'The vaginal microbiome of pregnant women is less rich and diverse, with lower prevalence of Mollicutes, compared to non-pregnant women', *Sci Rep*, 7: 9212.

Gajer, P., R. M. Brotman, G. Bai, J. Sakamoto, U. M. Schutte, X. Zhong, S. S. Koenig, L. Fu, Z. S. Ma, X. Zhou, Z. Abdo, L. J. Forney, and J. Ravel. 2012. 'Temporal dynamics of the human vaginal microbiota', *Sci Transl Med*, 4: 132-52.

Gong, Z., Y. Luna, P. Yu, and H. Fan. 2014. 'Lactobacilli inactivate Chlamydia trachomatis through lactic acid but not H2O2', *PLoS One*, 9: e107758.

Guven-Maiorov, E., C. J. Tsai, and R. Nussinov. 2017. 'Structural host-microbiota interaction networks', *PLoS Comput Biol*, 13: e1005579.

Haahr, T., J. S. Jensen, L. Thomsen, L. Duus, K. Rygaard, and P. Humaidan. 2016. 'Abnormal vaginal microbiota may be associated with poor reproductive outcomes: a prospective study in IVF patients', *Hum Reprod*, 31: 795-803.

Hilbert, D. W., W. L. Smith, S. G. Chadwick, G. Toner, E. Mordechai, M. E. Adelson, T. J. Aguin, J. D. Sobel, and S. E. Gygax. 2016. 'Development and validation of a highly accurate quantitative real-time pcr assay for diagnosis of bacterial vaginosis', *J Clin Microbiol*, 54: 1017-24.

Hyman, R. W., M. Fukushima, L. Diamond, J. Kumm, L. C. Giudice, and R. W. Davis. 2005. 'Microbes on the human vaginal epithelium', *Proc Natl Acad Sci U S A*, 102: 7952-7.

Hyman, R. W., C. N. Herndon, H. Jiang, C. Palm, M. Fukushima, D. Bernstein, K. C. Vo, Z. Zelenko, R. W. Davis, and L. C. Giudice. 2012. 'The dynamics of the vaginal microbiome during infertility therapy with in vitro fertilization-embryo transfer', *J Assist Reprod Genet*, 29: 105-15.

Li, J., J. McCormick, A. Bocking, and G. Reid. 2012. 'Importance of vaginal microbes in reproductive health', *Reprod Sci*, 19: 235-42.

Liversedge, N. H., A. Turner, P. J. Horner, S. D. Keay, J. M. Jenkins, and M. G. Hull. 1999. 'The influence of bacterial vaginosis on in-vitro fertilization and embryo implantation during assisted reproduction treatment', *Hum Reprod*, 14: 2411-5.

Mangot-Bertrand, J., F. Fenollar, F. Bretelle, M. Gamerre, D. Raoult, and B. Courbiere. 2013. 'Molecular diagnosis of bacterial vaginosis: impact on IVF outcome', *Eur J Clin Microbiol Infect Dis*, 32: 535-41.

Mendling, W. 2016. 'Vaginal Microbiota', *Adv Exp Med Biol*, 902: 83-93.

Moini, A., L. Mohammadi Yeganeh, M. Shiva, M. Ahmadieh, R. Salman Yazdi, F. Hasani, N. Bagheri Lankarani, and A. Sanati. 2017. 'Bacterial vaginosis and the risk of early miscarriage in women undergoing intracytoplasmic sperm injection cycles: a prospective cohort study', *Hum Fertil (Camb)*: 1-6.

Moreno, I., F. M. Codoner, F. Vilella, D. Valbuena, J. F. Martinez-Blanch, J. Jimenez-Almazan, R. Alonso, P. Alama, J. Remohi, A. Pellicer, D. Ramon, and C. Simon. 2016. 'Evidence that the endometrial microbiota has an effect on implantation success or failure', *Am J Obstet Gynecol*, 215: 684-703.

Nelson, D. B., S. Bellamy, I. Nachamkin, R. B. Ness, G. A. Macones, and L. Allen-Taylor. 2007. 'First trimester bacterial vaginosis, individual microorganism levels, and risk of second trimester pregnancy loss among urban women', *Fertil Steril*, 88: 1396-403.

Nelson, D. B., A. L. Hanlon, G. Wu, C. Liu, and D. N. Fredricks. 2015. 'First trimester levels of bv-associated bacteria and risk of miscarriage among women early in pregnancy', *Matern Child Health J*, 19: 2682-7.

Nugent, R. P., M. A. Krohn, and S. L. Hillier. 1991. 'Reliability of diagnosing bacterial vaginosis is improved by a standardized method of gram stain interpretation', *J Clin Microbiol*, 29: 297-301.

Nunn K, Wang Y-Y, Harit D, Cone R & Lai S 2014. 'Influence of vaginal microbiota on the diffusional barrier properties of cervicovaginal mucus', *AIDS Res Hum Retroviruses*, 6:e01084-15.

Plummer, E. L., S. M. Garland, C. S. Bradshaw, M. G. Law, L. A. Vodstrcil, J. S. Hocking, C. K. Fairley, and S. N. Tabrizi. 2017. 'Molecular diagnosis of bacterial vaginosis: Does adjustment for total bacterial load or human cellular content improve diagnostic performance?', *J Microbiol Methods*, 133: 66-68.

Ralph, S. G., A. J. Rutherford, and J. D. Wilson. 1999. 'Influence of bacterial vaginosis on conception and miscarriage in the first trimester: cohort study', *BMJ*, 319: 220-3.

Ravel, J., P. Gajer, Z. Abdo, G. M. Schneider, S. S. Koenig, S. L. McCulle, S. Karlebach, R. Gorle, J. Russell, C. O. Tacket, R. M. Brotman, C. C. Davis, K. Ault, L. Peralta, and L. J. Forney. 2011. 'Vaginal microbiome of reproductive-age women', *Proc Natl Acad Sci U S A*, 108 Suppl 1: 4680-7.

Salah, R. M., A. M. Allam, A. M. Magdy, and ASh Mohamed. 2013. 'Bacterial vaginosis and infertility: cause or association?', *Eur J Obstet Gynecol Reprod Biol*, 167: 59-63.

Srinivasan, S., and D. N. Fredricks. 2008. 'The human vaginal bacterial biota and bacterial vaginosis', *Interdiscip Perspect Infect Dis*, 2008: 750479.

Torra-Massana, M., M. Barragan, E. Bellu, R. Oliva, A. Rodriguez, and R. Vassena. 2018. 'Sperm telomere length in donor samples is not related to ICSI outcome', *J Assist Reprod Genet*, 35: 649-657.

van Oostrum, N., P. De Sutter, J. Meys, and H. Verstraelen. 2013. 'Risks associated with bacterial vaginosis in infertility patients: a systematic review and meta-analysis', *Hum Reprod*, 28: 1809-15.

Verstraelen, H., R. Vilchez-Vargas, F. Desimpel, R. Jauregui, N. Vankeirsbilck, S. Weyers, R. Verhelst, P. De Sutter, D. H. Pieper, and T. Van De Wiele. 2016. 'Characterisation of the human uterine microbiome in non-pregnant women through deep sequencing of the V1-2 region of the 16S rRNA gene', *PeerJ*, 4: e1602.

Wilson, J. D., S. G. Ralph, and A. J. Rutherford. 2002. 'Rates of bacterial vaginosis in women undergoing in vitro fertilisation for different types of infertility', *BJOG*, 109: 714-7.

Zariffard, M. R., M. Saifuddin, B. E. Sha, and G. T. Spear. 2002. 'Detection of bacterial vaginosis-related organisms by real-time PCR for Lactobacilli, Gardnerella vaginalis and Mycoplasma hominis', *FEMS Immunol Med Microbiol*, 34: 277-81.

Zozaya-Hinchliffe M, Lillis R, H. Martin D, J. Ferris, M. 2010. 'Quantitative PCR Assessments of Bacterial Species in Women with and without Bacterial Vaginosis', *J Clin Microbiol,* 48:1812-9.

SUMMARY OF THE RESULTS

Through the work presented in this thesis, we have inquired the mechanisms regulating implantation from a transcriptional perspective, with dissection of the embryonic and maternal responses. This approach allowed us to generate lists of molecules putatively involved in endometrial receptivity and implantation, to identify protein-protein interactions between the trophoblast and the endometrial epithelium, to characterize the biological pathways affected by the trophoblast-epithelium interaction and to speculate about the mechanisms that ultimately lead to pregnancy. Additionally, we have explored the environmental determinants influencing the establishment of pregnancy in order to find non-invasive markers of successful implantation for clinical application.

In **Chapter 1**, we describe an *in vitro* model using GFP expressing JEG-3 spheroids co-cultured with receptive Ishikawa or non-receptive HEC-1-A epithelia. After co-culturing Ishikawa cells with trophoblast spheroids, 310 and 298 genes increased or decreased their expression compared to non-co-cultured Ishikawa control cells, respectively; only 9 genes (5 up-regulated and 4 down-regulated) were differentially expressed in HEC-1-A upon co-culture with trophoblast spheroids. Compared to HEC-1-A, the trophoblast challenge to Ishikawa cells differentially regulated the expression of 495 genes; these differences in gene expression highlighted an important role for cell adhesion and ECM molecules in the trophoblast-epithelium interaction. Other pathways enriched in the Ishikawa epithelium included cell division, cell cycle regulation and metabolism. Both differential gene expression and functional analysis suggested that the trophoblast spheroid response depended on the receptivity of the substrate; a total of 1877 and 323 genes were up-regulated or down-regulated when co-cultured on Ishikawa compared to HEC-1-A cells, respectively. The GSEA results suggested that a number of pathways previously related to pregnancy (e.g. tissue remodelling, cell differentiation and angiogenesis) were enhanced in the trophoblast after co-culture with the receptive epithelium. On the other hand, the co-culture with non-receptive epithelium enriched pathways involving trophoblast cell proliferation and cell cycle regulation.

Using the same *in vitro* system, we further investigated the transcriptional dynamics of the trophoblast and the receptive epithelium in earlier stages during their interaction, as described in **Chapter 2**. After 8 hours of co-culture, 200 genes were up-regulated and 95 genes were down-regulated in the receptive epithelium. In the next stage from 8 to 24 hours, 127 and 131 were up- and down-regulated, respectively. Responding to the interaction with the trophoblast for 8 hours, the receptive epithelium showed a wave of transcriptional changes. The over-represented pathways

included EMT, cell movement, apoptosis, hypoxia, inflammation, allograft rejection, myogenesis and cell signalling (e.g., TNFa/NFkb, KRAS, JAK-STAT cascades). Some of these pathways did not vary in the subsequent stage until 24 hours (e.g. hypoxia, inflammation and apoptosis) but most of them were under-represented instead (*i.e.,* EMT, cell movement, allograft rejection, myogenesis and cell signalling). The trophoblast spheroids showed a more dynamic pattern of transcriptional changes upon co-culture with the receptive epithelium. A total of 1201 and 46 genes were up- and down-regulated after 8 hours, respectively; from 8 to 24 hrs, 458 genes were up-regulated and 23 were down-regulated. Some pathways were over-represented at both 8 and 24 hours (e.g. angiogenesis and hypoxia), while EMT and cell signalling were only over-represented at 8 hours and not changed at 24 hours. Stage II (from 8 to 24 hours) involved the over-representation of pathways such as inflammation and estrogen response.

Our *in silico* interactome network analysis described in **Chapter 3** predicted 21 direct protein-protein partners presumably involved in trophoblast-receptive epithelium crosstalk at 48 hours. From our time course study, 62 different protein-protein interactions were predicted at stage I (0 to 8 hours) and 16 protein-protein interactions at stage II (8 to 24 hours). We used specific antibodies to validate the co-localization of selected predicted protein-protein interacting pairs by immunofluorescence; unfortunately, we could not confirm it.

Finally, we investigated the microbial environment during implantation using an indirect, non-invasive approach. We correlated the vaginal microbiota profile at the day of embryo transfer and the reproductive outcomes in IVF cycles using donated oocytes (**Chapter 4**). Our results showed that samples varied in bacterial load but most of them were dominated by a single species (80.7%, 121/150). Specifically, most of them were dominated by *Lactobacillus spp*. (76.7%, 115/150) and 23.3% (35/150) were dominated by BV associated bacteria. Regarding the reproductive outcomes, women who achieved live birth and those who did not had similar distribution of *Lactobacillus*- or BVB-dominated microbiota profiles ($p = 0.43$). A significantly higher proportion of *L. crispatus*-dominated samples were found in women achieving live birth compared to those who did not ($p = 0.021$), as well as in women achieving biochemical pregnancy ($p = 0.039$) and confirmed clinical pregnancy ($p = 0.015$).

GENERAL DISCUSSION

Implantation is the major rate-limiting step in achieving pregnancy, both spontaneously and after IVF. Over 60% of embryos are lost, either due to failed implantation, immediately after implantation or soon after biochemical confirmation of the pregnancy (Macklon, Geraedts and Fauser, 2002). This early reproductive failure is a serious concern in IVF treatments, and the main question "what is it needed to establish a successful pregnancy?" remains unanswered. The major handicaps in answering this question in humans are the ethical concerns and technical difficulties to study human implantation and pregnancy. Embryonic or endometrial tissue from pregnant women is simply not available; human placenta can be obtained after voluntary elective terminations or pathological pregnancies, but it represents later stages of the process. On the other hand, *in vitro* research on human embryos is currently restricted to 14-days culture post-fertilization (on gastrulation, when the primitive streak emerges), either by law or scientific consensus (Hyun, Wilkerson and Johnston, 2016; Pera, 2017). As a consequence, the only currently available clinical approaches focus on assessing the embryo and the endometrium out of the context of human implantation. Importantly, these limitations hamper the development of clinical treatments for IVF patients suffering from RIF. It is a challenge for researchers to find approaches that model the *in vivo* scenario in order to understand the difficult to access time frame from conception until placentation, and to be able to translate it into the clinical setting.

Implantation requires a developmentally competent blastocyst, a receptive endometrium able to host it and a coordinated interaction between both compartments. These three factors seem to be equally important to the implantation success. It is estimated that embryo factors contribute to one third of implantation failures, while impaired endometrial receptivity and defective embryo-endometrial dialogue are responsible for the other two thirds of them (Craciunas et al., 2019). While the embryo has long been the focus of attention, the endometrium has been more recently recognized as an active player in implantation and gained relevance for the treatment of implantation failure. Far from just being a passive stratum for implantation, endometrial cells are able to migrate and to give a specific molecular response to the embryo. Many recent publications have focused on the stroma, revealing a relevant role in the implantation success mainly due to the unique activity of decidualized cells. Upon decidualization, stromal cells are able to sense embryo quality and to regulate tissue homeostasis, which is in turn linked to endometrial receptivity and remodelling (Teklenburg et al., 2010; Salker et al., 2012; Weimar et al., 2012; Brighton et al., 2017). However, some preclinical pregnancy losses could underlie defective embryo-endometrium crosstalk during early stages of implantation, i.e. apposition and attachment, and would not involve the decidua (at least as the main factor responsible for the failure). In this thesis, we have tried to

test this hypothesis from a molecular point of view by i) revealing the contribution of endometrial receptivity to the trophoblast-epithelium interactions during implantation (**Chapter 1**), ii) studying the temporal dynamics of the reciprocal trophoblast-epithelium molecular regulation during their successful interaction (**Chapter 2**) and iii) identifying the main protein networks that presumably contribute to the correct signalling during successful implantation (**Chapter 3**). Additionally, we analyzed the relationship of the vaginal microbiota with the reproductive outcomes as an indirect assessment of the uterine microenvironment during implantation (**Chapter 4**). In this section, we summarize and integrate our results, contextualize them with the current literature and discuss the mechanisms that might be involved in endometrial receptivity and implantation.

The intriguing mechanisms of endometrial receptivity acquisition

Our study results demonstrate that HEC-1-A and Ishikawa are good models for representing the non-receptive and receptive endometrial epithelium, respectively. The lack of receptivity observed in HEC-1-A substrate is clearly seen at the molecular level as a severe inability of this substrate to mount the proper transcriptional response, as seen in the receptive Ishikawa cell line, to the contact with a trophoblast spheroid. As expected, transcriptional profiling of both cell lines (Ishikawa and HEC-1-A) shows how different they are from the transcriptomic point of view; a total of 6628 genes were differentially expressed between Ishikawa and HEC-1-A cells. These genes include some previously related with the receptive status, e.g. *MAOA*, *GPX3*, *SPP1*, *ANXA-4*, *APOD*, *HOXA-10*, *EDNRB*, *DPP4*, *GBP2*, *APOD*, *ABCC3*, *COMP*, *G0S2*, *MAP3K5*, *EDNRB*, *IGFBP-1*, *DDX52*, *SERPING1*, *ARID5B*, *LAMB3*, *AOX1*, *IDO1*, *ANXA-2*, *HABP2*, *NDRG1*, *SFRP4*, *OLFM-1* and *MMP-7* (Altmae et al., 2017). Nevertheless, none of these genes has been proven to be essential for endometrial receptivity or implantation.

The initial interaction of trophoblast with the endometrial epithelium is thought to be critically dependent on destabilization of apicobasal polarity of both elements; this loss of polarity allows to trigger the correct signalling preceding adhesion at the apical cell poles (Hohn, Linke and Denker, 2000). In a previous study, HEC-1-A cells showed a strongly polarized phenotype with large basal lamina and absence of desmosomal contacts with trophoblast cells upon co-culture. In contrast, Ishikawa cells were less polarized and therefore highly invaded by trophoblast cells upon co-culture (Buck et al., 2015). These features regarding polarization of endometrial epithelial cell lines are representative of the non-receptive proliferative phase of the endometrial cycle (HEC-1-A) and the receptive secretory phase (Ishikawa). Processes influencing epithelial cell polarity would be, therefore, expected to influence endometrial receptivity and trophoblast adhesion.

Recently, epithelial polarity has been recognized as a critical regulator of EMT; apical–basal polarity integrity maintains epithelial cell–cell junctions by suppressing the EMT program, which limits tumour invasion (Jung et al., 2019). Although the results were obtained using a different system, these mechanisms could also govern the epithelial remodelling during the acquisition of the receptive status and barrier breaching for trophoblast invasion. In our results, pathways related to EMT, cell movement and cytoskeleton organization were enriched in the receptive endometrium compared to that non-receptive and also upon co-culture with the trophoblast for different time points (**Chapter 1** and **Chapter 2**).

The unfolded protein response (UPR) involves a network of intracellular signalling pathways that mediates endoplasmic reticulum-associated stress and regulates protein folding and post-translational modifications. UPR is up-regulated during decidualization of the endometrial stromal cells, allowing them to expand their endoplasmic reticulum to modify protein folding (Salker et al., 2012). Inhibition of UPR decreases the invasive ability of trophoblast spheroids co-cultured on monolayers of decidualized stromal cells *in vitro*. Additionally, endometrial samples from RIF patients have shown significantly decreased *TXNIP* expression in comparison with fertile women, suggesting that defective UPR may be related with impaired implantation (Grasso et al., 2018). The regulation of UPR in the luminal endometrial epithelium and its effect on the embryo-epithelium interaction have not been described. Interestingly, *TXNIP* which is a main mediator of the UPR was the most up-regulated gene in the receptive Ishikawa substrates after interacting with the trophoblast as well as in the analysis of differential expression patterns between I-co-S and I-c as compared to the differential expression patterns between H-co-S and H-c (**Supplementary File S4**, **Chapter 1**). Increased TXNIP levels promote the formation of large multiprotein complexes called inflammasomes that ultimately activate the inflammatory response and cytokine secretion (Lerner et al., 2012). Under prolonged activation, UPR can trigger autophagy and lead to cell death (Grootjans et al., 2016; Guzel et al., 2017). Inflammation and apoptosis were enriched in the receptive epithelium compared to that non-receptive and also after interaction with the trophoblast *vs*. non-co-cultured controls in our time course study. Interestingly, UPR was also dynamically regulated in the trophoblast compartment along co-culture time, as discussed in **Chapter 2**. Trophoblast UPR is related with hypoxia and oxidative stress that enhance the secretion of several anti-angiogenic factors, leading to placental disorders such as preeclampsia (Guzel et al., 2017). Further studies are needed to assess whether these processes are required to sustain embryo implantation and how cells achieve a balance between pro-inflammatory or anti-inflammatory signalling.

Physical and mechanical properties of the embryo-maternal interface

Ishikawa and HEC-1-A as well as other receptive and non-receptive epithelial cell lines have also been assessed to find the mechanical forces and ultrastructural features driving trophoblast-epithelium interactions in each model (Harduf, Goldman and Shalev 2007, 2009; Thie and Denker, 2002). As other tissue cells, embryos are sensitive to the mechanical properties of the substrates on which they implant (Discher, Janmey and Wang, 2005; Kolahi et al., 2012). Co-culture of mouse embryos on substrates with high stiffness has negative effects on embryo and placental development, suggesting that the preimplantation microenvironment affect pre- and post-implantation events (Kolahi et al., 2012). The organization of ECM, membrane and subcellular components such as the cytoskeleton determine cell stiffness (Ketene et al., 2012; Luo et al., 2016). In our study, we found striking gene expression differences between Ishikawa and HEC-1-A substrates after co-culture regarding cell adhesion and ECM molecules (e.g. integrins, collagens, claudins and metallopeptidases, **Chapter 1**) as well as genes involved in cytoskeleton organization and microtubule-based process (**Table III**, **Chapter 1**). Given that stiffness is linked to cell motility, it is possible that these differences led to the inability of HEC-1-A to be displaced by the trophoblast spheroids, leading to the absence of radial expansion upon co-culture in our *in vitro* model. Interestingly, Ishikawa cells showed dynamic regulation of pathways related with cell movement (e.g. actin-mediated cell contraction and movement, actin-myosin filament sliding and muscle filament sliding) with peaked enrichment at 8 hours and subsequent decrease up to 24 hours of co-culture, while HEC-1-A did not.

Ion channels have been proposed as mechanotransducers in endometrial epithelial cells, i.e. they are able to induce cellular responses to physical forces. The sodium channel mechanosensor in the endometrial epithelium has been proposed as a regulator of prostaglandin E2 production, which is required for embryo implantation (Ruan et al., 2012). A recent publication has shown that mechanical stimulation of primary endometrial epithelial cells results in calcium influxes that can be blocked by using inhibitors of mechanosensitive channels. Specifically, they focused on the characterization of PIEZO1, a member of the transient receptor potential superfamily of ion channels. As opposed to primary epithelial cells, HEC-1-A cells showed very low expression of ion channels including *PIEZO1* as well as altered patterns of calcium influx and release (Hennes et al., 2019). Interestingly, our results showed significantly decreased expression of *PIEZO1* in HEC-1-A non-co-cultured controls compared to Ishikawa non-co-cultured controls. Among the results of our time course study described in **Chapter 2**, some pathways enriched in the Ishikawa substrate were related to calcium transport (e. g. regulation of calcium ion import, regulation of

ryanodine-sensitive calcium-release channel activity and regulation of calcium ion transmembrane transporter activity; **Table I**, **Chapter 2**). Altogether, our results support the hypothesis that stiffness, mechanosensitivity and transduction could be important determinants of epithelial receptivity and might contribute to the different properties between Ishikawa and HEC-1-A cell lines.

Who leads, the trophoblast or the endometrial epithelium?

Whether juxtacrine molecular signals originate from the epithelial substrate or, conversely, are derived from the trophoblast remains a matter of debate. Based on our results, we propose that a specific endometrial transcriptional profile is required to elicit the correct reciprocal response in both the embryo and endometrium counterparts. Indeed, the trophoblast spheroids reacted differently to co-culture with receptive *vs*. non-receptive epithelia, suggesting that substrate input is required for the trophoblast to acquire highly invasive properties. This input seems to come from the endometrial side, which also underwent concordant transcriptional changes upon the interaction. As the trophoblast spheroids also attached to a lesser extent to the non-receptive cell line, their invasive ability could be due to the carcinoma origin of the studied cell line. Although not characterized at the transcriptional level, it was previously reported that carcinoma-derived trophoblast spheroids show minimal attachment to glass slides or to fibroblasts (Hohn, Linke and Denker, 2000; Wang et al., 2012). The behaviour of the trophoblast spheroids after co-culture on HEC-1-A resembled that of co-culture on these surfaces, suggesting that they needed any specific input to expand out of the sphere. In addition, the comparison of the trophoblast transcriptional profiles after co-culture on Ishikawa or HEC-1-A *vs*. non-co-cultured experimental controls confirmed that the morphological and transcriptional changes were induced by the interaction and not by the cell culture conditions.

That additional juxtacrine embryo-derived signals are required for implantation is a reasonable hypothesis but cannot be inferred from our experiments. It has been previously demonstrated that active embryo selection at the implantation sites requires the appropriate embryonic signals that can be recognized and translated by the endometrium through calcium signalling (Brosens et al., 2014). In fact, it would be reasonable to think that juxtacrine embryo-derived signals underlie some cases of ectopic pregnancies (i.e. the implantation of the embryo outside the uterine cavity, mostly in the fallopian tube). Recent work by Zernicka-Goetz's group has focused on the self-organizing ability of embryos and has demonstrated their developmental potential while attached to cell-free surfaces, in absence of maternal stimuli (Harrison et al., 2017; Shahbazi et al., 2017; Sozen et al., 2018). Nevertheless, even in ectopic pregnancies embryo-derived signals are likely not sufficient to

establish pregnancy. The fallopian tube expresses endometrial receptivity markers such as integrins; contrary to previous thinking, the expression pattern of these markers in the fallopian tube does not seem to mirror that followed during the endometrial cycle but are constitutively expressed instead (Sulz et al., 1998; Makrigiannakis et al., 2009; Brown et al., 2012). In addition, increased inflammatory tubal environment, local angiogenesis and hypoxia have been reported in women with ectopic pregnancies (Shaw et al., 2010), which were associated with implantation both in the literature and in our study. In women with impaired endometrial receptivity and defective embryo-tubal transport, these factors could increase the risk of ectopic pregnancy. Close resemblance between other reproductive tissues and the endometrium could underlie the etiology of ectopic pregnancy rather than a full control of implantation by the embryo.

The role of the microbial microenvironment in reproductive success

The microbiota of the female reproductive tract represents approximately 9% of the total human bacterial load (Moreno and Simon, 2018). Contrary to what was thought until relatively recently, the upper genital tract is not sterile; several reports have found a range of bacterial species within the endometrial cavity (Franasiak et al., 2016; Moreno et al., 2016; Verstraelen et al., 2016), which correlated with detrimental reproductive outcomes when those bacteria were pathological (Moreno et al., 2016). The fallopian tubes and the ovaries have also shown to harbour bacteria. In all of these sites of the human body and unlike other species, the most abundant bacteria are Lactobacilli (Franasiak and Scott, 2015). As discussed in **Chapter 4**, the relationship between vaginal microbiota and reproductive outcomes is highly controversial. Our results support the claim that the vaginal microbiota profile does not affect implantation and pregnancy. It is noteworthy to mention that the vaginal microbiome is affected by several factors such as sexual habits, hygiene or ethnicity. In view of this, the results are highly dependent on the study population. A recent systematic review and meta-analysis emphasizes the lack of heterogeneity among the studies currently available in the literature. While they concluded that BV is significantly associated with early spontaneous abortion, they did not find significant impact of the vaginal microbiota status on other reproductive outcomes such as live birth and clinical pregnancy rates. This discrepancy led the authors to recommend caution when interpreting their results. Furthermore, they found an association between BV and a certain population of women who were affected by tubal factor (Haahr et al., 2016). However, we did not assess the endometrial microbiota profile of the women included in our study and therefore we cannot exclude the existence of a unique endometrial composition that directly affects embryo implantation and pregnancy. Indeed, it has been demonstrated that the uterine microbiota composition differs from that found in paired vaginal

samples; this absence of correlation was proven both in healthy women and women affected by BV (Mitchell et al., 2015; Moreno et al., 2016). Nonetheless, the oral or vaginal administration of probiotics and/or prebiotics concurrently with antibiotics successfully restored the *Lactobacillus*-dominated endometrial profiles but failed to increase pregnancy rates, according to a recent pilot study (Kyono et al., 2019).

The mechanisms underlying the relationship between endometrial microbiota and reproductive outcomes are, so far, unknown. The microbiota of the human body influences local and systemic immunity (Hooper, Littman and Macpherson, 2012). As previously mentioned, inflammation and immune response are important determinants for the establishment of pregnancy. Both biological pathways are significantly modulated by the trophoblast during apposition and attachment, as suggested by our results described **Chapter 1** and **Chapter 2**. During the establishment of pregnancy, the mother faces several immunologic challenges, starting from the tolerance to allow the introduction of semen during fertilization until placentation. During implantation, the endometrial immune cells secrete a wide range of molecules such as chemokines and interleukins which are responsible for creating a non-cytotoxic, pro-inflammatory environment enabling trophoblast invasion. Key elements of this active maternal immune tolerance are the regulatory T cells (Treg cells) and the helper T cells (Th cells, i.e. Th1, Th2 and Th17). Th1 and Th2 produce pro- and anti- inflammatory effects, respectively. It has been suggested that a balanced ratio of Th1 and Th2 cells in the endometrium precedes implantation, showing decreased Th1 and increased Th2 levels towards pregnancy. Recently, Th17 has also been included in this regulatory system, which is involved in the immunological response against pathogens and transplant rejection by promoting inflammation. In contrast, Treg cells inhibit proliferation and cytokine production and are responsible for immunoregulation and induction of tolerance (Saito et al., 2010; Robertson, Care and Moldenhauer, 2018). The innate immune system detects pathogen-associated molecular patterns (PAMPs, e.g. cell wall components) through pattern recognition receptors (PRRs), such as toll-like receptors (TLRs) and NOD-like receptors (NLRs) (Takeuchi and Akira, 2010). PRRs exert different functions in the uterus; for example, TLRs and other PRRs are expressed by stromal and epithelial cells and are responsible for inducing a potent inflammatory response upon receptor recognition (Anders et al., 2017). The increasing knowledge of the gut microbiota suggest that the uterine microbiota might modulate the local immune cells entailing implications for implantation, tissue structure and defence against pathogens (Benner et al., 2018), **Figure 8**). Even in the gut, where the microbiome-host interactions have been extensively studied, their regulatory mechanisms have not been disclosed. Specific commensal bacteria have shown

protective roles in the intestinal mucosa through the interaction with Th17 cells (Ivanov et al., 2009). Similarly, the genus *Bacteroides* modulate the Th17 and Th1 responses in the gut influencing epithelial cell maturation and maintenance (Wexler, 2007; Maier, Anderson and Roy, 2014); interestingly, these bacteria have appeared in a number of endometrial studies using 16S rRNA (Mazmanian et al., 2005; Mazmanian, Round and Kasper, 2008; Johnson, Jones and Cobb, 2015). Of note, Th and Treg cells produce a wide variety of interleukins and other molecules related with inflammation and immune response such as LIF and TNF-α, which in turn could lead to epithelial remodelling, changes in barrier function and creating an environment suitable for implantation. These mechanisms could also be similar for other infections such as HIV, explaining the lower pregnancy found in infected women receiving donated oocytes compared to those non-infected (Mataro et al., 2017).

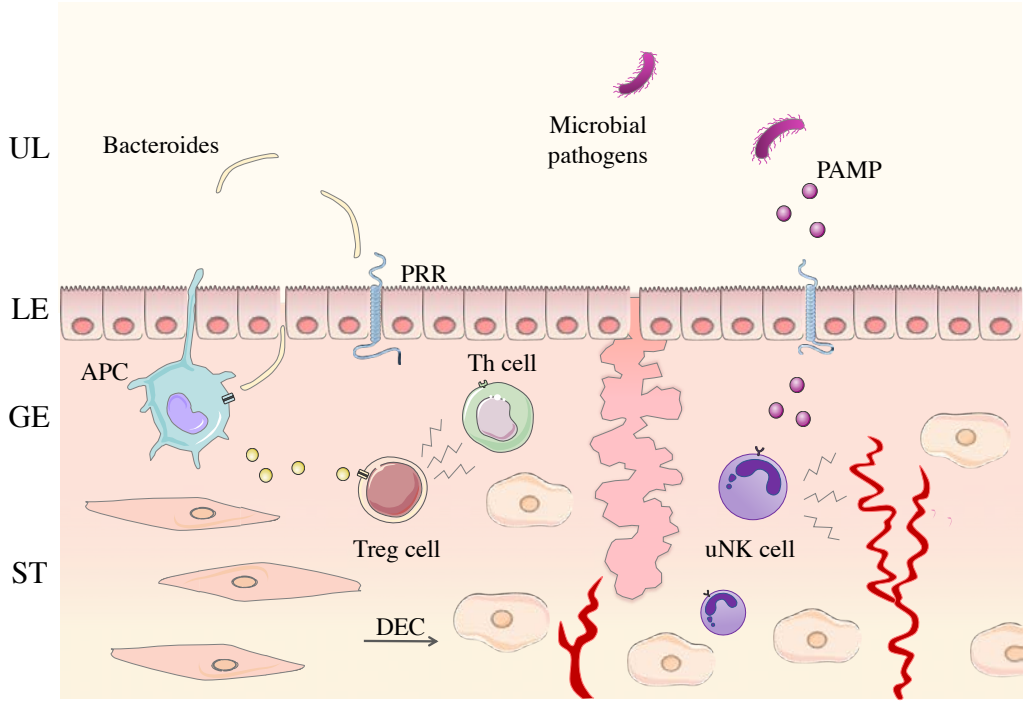

Figure 8. **Proposed mechanisms for the contribution of the endometrial microbiota to the physiology and function of the endometrium** (based on studies of gut microbiota-host interaction). Bacteria could be sensed by local immune cells by passing through the epithelial barrier or by pathogen-associated molecular patterns (PAMPs), initiating a signalling cascade. This might alter the T cell balance and the secreted cytokines could modulate the local immune environment, maternal vasculature and endometrial physiology. UL: uterine lumen; LE: luminal epithelium; GE: glandular epithelium; ST: stroma; DEC: decidualization; APC: antigen presenting cell; PRR: pattern recognition receptor; Th cells: T helper cells; Treg: regulatory T cell; uNK: uterine natural killer.

Recent results suggest that the uterus contains its own microbiota, similar but yet distinct from the microbiota of the vagina. However, the study of the uterine microbiota is hampered by technical difficulties regarding obtention of samples mainly due to contamination of endometrial fluid with vaginal bacteria. The endometrial microenvironment is the one that ultimately affects implantation, so it is required the development of sampling devices that are able to overcome this issue in a non-invasive manner in order to generate robust results. It will be important to establish the composition of the uterine microbiota and to determine the degree of interaction between both populations. It is possible that the endometrial microbiota may be affected by bacteria ascending from the lower genital tract, which is a reasonable explanation for the association of BV-like vaginal microbiota with pregnancy loss reported in the literature (Haahr et al., 2019). In **Chapter 4**, we concluded that previous evidences in the literature about any effect of BV on reproductive outcomes could derive from overall infection or abnormal immune conditions. It would be of great interest to assess the overall immunological status of women undergoing IVF simultaneously with their endometrial microbiota profile in order to determine the relationship between both of them.

Implantation is a dynamic process involving an early transient transcriptional wave in the endometrium and a less structured response of the trophoblast and is conditioned by the uterine microenvironment

As research progresses, the view of implantation has evolved from a neatly divided process involving apposition, attachment and invasion of the embryo into the uterus to a more dynamic multistep mechanism. We have identified several mechanisms involved in endometrial receptivity and implantation such as EMT, cell cycle regulation, cell movement, inflammation and immune responses in both the trophoblast and the endometrial epithelium. We highlight that implantation is highly complex and involves connections between many different processes in both compartments; therefore, the development of therapeutic avenues should take into account not only endometrial receptivity or embryo quality independently but also their transcriptional response upon interaction. Current approaches to therapy may not be effective due to their limited effect; for example, the literature is controversial about the benefits of performing endometrial scratching in IVF cycles, with unclear indications of when to perform it and to whom (Vitagliano et al., 2018; Lensen et al., 2019; van Hoogenhuijze et al., 2019; Vitagliano et al., 2019). Endometrial scratching, one of the options suggested to RIF patients, aims to promote the pro-inflammatory environment needed for implantation. However, as discussed above, inflammation is part of a wider signalling network including immune response, EMT, epithelial cell polarity… In all probability, a pro-inflammatory environment may be necessary but not sufficient to support

successful implantation. Likewise, the current tools to assess endometrial receptivity using transcriptomics (i.e. ERA® and the ER Map®) are based on predefined sets of genes that have been selected as differentially expressed between phases of the endometrial cycle, but not in the context of embryo implantation. In ERA®, these sets were defined in fertile women. In addition to the fact that infertility may be associated with specific transcriptional signatures that do not correspond to those in the fertile population, it could be possible that RIF patients had concordant differential expression of these selected genes but failed into triggering the correct response upon the contact with the embryo. This could explain the reported lack of robustness when using ERA® (Dahan and Tan, 2018).

Our results are concordant with those reported by Uchida and colleagues, who emphasised the role of EMT in endometrial epithelium barrier breaching due to depolarization and rearrangement of the cell surface to acquire receptivity. Upon embryo attachment, they propose that EMT is accelerated by signalling initiated by the binding of cell adhesion molecules. As a result, a descending motion of the epithelial cells concomitant with apoptosis create a breach in the epithelial layer for embryo penetration. After epithelial breaching and the initiation of embryo invasion, the epithelial cells start an ascending migration in order to reconstitute the luminal surface and when the EMT signal decreases, epithelial cells undergo MET (mesenchymal to epithelial transition) and proliferate (Uchida et al., 2016). **Figure 9** represents our speculative overview of how human implantation occurs based on the results of our experiments in addition to previous evidences reported in the literature. By the time of implantation, the endometrium acquires receptivity, a process in which the uterine microbiota might take part, and the blastocyst arrives to the luminal cavity. Embryo attachment (coinciding with 8 hours of co-culture in our experiments) induces a series of changes in the epithelial surface of the receptive endometrium; this includes over-representation of EMT, apoptosis, apical junction and cell motion together with concordant under-representation of epithelial cell polarity, which could facilitate the barrier breaching and subsequent embryo invasion. Allograft rejection and inflammatory response are also enriched, which could be linked to the regulation promoted by the uterine bacteria and the role of local immune cells previously discussed. Other over-represented pathways include estrogen response, myogenesis, cell differentiation and UPR. Simultaneously, there is over-representation in the trophoblast of hypoxia, angiogenesis, Wingless/β-catenin signalling and EMT as well as under-representation of cell proliferation and UPR, which suggest increased invasive activity of the embryo. Once the embryo has breached the endometrial surface, it is expected to invade the glandular epithelium and the stroma. During the attachment preceding early invasion (equivalent

to 24 hours in our experiments), the endometrial epithelium undergoes reverse changes compared to previous attachment, involving over-representation of epithelial cell polarity as well as under-representation of EMT, apoptosis, myogenesis, allograft rejection and apical junction. Other pathways do not change compared to the previous stage, such as hypoxia, cell motion, estrogen response, inflammatory response, cell differentiation and UPR. As Uchida et al. suggested, these changes could assist on recovering the epithelial integrity while allowing the embryo to invade the stroma. On the other hand, the embryo undergoes further enrichment of hypoxia and angiogenesis concomitant with over-representation of inflammatory and estrogen responses; cell proliferation and ROS (reactive oxygen species) pathways are under-represented, while EMT and UPR do not change. As discussed in **Chapter 2**, these changes suggest controlled trophoblast invasion and placental development, which are concordant with the establishment of pregnancy at this early stage.

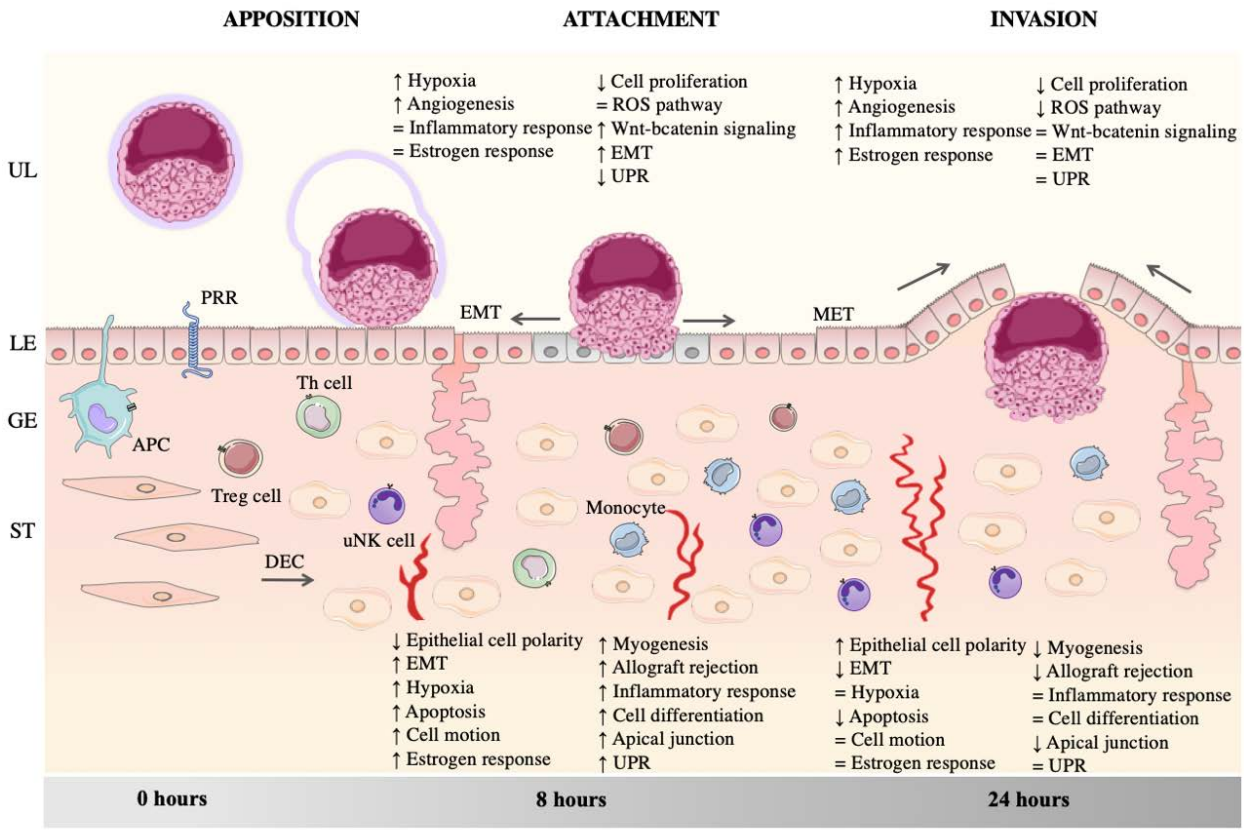

Figure 9. Proposed sequence of events regulating human implantation during the first 24 hours in the embryo (upper part) **and the endometrium** (bottom part). Arrow heads indicate over-represented (↑) and under-represented (↓) processes compared to the previous time-point. The symbol "=" indicates absence of changes. UL: uterine lumen; LE: luminal epithelium; GE: glandular epithelium; ST: stroma; DEC: decidualization; APC: antigen presenting cell; PRR: pattern recognition receptor; Th cells: T helper cells; Treg: regulatory T cell; uNK: uterine natural killer; EMT: epithelial to mesenchymal transition; MET: mesenchymal to epithelial transition; ROS: reactive oxygen species.

Strengths and limitations

We have devised a robust, reproducible *in vitro* model to study human implantation. Our experimental design using cell sorting allowed us to generate compartment-specific lists of candidate genes regulating the trophoblast-epithelium interaction. Our method provides a good representation of early implantation and is a good alternative to other systems such as using animal models or when using embryos is not feasible. As previously mentioned, this simple *in vitro* model presents some limitations due to the use of carcinoma-derived cell lines, the failure to represent physiological conditions (e.g. lack of endometrial cells, immune cells, glands and hormonal supplementation) as well as the use of trophoblast spheroids as a proxy for human embryos. It is noteworthy to mention that the GSEA allowed us to see whether a certain functionally related group of genes were enriched in the study samples; however, it is the signal transduction cascades and the up- or down-regulation of specific sets of genes which ultimately determines a biological response, which cannot be directly predicted from our results. We used a simple integrative *in silico* strategy which allowed us to identify protein-protein interactions between the trophoblast and the receptive epithelial endometrium. Although this approach was promising, we failed to validate some of these interactions by co-localization of the proteins using immunofluorescence. Further assays are needed to confirm these interactions in order to validate this technique. Still, co-localization is required but not sufficient to demonstrate physical interaction between proteins and the proposed protein pairs should be proven using proximity ligation assays.

In order to evaluate the effect of the microbial environment on the reproductive outcomes, we assessed the overall vaginal microbiota status at the moment of the embryo transfer using a straight-forward qPCR-based method. The careful selection of our study population gave robustness to our results; we only included SET of blastocysts and cycles of oocyte donation, all of them following the same protocols of endometrial preparation. However, we included few bacterial species and we did not use any other method to confirm the *Lactobacillus*-dominated or BVB-dominated profiles.

In conclusion, the original research included in this thesis has shed light on the regulation of embryonic and uterine epithelial implantation modulators in response to their reciprocal contact. We have generated extensive lists of candidates for functional studies in order to prove the embryo-endometrium interactions that ultimately regulate the establishment of pregnancy. The confirmation of these functional roles in primary endometrial cells and viable embryos will pave the way towards the development of clinically relevant biomarkers. Additionally, our work

supports the conclusion that the state of the vaginal microbiota at embryo transfer is not predictive of the reproductive outcome in women receiving oocytes and suggests the need to develop future studies that accurately determine the composition of the endometrial microbiota.

FUTURE PERSPECTIVES

Despite the growing knowledge concerning the mechanisms underlying the early establishment of pregnancy, many questions remain unanswered. In this thesis, some ideas and future experiments related to the presented work have been suggested. In this section we propose more specific questions whose answers could bring important advances to this field.

As mentioned, we performed comprehensive transcriptional studies but we did not focus on the protein level. The GSEA showed us which pathways were enriched in each compartment under certain conditions, but the up- or down-regulation of those functionally related genes needs to be confirmed. Performing complementary functional studies such as proliferation assays or focusing on specific functionally related sets of genes would provide deeper insights into those selected mechanisms and their contribution to the implantation process. Our transcriptomics analyses suggest a number of molecular biomarkers of endometrial receptivity and implantation. Regarding the trophoblast-endometrium interaction, the most valuable candidates would be those predicted as interacting protein partners by the *in silico* technique. Once protein-protein interactions were proven, a logical next step would be to determine their role in trophoblast attachment to the epithelium by functional assays. This could include gene editing by inhibition or over-expression of selected genes (e.g. using CRIPR/Cas9 technology) to assess the attachment rate. Additionally, the over-expression of any presumably relevant gene for attachment in the HEC-1-A cell line and the subsequent evaluation of the attachment rates upon co-culture would contribute to the selection of molecular candidates responsible for endometrial receptivity and implantation.

The final objective of our work would be not only to understand the mechanism underlying implantation but also to identify biomarkers of implantation success or failure with clinical applicability, so any mentioned study would involve confirmation in primary samples. It would be of great interest to look for mutations in certain genes which we identified differentially regulated between the receptive and non-receptive epithelium after the interactions with the trophoblast in RIF *vs*. fertile patients. Additionally, it would also be very interesting to determine which of these genes are hormone responsive; dose-response studies could be helpful to find personalised protocols for endometrial preparation.

General considerations to develop future *in vitro* models of implantation

The development of *in vitro* models must be oriented to answer a clearly stated research question and must be carefully designed. Lack of communication between the multiple elements of the system is a limitation for both the embryo and the endometrium. In order to develop more biologically relevant systems, future *in vitro* models of implantation should include glandular and

luminal epithelial cells, stromal cells and the variety of immune, endothelial and stem cells that conform the tissue *in vivo*. On the other hand, the trophoblast is required but not sufficient to establish a successful interaction with the receptive endometrium; the use of viable human embryos would significantly increase the value of future studies.

In vitro models can be as complex as desired; but this complexity needs to balance fidelity to represent the physiological conditions of the studied process with experimental feasibility and robustness of the results. Therefore, highly complex models could introduce too much variability to the system. For this, in addition to the technical difficulties of culturing different cell types together, the setup of an "all-in" *in vitro* system is very challenging. The advances in the field while facing this issue include the use of endometrial/trophoblast organoids and microfluidic cell culture devices.

The dimensionality of *in vitro* systems is important, as gene expression changes in 3-D *vs*. 2-D cell culture. 3-D culture also affects mechanotransduction and signalling (Baker and Chen, 2012). As previously mentioned, mechanosensitivity and other mechanical properties such as stiffness are important parameters for cellular and tissue function and should be also taken into account in order to represent implantation from a biologically relevant approach. These considerations are also very important when comparing heterogeneous groups of patients such as RIF *vs*. fertile women; the etiology of RIF is diverse and lacks consensus, so the conditions introduced in the study systems should be defined and controlled as much as possible in order to avoid confounders affecting the outcomes. Interestingly, 3-D *in vitro* models have also been developed to study host-microbe interactions in the endometrium (Laniewski et al., 2017).

Novel *in vitro* models of implantation

One of the biggest step-stones while studying the initial embryo-endometrium crosstalk is the difficulty of isolating and maintaining primary human endometrial epithelial cells. By optimizing the culture conditions, long-term, hormone-responsive endometrial organoids have been obtained that recapitulate the physiological endometrial glandular function *in vitro*. Glandular endometrial organoids contain progenitor/stem and differentiated cells and comprise different cell types, as they can differentiate into luminal ciliated cells (Boretto et al., 2017; Turco et al., 2017). These organoids not only represent the physiology of healthy endometrium but also of diseased endometrium, including endometriosis and endometrial carcinomas. Carcinoma organoids can be obtained from different grades and recapitulate the original gene instability of the tissue (Vankelecom, 2019, unpublished results). Although the use of endometrial organoids is a great

contribution to the field, they are only representative of the glandular epithelium but not of the luminal epithelium. Research directions go towards obtaining organoids that resemble the luminal epithelium as well as adding the plethora of different cell types comprising the endometrial environment (i.e. stromal, endothelial and immune cells). Likewise, this approach has been recently applied to the trophoblast element; the trophoblast organoids have been derived from first trimester placentas and can differentiate into both SCT and EVT (Haider et al., 2018; Turco et al., 2018). Trophoblast organoids seem to be a good alternative when using human embryos is not feasible.

Recently, compartmentalized 3-D microfluidic cell culture devices (usually referred as "organs-on-a-chip") are coming along to provide a holistic approach in embryo implantation studies. These bioengineering products are able to introduce heterogeneous cell compartments together with chemical and biomechanical controlled conditions. Technical advantages include long-term stability of the cell cultures, real-time imaging and selective experimental procedures on specific cell types due to the compartmentalization of each component. Using these kind of devices, recent publications have shed light on the interaction between the endometrial stromal and endothelial cells (Gnecco, Pensabene, et al., 2017; Gnecco et al., 2019), multi-organ communication during the menstrual cycle and pregnancy-like hormonal status in the female reproductive tract (Xiao et al., 2017), fetal membrane microenvironment and interaction between amnion epithelial cells and decidual cells (Gnecco, Anders, et al., 2017; Richardson et al., 2019), and invasive behaviour of placental trophoblast cells (Abbas et al., 2017). Hitherto, there is not any publication addressing human embryo implantation using a microfluidics chip device; some preliminary results showed that the addition of endothelial cells to the system induced EVT invasion while stromal fibroblast (non-decidualized) reduced it (Mainigi et al., 2019, unpublished results). This approach will provide insights into the regulation of the transcriptome, proteome and secretome in the presence of different cells. Nevertheless, as it happens with organoids, these systems need to be refined and adapted to include all the endometrial cell types involved in the process of implantation. Of note, the future use of microfluidic devices to explore not only normal physiological but also pathological conditions (e.g. infertility, endometriosis and cancer) would be of great interest and clinical relevance.

CONCLUSIONS

- Ishikawa and HEC-1-A cell lines are good models for receptive and minimally receptive human endometrial epithelium; their different molecular responses in our *in vitro* model reflect those expected during *in vivo* implantation.
- Endometrial receptivity entails a specific reciprocal transcriptional response underlying the trophoblast-epithelium crosstalk otherwise muted when the endometrium is non-receptive.
- This reciprocal transcriptional response is characterized by an overall early and transient transcriptional up-regulation in the receptive epithelium at 8 hours followed by down-regulation from 8 to 24 hours of co-culture.
- The transcriptional response in the trophoblast is more dynamic, with numerous differentially expressed genes and a less structured regulation of different molecular pathways at each time-point.
- Our integrative *in silico* approach allowed us to identify a number of protein-protein interactions among the receptive endometrial epithelium and the trophoblast at different time points.
- The overall vaginal microbiota status at the time of ET does not directly affect implantation after IVF in women receiving donated oocytes.

BIBLIOGRAPHY

Abbas, Y., C. M. Oefner, W. J. Polacheck, L. Gardner, L. Farrell, A. Sharkey, R. Kamm, A. Moffett, and M. L. Oyen. 2017. 'A microfluidics assay to study invasion of human placental trophoblast cells', *J R Soc Interface*, 14.

Aberkane, A., W. Essahib, C. Spits, C. De Paepe, K. Sermon, T. Adriaenssens, S. Mackens, H. Tournaye, J. J. Brosens, and H. Van de Velde. 2018. 'Expression of adhesion and extracellular matrix genes in human blastocysts upon attachment in a 2D co-culture system', *Mol Hum Reprod*, 24: 375-87.

Aboussahoud, W., C. Bruce, S. Elliott, and A. Fazeli. 2010. 'Activation of Toll-like receptor 5 decreases the attachment of human trophoblast cells to endometrial cells in vitro', *Hum Reprod*, 25: 2217-28.

Altmae, S., F. J. Esteban, A. Stavreus-Evers, C. Simon, L. Giudice, B. A. Lessey, J. A. Horcajadas, N. S. Macklon, T. D'Hooghe, C. Campoy, B. C. Fauser, L. A. Salamonsen, and A. Salumets. 2014. 'Guidelines for the design, analysis and interpretation of 'omics' data: focus on human endometrium', *Hum Reprod Update*, 20: 12-28.

Altmae, S., M. Koel, U. Vosa, P. Adler, M. Suhorutsenko, T. Laisk-Podar, V. Kukushkina, M. Saare, A. Velthut-Meikas, K. Krjutskov, L. Aghajanova, P. G. Lalitkumar, K. Gemzell-Danielsson, L. Giudice, C. Simon, and A. Salumets. 2017. 'Meta-signature of human endometrial receptivity: a meta-analysis and validation study of transcriptomic biomarkers', *Sci Rep*, 7: 10077.

Altmae, S., J. Reimand, O. Hovatta, P. Zhang, J. Kere, T. Laisk, M. Saare, M. Peters, J. Vilo, A. Stavreus-Evers, and A. Salumets. 2012. 'Research resource: interactome of human embryo implantation: identification of gene expression pathways, regulation, and integrated regulatory networks', *Mol Endocrinol*, 26: 203-17.

Anders, A. P., J. A. Gaddy, R. S. Doster, and D. M. Aronoff. 2017. 'Current concepts in maternal-fetal immunology: Recognition and response to microbial pathogens by decidual stromal cells', *Am J Reprod Immunol*, 77.

Aplin, J. D., and S. J. Kimber. 2004. 'Trophoblast-uterine interactions at implantation', *Reprod Biol Endocrinol*, 2: 48.

Armant, D. R., R. Fritz, B. A. Kilburn, Y. M. Kim, J. K. Nien, N. J. Maihle, R. Romero, and R. E. Leach. 2015. 'Reduced expression of the epidermal growth factor signaling system in preeclampsia', *Placenta*, 36: 270-8.

Arnold, J. T., D. G. Kaufman, M. Seppala, and B. A. Lessey. 2001. 'Endometrial stromal cells regulate epithelial cell growth in vitro: a new co-culture model', *Hum Reprod*, 16: 836-45.

Azkargorta, M., I. Escobes, I. Iloro, N. Osinalde, B. Corral, J. Ibanez-Perez, A. Exposito, B. Prieto, F. Elortza, and R. Matorras. 2018. 'Differential proteomic analysis of endometrial fluid suggests increased inflammation and impaired glucose metabolism in non-implantative IVF cycles and pinpoints PYGB as a putative implantation marker', *Hum Reprod*, 33: 1898-906.

Baker, B. M., and C. S. Chen. 2012. 'Deconstructing the third dimension: how 3D culture microenvironments alter cellular cues', *J Cell Sci*, 125: 3015-24.

Barbier, C. S., K. A. Becker, M. A. Troester, and D. G. Kaufman. 2005. 'Expression of exogenous human telomerase in cultures of endometrial stromal cells does not alter their hormone responsiveness', *Biol Reprod*, 73: 106-14.

Barbieri, R. L. 2014. 'The endocrinology of the menstrual cycle', *Methods Mol Biol*, 1154: 145-69.

Bassil, R., R. Casper, N. Samara, T. B. Hsieh, E. Barzilay, R. Orvieto, and J. Haas. 2018. 'Does the endometrial receptivity array really provide personalized embryo transfer?', *J Assist Reprod Genet*, 35: 1301-05.

Bastu, E., M. F. Mutlu, C. Yasa, O. Dural, A. Nehir Aytan, C. Celik, F. Buyru, and J. Yeh. 2015. 'Role of Mucin 1 and Glycodelin A in recurrent implantation failure', *Fertil Steril*, 103: 1059-64 e2.

Bender-Atik R., O. B. Christiansen, J. Elson, A. M. Kolte, S. Lewis, S. Middeldorp, W. Nelen, B. Peramo, S. Quenby, N. Vermeulen, M. Goddijn. 2018. 'ESHRE guideline: recurrent pregnancy loss', *Human Reproduction Open*, 2: 004.

Benner, M., G. Ferwerda, I. Joosten, and R. G. van der Molen. 2018. 'How uterine microbiota might be responsible for a receptive, fertile endometrium', *Hum Reprod Update*, 24: 393-415.

Bentin-Ley, U., T. Horn, A. Sjogren, S. Sorensen, J. Falck Larsen, and L. Hamberger. 2000. 'Ultrastructure of human blastocyst-endometrial interactions in vitro', *J Reprod Fertil*, 120: 337-50.

Bentin-Ley, U., A. Sjogren, L. Nilsson, L. Hamberger, J. F. Larsen, and T. Horn. 1999. 'Presence of uterine pinopodes at the embryo-endometrial interface during human implantation in vitro', *Hum Reprod*, 14: 515-20.

Berger, C., N. R. Boggavarapu, J. Menezes, P. G. Lalitkumar, and K. Gemzell-Danielsson. 2015. 'Effects of ulipristal acetate on human embryo attachment and endometrial cell gene expression in an in vitro co-culture system', *Hum Reprod*, 30: 800-11.

Berker, B., S. Taskin, K. Kahraman, E. A. Taskin, C. Atabekoglu, and M. Sonmezer. 2011. 'The role of low-molecular-weight heparin in recurrent implantation failure: a prospective, quasi-randomized, controlled study', *Fertil Steril*, 95: 2499-502.

Berneau, S. C., P. T. Ruane, D. R. Brison, S. J. Kimber, M. Westwood, and J. D. Aplin. 2019. 'Investigating the role of CD44 and hyaluronate in embryo-epithelial interaction using an in vitro model', *Mol Hum Reprod*, 25: 265-73.

Bilban, M., S. Tauber, P. Haslinger, J. Pollheimer, L. Saleh, H. Pehamberger, O. Wagner, and M. Knofler. 2010. 'Trophoblast invasion: assessment of cellular models using gene expression signatures', *Placenta*, 31: 989-96.

Blauer, M., P. K. Heinonen, P. M. Martikainen, E. Tomas, and T. Ylikomi. 2005. 'A novel organotypic culture model for normal human endometrium: regulation of epithelial cell proliferation by estradiol and medroxyprogesterone acetate', *Hum Reprod*, 20: 864-71.

Boggavarapu, N. R., C. Berger, C. von Grothusen, J. Menezes, K. Gemzell-Danielsson, and P. G. Lalitkumar. 2016. 'Effects of low doses of mifepristone on human embryo implantation process in a three-dimensional human endometrial in vitro co-culture system', *Contraception*, 94: 143-51.

Bohlmann, M. K., J. C. Hoerster, D. Bundschuh, P. Boemicke, D. W. Luedders, and F. Koster. 2014. 'Growth-modulatory effects of heparin and VEGF165 on the choriocarcinoma cell-line JEG-3 and its expression of heparanase', *Anticancer Res*, 34: 7071-6.

Boretto, M., B. Cox, M. Noben, N. Hendriks, A. Fassbender, H. Roose, F. Amant, D. Timmerman, C. Tomassetti, A. Vanhie, C. Meuleman, M. Ferrante, and H. Vankelecom. 2017. 'Development of organoids from mouse and human endometrium showing endometrial epithelium physiology and long-term expandability', *Development*, 144: 1775-86.

Bowen, J. A., and R. C. Burghardt. 2000. 'Cellular mechanisms of implantation in domestic farm animals', *Semin Cell Dev Biol*, 11: 93-104.

Brighton, P. J., Y. Maruyama, K. Fishwick, P. Vrljicak, S. Tewary, R. Fujihara, J. Muter, E. S. Lucas, T. Yamada, L. Woods, R. Lucciola, Y. Hou Lee, S. Takeda, S. Ott, M. Hemberger, S. Quenby, and J. J. Brosens. 2017. 'Clearance of senescent decidual cells by uterine natural killer cells in cycling human endometrium', *Elife*, 6.

Bromer, J. G., T. S. Aldad, and H. S. Taylor. 2009. 'Defining the proliferative phase endometrial defect', *Fertil Steril*, 91: 698-704.

Brosens, J. J., M. G. Parker, A. McIndoe, R. Pijnenborg, and I. A. Brosens. 2009. 'A role for menstruation in preconditioning the uterus for successful pregnancy', *Am J Obstet Gynecol*, 200: 615 e1-6.

Brosens, J. J., M. S. Salker, G. Teklenburg, J. Nautiyal, S. Salter, E. S. Lucas, J. H. Steel, M. Christian, Y. W. Chan, C. M. Boomsma, J. D. Moore, G. M. Hartshorne, S. Sucurovic, B. Mulac-Jericevic, C. J. Heijnen, S. Quenby, M. J. Koerkamp, F. C. Holstege, A. Shmygol, and N. S. Macklon. 2014. 'Uterine selection of human embryos at implantation', *Sci Rep*, 4: 3894.

Brown, J. K., J. L. Shaw, H. O. Critchley, and A. W. Horne. 2012. 'Human fallopian tube epithelium constitutively expresses integrin endometrial receptivity markers: no evidence for a tubal implantation window', *Mol Hum Reprod*, 18: 111-20.

Buck, V. U., B. Gellersen, R. E. Leube, and I. Classen-Linke. 2015. 'Interaction of human trophoblast cells with gland-like endometrial spheroids: a model system for trophoblast invasion', *Hum Reprod*, 30: 906-16.

Burleigh, D. W., C. M. Kendziorski, Y. J. Choi, K. M. Grindle, R. L. Grendell, R. R. Magness, and T. G. Golos. 2007. 'Microarray analysis of BeWo and JEG3 trophoblast cell lines: identification of differentially expressed transcripts', *Placenta*, 28: 383-9.

Burton, J. P., and G. Reid. 2002. 'Evaluation of the bacterial vaginal flora of 20 postmenopausal women by direct (Nugent score) and molecular (polymerase chain reaction and denaturing gradient gel electrophoresis) techniques', *J Infect Dis*, 186: 1770-80.

Caballero-Campo, P., F. Dominguez, J. Coloma, M. Meseguer, J. Remohi, A. Pellicer, and C. Simon. 2002. 'Hormonal and embryonic regulation of chemokines IL-8, MCP-1 and RANTES in the human endometrium during the window of implantation', *Mol Hum Reprod*, 8: 375-84.

Calderone, A., L. Castagnoli, and G. Cesareni. 2013. 'mentha: a resource for browsing integrated protein-interaction networks', *Nat Methods*, 10: 690-1.

Campbell, S., J. Larsen, M. W. Seif, T. D. Allen, F. Knox, C. J. Jones, and J. D. Aplin. 2000. 'Mosaic characteristics of human endometrial epithelium in vitro: analysis of secretory markers and cell surface ultrastructure', *Mol Hum Reprod*, 6: 41-9.

Carmeliet, P., and R. K. Jain. 2011. 'Molecular mechanisms and clinical applications of angiogenesis', *Nature*, 473: 298-307.

Carson, D. D., I. Bagchi, S. K. Dey, A. C. Enders, A. T. Fazleabas, B. A. Lessey, and K. Yoshinaga. 2000. 'Embryo implantation', *Dev Biol*, 223: 217-37.

Carver, J., K. Martin, I. Spyropoulou, D. Barlow, I. Sargent, and H. Mardon. 2003. 'An in-vitro model for stromal invasion during implantation of the human blastocyst', *Hum Reprod*, 18: 283-90.

Cervello, I., C. Gil-Sanchis, A. Mas, F. Delgado-Rosas, J. A. Martinez-Conejero, A. Galan, A. Martinez-Romero, S. Martinez, I. Navarro, J. Ferro, J. A. Horcajadas, F. J. Esteban, J. E. O'Connor, A. Pellicer, and C. Simon. 2010. 'Human endometrial side population cells exhibit genotypic, phenotypic and functional features of somatic stem cells', *PLoS One*, 5: e10964.

Cha, J., X. Sun, and S. K. Dey. 2012. 'Mechanisms of implantation: strategies for successful pregnancy', *Nat Med*, 18: 1754-67.

Chalmel, F., E. Com, R. Lavigne, N. Hernio, A. P. Teixeira-Gomes, J. L. Dacheux, and C. Pineau. 2014. 'An integrative omics strategy to assess the germ cell secretome and to decipher sertoli-germ cell crosstalk in the Mammalian testis', *PLoS One*, 9: e104418.

Chan, C., C. Virtanen, N. A. Winegarden, T. J. Colgan, T. J. Brown, and E. M. Greenblatt. 2013. 'Discovery of biomarkers of endometrial receptivity through a minimally invasive approach: a validation study with implications for assisted reproduction', *Fertil Steril*, 100: 810-7.

Chen, X., X. Jin, L. Liu, C. W. Man, J. Huang, C. C. Wang, S. Zhang, and T. C. Li. 2015. 'Differential expression of vascular endothelial growth factor angiogenic factors in different endometrial compartments in women who have an elevated progesterone level before oocyte retrieval, during in vitro fertilization-embryo transfer treatment', *Fertil Steril*, 104: 1030-36.

Chobotova, K., I. Spyropoulou, J. Carver, S. Manek, J. K. Heath, W. J. Gullick, D. H. Barlow, I. L. Sargent, and H. J. Mardon. 2002. 'Heparin-binding epidermal growth factor and its receptor ErbB4 mediate implantation of the human blastocyst', *Mech Dev*, 119: 137-44.

Christian, M., X. Zhang, T. Schneider-Merck, T. G. Unterman, B. Gellersen, J. O. White, and J. J. Brosens. 2002. 'Cyclic AMP-induced forkhead transcription factor, FKHR, cooperates with CCAAT/enhancer-binding protein beta in differentiating human endometrial stromal cells', *J Biol Chem*, 277: 20825-32.

Chung, T. W., M. J. Park, H. S. Kim, H. J. Choi, and K. T. Ha. 2016. 'Integrin alphaVbeta3 and alphaVbeta5 are required for leukemia inhibitory factor-mediated the adhesion of trophoblast cells to the endometrial cells', *Biochem Biophys Res Commun*, 469: 936-40.

Cicinelli, E., M. Matteo, R. Tinelli, A. Lepera, R. Alfonso, U. Indraccolo, S. Marrocchella, P. Greco, and L. Resta. 2015. 'Prevalence of chronic endometritis in repeated unexplained implantation failure and the IVF success rate after antibiotic therapy', *Hum Reprod*, 30: 323-30.

Clark, G. F., and D.J. Schust. 2013. 'Manifestations of immune tolerance in the human female reproductive tract', *Frontiers in immunology*, 4: 26.

Cohen, M., A. Meisser, and P. Bischof. 2006. 'Metalloproteinases and human placental invasiveness', *Placenta*, 27: 783-93.

Cornillie, F. J., J. M. Lauweryns, and I. A. Brosens. 1985. 'Normal human endometrium. An ultrastructural survey', *Gynecol Obstet Invest*, 20: 113-29.

Coticchio, G., M. Mignini Renzini, P. V. Novara, M. Lain, E. De Ponti, D. Turchi, R. Fadini, and M. Dal Canto. 2018. 'Focused time-lapse analysis reveals novel aspects of human fertilization and suggests new parameters of embryo viability', *Hum Reprod*, 33: 23-31.

Coughlan, C., W. Ledger, Q. Wang, F. Liu, A. Demirol, T. Gurgan, R. Cutting, K. Ong, H. Sallam, and T. C. Li. 2014. 'Recurrent implantation failure: definition and management', *Reprod Biomed Online*, 28: 14-38.

Cousins, F. L., P. M. Kirkwood, P. T. Saunders, and D. A. Gibson. 2016. 'Evidence for a dynamic role for mononuclear phagocytes during endometrial repair and remodelling', *Sci Rep*, 6: 36748.

Craciunas, L., I. Gallos, J. Chu, T. Bourne, S. Quenby, J. J. Brosens, and A. Coomarasamy. 2019. 'Conventional and modern markers of endometrial receptivity: a systematic review and meta-analysis', *Hum Reprod Update*, 25: 202-23.

Croxatto, H. B. 2002. 'Physiology of gamete and embryo transport through the fallopian tube', *Reprod Biomed Online*, 4: 160-9.

Croxtall, J. D., M. G. Elder, and J. O. White. 1990. 'Hormonal control of proliferation in the Ishikawa endometrial adenocarcinoma cell line', *J Steroid Biochem*, 35: 665-9.

Dahan, M. H., and S. L. Tan. 2018. 'Variations in the endometrial receptivity assay (ERA) may actually represent test error', *J Assist Reprod Genet*, 35: 1923-24.

De Geyter, C., C. Calhaz-Jorge, M. S. Kupka, C. Wyns, E. Mocanu, T. Motrenko, G. Scaravelli, J. Smeenk, S. Vidakovic, V. Goossens, I. V. F. monitoring Consortium for the European Society of Human Reproduction European, and Embryology. 2018. 'ART in Europe, 2014: results generated from European registries by ESHRE: The European IVF-monitoring Consortium (EIM) for the European Society of Human Reproduction and Embryology (ESHRE)', *Hum Reprod*, 33: 1586-601.

Diaz-Gimeno, P., J. A. Horcajadas, J. A. Martinez-Conejero, F. J. Esteban, P. Alama, A. Pellicer, and C. Simon. 2011. 'A genomic diagnostic tool for human endometrial receptivity based on the transcriptomic signature', *Fertil Steril*, 95: 50-60, 60 e1-15.

Diaz-Gimeno, P., M. Ruiz-Alonso, D. Blesa, N. Bosch, J. A. Martinez-Conejero, P. Alama, N. Garrido, A. Pellicer, and C. Simon. 2013. 'The accuracy and reproducibility of the endometrial receptivity array is superior to histology as a diagnostic method for endometrial receptivity', *Fertil Steril*, 99: 508-17.

Diaz-Gimeno, P., M. Ruiz-Alonso, P. Sebastian-Leon, A. Pellicer, D. Valbuena, and C. Simon. 2017. 'Window of implantation transcriptomic stratification reveals different endometrial subsignatures associated with live birth and biochemical pregnancy', *Fertil Steril*, 108: 703-10 e3.

Discher, D. E., P. Janmey, and Y. L. Wang. 2005. 'Tissue cells feel and respond to the stiffness of their substrate', *Science*, 310: 1139-43.

Dominguez, F., S. Avila, A. Cervero, J. Martin, A. Pellicer, J. L. Castrillo, and C. Simon. 2003. 'A combined approach for gene discovery identifies insulin-like growth factor-binding protein-related protein 1 as a new gene implicated in human endometrial receptivity', *J Clin Endocrinol Metab*, 88: 1849-57.

Dominguez, F., C. Simon, A. Quinonero, M. A. Ramirez, E. Gonzalez-Munoz, H. Burghardt, A. Cervero, S. Martinez, A. Pellicer, M. Palacin, F. Sanchez-Madrid, and M. Yanez-Mo. 2010. 'Human endometrial CD98 is essential for blastocyst adhesion', *PLoS One*, 5: e13380.

Durruthy-Durruthy, J., M. Wossidlo, S. Pai, Y. Takahashi, G. Kang, L. Omberg, B. Chen, H. Nakauchi, R. Reijo Pera, and V. Sebastiano. 2016. 'Spatiotemporal Reconstruction of the Human Blastocyst by Single-Cell Gene-Expression Analysis Informs Induction of Naive Pluripotency', *Dev Cell*, 38: 100-15.

Enciso, M., J. P. Carrascosa, J. Sarasa, P. A. Martinez-Ortiz, S. Munne, J. A. Horcajadas, and J. Aizpurua. 2018. 'Development of a new comprehensive and reliable endometrial receptivity map (ER Map/ER Grade) based on RT-qPCR gene expression analysis', *Hum Reprod*, 33: 220-28.

Estella, C., I. Herrer, S. P. Atkinson, A. Quinonero, S. Martinez, A. Pellicer, and C. Simon. 2012. 'Inhibition of histone deacetylase activity in human endometrial stromal cells promotes extracellular matrix remodelling and limits embryo invasion', *PLoS One*, 7: e30508.

Evans, G. E., J. A. Martinez-Conejero, G. T. Phillipson, P. H. Sykes, I. L. Sin, E. Y. Lam, C. G. Print, J. A. Horcajadas, and J. J. Evans. 2014. 'In the secretory endometria of women, luminal epithelia exhibit gene and protein expressions that differ from those of glandular epithelia', *Fertil Steril*, 102: 307-17 e7.

Evans, G. E., G. T. M. Phillipson, P. H. Sykes, L. A. McNoe, C. G. Print, and J. J. Evans. 2018. 'Does the endometrial gene expression of fertile women vary within and between cycles?', *Hum Reprod*, 33: 452-63.

Evans, J., R. D. Catalano, K. Morgan, H. O. Critchley, R. P. Millar, and H. N. Jabbour. 2008. 'Prokineticin 1 signaling and gene regulation in early human pregnancy', *Endocrinology*, 149: 2877-87.

Evans, J., L. A. Salamonsen, A. Winship, E. Menkhorst, G. Nie, C. E. Gargett, and E. Dimitriadis. 2016. 'Fertile ground: human endometrial programming and lessons in health and disease', *Nat Rev Endocrinol*, 12: 654-67.

Evron, A., S. Goldman, and E. Shalev. 2011. 'Effect of primary human endometrial stromal cells on epithelial cell receptivity and protein expression is dependent on menstrual cycle stage', *Hum Reprod*, 26: 176-90.

Fagerberg, L., K. Jonasson, G. von Heijne, M. Uhlen, and L. Berglund. 2010. 'Prediction of the human membrane proteome', *Proteomics*, 10: 1141-9.

Fest, S., P. B. Aldo, V. M. Abrahams, I. Visintin, A. Alvero, R. Chen, S. L. Chavez, R. Romero, and G. Mor. 2007. 'Trophoblast-macrophage interactions: a regulatory network for the protection of pregnancy', *Am J Reprod Immunol*, 57: 55-66.

Franasiak, J. M., M. D. Werner, C. R. Juneau, X. Tao, J. Landis, Y. Zhan, N. R. Treff, and R. T. Scott. 2016. 'Endometrial microbiome at the time of embryo transfer: next-generation sequencing of the 16S ribosomal subunit', *J Assist Reprod Genet*, 33: 129-36.

Frank, H. G., B. Gunawan, I. Ebeling-Stark, H. J. Schulten, H. Funayama, U. Cremer, B. Huppertz, G. Gaus, P. Kaufmann, and L. Fuzesi. 2000. 'Cytogenetic and DNA-fingerprint characterization of choriocarcinoma cell lines and a trophoblast/choriocarcinoma cell hybrid', *Cancer Genet Cytogenet*, 116: 16-22.

Galan, A., J. E. O'Connor, D. Valbuena, R. Herrer, J. Remohi, S. Pampfer, A. Pellicer, and C. Simon. 2000. 'The human blastocyst regulates endometrial epithelial apoptosis in embryonic adhesion', *Biol Reprod*, 63: 430-9.

Gardner, D. K., and B. Balaban. 2016. 'Assessment of human embryo development using morphological criteria in an era of time-lapse, algorithms and 'OMICS': is looking good still important?', *Mol Hum Reprod*, 22: 704-18.

Gargett, C. E., F. L. Lederman, T. M. Lau, N. H. Taylor, and P. A. Rogers. 1999. 'Lack of correlation between vascular endothelial growth factor production and endothelial cell proliferation in the human endometrium', *Hum Reprod*, 14: 2080-8.

Gargett, C. E., and P. A. Rogers. 2001. 'Human endometrial angiogenesis', *Reproduction*, 121: 181-6.

Gargett, C. E., K. E. Schwab, and J. A. Deane. 2016. 'Endometrial stem/progenitor cells: the first 10 years', *Hum Reprod Update*, 22: 137-63.

Gellersen, B., and J. J. Brosens. 2014. 'Cyclic decidualization of the human endometrium in reproductive health and failure', *Endocr Rev*, 35: 851-905.

Gellersen, B., K. Reimann, A. Samalecos, S. Aupers, and A. M. Bamberger. 2010. 'Invasiveness of human endometrial stromal cells is promoted by decidualization and by trophoblast-derived signals', *Hum Reprod*, 25: 862-73.

Gellersen, B., A. Wolf, M. Kruse, M. Schwenke, and A. M. Bamberger. 2013. 'Human endometrial stromal cell-trophoblast interactions: mutual stimulation of chemotactic migration and promigratory roles of cell surface molecules CD82 and CEACAM1', *Biol Reprod*, 88: 80.

Giacomini, E., R. Vago, A. M. Sanchez, P. Podini, N. Zarovni, V. Murdica, R. Rizzo, D. Bortolotti, M. Candiani, and P. Vigano. 2017. 'Secretome of in vitro cultured human embryos contains extracellular vesicles that are uptaken by the maternal side', *Sci Rep*, 7: 5210.

Gnecco, J. S., A. P. Anders, D. Cliffel, V. Pensabene, L. M. Rogers, K. Osteen, and D. M. Aronoff. 2017. 'Instrumenting a Fetal Membrane on a Chip as Emerging Technology for Preterm Birth Research', *Curr Pharm Des*, 23: 6115-24.

Gnecco, J. S., T. Ding, C. Smith, J. Lu, K. L. Bruner-Tran, and K. G. Osteen. 2019. 'Hemodynamic forces enhance decidualization via endothelial-derived prostaglandin E2 and prostacyclin in a microfluidic model of the human endometrium', *Hum Reprod*, 34: 702-14.

Gnecco, J. S., V. Pensabene, D. J. Li, T. Ding, E. E. Hui, K. L. Bruner-Tran, and K. G. Osteen. 2017. 'Compartmentalized Culture of Perivascular Stroma and Endothelial Cells in a Microfluidic Model of the Human Endometrium', *Ann Biomed Eng*, 45: 1758-69.

Godbole, G., P. Suman, S. K. Gupta, and D. Modi. 2011. 'Decidualized endometrial stromal cell derived factors promote trophoblast invasion', *Fertil Steril*, 95: 1278-83.

Golander, A., T. Hurley, J. Barrett, A. Hizi, and S. Handwerger. 1978. 'Prolactin synthesis by human chorion-decidual tissue: a possible source of prolactin in the amniotic fluid', *Science*, 202: 311-3.

Gonzalez, M., J. Neufeld, K. Reimann, S. Wittmann, A. Samalecos, A. Wolf, A. M. Bamberger, and B. Gellersen. 2011. 'Expansion of human trophoblastic spheroids is promoted by

decidualized endometrial stromal cells and enhanced by heparin-binding epidermal growth factor-like growth factor and interleukin-1 beta', *Mol Hum Reprod*, 17: 421-33.

Gonzalez, R. R., P. Caballero-Campo, M. Jasper, A. Mercader, L. Devoto, A. Pellicer, and C. Simon. 2000. 'Leptin and leptin receptor are expressed in the human endometrium and endometrial leptin secretion is regulated by the human blastocyst', *J Clin Endocrinol Metab*, 85: 4883-8.

Gonzalez, R. R., K. Leary, J. C. Petrozza, and P. C. Leavis. 2003. 'Leptin regulation of the interleukin-1 system in human endometrial cells', *Mol Hum Reprod*, 9: 151-8.

Grasso, E., S. Gori, E. Soczewski, L. Fernandez, L. Gallino, D. Vota, G. Martinez, M. Irigoyen, C. Ruhlmann, T. F. Lobo, G. Salamone, R. Mattar, S. Daher, C. P. Leiros, and R. Ramhorst. 2018. 'Impact of the Reticular Stress and Unfolded Protein Response on the inflammatory response in endometrial stromal cells', *Sci Rep*, 8: 12274.

Greening, D. W., H. P. Nguyen, K. Elgass, R. J. Simpson, and L. A. Salamonsen. 2016. 'Human Endometrial Exosomes Contain Hormone-Specific Cargo Modulating Trophoblast Adhesive Capacity: Insights into Endometrial-Embryo Interactions', *Biol Reprod*, 94: 38.

Greening, D. W., H. P. Nguyen, J. Evans, R. J. Simpson, and L. A. Salamonsen. 2016. 'Modulating the endometrial epithelial proteome and secretome in preparation for pregnancy: The role of ovarian steroid and pregnancy hormones', *J Proteomics*, 144: 99-112.

Grewal, S., J. G. Carver, A. J. Ridley, and H. J. Mardon. 2008. 'Implantation of the human embryo requires Rac1-dependent endometrial stromal cell migration', *Proc Natl Acad Sci U S A*, 105: 16189-94.

Grewal, S., J. Carver, A. J. Ridley, and H. J. Mardon. 2010. 'Human endometrial stromal cell rho GTPases have opposing roles in regulating focal adhesion turnover and embryo invasion in vitro', *Biol Reprod*, 83: 75-82.

Grootjans, J., A. Kaser, R. J. Kaufman, and R. S. Blumberg. 2016. 'The unfolded protein response in immunity and inflammation', *Nat Rev Immunol*, 16: 469-84.

Gurunath, S., Z. Pandian, R. A. Anderson, and S. Bhattacharya. 2011. 'Defining infertility--a systematic review of prevalence studies', *Hum Reprod Update*, 17: 575-88.

Guzel, E., S. Arlier, O. Guzeloglu-Kayisli, M. S. Tabak, T. Ekiz, N. Semerci, K. Larsen, F. Schatz, C. J. Lockwood, and U. A. Kayisli. 2017. 'Endoplasmic Reticulum Stress and Homeostasis in Reproductive Physiology and Pathology', *Int J Mol Sci*, 18.

Haahr, T., J. S. Jensen, L. Thomsen, L. Duus, K. Rygaard, and P. Humaidan. 2016. 'Abnormal vaginal microbiota may be associated with poor reproductive outcomes: a prospective study in IVF patients', *Hum Reprod*, 31: 795-803.

Haahr, T., J. Zacho, M. Brauner, K. Shathmigha, J. Skov Jensen, and P. Humaidan. 2019. 'Reproductive outcome of patients undergoing in vitro fertilisation treatment and diagnosed with bacterial vaginosis or abnormal vaginal microbiota: a systematic PRISMA review and meta-analysis', *BJOG*, 126: 200-07.

Haider, S., G. Meinhardt, L. Saleh, V. Kunihs, M. Gamperl, U. Kaindl, A. Ellinger, T. R. Burkard, C. Fiala, J. Pollheimer, S. Mendjan, P. A. Latos, and M. Knofler. 2018. 'Self-Renewing Trophoblast Organoids Recapitulate the Developmental Program of the Early Human Placenta', *Stem Cell Reports*, 11: 537-51.

Hakam, M. S., J. M. Miranda-Sayago, S. Hayrabedyan, K. Todorova, P. S. Spencer, A. Jabeen, E. R. Barnea, and N. Fernandez. 2017. 'Preimplantation Factor (PIF) Promotes HLA-G, -E, -F, -C Expression in JEG-3 Choriocarcinoma Cells and Endogenous Progesterone Activity', *Cell Physiol Biochem*, 43: 2277-96.

Handschuh, K., J. Guibourdenche, V. Tsatsaris, M. Guesnon, I. Laurendeau, D. Evain-Brion, and T. Fournier. 2007. 'Human chorionic gonadotropin expression in human trophoblasts from early placenta: comparative study between villous and extravillous trophoblastic cells', *Placenta*, 28: 175-84.

Hannan, N. J., R. L. Jones, C. A. White, and L. A. Salamonsen. 2006. 'The chemokines, CX3CL1, CCL14, and CCL4, promote human trophoblast migration at the feto-maternal interface', *Biol Reprod*, 74: 896-904.

Hannan, N. J., P. Paiva, E. Dimitriadis, and L. A. Salamonsen. 2010. 'Models for study of human embryo implantation: choice of cell lines?', *Biol Reprod*, 82: 235-45.

Haouzi, D., H. Dechaud, S. Assou, C. Monzo, J. de Vos, and S. Hamamah. 2011. 'Transcriptome analysis reveals dialogues between human trophectoderm and endometrial cells during the implantation period', *Hum Reprod*, 26: 1440-9.

Harduf, H., S. Goldman, and E. Shalev. 2007. 'Human uterine epithelial RL95-2 and HEC-1A cell-line adhesiveness: the role of plexin B1', *Fertil Steril*, 87: 1419-27.

Harduf, H., S. Goldman, and E. Shalev. 2009. 'Progesterone receptor A and c-Met mediates spheroids-endometrium attachment', *Reprod Biol Endocrinol*, 7: 14.

Harrison, S. E., B. Sozen, N. Christodoulou, C. Kyprianou, and M. Zernicka-Goetz. 2017. 'Assembly of embryonic and extraembryonic stem cells to mimic embryogenesis in vitro', *Science*, 356.

Hashimoto, T., M. Koizumi, M. Doshida, M. Toya, E. Sagara, N. Oka, Y. Nakajo, N. Aono, H. Igarashi, and K. Kyono. 2017. 'Efficacy of the endometrial receptivity array for repeated implantation failure in Japan: A retrospective, two-centers study', *Reprod Med Biol*, 16: 290-96.

Hempstock, J., T. Cindrova-Davies, E. Jauniaux, and G. J. Burton. 2004. 'Endometrial glands as a source of nutrients, growth factors and cytokines during the first trimester of human pregnancy: a morphological and immunohistochemical study', *Reprod Biol Endocrinol*, 2: 58.

Heneweer, C., H. G. Adelmann, L. H. Kruse, H. W. Denker, and M. Thie. 2003. 'Human uterine epithelial RL95-2 cells reorganize their cytoplasmic architecture with respect to Rho protein and F-actin in response to trophoblast binding', *Cells Tissues Organs*, 175: 1-8.

Heneweer, C., M. Schmidt, H. W. Denker, and M. Thie. 2005. 'Molecular mechanisms in uterine epithelium during trophoblast binding: the role of small GTPase RhoA in human uterine Ishikawa cells', *J Exp Clin Assist Reprod*, 2: 4.

Hennes, A., K. Held, M. Boretto, K. De Clercq, C. Van den Eynde, A. Vanhie, N. Van Ranst, M. Benoit, C. Luyten, K. Peeraer, C. Tomassetti, C. Meuleman, T. Voets, H. Vankelecom, and J. Vriens. 2019. 'Functional expression of the mechanosensitive PIEZO1 channel in primary endometrial epithelial cells and endometrial organoids', *Sci Rep*, 9: 1779.

Hevir-Kene, N., and T. L. Rizner. 2015. 'The endometrial cancer cell lines Ishikawa and HEC-1A, and the control cell line HIEEC, differ in expression of estrogen biosynthetic and metabolic genes, and in androstenedione and estrone-sulfate metabolism', *Chem Biol Interact*, 234: 309-19.

Ho, H., H. Singh, M. Aljofan, and G. Nie. 2012. 'A high-throughput in vitro model of human embryo attachment', *Fertil Steril*, 97: 974-8.

Hohn, H. P., M. Linke, and H. W. Denker. 2000. 'Adhesion of trophoblast to uterine epithelium as related to the state of trophoblast differentiation: in vitro studies using cell lines', *Mol Reprod Dev*, 57: 135-45.

Holmberg, J. C., S. Haddad, V. Wunsche, Y. Yang, P. B. Aldo, Y. Gnainsky, I. Granot, N. Dekel, and G. Mor. 2012. 'An in vitro model for the study of human implantation', *Am J Reprod Immunol*, 67: 169-78.

Hood, B. L., B. Liu, A. Alkhas, Y. Shoji, R. Challa, G. Wang, S. Ferguson, J. Oliver, D. Mitchell, N. W. Bateman, C. M. Zahn, C. A. Hamilton, M. Payson, B. Lessey, A. T. Fazleabas, G. L. Maxwell, T. P. Conrads, and J. I. Risinger. 2015. 'Proteomics of the human endometrial glandular epithelium and stroma from the proliferative and secretory phases of the menstrual cycle', *Biol Reprod*, 92: 106.

Hooper, L. V., D. R. Littman, and A. J. Macpherson. 2012. 'Interactions between the microbiota and the immune system', *Science*, 336: 1268-73.

Horne, A. W., E. N. Lalani, R. A. Margara, T. A. Ryder, M. A. Mobberley, and J. O. White. 2005. 'The expression pattern of MUC1 glycoforms and other biomarkers of endometrial receptivity in fertile and infertile women', *Mol Reprod Dev*, 72: 216-29.

Huang, M. Y., W. Q. Zhang, M. Zhao, C. Zhu, J. P. He, and J. L. Liu. 2018. 'Assessment of Embryo-Induced Transcriptomic Changes in Hamster Uterus Using RNA-Seq', *Cell Physiol Biochem*, 46: 1868-78.

Huang, T. T., K. Chinn, T. Kosasa, H. J. Ahn, and B. Kessel. 2016. 'Morphokinetics of human blastocyst expansion in vitro', *Reprod Biomed Online*, 33: 659-67.

Huang, X., M. Luthi, E. C. Ontsouka, S. Kallol, M. U. Baumann, D. V. Surbek, and C. Albrecht. 2016. 'Establishment of a confluent monolayer model with human primary trophoblast cells: novel insights into placental glucose transport', *Mol Hum Reprod*, 22: 442-56.

Hyun, I., A. Wilkerson, and J. Johnston. 2016. 'Embryology policy: Revisit the 14-day rule', *Nature*, 533: 169-71.

Ivanov, II, K. Atarashi, N. Manel, E. L. Brodie, T. Shima, U. Karaoz, D. Wei, K. C. Goldfarb, C. A. Santee, S. V. Lynch, T. Tanoue, A. Imaoka, K. Itoh, K. Takeda, Y. Umesaki, K. Honda, and D. R. Littman. 2009. 'Induction of intestinal Th17 cells by segmented filamentous bacteria', *Cell*, 139: 485-98.

Iwahashi, M., Y. Muragaki, A. Ooshima, M. Yamoto, and R. Nakano. 1996. 'Alterations in distribution and composition of the extracellular matrix during decidualization of the human endometrium', *J Reprod Fertil*, 108: 147-55.

Johnson, J. L., M. B. Jones, and B. A. Cobb. 2015. 'Polysaccharide A from the capsule of Bacteroides fragilis induces clonal CD4+ T cell expansion', *J Biol Chem*, 290: 5007-14.

Jung, H. Y., L. Fattet, J. H. Tsai, T. Kajimoto, Q. Chang, A. C. Newton, and J. Yang. 2019. 'Apical-basal polarity inhibits epithelial-mesenchymal transition and tumour metastasis by PAR-complex-mediated SNAI1 degradation', *Nat Cell Biol*, 21: 359-71.

Kabir-Salmani, M., H. Nikzad, S. Shiokawa, Y. Akimoto, and M. Iwashita. 2005. 'Secretory role for human uterodomes (pinopods): secretion of LIF', *Mol Hum Reprod*, 11: 553-9.

Kaitu'u-Lino, T. J., N. B. Morison, and L. A. Salamonsen. 2007. 'Neutrophil depletion retards endometrial repair in a mouse model', *Cell Tissue Res*, 328: 197-206.

Kajihara, T., K. Tanaka, T. Oguro, H. Tochigi, J. Prechapanich, S. Uchino, A. Itakura, S. Sucurovic, K. Murakami, J. J. Brosens, and O. Ishihara. 2014. 'Androgens modulate the morphological characteristics of human endometrial stromal cells decidualized in vitro', *Reprod Sci*, 21: 372-80.

Karmakar, S., R. Dhar, and C. Das. 2004. 'Inhibition of cytotrophoblastic (JEG-3) cell invasion by interleukin 12 involves an interferon gamma-mediated pathway', *J Biol Chem*, 279: 55297-307.

Kayisli, U. A., J. Luk, O. Guzeloglu-Kayisli, Y. Seval, R. Demir, and A. Arici. 2004. 'Regulation of angiogenic activity of human endometrial endothelial cells in culture by ovarian steroids', *J Clin Endocrinol Metab*, 89: 5794-802.

Kelleher, A. M., J. Milano-Foster, S. K. Behura, and T. E. Spencer. 2018. 'Uterine glands coordinate on-time embryo implantation and impact endometrial decidualization for pregnancy success', *Nat Commun*, 9: 2435.

Kervancioglu Demirci, E., L. A. Salamonsen, and M. Gauster. 2016. 'The role of CX3CL1 in fetal-maternal interaction during human gestation', *Cell Adh Migr*, 10: 189-96.

Ketene, A. N., P. C. Roberts, A. A. Shea, E. M. Schmelz, and M. Agah. 2012. 'Actin filaments play a primary role for structural integrity and viscoelastic response in cells', *Integr Biol (Camb)*, 4: 540-9.

King, A., L. Thomas, and P. Bischof. 2000. 'Cell culture models of trophoblast II: trophoblast cell lines-a workshop report', *Placenta*, 21 Suppl A: S113-9.

Kliman, H. J., R. F. Feinberg, and J. E. Haimowitz. 1990. 'Human trophoblast-endometrial interactions in an in vitro suspension culture system', *Placenta*, 11: 349-67.

Knofler, M. 2010. 'Critical growth factors and signalling pathways controlling human trophoblast invasion', *Int J Dev Biol*, 54: 269-80.

Kohler, P. O., and W. E. Bridson. 1971. 'Isolation of hormone-producing clonal lines of human choriocarcinoma', *J Clin Endocrinol Metab*, 32: 683-7.

Kolahi, K. S., A. Donjacour, X. Liu, W. Lin, R. K. Simbulan, E. Bloise, E. Maltepe, and P. Rinaudo. 2012. 'Effect of substrate stiffness on early mouse embryo development', *PLoS One*, 7: e41717.

Koopman, L. A., H. D. Kopcow, B. Rybalov, J. E. Boyson, J. S. Orange, F. Schatz, R. Masch, C. J. Lockwood, A. D. Schachter, P. J. Park, and J. L. Strominger. 2003. 'Human decidual natural killer cells are a unique NK cell subset with immunomodulatory potential', *J Exp Med*, 198: 1201-12.

Koot, Y. E., G. Teklenburg, M. S. Salker, J. J. Brosens, and N. S. Macklon. 2012. 'Molecular aspects of implantation failure', *Biochim Biophys Acta*, 1822: 1943-50.

Koot, Y. E., S. R. van Hooff, C. M. Boomsma, D. van Leenen, M. J. Groot Koerkamp, M. Goddijn, M. J. Eijkemans, B. C. Fauser, F. C. Holstege, and N. S. Macklon. 2016. 'An endometrial gene expression signature accurately predicts recurrent implantation failure after IVF', *Sci Rep*, 6: 19411.

Krikun, G., G. Mor, A. Alvero, S. Guller, F. Schatz, E. Sapi, M. Rahman, R. Caze, M. Qumsiyeh, and C. J. Lockwood. 2004. 'A novel immortalized human endometrial stromal cell line with normal progestational response', *Endocrinology*, 145: 2291-6.

Kuramoto, H., S. Tamura, and Y. Notake. 1972. 'Establishment of a cell line of human endometrial adenocarcinoma in vitro', *Am J Obstet Gynecol*, 114: 1012-9.

Kurarmoto, H., M. Hamano, and M. Imai. 2002. 'HEC-1 cells', *Hum Cell*, 15: 81-95.

Kyono, K., T. Hashimoto, S. Kikuchi, Y. Nagai, and Y. Sakuraba. 2019. 'A pilot study and case reports on endometrial microbiota and pregnancy outcome: An analysis using 16S rRNA gene sequencing among IVF patients, and trial therapeutic intervention for dysbiotic endometrium', *Reprod Med Biol*, 18: 72-82.

Lalitkumar, P. G., S. Lalitkumar, C. X. Meng, A. Stavreus-Evers, F. Hambiliki, U. Bentin-Ley, and K. Gemzell-Danielsson. 2007. 'Mifepristone, but not levonorgestrel, inhibits human blastocyst attachment to an in vitro endometrial three-dimensional cell culture model', *Hum Reprod*, 22: 3031-7.

Landgren, B. M., E. Johannisson, A. Stavreus-Evers, L. Hamberger, and H. Eriksson. 1996. 'A new method to study the process of implantation of a human blastocyst in vitro', *Fertil Steril*, 65: 1067-70.

Laniewski, P., A. Gomez, G. Hire, M. So, and M. M. Herbst-Kralovetz. 2017. 'Human Three-Dimensional Endometrial Epithelial Cell Model To Study Host Interactions with Vaginal Bacteria and Neisseria gonorrhoeae', *Infect Immun*, 85.

Lee, K. Y., and F. J. DeMayo. 2004. 'Animal models of implantation', *Reproduction*, 128: 679-95.

Lensen, S., D. Osavlyuk, S. Armstrong, C. Stadelmann, A. Hennes, E. Napier, J. Wilkinson, L. Sadler, D. Gupta, A. Strandell, C. Bergh, K. Vigneswaran, W. T. Teh, H. Hamoda, L. Webber, S. A. Wakeman, L. Searle, P. Bhide, S. McDowell, K. Peeraer, Y. Khalaf, and C. Farquhar. 2019. 'A Randomized Trial of Endometrial Scratching before In Vitro Fertilization', *N Engl J Med*, 380: 325-34.

Lerner, A. G., J. P. Upton, P. V. Praveen, R. Ghosh, Y. Nakagawa, A. Igbaria, S. Shen, V. Nguyen, B. J. Backes, M. Heiman, N. Heintz, P. Greengard, S. Hui, Q. Tang, A. Trusina, S. A. Oakes, and F. R. Papa. 2012. 'IRE1alpha induces thioredoxin-interacting protein to activate

the NLRP3 inflammasome and promote programmed cell death under irremediable ER stress', *Cell Metab*, 16: 250-64.

Lessey, B. A. 2000. 'Endometrial receptivity and the window of implantation', *Baillieres Best Pract Res Clin Obstet Gynaecol*, 14: 775-88.

Lessey, B. A., Y. Gui, K. B. Apparao, S. L. Young, and J. Mulholland. 2002. 'Regulated expression of heparin-binding EGF-like growth factor (HB-EGF) in the human endometrium: a potential paracrine role during implantation', *Mol Reprod Dev*, 62: 446-55.

Lessey, B. A., A. O. Ilesanmi, M. A. Lessey, M. Riben, J. E. Harris, and K. Chwalisz. 1996. 'Luminal and glandular endometrial epithelium express integrins differentially throughout the menstrual cycle: implications for implantation, contraception, and infertility', *Am J Reprod Immunol*, 35: 195-204.

Lessey, B. A., Young S.L. 2019. 'Chapter 9 - Structure, Function, and Evaluation of the Female Reproductive Tract' in *Yen and Jaffe's Reproductive Endocrinology (Eighth Edition). Physiology, Pathophysiology, and Clinical Management*.

Li, J., Y. Chen, C. Liu, Y. Hu, and L. Li. 2013. 'Intravenous immunoglobulin treatment for repeated IVF/ICSI failure and unexplained infertility: a systematic review and a meta-analysis', *Am J Reprod Immunol*, 70: 434-47.

Li, J., S. Mo, and Y. Chen. 2017. 'The effect of G-CSF on infertile women undergoing IVF treatment: A meta-analysis', *Syst Biol Reprod Med*, 63: 239-47.

Lin, J. J., R. D. Eppinga, K. S. Warren, and K. R. McCrae. 2008. 'Human tropomyosin isoforms in the regulation of cytoskeleton functions', *Adv Exp Med Biol*, 644: 201-22.

Lindenberg, S. 1991. 'Ultrastructure in human implantation: transmission and scanning electron microscopy', *Baillieres Clin Obstet Gynaecol*, 5: 1-14.

Lindenberg, S., M. H. Nielsen, and S. Lenz. 1985. 'In vitro studies of human blastocyst implantation', *Ann N Y Acad Sci*, 442: 368-74.

Liu, H., X. Liu, H. Jin, F. Yang, W. Gu, and X. Li. 2013. 'Proteomic analysis of knock-down HLA-G in invasion of human trophoblast cell line JEG-3', *Int J Clin Exp Pathol*, 6: 2451-9.

Lunghi, L., M. E. Ferretti, S. Medici, C. Biondi, and F. Vesce. 2007. 'Control of human trophoblast function', *Reprod Biol Endocrinol*, 5: 6.

Luo, Q., D. Kuang, B. Zhang, and G. Song. 2016. 'Cell stiffness determined by atomic force microscopy and its correlation with cell motility', *Biochim Biophys Acta*, 1860: 1953-60.

Macdonald, L. J., K. J. Sales, V. Grant, P. Brown, H. N. Jabbour, and R. D. Catalano. 2011. 'Prokineticin 1 induces Dickkopf 1 expression and regulates cell proliferation and decidualization in the human endometrium', *Mol Hum Reprod*, 17: 626-36.

Macklon, N. S., J. P. Geraedts, and B. C. Fauser. 2002. 'Conception to ongoing pregnancy: the 'black box' of early pregnancy loss', *Hum Reprod Update*, 8: 333-43.

Madawala, R. J., S. Dowland, C. E. Poon, L. A. Lindsay, and C. R. Murphy. 2014. 'Caveolins redistribute in uterine epithelial cells during early pregnancy in the rat: an epithelial polarisation strategy?', *Histochem Cell Biol*, 142: 555-67.

Magdi, Y., A. El-Damen, A. M. Fathi, A. M. Abdelaziz, M. Abd-Elfatah Youssef, A. A. Abd-Allah, M. Ahmed Elawady, M. Ahmed Ibrahim, and Y. Edris. 2017. 'Revisiting the management of recurrent implantation failure through freeze-all policy', *Fertil Steril*, 108: 72-77.

Maier, E., R. C. Anderson, and N. C. Roy. 2014. 'Understanding how commensal obligate anaerobic bacteria regulate immune functions in the large intestine', *Nutrients*, 7: 45-73.

Mainigi M., S. Mani, C. Blundell, J. Y. Park, R. young, D. Huh. 2019. 'Maternal decidual cells regulate trophoblast invasion: studies from a novel organ on-a-chip device'. Oral communication at the 66th Annual Scientific Meeting of the Society for Reproductive Investigation in Paris, France.

Makrigiannakis, A., M. Karamouti, G. Petsas, N. Makris, G. Nikas, and A. Antsaklis. 2009. 'The expression of receptivity markers in the fallopian tube epithelium', *Histochem Cell Biol*, 132: 159-67.

Maldonado-Estrada, J., E. Menu, P. Roques, F. Barre-Sinoussi, and G. Chaouat. 2004. 'Evaluation of Cytokeratin 7 as an accurate intracellular marker with which to assess the purity of human placental villous trophoblast cells by flow cytometry', *J Immunol Methods*, 286: 21-34.

Margalioth, E. J., A. Ben-Chetrit, M. Gal, and T. Eldar-Geva. 2006. 'Investigation and treatment of repeated implantation failure following IVF-ET', *Hum Reprod*, 21: 3036-43.

Mascarenhas, M. N., S. R. Flaxman, T. Boerma, S. Vanderpoel, and G. A. Stevens. 2012. 'National, regional, and global trends in infertility prevalence since 1990: a systematic analysis of 277 health surveys', *PLoS Med*, 9: e1001356.

Masuda, H., S. S. Anwar, H. J. Buhring, J. R. Rao, and C. E. Gargett. 2012. 'A novel marker of human endometrial mesenchymal stem-like cells', *Cell Transplant*, 21: 2201-14.

Mataro, D., D. Garcia, O. Coll, R. Vassena, and A. Rodriguez. 2017. 'Lower endometrial receptivity in HIV-infected women receiving oocyte donation: a comorbidity of HIV infection?', *Hum Reprod Open*, 2017: hox019.

Matsuoka, A., F. Kizuka, L. Lee, I. Tamura, K. Taniguchi, H. Asada, T. Taketani, H. Tamura, and N. Sugino. 2010. 'Progesterone increases manganese superoxide dismutase expression via a cAMP-dependent signaling mediated by noncanonical Wnt5a pathway in human endometrial stromal cells', *J Clin Endocrinol Metab*, 95: E291-9.

Mazmanian, S. K., C. H. Liu, A. O. Tzianabos, and D. L. Kasper. 2005. 'An immunomodulatory molecule of symbiotic bacteria directs maturation of the host immune system', *Cell*, 122: 107-18.

Mazmanian, S. K., J. L. Round, and D. L. Kasper. 2008. 'A microbial symbiosis factor prevents intestinal inflammatory disease', *Nature*, 453: 620-5.

McConkey, C. A., E. Delorme-Axford, C. A. Nickerson, K. S. Kim, Y. Sadovsky, J. P. Boyle, and C. B. Coyne. 2016. 'A three-dimensional culture system recapitulates placental syncytiotrophoblast development and microbial resistance', *Sci Adv*, 2: e1501462.

McRae, A. C., and T. G. Kennedy. 1983. 'Selective permeability of the blood-uterine lumen barrier in rats: importance of molecular size', *Biol Reprod*, 29: 879-85.

Melford, S. E., A. H. Taylor, and J. C. Konje. 2014. 'Of mice and (wo)men: factors influencing successful implantation including endocannabinoids', *Hum Reprod Update*, 20: 415-28.

Meng, C. X., K. L. Andersson, U. Bentin-Ley, K. Gemzell-Danielsson, and P. G. Lalitkumar. 2009. 'Effect of levonorgestrel and mifepristone on endometrial receptivity markers in a three-dimensional human endometrial cell culture model', *Fertil Steril*, 91: 256-64.

Mercader, A., J. A. Garcia-Velasco, E. Escudero, J. Remohi, A. Pellicer, and C. Simon. 2003. 'Clinical experience and perinatal outcome of blastocyst transfer after coculture of human embryos with human endometrial epithelial cells: a 5-year follow-up study', *Fertil Steril*, 80: 1162-8.

Meseguer, M., J. D. Aplin, P. Caballero-Campo, J. E. O'Connor, J. C. Martin, J. Remohi, A. Pellicer, and C. Simon. 2001. 'Human endometrial mucin MUC1 is up-regulated by progesterone and down-regulated in vitro by the human blastocyst', *Biol Reprod*, 64: 590-601.

Miller, P. B., B. A. Parnell, G. Bushnell, N. Tallman, D. A. Forstein, H. L. Higdon, 3rd, J. Kitawaki, and B. A. Lessey. 2012. 'Endometrial receptivity defects during IVF cycles with and without letrozole', *Hum Reprod*, 27: 881-8.

Mitchell, C. M., A. Haick, E. Nkwopara, R. Garcia, M. Rendi, K. Agnew, D. N. Fredricks, and D. Eschenbach. 2015. 'Colonization of the upper genital tract by vaginal bacterial species in nonpregnant women', *Am J Obstet Gynecol*, 212: 611 e1-9.

Mo, B., A. E. Vendrov, W. A. Palomino, B. R. DuPont, K. B. Apparao, and B. A. Lessey. 2006. 'ECC-1 cells: a well-differentiated steroid-responsive endometrial cell line with characteristics of luminal epithelium', *Biol Reprod*, 75: 387-94.

Moreno, I., F. M. Codoner, F. Vilella, D. Valbuena, J. F. Martinez-Blanch, J. Jimenez-Almazan, R. Alonso, P. Alama, J. Remohi, A. Pellicer, D. Ramon, and C. Simon. 2016. 'Evidence that the endometrial microbiota has an effect on implantation success or failure', *Am J Obstet Gynecol*, 215: 684-703.

Moreno, I., and C. Simon. 2018. 'Relevance of assessing the uterine microbiota in infertility', *Fertil Steril*, 110: 337-43.

Moreno-Moya, J. M., N. A. Franchi, S. Martinez-Escribano, J. A. Martinez-Conejero, S. Bocca, S. Oehninger, and J. A. Horcajadas. 2015. 'Transcriptome of early embryonic invasion at implantation sites in a murine model', *Reprod Fertil Dev*.

Motato, Y., M. J. de los Santos, M. J. Escriba, B. A. Ruiz, J. Remohi, and M. Meseguer. 2016. 'Morphokinetic analysis and embryonic prediction for blastocyst formation through an integrated time-lapse system', *Fertil Steril*, 105: 376-84 e9.

Nakagawa, K., J. Kwak-Kim, K. Ota, K. Kuroda, M. Hisano, R. Sugiyama, and K. Yamaguchi. 2015. 'Immunosuppression with tacrolimus improved reproductive outcome of women with repeated implantation failure and elevated peripheral blood TH1/TH2 cell ratios', *Am J Reprod Immunol*, 73: 353-61.

Nancy, P., E. Tagliani, C. S. Tay, P. Asp, D. E. Levy, and A. Erlebacher. 2012. 'Chemokine gene silencing in decidual stromal cells limits T cell access to the maternal-fetal interface', *Science*, 336: 1317-21.

Nejatbakhsh, R., M. Kabir-Salmani, E. Dimitriadis, A. Hosseini, R. Taheripanah, Y. Sadeghi, Y. Akimoto, and M. Iwashita. 2012. 'Subcellular localization of L-selectin ligand in the endometrium implies a novel function for pinopodes in endometrial receptivity', *Reprod Biol Endocrinol*, 10: 46.

Ng, Y. H., S. Rome, A. Jalabert, A. Forterre, H. Singh, C. L. Hincks, and L. A. Salamonsen. 2013. 'Endometrial exosomes/microvesicles in the uterine microenvironment: a new paradigm for embryo-endometrial cross talk at implantation', *PLoS One*, 8: e58502.

Niakan, K. K., J. Han, R. A. Pedersen, C. Simon, and R. A. Pera. 2012. 'Human pre-implantation embryo development', *Development*, 139: 829-41.

Nishida, M., K. Kasahara, M. Kaneko, H. Iwasaki, and K. Hayashi. 1985. '[Establishment of a new human endometrial adenocarcinoma cell line, Ishikawa cells, containing estrogen and progesterone receptors]', *Nihon Sanka Fujinka Gakkai Zasshi*, 37: 1103-11.

Noyes, R. W., A. T. Hertig, and J. Rock. 1975. 'Dating the endometrial biopsy', *Am J Obstet Gynecol*, 122: 262-3.

Pandian, Z., A. Gibreel, and S. Bhattacharya. 2015. 'In vitro fertilisation for unexplained subfertility', *Cochrane Database Syst Rev*: CD003357.

Paternot, G., S. Debrock, D. De Neubourg, T. M. D'Hooghe, and C. Spiessens. 2013. 'Semi-automated morphometric analysis of human embryos can reveal correlations between total embryo volume and clinical pregnancy', *Hum Reprod*, 28: 627-33.

Payne, D., S. P. Flaherty, M. F. Barry, and C. D. Matthews. 1997. 'Preliminary observations on polar body extrusion and pronuclear formation in human oocytes using time-lapse video cinematography', *Hum Reprod*, 12: 532-41.

Pera, M. F. 2017. 'Human embryo research and the 14-day rule', *Development*, 144: 1923-25.

Petersen, A., U. Bentin-Ley, V. Ravn, K. Qvortrup, S. Sorensen, H. Islin, A. Sjogren, S. Mosselmann, and L. Hamberger. 2005. 'The antiprogesterone Org 31710 inhibits human blastocyst-endometrial interactions in vitro', *Fertil Steril*, 83 Suppl 1: 1255-63.

Petraglia, F., G. I. Serour, and C. Chapron. 2013. 'The changing prevalence of infertility', *Int J Gynaecol Obstet*, 123 Suppl 2: S4-8.

Pierro, E., F. Minici, O. Alesiani, F. Miceli, C. Proto, I. Screpanti, S. Mancuso, and A. Lanzone. 2001. 'Stromal-epithelial interactions modulate estrogen responsiveness in normal human endometrium', *Biol Reprod*, 64: 831-8.

Plant, T. M. 2015. '60 years of neuroendocrinology: The hypothalamo-pituitary-gonadal axis', *J Endocrinol*, 226: T41-54.

Polanski, L. T., M. N. Baumgarten, S. Quenby, J. Brosens, B. K. Campbell, and N. J. Raine-Fenning. 2014. 'What exactly do we mean by 'recurrent implantation failure'? A systematic review and opinion', *Reprod Biomed Online*, 28: 409-23.

Popovici, R. M., N. K. Betzler, M. S. Krause, M. Luo, J. Jauckus, A. Germeyer, S. Bloethner, A. Schlotterer, R. Kumar, T. Strowitzki, and M. von Wolff. 2006. 'Gene expression profiling of human endometrial-trophoblast interaction in a coculture model', *Endocrinology*, 147: 5662-75.

Qiong, Z., H. Jie, W. Yonggang, X. Bin, Z. Jing, and L. Yanping. 2017. 'Clinical validation of pinopode as a marker of endometrial receptivity: a randomized controlled trial', *Fertil Steril*, 108: 513-17 e2.

Quenby, S., M. Bates, T. Doig, J. Brewster, D. I. Lewis-Jones, P. M. Johnson, and G. Vince. 1999. 'Pre-implantation endometrial leukocytes in women with recurrent miscarriage', *Hum Reprod*, 14: 2386-91.

Quenby, S., H. Nik, B. Innes, G. Lash, M. Turner, J. Drury, and J. Bulmer. 2009. 'Uterine natural killer cells and angiogenesis in recurrent reproductive failure', *Hum Reprod*, 24: 45-54.

Quinn, C. E., and R. F. Casper. 2009. 'Pinopodes: a questionable role in endometrial receptivity', *Hum Reprod Update*, 15: 229-36.

Richards, J. S. 2018. 'The Ovarian Cycle', *Vitam Horm*, 107: 1-25.

Richardson, L., J. Gnecco, T. Ding, K. Osteen, L. M. Rogers, D. M. Aronoff, and R. Menon. 2019. 'Fetal Membrane Organ-On-Chip: An Innovative Approach to Study Cellular Interactions', *Reprod Sci*: 1933719119828084.

Robertson, S. A., A. S. Care, and L. M. Moldenhauer. 2018. 'Regulatory T cells in embryo implantation and the immune response to pregnancy', *J Clin Invest*, 128: 4224-35.

Rothbauer, M., N. Patel, H. Gondola, M. Siwetz, B. Huppertz, and P. Ertl. 2017. 'A comparative study of five physiological key parameters between four different human trophoblast-derived cell lines', *Sci Rep*, 7: 5892.

Ruan, Y. C., J. H. Guo, X. Liu, R. Zhang, L. L. Tsang, J. D. Dong, H. Chen, M. K. Yu, X. Jiang, X. H. Zhang, K. L. Fok, Y. W. Chung, H. Huang, W. L. Zhou, and H. C. Chan. 2012. 'Activation of the epithelial Na+ channel triggers prostaglandin E(2) release and production required for embryo implantation', *Nat Med*, 18: 1112-7.

Ruane, P. T., S. C. Berneau, R. Koeck, J. Watts, S. J. Kimber, D. R. Brison, M. Westwood, and J. D. Aplin. 2017. 'Apposition to endometrial epithelial cells activates mouse blastocysts for implantation', *Mol Hum Reprod*, 23: 617-27.

Rubio, C., C. Simon, A. Mercader, J. Garcia-Velasco, J. Remohi, and A. Pellicer. 2000. 'Clinical experience employing co-culture of human embryos with autologous human endometrial epithelial cells', *Hum Reprod*, 15 Suppl 6: 31-8.

Ruiz-Alonso, M., D. Blesa, P. Diaz-Gimeno, E. Gomez, M. Fernandez-Sanchez, F. Carranza, J. Carrera, F. Vilella, A. Pellicer, and C. Simon. 2013. 'The endometrial receptivity array for diagnosis and personalized embryo transfer as a treatment for patients with repeated implantation failure', *Fertil Steril*, 100: 818-24.

Rutanen, E. M., R. Koistinen, T. Wahlstrom, H. Bohn, T. Ranta, and M. Seppala. 1985. 'Synthesis of placental protein 12 by human decidua', *Endocrinology*, 116: 1304-9.

Saito, S., A. Nakashima, T. Shima, and M. Ito. 2010. 'Th1/Th2/Th17 and regulatory T-cell paradigm in pregnancy', *Am J Reprod Immunol*, 63: 601-10.

Salamonsen, L. A., J. Evans, H. P. Nguyen, and T. A. Edgell. 2016. 'The Microenvironment of Human Implantation: Determinant of Reproductive Success', *Am J Reprod Immunol*, 75: 218-25.

Salker, M. S., J. Nautiyal, J. H. Steel, Z. Webster, S. Sucurovic, M. Nicou, Y. Singh, E. S. Lucas, K. Murakami, Y. W. Chan, S. James, Y. Abdallah, M. Christian, B. A. Croy, B. Mulac-Jericevic, S. Quenby, and J. J. Brosens. 2012. 'Disordered IL-33/ST2 activation in decidualizing stromal cells prolongs uterine receptivity in women with recurrent pregnancy loss', *PLoS One*, 7: e52252.

Samalecos, A., K. Reimann, S. Wittmann, H. M. Schulte, J. J. Brosens, A. M. Bamberger, and B. Gellersen. 2009. 'Characterization of a novel telomerase-immortalized human endometrial stromal cell line, St-T1b', *Reprod Biol Endocrinol*, 7: 76.

Schaefer, W. R., L. Fischer, W. R. Deppert, A. Hanjalic-Beck, L. Seebacher, M. Weimer, and H. P. Zahradnik. 2010. 'In vitro-Ishikawa cell test for assessing tissue-specific chemical effects on human endometrium', *Reprod Toxicol*, 30: 89-93.

Schropfer, A., U. Kammerer, M. Kapp, J. Dietl, S. Feix, and J. Anacker. 2010. 'Expression pattern of matrix metalloproteinases in human gynecological cancer cell lines', *BMC Cancer*, 10: 553.

Schwab, K. E., and C. E. Gargett. 2007. 'Co-expression of two perivascular cell markers isolates mesenchymal stem-like cells from human endometrium', *Hum Reprod*, 22: 2903-11.

Sebastian-Leon, P., N. Garrido, J. Remohi, A. Pellicer, and P. Diaz-Gimeno. 2018. 'Asynchronous and pathological windows of implantation: two causes of recurrent implantation failure', *Hum Reprod*, 33: 626-35.

Senbanjo, L. T., and M. A. Chellaiah. 2017. 'CD44: A Multifunctional Cell Surface Adhesion Receptor Is a Regulator of Progression and Metastasis of Cancer Cells', *Front Cell Dev Biol*, 5: 18.

Shahbazi, M. N., A. Scialdone, N. Skorupska, A. Weberling, G. Recher, M. Zhu, A. Jedrusik, L. G. Devito, L. Noli, I. C. Macaulay, C. Buecker, Y. Khalaf, D. Ilic, T. Voet, J. C. Marioni, and M. Zernicka-Goetz. 2017. 'Pluripotent state transitions coordinate morphogenesis in mouse and human embryos', *Nature*, 552: 239-43.

Shannon, P., A. Markiel, O. Ozier, N. S. Baliga, J. T. Wang, D. Ramage, N. Amin, B. Schwikowski, and T. Ideker. 2003. 'Cytoscape: a software environment for integrated models of biomolecular interaction networks', *Genome Res*, 13: 2498-504.

Sharma, S., G. Godbole, and D. Modi. 2016. 'Decidual Control of Trophoblast Invasion', *Am J Reprod Immunol*, 75: 341-50.

Shaw, J. L., S. K. Dey, H. O. Critchley, and A. W. Horne. 2010. 'Current knowledge of the aetiology of human tubal ectopic pregnancy', *Hum Reprod Update*, 16: 432-44.

Shi, J., Q. Chen, X. Li, X. Zheng, Y. Zhang, J. Qiao, F. Tang, Y. Tao, Q. Zhou, and E. Duan. 2015. 'Dynamic transcriptional symmetry-breaking in pre-implantation mammalian embryo development revealed by single-cell RNA-seq', *Development*, 142: 3468-77.

Shohayeb, A., and W. El-Khayat. 2012. 'Does a single endometrial biopsy regimen (S-EBR) improve ICSI outcome in patients with repeated implantation failure? A randomised controlled trial', *Eur J Obstet Gynecol Reprod Biol*, 164: 176-9.

Shyu, M. K., M. C. Lin, C. H. Liu, Y. R. Fu, J. C. Shih, C. N. Lee, H. Y. Chen, J. Huang, M. C. Huang, and F. J. Hsieh. 2008. 'MUC1 expression is increased during human placental development and suppresses trophoblast-like cell invasion in vitro', *Biol Reprod*, 79: 233-9.

Simon, C., M. J. Gimeno, A. Mercader, J. E. O'Connor, J. Remohi, M. L. Polan, and A. Pellicer. 1997. 'Embryonic regulation of integrins beta 3, alpha 4, and alpha 1 in human endometrial epithelial cells in vitro', *J Clin Endocrinol Metab*, 82: 2607-16.

Simon C., I.K. Vladimirov, G. Castillon Cortes, I. Ortega, S. Cabanillas, C. Vidal, J. Gilesf, A. Izquierdo, S. Portela, I. Fernandez, M. Ferrando, S. Mackens, S. Barrera, A. Pellicer. 2016. 'Prospective, randomized study of the endometrial receptivity analysis (ERA) test in the infertility work-up to guide personalized embryo transfer versus fresh transfer or deferred embryo transfer', *Fertility and Sterility*, 106, 3: e46 - e47.

Simon, C., A. Mercader, J. Garcia-Velasco, G. Nikas, C. Moreno, J. Remohi, and A. Pellicer. 1999. 'Coculture of human embryos with autologous human endometrial epithelial cells in patients with implantation failure', *J Clin Endocrinol Metab*, 84: 2638-46.

Singh, H., and J. D. Aplin. 2015. 'Endometrial apical glycoproteomic analysis reveals roles for cadherin 6, desmoglein-2 and plexin b2 in epithelial integrity', *Mol Hum Reprod*, 21: 81-94.

Singh, H., L. Nardo, S. J. Kimber, and J. D. Aplin. 2010. 'Early stages of implantation as revealed by an in vitro model', *Reproduction*, 139: 905-14.

Somigliana, E., P. Vigano, A. Busnelli, A. Paffoni, W. Vegetti, and P. Vercellini. 2018. 'Repeated implantation failure at the crossroad between statistics, clinics and over-diagnosis', *Reprod Biomed Online*, 36: 32-38.

Sozen, B., G. Amadei, A. Cox, R. Wang, E. Na, S. Czukiewska, L. Chappell, T. Voet, G. Michel, N. Jing, D. M. Glover, and M. Zernicka-Goetz. 2018. 'Self-assembly of embryonic and two extra-embryonic stem cell types into gastrulating embryo-like structures', *Nat Cell Biol*, 20: 979-89.

Stavreus-Evers, A., L. Aghajanova, H. Brismar, H. Eriksson, B. M. Landgren, and O. Hovatta. 2002. 'Co-existence of heparin-binding epidermal growth factor-like growth factor and pinopodes in human endometrium at the time of implantation', *Mol Hum Reprod*, 8: 765-9.

Stevens, V. C. 1997. 'Some reproductive studies in the baboon', *Hum Reprod Update*, 3: 533-40.

Stewart-Akers, A. M., J. S. Krasnow, J. Brekosky, and J. A. DeLoia. 1998. 'Endometrial leukocytes are altered numerically and functionally in women with implantation defects', *Am J Reprod Immunol*, 39: 1-11.

Stirparo, G. G., T. Boroviak, G. Guo, J. Nichols, A. Smith, and P. Bertone. 2018. 'Integrated analysis of single-cell embryo data yields a unified transcriptome signature for the human pre-implantation epiblast', *Development*, 145.

Sugihara, K., D. Sugiyama, J. Byrne, D. P. Wolf, K. P. Lowitz, Y. Kobayashi, M. Kabir-Salmani, D. Nadano, D. Aoki, S. Nozawa, J. Nakayama, T. Mustelin, E. Ruoslahti, N. Yamaguchi, and M. N. Fukuda. 2007. 'Trophoblast cell activation by trophinin ligation is implicated in human embryo implantation', *Proc Natl Acad Sci U S A*, 104: 3799-804.

Suhorutshenko, M., V. Kukushkina, A. Velthut-Meikas, S. Altmae, M. Peters, R. Magi, K. Krjutskov, M. Koel, F. M. Codoner, J. F. Martinez-Blanch, F. Vilella, C. Simon, A. Salumets, and T. Laisk. 2018. 'Endometrial receptivity revisited: endometrial transcriptome adjusted for tissue cellular heterogeneity', *Hum Reprod*, 33: 2074-86.

Sulz, L., J. P. Valenzuela, A. M. Salvatierra, M. E. Ortiz, and H. B. Croxatto. 1998. 'The expression of alpha(v) and beta3 integrin subunits in the normal human Fallopian tube epithelium suggests the occurrence of a tubal implantation window', *Hum Reprod*, 13: 2916-20.

Tabibzadeh, S., B. Lessey, and P. G. Satyaswaroop. 1998. 'Temporal and site-specific expression of transforming growth factor-beta4 in human endometrium', *Mol Hum Reprod*, 4: 595-602.

Takahashi, H., T. Takizawa, S. Matsubara, A. Ohkuchi, T. Kuwata, R. Usui, H. Matsumoto, Y. Sato, H. Fujiwara, A. Okamoto, M. Suzuki, and T. Takizawa. 2014. 'Extravillous trophoblast cell invasion is promoted by the CD44-hyaluronic acid interaction', *Placenta*, 35: 163-70.

Takeuchi, O., and S. Akira. 2010. 'Pattern recognition receptors and inflammation', *Cell*, 140: 805-20.

Tamm, K., M. Room, A. Salumets, and M. Metsis. 2009. 'Genes targeted by the estrogen and progesterone receptors in the human endometrial cell lines HEC1A and RL95-2', *Reprod Biol Endocrinol*, 7: 150.

Tamm-Rosenstein, K., J. Simm, M. Suhorutshenko, A. Salumets, and M. Metsis. 2013. 'Changes in the transcriptome of the human endometrial Ishikawa cancer cell line induced by estrogen, progesterone, tamoxifen, and mifepristone (RU486) as detected by RNA-sequencing', *PLoS One*, 8: e68907.

Teixeira, J., B. R. Rueda, and J. K. Pru. 2008. 'Uterine stem cells.' in, *StemBook* (Cambridge (MA)).

Teklenburg, G., M. Salker, M. Molokhia, S. Lavery, G. Trew, T. Aojanepong, H. J. Mardon, A. U. Lokugamage, R. Rai, C. Landles, B. A. Roelen, S. Quenby, E. W. Kuijk, A. Kavelaars, C. J. Heijnen, L. Regan, J. J. Brosens, and N. S. Macklon. 2010. 'Natural selection of human embryos: decidualizing endometrial stromal cells serve as sensors of embryo quality upon implantation', *PLoS One*, 5: e10258.

Thie, M., and H. W. Denker. 2002. 'In vitro studies on endometrial adhesiveness for trophoblast: cellular dynamics in uterine epithelial cells', *Cells Tissues Organs*, 172: 237-52.

Thornhill, A. R., C. E. deDie-Smulders, J. P. Geraedts, J. C. Harper, G. L. Harton, S. A. Lavery, C. Moutou, M. D. Robinson, A. G. Schmutzler, P. N. Scriven, K. D. Sermon, L. Wilton, and Eshre Pgd Consortium. 2005. 'ESHRE PGD Consortium 'Best practice guidelines for clinical preimplantation genetic diagnosis (PGD) and preimplantation genetic screening (PGS)'', *Hum Reprod*, 20: 35-48.

Turco, M. Y., L. Gardner, J. Hughes, T. Cindrova-Davies, M. J. Gomez, L. Farrell, M. Hollinshead, S. G. E. Marsh, J. J. Brosens, H. O. Critchley, B. D. Simons, M. Hemberger, B. K. Koo, A. Moffett, and G. J. Burton. 2017. 'Long-term, hormone-responsive organoid cultures of human endometrium in a chemically defined medium', *Nat Cell Biol*, 19: 568-77.

Turco, M. Y., L. Gardner, R. G. Kay, R. S. Hamilton, M. Prater, M. S. Hollinshead, A. McWhinnie, L. Esposito, R. Fernando, H. Skelton, F. Reimann, F. M. Gribble, A. Sharkey, S. G. E. Marsh, S. O'Rahilly, M. Hemberger, G. J. Burton, and A. Moffett. 2018. 'Trophoblast organoids as a model for maternal-fetal interactions during human placentation', *Nature*, 564: 263-67.

Uchida, H., T. Maruyama, H. Masuda, S. Uchida, F. Miki, H. Hihara, S. Katakura, Y. Yoshimasa, and M. Tanaka. 2016. 'How to Create an Embryo Penetration Route', *Am J Reprod Immunol*, 75: 326-32.

Uchida, H., T. Maruyama, K. Ohta, M. Ono, T. Arase, M. Kagami, H. Oda, T. Kajitani, H. Asada, and Y. Yoshimura. 2007. 'Histone deacetylase inhibitor-induced glycodelin enhances the initial step of implantation', *Hum Reprod*, 22: 2615-22.

Uhlen, M., L. Fagerberg, B. M. Hallstrom, C. Lindskog, P. Oksvold, A. Mardinoglu, A. Sivertsson, C. Kampf, E. Sjostedt, A. Asplund, I. Olsson, K. Edlund, E. Lundberg, S. Navani, C. A. Szigyarto, J. Odeberg, D. Djureinovic, J. O. Takanen, S. Hober, T. Alm, P. H. Edqvist, H. Berling, H. Tegel, J. Mulder, J. Rockberg, P. Nilsson, J. M. Schwenk, M. Hamsten, K. von Feilitzen, M. Forsberg, L. Persson, F. Johansson, M. Zwahlen, G. von Heijne, J. Nielsen, and F. Ponten. 2015. 'Proteomics. Tissue-based map of the human proteome', *Science*, 347: 1260419.

Usadi, R. S., M. J. Murray, R. C. Bagnell, M. A. Fritz, A. I. Kowalik, W. R. Meyer, and B. A. Lessey. 2003. 'Temporal and morphologic characteristics of pinopod expression across the secretory phase of the endometrial cycle in normally cycling women with proven fertility', *Fertil Steril*, 79: 970-4.

van der Gaast, M. H., K. Beier-Hellwig, B. C. Fauser, H. M. Beier, and N. S. Macklon. 2003. 'Endometrial secretion aspiration prior to embryo transfer does not reduce implantation rates', *Reprod Biomed Online*, 7: 105-9.

van Hoogenhuijze, N. E., J. C. Kasius, F. J. M. Broekmans, J. Bosteels, and H. L. Torrance. 2019. 'Endometrial scratching prior to IVF; does it help and for whom? A systematic review and meta-analysis', *Hum Reprod Open*, 2019: hoy025.

Vankelecom, H. 2019. 'Organoid modeling of healthy and diseased endometrium. Oral communication at the 66th Annual Scientific Meeting of the Society for Reproductive Investigation in Paris, France.'.

Vassena, R., S. Boue, E. Gonzalez-Roca, B. Aran, H. Auer, A. Veiga, and J. C. Izpisua Belmonte. 2011. 'Waves of early transcriptional activation and pluripotency program initiation during human preimplantation development', *Development*, 138: 3699-709.

Vento-Tormo, R., M. Efremova, R. A. Botting, M. Y. Turco, M. Vento-Tormo, K. B. Meyer, J. E. Park, E. Stephenson, K. Polanski, A. Goncalves, L. Gardner, S. Holmqvist, J. Henriksson, A. Zou, A. M. Sharkey, B. Millar, B. Innes, L. Wood, A. Wilbrey-Clark, R. P. Payne, M. A. Ivarsson, S. Lisgo, A. Filby, D. H. Rowitch, J. N. Bulmer, G. J. Wright, M. J. T. Stubbington, M. Haniffa, A. Moffett, and S. A. Teichmann. 2018. 'Single-cell reconstruction of the early maternal-fetal interface in humans', *Nature*, 563: 347-53.

Verstraelen, H., R. Vilchez-Vargas, F. Desimpel, R. Jauregui, N. Vankeirsbilck, S. Weyers, R. Verhelst, P. De Sutter, D. H. Pieper, and T. Van De Wiele. 2016. 'Characterisation of the human uterine microbiome in non-pregnant women through deep sequencing of the V1-2 region of the 16S rRNA gene', *PeerJ*, 4: e1602.

Vilella, F., L. B. Ramirez, and C. Simon. 2013. 'Lipidomics as an emerging tool to predict endometrial receptivity', *Fertil Steril*, 99: 1100-6.

Vitagliano, A., A. Andrisani, C. Alviggi, S. G. Vitale, G. Valenti, F. Sapia, A. Favilli, W. P. Martins, N. Raine-Ferring, L. Polanski, and G. Ambrosini. 2019. 'Endometrial scratching for infertile women undergoing a first embryo transfer: a systematic review and meta-analysis of published and unpublished data from randomized controlled trials', *Fertil Steril*, 111: 734-46 e2.

Vitagliano, A., A. Di Spiezio Sardo, G. Saccone, G. Valenti, F. Sapia, M. S. Kamath, M. Blaganje, A. Andrisani, and G. Ambrosini. 2018. 'Endometrial scratch injury for women with one or more previous failed embryo transfers: a systematic review and meta-analysis of randomized controlled trials', *Fertil Steril*, 110: 687-702 e2.

Wang, H., S. Bocca, S. Anderson, L. Yu, B. S. Rhavi, J. Horcajadas, and S. Oehninger. 2013. 'Sex steroids regulate epithelial-stromal cell cross talk and trophoblast attachment invasion in a three-dimensional human endometrial culture system', *Tissue Eng Part C Methods*, 19: 676-87.

Wang, H., and S. K. Dey. 2006. 'Roadmap to embryo implantation: clues from mouse models', *Nat Rev Genet*, 7: 185-99.

Wang, H., F. Pilla, S. Anderson, S. Martinez-Escribano, I. Herrer, J. M. Moreno-Moya, S. Musti, S. Bocca, S. Oehninger, and J. A. Horcajadas. 2012. 'A novel model of human implantation: 3D endometrium-like culture system to study attachment of human trophoblast (Jar) cell spheroids', *Mol Hum Reprod*, 18: 33-43.

Wang, J., L. Mayernik, J. F. Schultz, and D. R. Armant. 2000. 'Acceleration of trophoblast differentiation by heparin-binding EGF-like growth factor is dependent on the stage-specific activation of calcium influx by ErbB receptors in developing mouse blastocysts', *Development*, 127: 33-44.

Weimar, C. H., A. Kavelaars, J. J. Brosens, B. Gellersen, J. M. de Vreeden-Elbertse, C. J. Heijnen, and N. S. Macklon. 2012. 'Endometrial stromal cells of women with recurrent miscarriage fail to discriminate between high- and low-quality human embryos', *PLoS One*, 7: e41424.

Wexler, H. M. 2007. 'Bacteroides: the good, the bad, and the nitty-gritty', *Clin Microbiol Rev*, 20: 593-621.

Wilcox, A. J., D. D. Baird, and C. R. Weinberg. 1999. 'Time of implantation of the conceptus and loss of pregnancy', *N Engl J Med*, 340: 1796-9.

Wira, C. R., K. S. Grant-Tschudy, and M. A. Crane-Godreau. 2005. 'Epithelial cells in the female reproductive tract: a central role as sentinels of immune protection', *Am J Reprod Immunol*, 53: 65-76.

Wongwananuruk, T., T. Sato, T. Kajihara, S. Matsumoto, M. Akita, K. Tamura, J. J. Brosens, and O. Ishihara. 2016. 'Endometrial androgen signaling and decidualization regulate trophoblast expansion and invasion in co-culture: A time-lapse study', *Placenta*, 47: 56-62.

Xiao, S., J. R. Coppeta, H. B. Rogers, B. C. Isenberg, J. Zhu, S. A. Olalekan, K. E. McKinnon, D. Dokic, A. S. Rashedi, D. J. Haisenleder, S. S. Malpani, C. A. Arnold-Murray, K. Chen, M. Jiang, L. Bai, C. T. Nguyen, J. Zhang, M. M. Laronda, T. J. Hope, K. P. Maniar, M. E. Pavone, M. J. Avram, E. C. Sefton, S. Getsios, J. E. Burdette, J. J. Kim, J. T. Borenstein, and T. K. Woodruff. 2017. 'A microfluidic culture model of the human reproductive tract and 28-day menstrual cycle', *Nat Commun*, 8: 14584.

Xiao, S., H. Diao, F. Zhao, R. Li, N. He, and X. Ye. 2014. 'Differential gene expression profiling of mouse uterine luminal epithelium during periimplantation', *Reprod Sci*, 21: 351-62.

Xiong, T., Y. Zhao, D. Hu, J. Meng, R. Wang, X. Yang, J. Ai, K. Qian, and H. Zhang. 2012. 'Administration of calcitonin promotes blastocyst implantation in mice by up-regulating integrin beta3 expression in endometrial epithelial cells', *Hum Reprod*, 27: 3540-51.

Yeaman, G. R., P. M. Guyre, M. W. Fanger, J. E. Collins, H. D. White, W. Rathbun, K. A. Orndorff, J. Gonzalez, J. E. Stern, and C. R. Wira. 1997. 'Unique CD8+ T cell-rich lymphoid aggregates in human uterine endometrium', *J Leukoc Biol*, 61: 427-35.

Yu, N., B. Zhang, M. Xu, S. Wang, R. Liu, J. Wu, J. Yang, and L. Feng. 2016. 'Intrauterine administration of autologous peripheral blood mononuclear cells (PBMCs) activated by HCG improves the implantation and pregnancy rates in patients with repeated implantation failure: a prospective randomized study', *Am J Reprod Immunol*, 76: 212-6.

Yuhki, M., T. Kajitani, T. Mizuno, Y. Aoki, and T. Maruyama. 2011. 'Establishment of an immortalized human endometrial stromal cell line with functional responses to ovarian stimuli', *Reprod Biol Endocrinol*, 9: 104.

Zegers-Hochschild, F., G. D. Adamson, J. de Mouzon, O. Ishihara, R. Mansour, K. Nygren, E. Sullivan, S. van der Poel, Technology International Committee for Monitoring Assisted Reproductive, and Organization World Health. 2009. 'The International Committee for Monitoring Assisted Reproductive Technology (ICMART) and the World Health Organization (WHO) Revised Glossary on ART Terminology, 2009', *Hum Reprod*, 24: 2683-7.

Zhang, K., and G. W. Smith. 2015. 'Maternal control of early embryogenesis in mammals', *Reprod Fertil Dev*, 27: 880-96.

Zhang, S., H. Lin, S. Kong, S. Wang, H. Wang, H. Wang, and D. R. Armant. 2013. 'Physiological and molecular determinants of embryo implantation', *Mol Aspects Med*, 34: 939-80.

Zhou, J. Z., S. S. Way, and K. Chen. 2018. 'Immunology of Uterine and Vaginal Mucosae: (Trends in Immunology 39, 302-314, 2018)', *Trends Immunol*, 39: 355.

Zhu, L. H., L. H. Sun, Y. L. Hu, Y. Jiang, H. Y. Liu, X. Y. Shen, X. Y. Jin, X. Zhen, H. X. Sun, and G. J. Yan. 2013. 'PCAF impairs endometrial receptivity and embryo implantation by down-regulating beta3-integrin expression via HOXA10 acetylation', *J Clin Endocrinol Metab*, 98: 4417-28.

Zinaman, M. J., E. D. Clegg, C. C. Brown, J. O'Connor, and S. G. Selevan. 1996. 'Estimates of human fertility and pregnancy loss', *Fertil Steril*, 65: 503-9.

Zygmunt, M., D. Hahn, K. Munstedt, P. Bischof, and U. Lang. 1998. 'Invasion of cytotrophoblastic JEG-3 cells is stimulated by hCG in vitro', *Placenta*, 19: 587-93.